

MS

STUTZMAN



**USNC/URSI
National Radio
Science Meeting
1998**

1998 Digest

Atlanta, Georgia June 21-26, 1998

**Antennas: Gateways to the
Global Network**



**Sponsored by USNC/URSI
in conjunction with:
1998 IEEE AP-S International Symposium**



2 8,9

142, 145

262

270, 271, 272

290

Welcome to the
**1998 AP-S International Symposium
and URSI National Radio Science Meeting**
in
Atlanta Georgia

The Steering Committee gratefully acknowledges the gracious support of the following organizations in planning this conference.

BMW Manufacturing Corporation

Georgia Institute of Technology

Georgia Tech Research Institute

Clemson University

Electromagnetic Sciences

Scientific Atlanta

Spartech Associates

Millimeter Wave Technology

Wang Electro-Opto Corporation



**National Academies of Science and Engineering
National Research Council of the United States of America**

**United States National Committee
International Union of Radio Science**



1998 Digest

USNC/URSI National Radio Science Meeting

**June 21 - 26, 1998
Atlanta, Georgia**

Antennas: Gateways to the Global Network

**Sponsored by USNC/URSI in conjunction with:
1998 IEEE AP-S International Symposium**



Chairman's Welcome



Andrew F. Peterson

Welcome to Atlanta!

During the week of June 21-26 Atlanta will host the *1998 IEEE International Antennas and Propagation Symposium and USNC/URSI National Radio Science Meeting*. Our steering committee has prepared a full technical and social program and we hope that you can attend! We also offer a variety of short courses and a broad range of exhibitors.

The conference will be at the Renaissance Waverly Hotel (Galleria complex), located approximately 10 miles northwest of downtown Atlanta near the intersection of US 41 and I-285.

To enhance the technical program, the Technical Program Committee, chaired by Wilson Pearson and Anthony Martin, has worked to reduce the number of parallel technical sessions. We have modified the format of the Plenary Session, distributing keynote speakers throughout the week. We also offer an interactive forum, which may be more appropriate for presenting demonstrations or a large volume of technical data.

The major change of this symposium has been the emphasis on electronic submission, electronic internal processing, and electronic delivery of the conference papers and abstracts. Thanks to the extensive pre-conference planning by Anthony Martin and others, this undertaking appears to be working well.

As you can see, we are conducting a number of experiments this year. Please give us your feedback so that future symposia can learn from our experience!

Andrew F. Peterson, *General Chair*
School of Electrical & Computer Engineering
Georgia Institute of Technology
Atlanta, GA 30332-0250

Steering Committee

Honorary Chair:	Donald G. Bodnar
General Chair:	Andrew F. Peterson
General Co-Chair:	James C. Wiltse
Finance:	Neal T. Alexander
Printing and CD-ROM:	Hugh Denny
Publicity:	Jagjeet S. Sidhu
URSI Liaison:	David P. Millard
Registration:	Dennis J. Kozakoff
Short Courses & Workshops:	Paul Harms
Technical Program Chair:	Gary Brown
Technical Program Co-Chair:	E. Jerry Archbold
Publications Preparation:	William P. Cooke
Special Sessions:	Victor K. Tripp
Interactive Forum:	L. Wilson Pearson
Student Paper Contest:	Anthony Q. Martin
Social Program:	Don Black
Awards Banquet:	James A. Fuller
Webmaster:	Cathy Freeman
Hotel Arrangements:	Doren W. Hess
Exhibits:	J. P. Montgomery
Members at large:	Cathy Freeman
	Joy Laskar
	D. Ray Lewis
	W. R. Scott, Jr
	David P. Millard
	Mark Mitchell
	Don Runyon
	J. W. Dees
	William A. Guzak
	Johnson J. H. Wang

Richard E. Tracy served as Editorial Assistant to the Technical Program Committee.

Technical Program Committee

Weng Chew	Christos Christodoulou
Afshin Daryoush	Bob Dybdal
Tom Fontana	David A. Hill
Glenn Hopkins	John Huang
William Imbraile	Akira Ishimaru
Magdy Iskander	Paul Ingerson
Linda Katehi	Ed Kuester
Ray Leubbers	James Lin
Theresa Maldonado	Krys Michalski
Amir Mortazawi	John Norgard
Sadisiva Rao	Ross Stone
Fred Tesche	Piergiorgio Uslenghi
Kathie Virga	Wohhart Vogel
John Volakis	Parveen Wahid
Don Wilton	Amir Zaghloul

Special Session Organizers

I. M. Besieris	A. C. Cangellaris	P. R. Cox	N. Engheta	J. A. Fuller
D. W. Hess	R. W. Kreutel	R. J. Luebbers	T. S. Rappaport	A. E. Ruehli
M. Sancer	R. A. York	J. L. Volakis		

Conference Facilitators

Three Dimensions

Mary Ellen Vegter
Bonnie Grosek
Theodora Dirksen

phone: 562-860-8180 FAX: 562-860-5262
On-line Registration: <http://www.threedimensions.com>

Table of Contents

Monday

SESSION	TITLE	PAGE	
URSI B	Session 2	Microstrip and Printed Antennas.....	1
URSI B	Session 3	Inverse Scattering from Theory to Application.....	13
URSI B	Session 4	Microwave and Radar Imaging.....	21
URSI B	Session 11	Numerical Methods for Transient Problems	27
URSI B	Session 14	<i>Special Session:</i> Domain Decomposition and Diakoptics for Efficient Electromagnetic Computation	39
URSI B	Session 15	High Frequency Techniques.....	45
URSI B	Session 21	Antenna Arrays: Theory and Design.....	55
URSI B	Session 22a	<i>Interactive Forum:</i> FDTD Methods	65
URSI B	Session 22b	<i>Interactive Forum:</i> Mesh Truncation Conditions	77

Tuesday

SESSION	TITLE	PAGE	
URSI B	Session 25	Hybrid Computational Approaches Involving Finite Methods	89
URSI B	Session 29	Efficiency Issues in Integral Equation Computations	101
URSI B/D	Session 31	<i>Session Session:</i> Antenna Applications of Photonic- Band-Gap Materials	113
AP/URSI B	Session 32	<i>Special Session:</i> Novel Trends in Theoretical Electromagnetics	125
AP/URSI B	Session 33	<i>Special Tribute</i> in Honor of the Career of Prof. Robert E. Collin.....	AP Vol. 2

AP/URSI B	Session 36	Scattering and Imaging from the Surface, Ground and Buried Objects.....	135
URSI F	Session 38	Mobile Propagation Studies for Outdoor and Indoor Scenarios	137
AP/URSI D	Session 40	Electronics and Photonics	147
URSI B	Session 42	Electromagnetic Theory	157

Wednesday

SESSION	TITLE	PAGE	
URSI B	Session 48	Transient Fields, Effects, and Systems.....	165
URSI B	Session 49	Random Media Effects on Propagation and Scattering	175
URSI K	Session 53	Biological Effects of Electromagnetic Fields.....	187
URSI B	Session 55	Issues in Differential Equation Based Methods	199
URSI B	Session 58	EM Scattering from Finite and Extended Bodies.....	211
URSI B	Session 60	Adaptive and Configurable Antenna Arrays.....	221
AP/URSI A	Session 61	Electromagnetic Measurement Techniques	227
URSI K	Session 64	Medical Applications of Electromagnetic Fields	237
AP/URSI B	Session 65	Wavelet Methods.....	243
URSI B/D	Session 67	Special Session: Microelectromechanical Systems, MEMS.....	247

Thursday

SESSION	TITLE	PAGE	
URSI B	Session 70	Reflectors and Broadband Antenna Design	255
AP/URSI F	Session 71	Tropospheric and Ionospheric Propagation.....	267
URSI K	Session 74	Antennas for Mobile Communications	269
URSI B	Session 75	Waveguiding Structures, Circuits, and Discontinuities	275

AP/URSI K	Session 76	Biological Effects and Medical Applications.....	287
URSI B	Session 79	Wire and Active Antenna Elements.....	289
URSI B	Session 82	Formulations for Integral Equation Solutions.....	301
URSI B	Session 86	Complex Media.....	313
URSI B	Session 91	Combining Method of Moments with High Frequency Techniques.....	319
URSI B	Session 92	Inverse Scattering for Target Recognition	325

Microstrip and Printed Antennas

D. R. Jackson and W. Stutzman

Analysis of a New Wideband Printed Antenna Element (the Foursquare) using FDTD Techniques	2
<i>C. G. Buxton*, W. L. Stutzman, J. R. Nealy, Virginia Polytechnic Institute and State University, USA</i>	
A Full-wave Time Domain Analysis of a Broadband U-slot Microstrip Array Antenna	3
<i>Y. X. Guo*, K. M. Luk, C. L. Mak, City University of Hong Kong, Hong Kong, P. R. China, P. R. China</i>	
Design of an L-Band High Efficiency Circularly Polarized Microstrip Antenna	4
<i>M. M. Faiz*, P. F. Wahid, University of Central Florida, USA</i>	
Microstrip Patch Antenna Performance on a Photonic Bandgap Substrate	5
<i>P. K. Kelly*, Ball Aerospace & Technologies Corp., USA, M. Piket-May, I. Rumsey, A. Bhobe, University of Colorado, USA</i>	
A General Method for Constructing Reduced Surface Wave Microstrip Antennas	6
<i>D. R. Jackson*, A. Mehrotra, J. T. Williams, S. A. Long, University of Houston, USA</i>	
Microstrip Zero-sum Antenna: CAD and Experimental Study	7
<i>E. Niver*, T. Lam, New Jersey Institute of Technology, USA, R. Kapadia, Zeland Software, Inc., USA</i>	
FDTD Analysis of Dual-frequency Planar Inverted-f Microstrip Antennas for Mobile Telephone Handsets	8
<i>M. Tong*, Y. Chen, Hong Kong Polytechnic University, Hong Kong, P. R. China, K. Sun, NEC, USA, R. Mittra, Penn State University, USA</i>	
Frequency Tunable Microstrip Patch Antennas using Ferroelectric-loaded Gaps	9
<i>L. I. Basilio*, J. T. Williams, D. R. Jackson, S. A. Long, University of Houston, USA</i>	
Design Considerations for Notch Feeding of a Patch Antenna	10
<i>A. Zaman*, R. Q. Lee, NASA Lewis Research Center, USA</i>	
Efficient Moment-method Analysis of a Class of Wideband Microstrip Patch Antennas	11
<i>D. Chatterjee*, R. G. Plumb, University of Kansas, USA</i>	
Creeping Wave Considerations in Cylindrical Microstrip Patch Arrays	12
<i>D. Chatterjee*, R. G. Plumb, G. Prescott, University of Kansas, USA</i>	

Analysis of a New Wideband Printed Antenna Element (the Foursquare) Using FDTD Techniques

C. G. Buxton*, W. L. Stutzman, and J. R. Nealy

The Bradley Department of Electrical and Computer Engineering

Virginia Polytechnic Institute and State University

Blacksburg, VA 24061-0111

www.ee.vt.edu/antenna

A new planar antenna element was developed at Virginia Tech for use in phased arrays. Experimental and numerical investigations both show that the new element, called the Foursquare, is capable of 50% bandwidth. The perimeter is square and at midband the diagonal dimension is about a half-wavelength and the depth is about a quarter-wavelength. A patent application has been filed.

It was not obvious how the Foursquare operated. Therefore, a numerical study was performed to investigate the antenna further. FDTD was selected because of its ability to treat three-dimensional structures, including dielectrics. An FDTD model of the Foursquare was developed to examine the radiation pattern, gain, and current distribution. The FDTD code uses cubic Yee cells and second order Higdon absorbing boundary conditions. The phasor electric and magnetic field values are determined on a closed surface surrounding the antenna. These field components provide the equivalent electric and magnetic surface currents that are examined directly. In addition, using the surface equivalence theorem, the far field pattern is obtained by performing a discrete Fourier transform.

The Foursquare antenna consists of four square, thin, metal plates and is fed across diagonally opposing plates. This feed configuration does not lend itself easily to a rectangular grid. Therefore, an equivalent feed configuration, using four sources, is used to conform to the rectangular grid of the FDTD code.

Results for the FDTD model of the antenna will be compared to the measured data of a prototype Foursquare antenna in the presentation. Gain values as a function of frequency computed using the four source feed configuration will also be presented.

A full-wave time domain analysis of a broadband U-slot microstrip array antenna

Y. X. Guo K. M. Luk C. L. Mak

Department of Electronic Engineering, City University of Hong Kong
Tat Chee Avenue, Kowloon, Hong Kong SAR, P. R. China

Many advantages of microstrip array antenna have made it very attractive for practical applications. Much progress has been made in recent years. Up to now there are two conventional techniques: the element-by-element method and the modified infinite periodic structure method. They are all in frequency domain. The full-wave integrated time domain analysis of finite structure microstrip array antenna is first introduced in this paper.

In this study, for the analysis of the our newly developed 1×4 elements U-slot microstrip array antenna, we use the frequency difference-time domain(FD-TD) method which may provide the wide band information. Because the frequency parameters of microstrip structure are much sensitive to the errors of time -domain numerical results, the key point in improving computation accuracy is to reduce the reflection of the absorbing boundary. Here the modified Berenger PML(MPML) absorbing condition developed by B. Chen and D. G. Fang is first used in the analysis. The MPML is more efficient in absorbing the evanescent energy and keeping the same performance for propagating modes than Berenger PML. This good behaviour of MPML is important in our analysis. The 1×4 elements U-slot microstrip array antenna is edged-fed with uniform amplitude and phase. Compared to isolated microstrip antenna, more slow decay evanescent waves are included near microstrip antenna array. It is shown that the MPML results are more accurate than the PML those.

Meanwhile, the broadband characteristics of dielectric rectangular U-slot microstrip array antenna is first investigated. Recently, the single-layer coaxially fed U-slot rectangular patch antenna with over 30% impedance bandwidth and good pattern characteristics has aroused much interest. The impedance bandwidth, and far-field radiation pattern are presented and verified by measurement. A good agreement is obtained.

DESIGN OF AN L-BAND HIGH EFFICIENCY CIRCULARLY POLARIZED MICROSTRIP ANTENNA

M. M. Faiz* and P. F. Wahid
Electrical and Computer Engineering Department
University of Central Florida
Orlando, Florida 32816

ABSTRACT

Microstrip antennas suffer inherently from low efficiency and narrow bandwidth. One way to improve the efficiency of microstrip antennas is to use substrates with lower permittivity (J R James & P S Hall, *Handbook of Microstrip antennas*, Vol. 1). Present day applications of microstrip antennas in mobile communications demand the need of high efficiency antennas. The research undertaken here deals with the design of a high efficiency circularly polarized rectangular patch antenna. Circular polarization is obtained by feeding the patch at a corner.

In order to attain lower permittivity substrate a combination of two dielectric layers, Rohacell hard foam, 3 mm thick with $\epsilon_r = 1.08$ and Rogers RT/Duroid 5880, 0.127 mm thick with $\epsilon_r = 2.2$, are used. The whole combination results in a better efficiency. The radiation pattern as well as the overall performance of the antenna will be presented.

The patch dimensions are 139.1 mm X 134 mm for a resonance frequency of 1.004 GHz. The efficiency of the patch was found to be around 94%. A superstrate consisting of Rogers RT/Duroid 5880, 0.0127 mm thick was introduced to study the effects on efficiency. The geometry of the antenna is shown in Figure 1 below. Results on the efficiency of the antenna will be presented in detail.

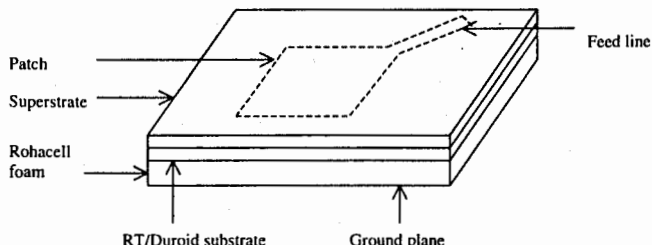


Figure 1: Circularly polarized microstrip patch

Microstrip Patch Antenna Performance on a Photonic Bandgap Substrate

P. Keith Kelly*
P.O. Box 1538
Broomfield, CO 80038-1538

Ball Aerospace

U of Col.

Melinda Piket-May, Ian Rumsey, Alpesh Bhobe
Office Tower, ECOT 436
Campus Box 425
Boulder, CO 80309-0425

Others have suggested that a photonic bandgap substrate could lead to enhanced bandwidth (P. K. Kelly, et. al. URSI, p. 10, Jan. 1998) and pattern performance (H. D. Yang, et. al., IEEE Trans. APS, 185-187, 1997). This paper reports the findings of an investigation conducted to explore the performance of a microstrip patch antenna on a photonic bandgap substrate, PBGS. The theoretical and experimental findings of this investigation and the construction techniques will be presented.

Researchers have been investigating the properties of a periodic dielectric structure exhibiting a photonic bandgap since 1987. This photonic bandgap structure prevents electromagnetic propagation in any direction (in two dimensions for the 2D structure). The geometries examined have been two and three-dimensionally periodic with lattice structures typically being triangular or rectangular. The investigation of the photonic bandgap structures had been confined to theory until about 1994 when researchers constructed and characterized through measurement the properties of a finite 2D structure (P. K. Kelly, et. al. IEEE APS Intl. Sym., 718-721, 1994). Recently, researchers have suggested using the photonic bandgap structure as a substrate (H. D. Yang, MTT-S, 1997). Potential benefits from using the PBGS are increased bandwidth or gain depending on the resonance of the antenna relative to the frequency bandgap of the PBGS.

Many unknowns are involved when considering the use of the PBGS. First, a choice of lattice must be made which is amenable to the microstrip patch geometry. Second and equally important are the lattice constant (periodicity of the structure) and the dielectric constant of the material to be used. The tools used to design the substrate and the microstrip patch antenna involve both the Plane Wave Spectrum (PWS) method and the Finite Difference Time Domain method. The PWS method is used to determine the performance of the PBG structure in two dimensions and the FDTD method is used to characterize the performance of the PBGS and the microstrip antenna together. Our findings on the parameter selection and associated impact on the microstrip patch performance will be presented.

A GENERAL METHOD FOR CONSTRUCTING REDUCED SURFACE WAVE MICROSTRIP ANTENNAS

David R. Jackson*, Amit Mehrotra, Jeffery T. Williams, and Stuart A. Long

Department of Electrical and Computer Engineering

University of Houston

Houston, TX 77204-4793

It was recently demonstrated that reduced surface wave microstrip antennas can be constructed by using a modified circular patch geometry (D. R. Jackson, J. T. Williams, A. K. Bhattacharyya, R. Smith, S. J. Buchheit, and S. A. Long, IEEE Trans. Antennas and Propagat., Vol. 41, pp. 1026-1037, Aug. 1993). These reduced surface wave antennas have a dominant-mode electric field distribution inside the patch cavity that results in an equivalent magnetic current at the boundary that does not excite the TM_0 surface wave of the grounded substrate. Although very good reduced surface wave performance can be achieved with these designs, the geometries are restricted to patches of circular shape.

In this presentation, a new method for constructing reduced surface wave antennas of *arbitrary shape* will be discussed. The method starts by taking a planar microstrip patch element of arbitrary shape on a grounded substrate of relative permittivity ϵ_r , and replaces the substrate material inside the patch cavity with a material having a relative permittivity ϵ_{rc} . The filling material inside the patch cavity is chosen to have a relative permittivity $\epsilon_{rc} = (\beta_{TM0} / k_0)^2$, where β_{TM0} is the propagation constant of the TM_0 surface wave on the grounded substrate. If the patch is resonant, the electric field inside the patch cavity will always correspond to an equivalent magnetic current at the boundary of the patch that does not excite the TM_0 surface wave, regardless of the patch shape. A proof of this theorem will be presented during the presentation.

In practice, the required relative permittivity ϵ_{rc} can be achieved by creating an artificial dielectric in the cavity region below the planar patch element. One way to do this is to drill closely spaced holes in the substrate underneath the patch. Another method is to core out part of the dielectric inside the cavity, so that the cavity is partially filled with a horizontal sheet of dielectric having a relative permittivity ϵ_r . In either case, simple formulas for the effective permittivity can be obtained, and the theorem discussed above provides simple design rules for the construction of the filling material inside the cavity.

Examples will be presented to illustrate the application of the method to patches of different shapes.

MICROSTRIP ZERO-SUM ANTENNA; CAD AND EXPERIMENTAL STUDY

Edip Niver, Tuan Lam* and Rajesh Kapadia

Electrical and Computer Engineering Department
New Jersey Institute of Technology
Newark, NJ 07102

* Zeland Software, Inc.
Eastern Office
25 Rose Street
South River, NJ 08882

A microstrip antenna array consisting of two elements combined with a stripline hybrid (rat-race) ring coupler is used to implement a zero-sum antenna. Numerical optimization of individual antenna elements in terms of feed location and patch size was achieved using IE3D (Zeland Software Inc., Fremont, CA), a fullwave 3-D planar electromagnetic simulation software. Further, design of a hybrid (rat-race) ring coupler in a stripline environment was carried out, yielding the sum and difference functions as 0.5 dB and 40 dB, respectively. A combination of a two-element antenna array and a hybrid (rat-race) ring coupler as a zero sum antenna has been studied numerically revealing that 40 dB differences can be expected between the sum and difference patterns in the forward direction at the operating frequency. Experimental results using MCS material ($\epsilon_r=3.26$ and thickness $t=60$ mils) (Glasteel Industrial Laminates, Collierville, TN) have shown that satisfactory performance can be achieved at the chosen operating frequency.

FDTD Analysis of Dual-Frequency Planar Inverted-F Microstrip Antennas for Mobile Telephone Handsets

¹*Ming-Sze Tong, ¹Yinchao Chen, ²Kunquan Sun, and ³Raj Mittra*

¹*Department of Electronic Engineering, Hong Kong Polytechnic University, Hong Kong*

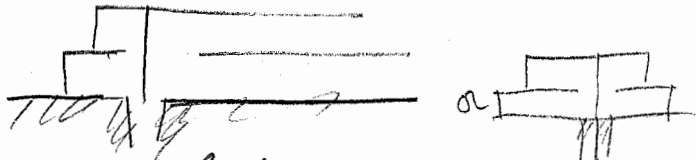
²*Wireless Communications Division, NEC America, Irving, TX, USA*

³*EMC Research Laboratory, 319 EEE, Penn State, University Park, PA*

Recent years have seen an explosive growth in market demand for cellular communication systems. In many regions of the world, two operating frequency systems are simultaneously used for mobile communication, *viz.*, the GSM and DCS 1800 systems operating at 0.9 GHz and 1.8 GHz, respectively. Hence, it is highly desirable to design a dual-band antenna for cellular telephone handsets that can operate in dual-mode, and meets the requirement for built-in antennas for both the GSM and DCS 1800 systems concurrently.

In this paper we describe the design of a planar inverted-F microstrip antenna which not only satisfies the dual mode requirement, but also significantly reduces the power absorbed in the head of the user of the hand-held telephone. We analyze the antenna by using the Finite Difference Time Domain (FDTD) method, applied in conjunction with an unsplit, anisotropic perfectly matched layer (APML) approach for mesh truncation of the computational domain. To obtain the desirable accuracy of computation for the PIFA design, we employ PML terminations that include all truncation surfaces, edges, and corners.

The PIFA is designed by using an S-parameter approach to meet the design criteria for resonance at the two designated frequencies, and to satisfy the corresponding bandwidth requirements. Next, the near-to-far-field transformation is employed to compute the radiation patterns of the dual-band antenna at its two resonant frequencies, to ascertain that the PIFA is effective in receiving incoming signals over a broad angular range.



Small ground plane

44 x 44 x 8 mm

Size Bandwidth is still a problem

Frequency Tunable Microstrip Patch Antennas Using Ferroelectric-Loaded Gaps

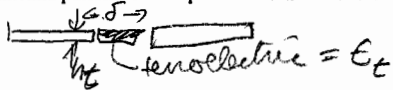
Lorena I. Basilio, Jeffery T. Williams, David R. Jackson,
and Stuart A. Long

Applied Electromagnetics Laboratory
Department of Electrical Engineering
University of Houston
Houston, TX 77204-4793

Due to the inherently narrow-band character of microstrip patch antennas, a considerable effort has been expended towards the development of tunable microstrip patches. A tunable microstrip patch antenna allows not only for relatively wide-band frequency diversity but also for the electronic correction of errors introduced by changes in temperature, environment, and manufacturing imperfections. In the past the tunable patch designs have included non-linear devices such as reverse-biased diodes. However, the use of these non-linear devices introduces design and fabrication complications as well as potential non-linear effects.

In this presentation we will discuss a new microstrip patch antenna that uses a ferroelectric-filled gap etched into the patch to obtain passive electronic frequency tuning. This gap design essentially represents a tuning capacitor that is introduced into the microstrip antenna. Although ferroelectric materials typically have high loss tangents, the loss effect is minimized by using a ferroelectric capacitor rather than a ferroelectric substrate for the microstrip patch. Since the effects of manufacturing tolerances and other external variables tend to especially influence the resonant frequency of patches etched on high permittivity substrates, the use of a ferroelectric loaded gap is ideal for tuning in these cases.

We will present a model, developed and verified, for the microstrip gap tuned patch. From this model the tunability and sensitivity of the gap-tuned antenna as a function of dielectric constant, gap size, and gap design will be examined. In addition, this presentation will also include results showing the electrical properties of ferroelectric-loaded gap patch antennas. Examples for the antenna patterns and impedance characteristics will be presented.



Tuning BW = 31%



Talking to phys. cs Dept. about materials

DESIGN CONSIDERATIONS FOR NOTCH FEEDING OF A PATCH ANTENNA

Afroz Zaman* and Richard Q. Lee

NASA Lewis Research Center

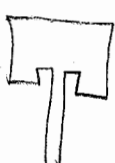
21000 Brookpark Rd., Cleveland, OH 44135, U.S.A.

An essential element in the design of a microstrip patch antenna is a proper feed structure. Without adequate attention to the feed design the actual antenna performance will be impacted. One widely used feed structure is a microstrip line which has the advantages of simplicity and fabrication ease. In general, the microstrip line can be placed either perpendicular to the radiating edge or non-radiating edge of a patch antenna. In case of square patches, it is often desirable to place the feed along the center line of the radiating edge to maintain a single mode operation with low cross-polarization. Since feeding a patch antenna at the edge usually results in high return losses due to high electric fields along the radiating edge, a notch feed which extends the feed line into the interior of the patch has often been used to achieve impedance match to a 50Ω line. Although the notch feeding technique has been applied successfully by many researchers[1-2], the design approach is still not well understood particularly in the design of the microstrip-notch transition. It is not clear whether the notch feed behaves like a conductor-backed coplanar waveguide or simply a microstrip extension.

In this paper, we will report a theoretical and an experimental investigations of what effects various parameters of a notch feed have on the antenna performance, namely, how the change of the slot width and depth impacts the input impedance, return loss (S_{11}), and resonant frequency of a square patch antenna. Based on these result, we will try to establish some design guideline and characteristic curves for notch feeding a patch antenna. The patch used in the experiment was fabricated on 10 mil thick RT/Duroid substrate with $\epsilon_r = 2.2$ and was excited for linear polarization by a notch feed of varying depths and slot widths. The square patch of 4.91 mm in dimensions was designed to operate around 20 GHz. Preliminary result indicate that both the notch depth and slot width affect the input impedance, S_{11} and the resonant frequency of the antenna. In particular, varying the notch depth profoundly impacts both the S_{11} and the input impedance and set the initial match of the input point to the feed network. However, varying the slot width provides only fine tuning of the S_{11} and the input impedance, but the effect is more prominent for a small input impedance than a large input impedance near the radiating edge. Finally, terminating the notch feed in open circuit by joining the two slots on both sides introduces large inductance which must be compensated with large capacitance to achieve good impedance match.

Reference:

- [1] K.R.Carver, Proc. Of the workshop on P.C.A.T. New Mexico State University, Las Cruces, New Mexico, U.S.A., 1979
- [2] H.D. Weinschel, Proc. Of the workshop on P.C.A.T. New Mexico State University, Las Cruces, New Mexico, U.S.A., 1979



Used Ensemble code
No experiments

EFFICIENT MOMENT-METHOD ANALYSIS OF A CLASS OF WIDEBAND MICROSTRIP PATCH ANTENNAS

D. Chatterjee* and R. G. Plumb

Radar Systems and Remote Sensing Laboratory
Department of Electrical Engineering and Computer Science
University of Kansas, Lawrence, KS 66045-2969

Modeling probe-fed, wideband microstrip antennas requires special attention for characterizing the probe-to-patch junction. This junction plays an increasingly dominant role as the frequency of the microstrip patch antenna increases. While it is relatively easier to fabricate a probe-fed patch, its analysis can be substantially complicated to warrant a rigorous analysis [D. H. Schaubert *et. al.* *IEEE Trans. Antennas Propagat.*, pp. 677-683, June 1989]. An improved feed model was subsequently used to model wideband arrays [J. T. Aberle and D. M. Pozar, *Proc. IEE*, Part H, pp. 110-119, April 1989] and single elements [J. T. Aberle and D. M. Pozar, *IEEE Antennas and Propagation Symp. Digest*, vol. 1, pp. 350-353, May 1990]. The results showed remarkable agreement in the high-frequency region when compared with experimental data. This was achieved by introducing the attachment mode expansion function in a method-of-moment (MoM) solution to model the rapidly varying current near the probe-to-patch junction. However this expansion function is an infinite eigenfunction series and is computationally intensive, particularly in spectral-domain regimes. Recently this infinite series was reduced to a residue series that required only one or two term(s) when compared to about fifty-five terms of the eigenfunction series [D. Chatterjee and R. G. Plumb, *IEEE Trans. Antennas Propagat.*, pp. 677-686, May 1996]. The concept of using the residue series in calculating the elements of the impedance matrix was presented in [D. Chatterjee and R. G. Plumb, *IEEE AP-S and URSI/USNC Symp. Dig.*, vol. 2, pp. 602-605, July 1997]. Additional investigations have shown that the application of the residue series can enhance the convergence properties of an MoM solution. This is feasible since the residue series form for the attachment mode expansion function requires only one term. Furthermore, since the calculations of the elements of the impedance matrix are done in space domain [M. I. Aksun and R. Mittra, *IEEE Trans. Microwave Theory Tech.*, pp. 503-509, March 1993], the fill time for the elements of the impedance matrix is substantially reduced. In the proposed MoM solution, the elements of the voltage matrix are evaluated in the spectral domain and, hence, the overall MoM approach is a hybrid technique. In this presentation some important features of this hybrid MoM formulation will be discussed. The various numerical issues regarding the computer implementation of this technique shall also be addressed. Finally, results for the input impedance will be compared against available measured data to demonstrate the validity and applicability of the residue series for the attachment mode when applied to modeling of wideband, coaxially fed, microstrip arrays.

Swingneen active element patterns

CREEPING WAVE CONSIDERATIONS IN CYLINDRICAL MICROSTRIP PATCH ARRAYS

D. Chatterjee, R. G. Plumb and G. Prescott

Radar Systems and Remote Sensing Laboratory (RSL)
Department of Electrical Engineering and Computer Science
University of Kansas, Lawrence, KS 66045-2969

Base-station antennas in microcellular communication systems must have complete azimuth beam-scanning capability and improved space diversity for spatial frequency reuse. In the recent past it has been proposed that a conformal cylindrical array be used for base-station applications with suitable amplitude and phase tapers across the individual elements [D. Chatterjee and R. G. Plumb, *IEEE AP-S and USNC/URSI Symp. Dig.*, vol. 1, pp. 714-717, July 1996], [D. Chatterjee and R. G. Plumb, *IEEE AP-S and USNC/URSI Symp. Dig.*, URSI Abstracts, p. 50, July 1997]. However, in these preliminary investigations a method of synthesis for the array excitation was realized without considering the actual radiating element characteristics. Recently cellular SDMA (Space Division Multiple Access) technology, using conformal cylindrical structures for multiple beam forming using rectangular microstrip patches, has been advocated [D. Loffler *et. al.*, *IEEE AP-S and USNC/URSI Symp. Dig.*, vol. 3, 1533-1536, July 1997]. However, in these analyses the effects of mutual coupling due to creeping wave propagation around the cylinder have not been addressed explicitly. It is of course well-known that in cylindrical arrays the creeping waves can cause beam spoilage near the boresight [J. C. Herper *et. al.*, *IEEE Trans. Antennas. Propagat.*, pp. 259-272, March 1985]. As discussed in [A. Hessel, p. 275, Fig. 4, in *Phased Array Antennas*, A. A. Oliner and G. H. Knittel (eds.), Artech House, USA, 1972], the creeping and space waves interfere destructively in a cylindrical (or non-planar) array environment causing significant reduction in boresight gain and mainbeam distortion. A criterion to suppress such effects was developed for waveguide apertures [J. C. Sureau and A. Hessel, *IEEE Trans. Antennas Propagat.*, Jan. 1971] but no substantial analysis has been performed for conformal cylindrical structures. An overview of full-wave analysis will be presented following some relevant earlier investigations [J. Ashkenazy *et. al.*, *IEEE Trans. Antennas Propagat.*, pp. 295-300, March 1985], [K. Naishadham and L. B. Felsen, *IEEE Trans. Antennas. Propagat.*, pp. 304-313, March 1993]. The effects of the grid spacings, cylinder electrical radius, substrate permittivity on the creeping wave propagation and radiation in such array environments will also be discussed through appropriate numerical results. It is expected that these criteria will be directly useful in design of conformal cylindrical arrays for applications to cellular communication systems.

Naugle et al. IEEE T-AP Aug 1997
improved capacity of narrow beams.

Inverse Scattering from Theory to Application

R. V. McGahan and K. J. Langenberg

On the Well-Posedness of Back Propagation Algorithms in Inverse Electromagnetics	14
<i>G. Crosta*, University of Milano, Italy</i>	
Three-dimensional Microwave Imaging of Buried Objects	15
<i>K. Langenberg*, M. Brandfab, K. Mayer, A. Piisch, University of Kassel, Germany</i>	
Herglotz Function Methods in the Reconstruction of Scatterers from Experimental Electromagnetic Scattering Data	16
<i>P. Maponi*, L. Misici, Universita di Camerino, Italy, F. Zirilli, Universita di Roma La Sapienza, Italy</i>	
An Improved Iterative Scheme with Incorporated a priori Information Applied to Real Scattering Data	17
<i>W. Rieger*, M. Haas, C. Huber, G. Lehner, W. M. Rucker, University at Stuttgart, Germany</i>	
Fast Solution of a 2D-electromagnetic Inverse Problem using the Distorted Born Iterative and Fast Multipole Method	18
<i>M. Brandfass*, W. Chew, J. Zhao, University of Illinois, USA</i>	
Imaging Ipswich Targets using Cepstral Filtering	19
<i>R. V. McGahan*, AFRL/SNHE, USA, A. Morales-Porras, University of Massachusetts, USA, J. B. Morris, AFRL/SNHE, USA, M. A. Fiddy, University of Massachusetts, USA</i>	

ON THE WELL - POSEDNESS OF BACK PROPAGATION ALGORITHMS IN INVERSE ELECTROMAGNETICS

GIOVANNI F CROSTA

UNIVERSITÀ DEGLI STUDI DI MILANO

Dipartimento di Scienze dell'Ambiente e del Territorio

via Emanuele, 15 - I 20126 MILANO (IT); e-mail: crosta@imiucca.csi.unimi.it

Approximate backpropagation (ABP) methods have been used by the author to identify the shape of simple scatterers in the resonance region from full aperture data both in the acoustic and electromagnetic case. ABP methods rely on a relation between the expansion coefficients, which represent the scattered wave in the far zone and, respectively, on the obstacle boundary, Γ , and lead to minimization algorithms.

In spite of satisfactory computational results, the well - posedness of ABP generally remains an open problem. A related result, which may eventually justify the method, pertains to a *forward* propagator i.e., to the affine map $N[\cdot] := \mathcal{A}[\cdot] + b$, which appears in the solution of the direct scattering problem.

Very briefly, if both the scattered wave and its normal derivative on Γ are represented by uniformly converging series according to a suitable basis in $L^2(\Gamma)$, if $N[\cdot]$ is bounded and maps ℓ_2 sequences of scattering coefficients into ℓ_2 sequences and if the spectral radius $r_o[\mathcal{A}]$ of \mathcal{A} satisfies $r_o[\mathcal{A}] < 1$, then $\forall b \in \ell_2$ there exists a unique fixed point, f , for the map $p[t+1] = b + \mathcal{A}[\cdot] \cdot p[t]$, $t = 0, 1, 2, \dots$, obtained by successive approximations and started with an arbitrary $p[0] \in \ell_2$.

One then derives the convergence and consistency properties of the approximate forward propagator, which relates finite subsequences of coefficients.

These results are applied to a class of numerical problems, which include the inversion of the Irswich Data.

Three-dimensional microwave imaging of buried objects

K.J. Langenberg

M. Brandfäß

K. Mayer

A. Pitsch

Department of Electrical Engineering

University of Kassel

34109 Kassel, Germany

Very often, measured microwave scattering data are considered as scalar data, for example the output voltage of a Ground Probing Radar, which allows the application of scalar imaging algorithms like the Fourier Diffraction Slice Theorem, far-field Fourier inversion, time domain back propagation, $K\omega$ -migration etc. All these algorithms can be summarized as diffraction tomography which is a general solution of the scalar inverse scattering problem when the latter is linearized in terms of the Born or Kirchhoff approximation. In this context, the paper reports a "missing link": Instead of applying the Fourier Diffraction Slice Theorem to *near-field* data, the much simpler *far-field* algorithm can be immediately utilized on near-field data with a novel proper K -space mapping. This procedure proves to be advantageous for *electromagnetic vector* data — these include polarization information —, because recently a polarimetric far-field algorithm based on the Kirchhoff approximation has been derived (K.J. Langenberg et al.; in: Radar Target Imaging, Springer-Verlag, Berlin 1994), which is, concerning the obtained image quality, far superior to scalar algorithms: With that novel mapping, an explicit near-field — far-field transform based on the electromagnetic version of Huygens' principle, which was previously necessary, can be deprecated. We apply the resulting scheme to parametric studies of microwave imaging of buried objects, for instance metallic tendon ducts below variable mesh size steel reinforcement in concrete and various models of land mines in dry soil. The air-ground interface is accounted for by observing Snell's law of refraction and disregarding multiple scattering effects; the Kirchhoff approximation, inherent in the inverse scattering scheme, does that anyway. Synthetic data for these problems are computed with the time domain module of the MAFIA code.

Herglotz function methods in the reconstruction of scatterers from experimental electromagnetic scattering data

Pierluigi Maponi
Dipartimento di Matematica e Fisica
Universita di Camerino
62032 Camerino Italy

Luciano Misici
Dipartimento di Matematica e Fisica
Universita di Camerino
62032 Camerino Italy

Francesco Zirilli
Dipartimento di Matematica G Castelnuovo
Universita di Roma La Sapienza
00185 Roma Italy

We consider the reconstruction of scatterers from experimental data relative to time harmonic electromagnetic scattering. These data are the so called IPSWICH dataset provided by the Rome Laboratory of the AIR FORCE. The scatterers considered have cylindrical symmetry and only VV, Vertical Vertical, or HH, Horizontal Horizontal, scattering is considered. In this hypothesis using the symmetry the problem can be reduced to a two dimensional inverse problem for the scalar Helmholtz equation, see 1. The IPSWICH data set has been used by several authors to test reconstruction methods on experimental data instead than synthetic data as more usual. See for example the relative special section in IEEE APS Symposium of 1996 and 1997. The scatterers considered include conductors, penetrable media and hybrid scatterers that contain both conductors and penetrable media. The problem obtained for the scalar Helmholtz equation after using the cylindrical symmetry can be interpreted in acoustic terminology. For example VV scattering of perfect conductors corresponds to scattering of acoustically soft impenetrable obstacles; VV scattering of penetrable scatterers correspond to the scattering due to the refraction index of an inhomogeneity. In 1 we have treated the IPSWICH data using a variation of the Born approximation. Several authors, see IEEE APS 1996, 1997, have considered nonlinear approaches to the inverse problems considered above. However all these methods involve the formulation of the inverse problem as a nonlinear optimization problem where the function evaluation involves the numerical solution of the direct scattering problem that is the solution of a boundary value problem for the Helmholtz equation. The need to solve iteratively the direct scattering problem makes the optimization procedure computationally expensive. The use of Herglotz function methods avoids the iterative solution of the direct problem when solving the inverse problem. Herglotz function methods have been introduced in 2 in the context of obstacle scattering and further developed in 3. Later they have been extended to inverse inhomogeneous media and electromagnetic scattering. To our knowledge this is the first attempt to use Herglotz function methods on experimental data. We will show how the Herglotz function methods have been adapted to the IPSWICH environment and the results obtained.

References

- 1 P. Maponi, L. Misici, F. Zirilli: A numerical method to solve the inverse medium problem: an application to the IPSWICH data
IEEE Antennas and Propagation Magazine 39, 1997, 14-19
- 2 D. Colton, P. Monk: The numerical solution of the three dimensional inverse scattering problem for time harmonic acoustic waves

An Improved Iterative Scheme with Incorporated a priori Information applied to Real Scattering Data

W. Rieger, M. Haas, C. Huber, G. Lehner and W.M. Rucker

Institut für Theorie der Elektrotechnik, Universität Stuttgart

Pfaffenwaldring 47, 70569 Stuttgart, Germany

E-mail: wolfgang.rieger@ite.uni-stuttgart.de

The 2D inverse electromagnetic scattering problem of reconstructing the material properties of inhomogeneous lossy dielectric cylindrical objects is considered. The material properties are reconstructed from measured far-field scattering data provided by the USAF Rome Laboratory Electromagnetic Measurement Facility in Ipswich. The targets in the Ipswich data set include perfectly conducting targets, penetrable targets and hybrid targets. The measured data are available either for TM- or TE-polarized incident fields and have to be calibrated for the use in our reconstruction algorithm.

In our previous paper (W. Rieger, M. Haas, C. Huber, G. Lehner, W.M. Rucker, Image Reconstruction from Real Scattering Data Using an Iterative Scheme with Incorporated a priori Information, submitted to IEEE Antennas and Propagation Magazine) we proposed an iterative scheme to solve numerically the inverse scattering problem formulated as unconstrained optimization problem which incorporates a priori information about the material properties. The material properties are described by the refractive index

$$n^2(r) = \frac{1}{\epsilon_0} \left(\epsilon(r) + j \frac{\kappa(r)}{\omega} \right) = 1 - m(r), \quad (1)$$

where $\epsilon(r)$ denotes the permittivity, $\kappa(r)$ the conductivity and ω the angular frequency of the incident fields. The aim of the inverse medium scattering problem is to reconstruct the contrast $m(r)$. In order to ensure physically meaningful quantities $\epsilon(r)$ and $\kappa(r)$ we write $m(r)$ as

$$m(r) = -\eta(r)\eta(r) - j\xi(r)\xi(r) \quad (2)$$

where $\eta(r)\eta(r) = \frac{\epsilon(r)}{\epsilon_0} - 1 \geq 0$ and $\xi(r)\xi(r) = \frac{\kappa(r)}{\epsilon_0\omega} \geq 0$. Instead of searching directly for complex functions $m(r)$ the real functions $\eta(r)$ and $\xi(r)$ have to be found.

In this paper we propose an improved reconstruction algorithm with a variable calibration factor. The calibration factor is incorporated into the iterative scheme as an unknown complex parameter which has to be determined during the optimization process.

The proposed method was successfully applied to the measured data.

Fast Solution of a 2D-Electromagnetic Inverse Problem using the Distorted Born Iterative and Fast Multipole Method

M. Brandfass*, W.C. Chew and J.-S. Zhao

Department of Electrical and Computer Engineering
University of Illinois, 1406 West Green Street
Urbana, IL 61801-2991

Abstract

Several procedures are available to solve the nonlinear inverse scattering problem. In principle, there are two ways of dealing with inverse scattering. (i) To linearize the nonlinear inverse problem by approximating (i.e. Born, Rytov or Kirchhoff) the total electromagnetic field on or within the scatterer to ignore the multiple interaction of scatterer and scattered field. The advantage of such methods is that usually a closed form expression can be derived for the object function, representing the scatterer. However, linearized inverse scattering models suffer from bad reconstructions if multiple reflections occur on the surface of highly conducting scatterers or if the wavenumber contrast ratio of the dielectric scatterer is high. (ii) To discretize the nonlinear inverse scattering problem representing it by matrix equations which can be inverted in an iterative manner to obtain the object function. Usually the computational cost of these iteration schemes is high because the scattered field (forward problem) must be computed for each incident angle and each frequency of the exciting field for every object function update.

Here we want to accelerate the computation of the forward problem as well as the inverse problem. We used the distorted Born iterative method (W.C. Chew and Y.M. Wang, IEEE Trans. Med. Imag., 4, 155-162, 1984) for perfectly conducting scatterers. Considering the two-dimensional transverse electric case for perfectly conducting scatterers, we discretized the magnetic field integral equation using the method of moments with two-dimensional pulse basis functions and point matching. We rearranged the Fréchet operator equation and introduced a matrix expansion, so that an inverse matrix, which is part of the Fréchet operator equation, need not be calculated while inverting the Fréchet operator equation for the next object function update.

The forward problem which still needs to be solved, is computed by a Multilevel Fast Multipole Algorithm code (MLFMA) which recursively subdivides the reconstruction domain in a bottom-up construction scheme before aggregating the divided subscatterers from the finest to the coarsest level. Such MLFMA code has $O(N \ln(N))$ computational complexity where N is the number of unknowns of the forward solver. Numerical results will be given to compare the computational time and the accuracy of the presented procedure here with usual evaluation methods using a conjugate gradient scheme.

Imaging Ipswich Targets using Cepstral Filtering

R. V. McGahan , A. Morales-Porras*, J. B. Morris and M. A. Fiddy*

AFRL/SNHE, 31 Grenier St., Hanscom AFB, MA 01731-3010

*Department of Electrical & Computer Engineering, University of Massachusetts, Lowell, MA 01854

Only when a target is weakly scattering can the target structure be readily deduced from far field scattering data. Under these conditions, when the first Born approximation is valid, there is a simple relation between the scattered field data, mapped into wave vector or k -space, and the spectral component of the target. With a sufficiently large data set, i.e. with a sufficiently large coverage of k -space, an inverse Fourier transformation yields an image of the target. One can view the scattered field data acquired for each incident field direction as providing information about spectral components of the target on a locus of points in k -space. Inverse Fourier transformation of one such data set is formally equivalent to backpropagating these far-field data into the target domain. Clearly this only provides an estimate of the product of the permittivity distribution, V , since it is convolved with a point spread function, the Fourier transform of the locus of points. Typically, this locus is the perimeter of a circle leading to a symmetric and reasonably narrow point spread function, a J_0 function. In the case of a strongly scattering target, the same approach leads to an estimate not of V but of the product of V with the total field inside the scatterer, Ψ . This field is no longer known or well approximated by the incident field, as can be assumed in the first Born approximation.

Having obtained an estimate of $V\Psi$ one can take the Fourier transform of the logarithm of this function. This spectral or "cepstral" information has the cepstrum of V added to the cepstrum of Ψ allowing simple filtering to be employed to separate one from the other. Care has to be taken in calculating the cepstrum since sampling rates are important and small values of $V\Psi$ must be avoided. For this reason we filter the spectrum of $\log(1 + |V\Psi|)$ and explain the implications of this for optimal filtering. The filtering carried out to date has been low-pass on the assumption that the spatial frequency content of Ψ is on average higher than that of V . This assumption held true reasonably well for most of the cases we have considered. It failed, however, for some of the Ipswich data sets, in particular for IPS008 and IPS012. For these penetrable and strongly scattering targets a more selective filter is required. We describe how this filter is designed and show images of the targets following filtering.

Microwave and Radar Imaging

K. Sarabandi and H. Ling

Spatial Frequency Spectrum Extension for Microwave Images of a Corner Reflector	22
<i>G. Tricole*, GDE Systems Inc., USA</i>	
ISAR Feature Extraction from Targets with Rotating Components using Adaptive Joint Time-frequency Processing.....	23
<i>Y. Wang*, H. Ling, University of Texas at Austin, USA, V. C. Chen, Naval Research Laboratory, USA</i>	
Compression and Denoising of Scattering Data in UWB Radar using Wavelet Transform.....	24
<i>B. Zhang*, S. Primak, J. LoVetri, University of Western Ontario, Canada, S. Kashyap, Defence Research Establishment, Canada</i>	
Time Domain Interferometric Radar Simulation for Urban Areas	25
<i>B. Houshmand*, California Institute of Technology, USA</i>	
Method of Nyquist Interpolation of Radar Image for Antenna Resolution Improvement	26
<i>A. V. Grechka*, Moscow Radioengineering Institute of Russian Academy of Science, Russia</i>	

Spatial frequency spectrum extension for microwave images of a corner reflector

G. Tricoles

GDE Systems Inc., P.O. Box 509009, San Diego CA 92150-9009;
telephone: (619) 675-2818 fax: (619) 675-1999

Analytically continuing an object's spatial frequency spectrum has been shown theoretically to improve resolution for two point sources, and extension of image spectra has been proposed (J.L. Harris J.O.S.A., 54 p. 931 (1964). Measurement noise may be a problem (J. L. Goodman, Introduction to Fourier Optics). We applied continuation to improve images of a subwavelength diffracting slit and a ground-based, broadcast band antenna.

This paper describes application of continuation to a microwave image of an extended object, a dihedral corner with each side 3.9 wavelength. The first step was measuring reflectance at 10Ghz with a monostatic antenna translated on a linear path, 36 wavelengths from the reflector's aperture. An image was then computed, with Kirchoff diffraction theory. To test the image we probed the scattered field, one wavelength from the aperture, the distance for which the image was calculated. The image and scattered field magnitudes showed oscillations, but the period for the probed field was half that for the image.

Analytic continuation was done by Fourier transforming the computed image and applying the sampling theorem to extend the spectrum, according to Harris' procedure. The images from continuation had period close to that of the probe data; however, the magnitudes at peaks and minima differed somewhat. In summary, resolution and image fidelity were improved.

ISAR FEATURE EXTRACTION FROM TARGETS WITH ROTATING COMPONENTS USING ADAPTIVE JOINT TIME-FREQUENCY PROCESSING

Yuanxun Wang* and Hao Ling

Department of Electrical and Computer Engineering,
The University of Texas at Austin, Austin, TX 78712-1084

Victor C. Chen

Airborne Branch, Naval Research Laboratory
Washington, DC 20375

It is well known that when rotating components exist on a target such as gimbaled antennas or propeller blades, image artifacts are introduced in the Doppler dimension of the inverse synthetic aperture radar (ISAR) image. These smeared features oftentimes overshadow the target geometrical features and hinder the proper interpretation of the ISAR image. In this paper, a technique is presented to remove such Doppler smear and produce a clear ISAR image of the target based on adaptive joint time-frequency processing (H. Ling, Y. Wang and V. Chen, SPIE AeroSense 97, 424-432, Orlando, FL, Apr. 1997). The technique entails adaptively searching for the linear chirp bases which best represent the time-frequency behavior of the signal. This is accomplished by projecting the signal onto all possible chirp bases and finding the one with the maximum projection value. After the optimal basis is found, the signal component associated with this basis is subtracted from the original signal. By iterating this search procedure, the signal can be fully parameterized with a set of chirp basis functions. Since the Doppler frequency due to the rotating component is both larger and more rapidly varying (in dwell time) than that from the target body, the signal components due to the fast rotating part are associated with those chirp bases having large displacement and slope parameters. On the other hand, the signal components due to the target body motion are represented by those chirp bases which have relatively small displacement and slope parameters. By sorting these chirp bases according to their slopes and displacements, the scattering due to the fast rotating part can be separated from that due to the target body. Consequently a cleaned ISAR image of the target body can be reconstructed by using only those bases associated with the body motion. Furthermore, if the pulse repetition rate of the radar is high enough, an image of the rotating part can also be constructed by removing the body interference. We shall present the results of applying this algorithm to both simulated data from the radar prediction code Xpatch and real measured ISAR data.

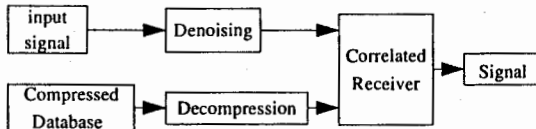
COMPRESSION AND DENOISING OF SCATTERING DATA IN UWB RADAR USING WAVELET TRANSFORM

B. Zhang*, S. Primak*, J. LoVetri*, S. Kashyap**

*Department of Electrical and Computer Engineering
The University of Western Ontario, London, Ontario, Canada N6A 5B9

**Defence Research Establishment Ottawa, 3701 Carling Ave.,
Ottawa, Ontario, Canada K1A 0Z4

Introduction. Electromagnetic Scattering from various objects and the subsequent ISAR imaging have been studied intensively in recent years. Some of these studies have been focused on the efficiency of storing collected wideband scattering data (E. J. Rothwell, K.M. Chen, D.P. Nyquist, J. E. Ross, R. Bebermeyer, IEEE Trans. AP, Vol. 42, # 7, pp. 1033-1037, 1994). Filtering of the measurement data in order to remove measurement noise, or *denoising*, has also attracted some attention. A great reduction in the required computer memory can be achieved and a better Signal-to-Noise Ratio (SNR) can be obtained with the simultaneous implementation of data compression and denoising. Various mathematical transforms exist which may achieve some results in either of these goals but the Wavelet Transform has many characteristics which make it useful for achieving both goals. Using the Wavelet Transform, the signal can be compressed considerably (compression ratio varies for scattering signals from different objects) while retaining the characteristics of the signal which are important for identification procedures. In this paper we investigate the performance of different compression and denoising schemes and their effects on target discrimination and ISAR imaging.



Method. The general approach is to analyze the signal using the Wavelet Transform technique, discard the decomposition coefficients with magnitude below a certain threshold and then synthesize a new signal using only the remaining coefficients. A number of targets have been investigated in this study, such as a PEC plate, sphere, and cylinder, for which the data is simulated using an FDTD code, and a rectangular cavity, for which the data is obtained from Ultra-wideband (2-18GHz) Radar measurements. Effects of using various different *mother* wavelets on the false discrimination using a correlation receiver and the quality of ISAR images obtained are also investigated in this research.

Time Domain Interferometric Radar Simulation for Urban Areas

Bijan Houshmand
Jet Propulsion Laboratory
California Institute of technology
4800 Oak Grove Drive
Pasadena, CA 91109-8099 U.S.A.
bh@athena.jpl.nasa.gov

Accurate modeling of the radar signal interaction with the urban environment is useful for interpretation of the interferometric measurements. In urban areas, the derived topography from the interferometric measurements is affected by multiple reflections, shadowing, geometrical structures, and penetrable surfaces. A geometrical optics based simulation for urban areas shows the general characteristics of the derived topography where shadowing and multiple reflections are present (B. Houshmand, Proceedings of URSI, Montreal, 1997). In this talk a time domain simulation is used to include the effects of the surface material property as well as geometry comparable to the signal wavelength. The interferometric simulation is carried out in two steps. First the forward scattering information is generated in the time domain for two observation locations. The second step is to invert the interferometric measurements to derive the topography. The forward scattering information is generated by the application of the Finite-Difference Time-Domain algorithm in combination with the Time-Domain Huygen's principle. A 2-D geometry is used for this simulation where the multiple scattering and shadowing effects are present. The forward scattering simulation produces the time-domain received signals at the observation locations. In order to derive the topography the received signals are compressed and coregistered to produce an interferometric phase. The interferometric phase is then related to the ground topography using the imaging geometry. In this talk, a number of examples are used to present the effects of complex geometry and material properties on the reconstructed topography. The simulation results will be compared with the interferometric measurements at C- and X- band.

METHOD OF NYQUIST INTERPOLATION OF RADAR IMAGE FOR ANTENNA RESOLUTION IMPROVEMENT

Grechka A.V. Moscow radioengineering institute of Russian Academy of Science.

Radar image reconstruction with high accuracy characteristics attracts a huge interest of specialists now. Special spectrum analysis methods are usually applied for solving this problem. Suggested linear method of Nyquist interpolation of radar image (MNIRI) belong to these methods group.

The basic MNIRI expressions are based on following statements. It is well known, that any image making system is described by expression

$$B(\xi) = \int G(\xi, x) \cdot A(x) dx, \quad (1)$$

were $A(x)$ and $B(\xi)$ - are real and restoring image accordingly; $G(\xi, x)$ - kernel of transform. For radar system it is antenna pattern. Image reconstruction problem consists in solving of integral equation (1). If we will find a equation (1) solution in the form of response on real object by virtual extended antenna, and apply Nyquist's sampling theorem for $A(x)$ and $B(\xi)$ presentation, than it is possible to transform integral equation (1) into linear system of equations

$$\frac{1}{p} \mathbf{S} \mathbf{E} = \mathbf{F}, \quad (2)$$

were \mathbf{S} - transform matrix; \mathbf{E} - reconstruction image vector; \mathbf{F} - primary image vector produced by initial antenna; p - virtual antenna extension value.

Equation (2) is a basic expression of MNIRI. The solution of this equation provides radar image reconstruction with improved characteristics. In particular, resolution ability improves and it is possible to resolve two close arranged targets, which have not been resolved by initial antenna. The result of MNIRI application is shown in Figure 1. Targets are marked in arrows.

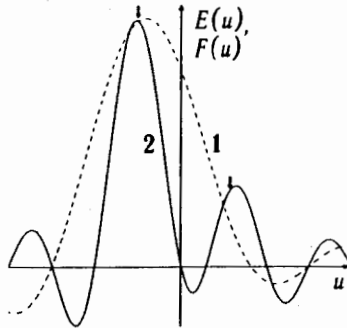


Figure 1. The result of MNIRI application. 1- $F(u)$; 2- $E(u)$.

Base radar characteristics research was made by computer simulation. For single target amplitude and angle definition accuracy are defined. Moreover, these characteristics are defined for resolve two close arranged targets situation. All obtained characteristics are compared with potential ability of radar measurement system (Kramer-Rao limits). Area of deviation of virtual antenna extension factor and signal/noise ratio, provided quite right tolerance of radar image reconstruction, are defined.

Obtained characteristics confirms the statement that MNIRI provides high targets parameters accuracy definition and radar image reconstruction with superresolution.

Numerical Methods for Transient Problems

S. P. Castillo and R. J. Luebbers

A Stability Analysis of the Path Integral Time-Domain Equations	28
<i>R. Nevels*, J. Miller, Texas A&M University, USA</i>	
The Path Integral Time-Domain Method: An Investigation of Numerical Dispersion	29
<i>J. Miller*, R. Nevels, Texas A&M University, USA</i>	
Stability Analysis of the Piecewise Linear Recursive Convolution Method in One and Three Dimensions.....	30
<i>D. F. Kelley*, R. J. Luebbers, Pennsylvania State University, USA</i>	
A Frequency-dependent PSTD Algorithm for General Dispersive Media.....	31
<i>Q. H. Liu*, G. Fan, New Mexico State University, USA</i>	
Analyses of Passive Optical Structures Based on the Fourier Pseudo-spectral Method	32
<i>Y. F. Leung*, C. H. Chan, City University of Hong Kong, Hong Kong, P. R. China</i>	
The Application of Meshless Methods to the Numerical Solution of Transient Electromagnetic Field Problems.....	33
<i>S. Buckles*, S. Castillo, New Mexico State University, USA</i>	
High Order, Finite Difference Procedure for the Temporally Dependent Maxwell's Equations	34
<i>J. F. Nystrom*, J. L. Young, University of Idaho, USA</i>	
Development of an Accurate FDTD Technique and its Applications.....	35
<i>A. Abdin*, A. Z. Elsherbeni, C. E. Smith, University of Mississippi, USA</i>	
Numerical Modeling of Printed Antennas and Circuits with Unstructured FVTD Method	36
<i>A. H. Mohammadian*, V. Shankar, W. F. Hall, C. Rowell, Rockwell International Science Center, USA</i>	
A Combined Finite-Element and Spectral Lanczos Decomposition Method for Efficient Analysis of Maxwell's Equations in Frequency and Time Domains.....	37
<i>M. Zunoubi*, J. Jin, W. C. Chew, University of Illinois, USA</i>	

A Stability Analysis of the Path Integral Time-Domain Equations

Robert Nevels* and Jeffrey Miller
Department of Electrical Engineering
Texas A&M University
College Station, TX 77843-3128

Here we will present a stability analysis and a stability condition for the path integral time-domain (PITD) method. The PITD method is a new electromagnetic field scattering technique based on a Feynman path integral formulation that gives a propagator solution to the time domain form of Maxwell's differential equations. The essence of the method is that the present time electric and magnetic field components are first Fourier transformed into the spectral domain and multiplied by a state transition matrix that accomplishes time stepping and then inverse transformed back to the spatial domain. Fourier transformation is a unitary operation and therefore is unconditionally stable. Since the product of unitary operators is also unitary, the operator here ($\bar{F}\bar{A}\bar{F}^{-1}$), which consist of forward and inverse Fourier transforms (F , F^1) and multiplication by the transition matrix (\bar{A}), is unitary if it can also be shown that the matrix \bar{A} is unitary.

In the theory of state variables it is well known that the eigenvalues of \bar{S} in the evolution operator $e^{\bar{S}t}$, which becomes the state transition matrix \bar{A} , are the poles of the transfer function. It can be shown that for the electromagnetic field in a lossless region these poles lie in symmetric pairs on the complex axis. The analytic operator \bar{A} is therefore said to be marginally stable. However, through roundoff error, the numerical operator \bar{A} can incur an instability that is manifest as numerical field amplitudes that gradually grow in time. This situation is remedied by adding a small amount of loss everywhere in the numerical scattering region. The eigenvalues of \bar{S} will then contain a small negative real part. The poles of the transfer function are thereby moved a short distance into the left half of the complex plane, thus preventing numerical instability in the computed fields.

Examples will be shown illustrating improved stability when a plane wave Gaussian pulse scatters from a dielectric slab. An advantage of the PITD technique is that it's stability in one, two or three dimensions does not depend upon the relationship between the time step τ and the spatial increment Δx as it does for example with the finite-difference time-domain method.

The Path Integral Time-Domain Method: An investigation of Numerical Dispersion

Jeffrey Miller* and Robert Nevels
Department of Electrical Engineering
Texas A&M University
College Station, TX 77843-3128

A new numerical method for electromagnetic scattering based on the path integral was presented at the 1997 AP-S/URSI conference (R. Nevels, J. Miller, and R. Miller, "The Path Integral Time-Domain Method: A New Numerical Method for Electromagnetic Scattering", AP-S/URSI International Symposium, Montreal, Canada, July 1997, p. 263). An unusual aspect of the path integral time-domain method is that the time steps can also be performed analytically for some boundary value problems. Examples include wave propagation in free space and scattering from a planar perfect conductor. Numerically, the Fourier transform is accomplished by a discrete Fourier transform, which is implemented as a Fast Fourier Transform. It is necessary to examine this discrete system to determine the numerical dispersion. In this paper we will present an analysis of the numerical dispersion of the path integral time-domain method.

An expression for dispersion is obtained by the following procedure:

- 1) The initial field is specified as a monochromatic plane wave. The resultant field is also specified as a monochromatic plane wave but advanced by one time step.
- 2) The path integral equations are then cast into a matrix equation form $\bar{P}f = 0$. The vector f contains all electric and magnetic field components and the matrix \bar{P} contains the forward and inverse Fourier transforms and the state transition matrix. The terms of the matrix \bar{P} are simplified by applying the convolution theorem to reduce the path integral expression to a single convolution in the spatial domain.
- 3) The determinant of \bar{P} is the dispersion relation.

Analytical and numerical dispersion results will be shown for 2-D line source excitation. The expression obtained by this analysis can be shown to give the free space dispersion relation in the limiting case where the spatial grid size $\Delta x \rightarrow 0$ and the time step size $\tau \rightarrow 0$.

STABILITY ANALYSIS OF THE PIECEWISE LINEAR RECURSIVE CONVOLUTION METHOD IN ONE AND THREE DIMENSIONS

David F. Kelley* and Raymond J. Luebbers
Electrical Engineering Department
The Pennsylvania State University
University Park, Pennsylvania 16802

The Piecewise Linear Recursive Convolution (PLRC) extension to the Finite Difference Time Domain (FDTD) method is an accurate and computationally efficient approach for the analysis of electromagnetic wave propagation through linear isotropic dispersive media. This paper presents a stability analysis of the PLRC method based on an approach described by Petropoulos in the January 1994 issue of the *IEEE Transactions on Antennas and Propagation*. The cases of propagation through both Debye and Lorentz media are considered.

The analysis approach involves the transformation of the FDTD field update equations into the Fourier domain. The independent solutions are expressed as products of an eigenvector, a scalar amplification factor, and a phase factor, and the system of transformed update equations is cast into the form of a matrix equation. The determinant of the matrix set equal to zero produces a polynomial whose roots are equal to the amplification factors corresponding to each independent solution. Each amplification factor is a function of frequency. The solution at a given frequency at time step n is proportional to the amplification factor evaluated at that frequency raised to the power n . Thus, if the amplification factor has a magnitude greater than unity at any frequency, the FDTD solution is unstable.

Evaluation of the determinant is not difficult for problems involving plane wave propagation in one dimension, since the matrix is only 3x3 in size for Debye problems and 4x4 for Lorentz problems. For problems involving propagation through Lorentz media in three dimensions, however, the resulting matrix is 12x12 in size. It will be shown that results obtained for 1-D problems can be applied to the 3-D case, avoiding the task of evaluating determinants of large matrices.

It will also be shown that the stability analysis approach cannot be applied to the PLRC method for Lorentz media in its original form, which makes use of complex-valued arithmetic. A new formulation for Lorentz media that avoids the use of complex quantities will be employed to permit the use of the analysis approach. Finally, though the presentation will focus on results for the total field formulation of the FDTD method, application to the scattered field formulation will also be considered.

A FREQUENCY-DEPENDENT PSTD ALGORITHM FOR GENERAL DISPERSIVE MEDIA

QING HUO LIU* AND GUO-XIN FAN

KLIPSCH SCHOOL OF ELECTRICAL AND COMPUTER ENGINEERING
NEW MEXICO STATE UNIVERSITY
LAS CRUCES, NM 88003

Email: qhliu@nmsu.edu

A three-dimensional pseudospectral time-domain (PSTD) algorithm is developed for general inhomogeneous, dispersive, lossy media. It is well known that in many applications such as those involving earth, biological materials, artificial dielectrics, and optical materials, the electromagnetic parameters of the medium are functions of frequency. This frequency dispersion property may significantly change the electromagnetic response in the medium, and hence has to be accurately modeled. Previously, significant efforts on simulations of transient electromagnetic waves have been made by utilizing the frequency-dependent finite-difference time-domain (FDTD) method. In this work, we extend the pseudospectral time-domain (PSTD) algorithm with perfectly matched layer (PML) absorbing boundary condition (ABC) to simulating waves in general dispersive media. In the PML formulation, the modified time-domain Maxwell's equations for dispersive media are expressed in terms of coordinate-stretching variables. With an arbitrary dispersive medium, the dispersion relation is modeled by a general form. The temporal convolution arising from the dispersion is approximated by the recursive convolution (RC) and the piecewise linear recursive convolution (PLRC). In contrast to the FDTD method, the PSTD algorithm uses the fast Fourier transform to calculate the spatial derivatives in Maxwell's equations. The wraparound effect due to the use of FFT is removed by the PML buffer zones. With this new PSTD algorithm for dispersive media, the number of unknowns can be reduced to the Nyquist limit, i.e., two cells per minimum wavelength, greatly increasing the scale of problems solvable on any given computers. The numerical results are validated by analytical solutions to several canonical problems, and by a frequency dispersive FDTD method. Applications to ground-penetrating radar and plasma will be demonstrated for large scale problems.

Analyses of Passive Optical Structures Based on the Fourier Pseudo-Spectral Method

Y. F. Leung* and C. H. Chan

Department of Electronic Engineering
City University of Hong Kong

83 Tat Chee Ave
Kowloon
Hong Kong

Abstract

Finite-difference time-domain (FDTD) method is one of the most popular electromagnetic analysis tools. This versatile method has been applied to a wide variety of problems such as active antennas, electronic packaging and dielectric waveguides, etc. However, it is not suitable for large-scale optical structures as 10 to 20 grid points per linear wavelength is required. The enormous memory requirement prohibits the use of FDTD for problems with large electrical size.

Recently, two competing schemes emerge to be potential candidates in alleviating the memory problem encountered by the FDTD method. Similar to FDTD, both schemes employ a leap-frog in time but only require 2 sample points per linear wavelength for accurate solutions. The first method is the wavelet-Galerkin method and the second one is the Fourier pseudo-spectral method. The wavelet-Galerkin method entails the use of scaling functions as basis function and testing functions in the time-domain integral equation formulation. Due to the multiresolution capability of the wavelets, the method provides excellent accuracy for a discretization close to the Nyquist limit. The second approach is the Fourier pseudo-spectral method which projects the spatial equation into Fourier space. The spatial derivatives in Maxwell's equations are performed analytically in the spectral domain. The only approximation is the use of FFT to convert the field quantities back into the spatial domain. Therefore, the spatial discretization in a homogeneous medium is only limited by the Nyquist rate. While both schemes alleviate the memory burden of the FDTD method, recent findings suggests that the pseudo-spectral method performs better than the wavelet-Galerkin method. For the wave-equation examples given in the literature, it was found that the spectral method was most efficient while the wavelet-Galerkin method requires less memory storage but more CPU time than the finite-difference method. Therefore, we adopt the use of Fourier pseudo-spectral method.

While the pseudo-spectral method may not suitable for other electromagnetic applications that deal with highly inhomogeneous structures, it is perfect for optical device structures that are electrically large but fairly homogeneous. In this paper, we will present our findings in using the Fourier pseudo-spectral method for the analyses of passive devices for optical applications.

THE APPLICATION OF MESHLESS METHODS TO THE NUMERICAL SOLUTION OF TRANSIENT ELECTROMAGNETIC FIELD PROBLEMS

Steffany Buckles and Steven Castillo
The Klipsch School of Electrical and Computer Engineering
New Mexico State University
Dept. 3-O, Box 30001
Las Cruces, NM 88003

Traditional finite-element, finite-difference, and method-of-moment integral equation solution methods have become the primary techniques for solving Maxwell's equations over the last thirty years. Each of these methods involves the use of a static grid over which some type of approximation for the unknown variables is applied. The combination of the grid "density" and approximation type has to be such that the resulting numerical solution is of sufficient accuracy. For transient electromagnetic problems, this forces the use of an extremely dense grid throughout the domain when in fact a high rate of sampling is required only in regions containing high field gradients. Recently, this has been addressed to some extent by the use of the MR/FDTD method (Johnson and Rahmat-Samii, 1997). However, the MR/FDTD method still uses a static grid which is not conducive for tracking a steep gradient that is traveling through the domain.

Gridless methods have been developed over the last twenty years by the computational fluid dynamics community. These techniques include Smooth Particle Hydrodynamics (SPH), moving least square approximations, and Element Free Galerkin (EFG) methods. Each of these methods is unconstrained by a background mesh for discretizing the domain of interest. The fields are approximated over a set of points which can be allowed to move through the domain in a pure Lagrangian (moving mesh) frame. The simplest of these methods is SPH which was developed by Lucy (1977), Gingold and Monaghan (1977) for astrophysical calculations. SPH uses kernel interpolation to compute gradients of field quantities eliminating the need for a background grid.

In this paper we examine the use of SPH for solving transient electromagnetic field problems. We demonstrate the use of SPH as an adaptive technique for efficiently "tracking" steep field gradients with a minimum number of unknowns. Particle splitting and merging will be used to improve the dynamic range that is inherent in the method. The resulting multiple spatial and time scales are treated using asynchronous time stepping. The method will be demonstrated for both one-dimensional and two-dimensional transient electromagnetic field problems.

HIGH-ORDER, FINITE-DIFFERENCE PROCEDURE FOR THE TEMPORALLY-DEPENDENT MAXWELL'S EQUATIONS

James F. Nystrom* and Jeffrey L. Young

Department of Electrical Engineering/MRC Institute

University of Idaho

Moscow, ID 83844-1023

The classic Finite-Difference, Time-Domain (FDTD) method is well known to be second-order accurate in both time and space. For electrically small problems, second-order accuracy suffices since phase error accumulation can be rendered negligible for sufficiently refined grids. For electrically large problems and relatively accurate solutions, a refined grid implies a prohibitive amount of memory and CPU time from the computational machine, especially for three-dimensional simulations.

To reduce memory and CPU requirements, we demonstrate that certain high-order schemes are viable methodologies for modeling transient electromagnetic phenomenon in conjunction with the electrically large problem. For example, in the context of finite-difference, nodally collocated solvers, a class of compact central numerical operators are considered for the approximation of the spatial derivative. These numerical operators are designed using recently developed k -space techniques in conjunction with classical system theory. To advance the equations in time, the four-stage Runge-Kutta integrator is invoked. The resulting fully discrete systems are conditionally stable with Courant numbers ranging between one and two. Due to the compact nature of the spatial numerical operator, the problem of boundary conditions near perfectly conducting boundaries is manageable via interpolation methods.

Comparisons between various time-domain solvers, including the popular Yee scheme, manifest the effects of Courant number and spatial grid size on the phase error. Moreover, the aforementioned procedure is substantiated with numerical data associated with wave propagation in one-dimensional and three-dimensional spaces. For example, the one-dimensional periodic domain and the one-dimensional cavity is contrived to demonstrate the schemes' stability and minimal error characteristics.

DEVELOPMENT OF AN ACCURATE FDTD TECHNIQUE AND ITS APPLICATIONS

A. Abdin,* Atef Z. Elsherbeni, and Charles E. Smith, E-mail address:atef@olemiss.edu, Electrical Eng. Dept., U. of Mississippi, Anderson Hall, Room # 314, University, MS 38677,

Abstract- In this paper, the total field formulation of the fourth order accurate FDTD scheme (4x4) in one, two and three dimensional space for lossy and lossless media is presented. The fundamental performance of this algorithm, which includes accuracy, memory requirements and dispersion, are presented and compared with Yee's second order accurate FDTD scheme (2x2) through several numerical experiments for different dimensional spaces. In a three dimensional space, the fourth order FDTD technique is used to compute the resonant frequencies of a rectangular cavity resonator with different discretizations in space, and the results are compared with that of the second order algorithm and the exact solution. The propagation of a plane wave with a Gaussian pulse waveform is also investigated in a free space medium and with the existence of a lossy or lossless dielectric slab or magnetic slab. The numerical results in this case for the (2x2) and the (4x4) orders are analyzed and compared with the second order in time and fourth order in space (2x4) technique. The modeling of planar microstrip circuits such as microstrip transmission lines and low-pass filters is also investigated with these FDTD schemes. The computed reflection and transmission parameters for a filter are compared with the available experimental data, and the results show good agreement. The soft voltage source and the matched load are modeled for the fourth order FDTD technique to excite and absorb the traveling wave that reaches the load or the source terminal. A similar analysis is performed for the one and two dimensional space.

This numerical analysis investigation shows that the fourth order scheme has higher accuracy and reduced computer resources as compared to the second order FDTD technique.

Numerical Modeling of Printed Antennas and Circuits With Unstructured FVTD Method

A. H. Mohammadian^{†*}, V. Shankar, W. F. Hall, and C. Rowell

Rockwell International Science Center

1049 Camino Dos Rios

Thousand Oaks, California 91360

†E-mail: ahm@rsc.rockwell.com

Electronic printed boards today often contain a mixture of analog and digital circuits carrying digital, analog and mixed signals. Whether these circuits are part of a communication system or perform control functions, the necessity for utilization of higher frequencies and signals with faster rise times poses a serious challenge to the quasi-static circuit theory approaches of the past to analyze and design these circuits. On the other hand, there is a need to integrate antennas with the supporting circuitry and analyze the resulting system simultaneously. Therefore, full wave numerical methods for solving Maxwell's equations that can model details of a circuit board are of interest to electronics industry.

In this paper, we first present a brief overview of our new unstructured explicit finite-volume time-domain (FVTD) solver for Maxwell's equations. This solver is based on a fourth-order Runge-Kutta integration scheme. Electric and magnetic field vectors in this scheme are collocated. Therefore, only a single grid has to be created. The grid is made of either tetrahedral or hexahedral cells. The algorithm also allows for a mix of the two types of cells, but at this point the computer code is limited to a single kind.

We have demonstrated the accuracy of this scheme in the area of radar cross section (RCS) computations for both canonical and real life objects, including a full fighter plane. The objective of the present research is to show its application to commercial electronics problems. Results for scattering parameters and radiation patterns of some candidate printed antennas for personal communication systems (PCS) and also scattering parameters for some circuit discontinuities will be shown.

A Combined Finite-Element and Spectral Lanczos Decomposition Method for Efficient Analysis of Maxwell's Equations in Frequency and Time Domains

Mohammad Zunoubi*, Jian-Ming Jin, and Weng Chow Chew

Center for Computational Electromagnetics
Department of Electrical and Computer Engineering
The University of Illinois at Urbana-Champaign
Urbana, IL 61801-2991

A popular method for the transient analysis of electromagnetic fields is the finite-difference time-domain (FDTD) technique. Despite its simplicity in programming and minimum book keeping requirements, the FDTD method, in its original form, involves the staircasing approximation when modeling arbitrary shaped objects. Hybrid FDTD schemes have been developed which eliminate such approximation by conforming to the surfaces of all boundaries in the solution region. Additionally, the FDTD method is an explicit scheme which is only conditionally stable. As an alternative approach to overcome the aforementioned difficulties, the time-domain finite-element methods (TD-FEM) have been introduced in recent years. The explicit TD-FEM schemes are conditionally stable with time steps equal to or smaller than those imposed in the FDTD method. The implicit TD-FEM techniques, although unconditionally stable, require the solution of a system of equations at each time step. As a result, for the implicit methods to be computationally efficient, the system of equations must be treated in an efficient manner.

Recently, Zunoubi *et al* (1997 *J. Electromagn. Waves Applicat.*, vol. 11, pp. 1389-1406, and 1997 *Proc. IEEE APS-URSI Symp.*, p. 39) have employed the spectral Lanczos decomposition method (SLDM) (1995 *Radio Science*, vol. 29, pp. 937-953) to analyze the axisymmetric and three-dimensional diffusion problems. It is illustrated that accurate results are obtained at many frequencies by performing the Lanczos process only at the smallest frequency of interest while evaluating the fields at the remaining frequencies in a negligible amount of extra computing time.

In the present work, we combine the finite-element method based on Whitney forms and the SLDM to solve Maxwell's equations, in their general form, in both frequency and time domains. First, the electromagnetic fields are evaluated in lossless media using a second-order differential equation. Second, we consider solution regions containing losses and employ the first order differential equations to solve for both the electric and magnetic fields. Finally, we illustrate the efficiency, validity, and effectiveness of our formulations by presenting numerical results of an air-filled and a lossy dielectric-loaded cavity.

**Special Session Domain Decomposition and Diakoptics for Efficient
Electromagnetic Computation**

A. C. Cangellaris and A. E. Ruehli

A Domain Decomposition Approach to Capacitance Calculation of Interconnect Structures.....	40
<i>V. Veremey*, R. Mittra, Pennsylvania State University, USA</i>	
Cloning Macro Elements for Efficient Finite Element Partitioning.....	41
<i>I. Bardi*, Z. Cendes, Ansoft Corporation, USA</i>	
The Advantages of Domain Decomposition for FEM	42
<i>R. Lee*, P. Sadayappan, Ohio State University, USA</i>	
Mesh Partitioning Methods for Efficient Parallel Solutions for Finite Element Methods.....	43
<i>S. D. Gedney*, U. Navsariwala, University of Kentucky, USA, C. T. Wolfe, Lexmark International, USA</i>	
Partitioning in Electromagnetics	44
<i>A. Ruehli*, IBM Research, USA, A. Cangellaris, University of Illinois, USA</i>	

A Domain Decomposition Approach to Capacitance Calculation of Interconnect Structures

Vladimir Veremey and Raj Mitra

Electromagnetic Communication Research Laboratory
Pennsylvania State University, 319 Electrical Engineering East
University Park, PA 16802-2705

e-mail: RIMECE@engr.psu.edu or vvv2@psu.edu

Simulation of realistic configurations of VLSI interconnect structures, comprised of multiple metal layers embedded in a stratified dielectric medium, can be very demanding in terms of the CPU memory and time requirements. This is true irrespective of the technique used for modeling these structures, including the boundary elements method, the PEEC technique, or Finite methods that utilize efficient iterative solvers for sparse matrices.

One approach to circumventing this problem is to employ a domain decomposition scheme, *i.e.*, a "divide and conquer" approach. In this method the original interconnect structure is subdivided into some manageable-size domains and the problem is solved iteratively in each of these subdomains. The principal difficulty in this approach is to find an efficient and reliable iterative algorithm that takes into account of the interaction between the elements of the VLSI interconnect located in various subdomains. The Finite methods appear to be better-suited for use in conjunction with iteration algorithms and have been employed in this work.

The various steps in the iteration algorithm based on the domain decomposition scheme are presented below:

1. Divide of the interconnect structure, and the computational domain into subdomains that have overlapping boundaries.
2. Solve for the potential function in the subdomain that contains the active line, *i.e.*, the principal subdomain, by using a suitable mesh truncation technique, *e.g.*, the Perfectly Matched Layer (PML).
3. Calculate the potential function in the neighboring subdomains using the values of the potential in the principal subdomain, obtained in the previous step, as initial boundary values.
4. Use the results of Step-3 to update the potentials at the boundary of the first subdomain.
5. Repeat Steps 2, 3 and 4 until the desired accuracy is achieved.

The above scheme has been applied to a multilayer interconnect structure and numerical results that illustrate the efficiency of the scheme are included in the paper.

Cloning Macro Elements for Efficient Finite Element Partitioning

I. Bardi and Z. Cendes
Ansoft Corporation
Four Station Square
Suite 660
Pittsburgh, PA 15219-1119

Partitioning and diakoptics have often been proposed as a solution method for complex electromagnetic problems. The idea is to break complex problems up into many smaller pieces, each one of which can be solved more easily than original large problem. However, difficulties arise in putting these pieces together. If one does not allow for detailed electromagnetic coupling, one is essentially reduced to circuit theory. If one allows detailed coupling, large dense matrices arise. It can be shown that the complete, rigorous process is actually much less efficient than solving the entire problem at once.

There exist, however, certain special cases where partitioning and diakoptics can be used with great efficiency. One such case is that of repetitive structures that are found in filters and phase array antennas. In the case of a repetitive structure, one can create the finite element matrix for one part of the repeated structure in isolation, and use substructuring to eliminate internal variables. The result is a *macro element* that may be used to represent the repeated part over and over again. This, by itself, would not lead to any efficiencies. However, by introducing the idea of cloning, great efficiency improvements are possible. Cloning is a variation of ballooning, invented by Silvester et. al. (Proc. IEE, 124, pp. 1267-1270, 1977) to model open region problems. In cloning, the macro element is first copied and then joined. The interior variables in this composite macro element are then eliminated; creating a new "two part macro element" that represents two of the repeated parts. This process is then iterated, combining the two-part macro element into a four-part macro element, and so on, until a large number of repeated parts are modeled by a single "super" macro element. The beauty of this process is that the size of the solution region grows geometrically while the computational requirements grow linearly. Great efficiencies are thus possible with highly repetitive structures.

This paper will present the basic procedures for creating macro elements and for their cloning. It will also demonstrate the procedures by application to microwave filters and phased array antennas.

THE ADVANTAGES OF DOMAIN DECOMPOSITION FOR FEM

R. Lee

ElectroScience Laboratory
Department of Electrical Engineering
The Ohio State University
1320 Kinnear Rd.
Columbus, Ohio 43212

P. Sadayappan

Department of Computer and Information Sciences
The Ohio State University
2015 Neil Ave.
Columbus, Ohio 43210

Solving electromagnetic problems involving large complex geometries with the finite element method (FEM) is very difficult. The large number of unknowns requires large amounts of computer memory for storage and powerful CPU's to perform the matrix solve. In addition, the associated grid may be so complex that the grid generator fails to produce a reasonably well-shaped grid.

Domain decomposition methods offer a possible way to reduce the computational costs as well as a means to alleviate the problems associated with grid generation. To illustrate our point, we consider a specific domain decomposition method, which we call the partitioning FEM (Y. S. Choi-Grogan, K. Eswar, P. Sadayappan, and R. Lee, *IEEE Trans. Antennas and Propagat.*, AP-44, pp. 1609-1616, Dec. 1996). In this method the computational domain is divided into subregions. Within each subregion, finite element solutions are generated independent of the other subregions. The solution within each subregion is then coupled together by a global matrix equation. On a single processor computer, it can be shown that this method requires a significantly smaller amount of memory than the traditional finite element method. For a parallel computer the partitioning method is even better. Because the finite element solution for each subregion is computed independently, the computation for each subregion can be done on separate processors without any need for interprocessor communication at this step. Thus, it is easier to implement onto a parallel computer than the traditional FEM. Furthermore, the parallel efficiency for the partitioning FEM is much higher than for the traditional FEM. For the partitioning FEM the grids for each subregion can be generated independently of the other subregions; therefore, the grid generation is greatly simplified. Also, the grid density in each subregion can be different which gives us better control for obtaining a more accurate solution.

Mesh Partitioning Methods for Efficient Parallel Solutions for Finite Element Methods

S. D. Gedney and U. Navsariwala
Department of Electrical Engineering
University of Kentucky
Lexington, KY 40506-0046
gedney@engr.uky.edu

C. T. Wolfe
Lexmark International
Lexington, KY 40511

Unstructured meshes are commonly used for the analysis of large-scale engineering problems by finite element methods and finite volume methods. Due to the increased resources of today's high performance parallel computers, very large practical problems can be analyzed successfully using these techniques. To enable efficient solutions to problems on distributed memory parallel computers, one must optimize the available resource, viz., load balance must be maintained throughout the computation, interprocessor communication must be minimized, synchronization should be avoided, and serial computation should be minimized. The challenge has been the development of parallel algorithms with such characteristics for the solution of large sparse systems.

Parallel finite element methods (FEM) are typically based on a spatial decomposition of the mesh, or a mesh partitioning. Subsequently, the mesh is broken up into contiguous subregions that are shared by common boundaries and possibly small overlapping regions. Typically, each subregion is mapped to a processor and a local FEM matrix is assembled completely in parallel. Operations involving each local submatrix are also done strictly in parallel as well. Then, the principal task of the spatial decomposition algorithm is to partition the unstructured grid into non-overlapping contiguous sub domains. The resulting decomposition should: 1) provide an optimal load balance, such that all processors have an equivalent number of floating-point operations and instructions to perform during each time-iteration, 2) minimize the number of edges and faces on the shared boundaries to minimize the amount of interprocessor communication, and 3) handle irregular and unstructured meshes automatically.

In this paper, we will present two parallel algorithms for analyzing time-dependent or frequency dependent finite-element problems. Specifically, a divide and conquer scheme based on a Conjugate Gradient method, and a hybrid iterative/direct method based on the finite-element tearing and interconnecting (FETI) scheme. It is shown that the FETI algorithm provides superior speed up as compared to the divide and conquer scheme. It also has a distinct advantage for the solution of frequency dependent FEM methods employing a perfectly matched layer material medium for mesh truncation. Secondly, in this paper, a survey of mesh partitioning techniques and the advantages and disadvantages of each will be discussed. In general, it has been found that the METIS algorithm (G. Karypis and V. Kumar, Technical Report TR 95-035, Dept. of C.S., Univ. Minn., 1995) is superior to most competitive techniques for the decomposition of three-dimensional unstructured meshes in terms of efficiency and quality of the partition.

Partitioning in Electromagnetics

Albert Ruehli[†] and Andreas Cangellaris^{††}

† IBM Research, T. J. Watson Research Center, Yorktown Heights, NY 10598

†† ECE Department, University of Illinois, Urbana-Champaign, IL 61801

The ideas of partitioning a systems into smaller entities has been applied in many different forms in several disciplines such as mathematics and engineering as well as electromagnetics (EM). Partitioning is know by various names in engineering and mathematics like diaoptics, splitting, domain decomposition, tearing or sub-dividing. In this paper we attempt to identify the use of partitioning in electromagnetics in a systematic way. The ever increasing size of EM problems necessitates the use of various techniques based on partitioning. Many of the parallel processing based algorithms employ partitioning in different forms. The opportunities for partitioned solutions are clearly increasing in the future with the rapid increase in workstation compute power to price performance and the increased availability of parallel processors.

Today, the various partitioning algorithms and techniques are not identified and characterized in a systematic way especially in EM. This may be due to the fact that they have different origins. Some of these techniques have been applied quite successfully especially for circuit problems and mathematical problems. In fact, partitioning has been applied to electrical machines more than fifty years ago by Kron. Various techniques in EM employ partitioning related approaches in approximate and other solutions. In this talk, we will identify such approaches and will point out other problems for which partitioning can be employed. The structure of the problem to be solved is of key importance to the applicability of a particular technique. For example a homogeneous problem consisting of a single domain with uniform properties needs to be solved much differently than a heterogeneous problem with multiple domains where each domain may have different properties. An important heterogeneous multi-domain example is an EM problem which is connected to a VLSI circuit. Most likely the best solution technique for such a heterogeneous problem will also be heterogeneous in nature. Domain decomposition has also been applied to heterogeneous problems with boundaries which are ideally suited for partitioning like apertures.

The challenges for partitioned solutions are very much problem dependent. Two of the issues are how a systems is best subdivided and what the optimal number of subsystems is. This is related to another question on how the boundary conditions are enforced between the subsystems. Numerous techniques can be applied both in the time and the frequency domain. Subsystem coupling may be unidirectional (one-way) or both ways. In time domain, iterative waveform techniques may be used like the *waveform relaxation* approach. Another issue is the best suitable formulation for a subsystem or subdomain. Solutions with mixed formulations are quite common especially for heterogeneous problems. Other aspects which are important are the best iterative or direct matrix solution especially if the overall solution approach involves a single, large domain only. Multiple domain problems may involve a domain or subsystem which is described in terms of an integral equation technique while the other domain is described by a differential technique like finite difference time domain (FDTD) or a finite element (FE) technique. To further complicate the problem, these domains or subsystems may be coupled to a circuit domain which is described by the modified nodal analysis (MNA) circuit formulation.

High Frequency Techniques

P. H. Pathak and G. Manara

UTD Prediction of Radiation-pattern Platform Effects on Fully Realistic Aircraft Models	46
<i>P. Hussar*, IIT Research Institute, USA, V. Oliker, Matis, Inc., USA</i>	
Enhancing a Cavity Backscatter Solution Obtained through a Geometrical Optics Aperture Integration Scheme: A Fuzzy Approach	47
<i>S. M. Khan*, Kansas State University, USA</i>	
Two Dimensional Ray Tracing Simulator for Radio Wave Propagation in Urban Areas with Arbitrary Building Shape and Terrain Profile	48
<i>D. Erricolo*, P. L. E. Uslenghi, University of Illinois at Chicago, USA</i>	
A TD-UTD for Transient Mutual Coupling Directly by Pulsed Antennas Placed on a Smooth Convex Surface	49
<i>H. Chou*, P. H. Pathak, Ohio State University, USA, P. Rousseau, Aerospace Corp., USA</i>	
Three Dimensional Numerical Diffraction Coefficients of Generic Conducting Wedges using FDTD	50
<i>V. Anantha*, Motorola Inc., USA, A. Taflove, Northwestern University, USA</i>	
Fast Gaussian Beam Analysis of Ellipsoidal Reflector Antennas	51
<i>H. Chou*, P. H. Pathak, Ohio State University, USA</i>	
Radiation Fields Excited by Incident Whispering Gallery Mode Over Concave-to-convex Boundary	52
<i>T. Ishihara*, K. Goto, S. Sayama, National Defense Academy, Japan</i>	
High-frequency Scattering at Edges in Thin Dielectric Slabs Loaded by Periodic Strip Gratings	53
<i>A. Armogida, G. Manara*, A. Monorchio, P. Nepa, University of Pisa, Italy</i>	
A Heuristic High-frequency Formulation for the Diffraction by Dielectric Screens	54
<i>M. Baroni*, F. Mioc, A. Toccafondi, R. Tiberio, University of Siena, Italy</i>	

UTD PREDICTION OF RADIATION-PATTERN PLATFORM EFFECTS ON FULLY REALISTIC AIRCRAFT MODELS

Paul Hussar[†]
IIT Research Institute
185 Admiral Cochrane Drive
Annapolis, MD 21401

Vladimir Oliker[†]
Matis, Inc.
1565 Adelia Place
Atlanta, GA 30329

Prediction of platform effects on antenna radiation patterns in the high-frequency regime has traditionally relied on two standard techniques, these being the Physical Theory of Diffraction (PTD) and the Uniform Geometrical Theory of Diffraction (UTD). A comparison of existing computer codes based on these two approaches indicates that their relative merits can be characterized as geometrical flexibility/faithfulness vs. accuracy in the shadow region (J. J. Kim and O. B. Kesler, 1997 North American Radio Science Meeting, July 13-18, 1997). Current PTD codes rely on realistic flat-faceted platform CAD models and provide a highly accurate lit-region representation, but are limited in their ability to represent the shadow region by virtue of their failure to include creeping-wave contributions. Existing UTD codes include the creeping-wave, but employ a simplified platform representation as an assortment of elementary shapes such as cylinders, ellipsoids, plates, etc. Recently, a novel approach that employs the UTD together with realistic flat-faceted aircraft CAD models was introduced to address the aircraft inter-antenna coupling problem (V. Oliker and P. Hussar, 1997 North American Radio Science Meeting, July 13-18, 1997). Here, this novel approach will be adapted to address the radiation-pattern platform-effects problem. A geometrical procedure that identifies UTD propagation paths linking a source point located in the vicinity of a single flat-faceted geometrical object of general shape with a field point at infinity will be described. The employment of paths thereby obtained, as well as associated geometrical data, to predict radiation-pattern platform effects computed in terms of UTD reflection, wedge-diffraction and surface-diffraction mechanisms will also be described.

[†] Order is alphabetical

Enhancing a cavity backscatter solution obtained through a Geometrical Optics Aperture Integration Scheme: A Fuzzy Approach

Dr. Saeed M. Khan
Electrical Engineering Technology
Kansas State University-Salina
Salina, KS 67401

Several techniques have been proposed for the numerical evaluation of backscattered fields from large arbitrarily shaped cavities, these include, the finite difference (time domain and frequency domain), the approximate modal technique, the ray tracing approach (geometrical optics aperture integration scheme or GO-AI) and other techniques that hybridize some of these same schemes. The ray tracing method, whether used by itself or in combination with another technique has always presented some advantages. Its ability to deal with arbitrary shapes and materials make it a robust choice for many backscattering problems (like jet inlets and antenna feeds). The GO-AI approach also has the disadvantage of not being very accurate. In the conventional geometrical optics ray tracing scheme the field incident on the cavity opening is collimated into tubes of equal cross section at the aperture and traced back to the aperture after bouncing it around inside the structure. The angle and cross section of the exiting tubes depend on the structure of the cavity. The ray tube neglects the effects of the diffraction centers and assumes that power is conserved inside the tube. Both of the previously mentioned assumptions are an attempt at reducing the complexity of the overall problem; this deliberately introduces uncertainty (leading to inaccuracies) into the scheme. This paper uses fuzzy logic to manage the aforementioned uncertainty.

In this approach the power inside the tubes are not considered to be conserved anymore and accommodation is made for dissipation based on exit angle and cavity structure. The results obtained by studying the backscattering of an offset bend using this fuzzy logic enhanced scheme are compared with the conventional GO-AI results and a more accurate baseline (using a hybrid modal technique). The gain or loss of accuracy is discussed as a function of field distribution inside the subapertures.

Two dimensional ray tracing simulator for radio wave propagation in urban areas with arbitrary building shape and terrain profile.

Danilo Erricolo, Piergiorgio L. E. Uslenghi

Department of EECS (M/C 154)

University of Illinois at Chicago

851 South Morgan Street, Chicago, IL, 60607, USA

Radio wave propagation in urban areas is a very important topic for wireless communications in general; however instead of a very well established theory there have been suggested many different approaches that apply to particular situations. Some researchers introduced two dimensional propagation simulators which modeled building obstacles in an urban environment as knife edges. This kind of approximation leads to inaccurate results, as it has been previously pointed out by the authors (Knife-edge versus double wedge modeling of buildings for ray tracing propagation methods in urban areas, National Radio Science Meeting, Boulder, Colorado, USA, 5-9 January 1998) who presented a two dimensional simulator where building profiles were modeled as having a rectangular shape. The terrain on which the buildings were built was assumed to be flat.

An improvement of the previous simulator that features both the capability of handling arbitrary shape buildings and hilly terrain profile is the purpose of this work. This means that each building has its own shape and that the spacing between two consecutive buildings and their heights are usually different. Wave propagation is studied using ray tracing methods with the assumptions that rays propagate from the transmitter to the receiver neglecting all backscatterings. No limitations are put on the transmitter and receiver height. Street canyon around either the transmitter or the receiver are considered since they might provide strong reflection contributions. Reflections are allowed to happen on any building surface or on the hilly terrain. Diffractions at the edges are calculated by the Uniform Theory of Diffraction. A proper algorithm that considers all the rays under the previous assumptions has been developed. From the point of view of the electric characterization of the buildings, each building wall is represented by its own value of surface impedance. The terrain profile is also allowed to have a surface impedance that is not the same everywhere.

A TD-UTD for Transient Mutual Coupling by Pulsed Antennas Placed Directly On a Smooth Convex Surface

Hsi-tseng Chou*, P.H. Pathak and P. Rousseau[†]

The Ohio State University ElectroScience Laboratory

1320 Kinnear Road, Columbus, Ohio 43212, USA

[†] Aerospace Corp., El Segundo, Calif., USA

A time domain (TD) version of the uniform geometrical theory of diffraction (UTD), or TD-UTD has been developed for analytically describing the transient electromagnetic scattering by a perfectly conducting arbitrary curved wedge, and an arbitrary smooth convex surface, respectively, when each of these is excited by an arbitrary time impulsive astigmatic waveform (P.R. Rousseau, Ph.D. dissertation, Dept. of Electrical Engineering, The Ohio State Univ., Columbus, Ohio, USA, 1995). More recently, a TD-UTD has been developed for describing the transient electromagnetic radiation by pulsed antennas placed directly on a smooth convex surface(H.T. Chou et al., 1997 Intl. IEEE AP-S and National URSI Radio Science Meeting, URSI digest pp. 293). In this paper, the TD-UTD is extended for analytically predicting the transient mutual coupling between elemental pulsed antennas located directly on a perfectly conducting arbitrary convex surface. Here, current moments associated with the elemental (point) antennas are assumed to behave as a step function in time. This TD-UTD solution, like the previous ones, has also been constructed from the corresponding frequency domain UTD solution (P.H. Pathak & N. Wang, IEEE Trans AP-29, no.6, pp. 911-922, Nov., 1981) by an application of the analytic time transform (ATT). An important advantage of the ATT is that it avoids some of the serious difficulties that result in the use of conventional Laplace/Fourier inversion techniques. Furthermore, the ATT allows one to essentially obtain a closed form (as opposed to numerical) convolution when the TD-UTD response to a realistic finite energy pulse excitation is to be obtained from the TD-UTD response to a time impulsive excitation; this is also a significant advantage which maintains the efficiency of the TD-UTD ray analysis. In addition, TD-UTD employs the same ray paths as in the UTD, and like the UTD it remains uniformly valid across the geometrical optics shadow boundary transition regions. The major analytical difficulty in the development of this TD-UTD solution for mutual coupling results from the presence of the mutual coupling type Fock integrals in the frequency domain UTD fields which are to be inverted into the TD via ATT. However, this difficulty has been overcome with the development of a relatively simple and efficient TD-UTD algorithm, in a manner somewhat analogous to that developed earlier for the TD-UTD solution for the scattering by a smooth convex surface mentioned above. It is noted that the Fock functions pertaining to the previous UTD solutions for scattering and radiation from smooth convex surfaces, respectively, are different from those of the Fock functions which describe the UTD mutual coupling on a convex surface and provide a uniform ray solution for this problem of interest. Some numerical results illustrating the utility of this TD-UTD solution will be presented. The TD-UTD analysis of more general conformal antennas on a convex body can be obtained via an appropriate superposition of the response to the elemental antennas.

THREE DIMENSIONAL NUMERICAL DIFFRACTION COEFFICIENTS OF GENERIC CONDUCTING WEDGES USING FDTD

Veeraraghavan Anantha
EMCID,
Cellular Infrastructure Group,
Motorola Inc.
Rolling Meadows, IL 60008

Allen Taflove
ECE Department
McCormick School of Engineering
Northwestern University
Evanston, IL 60208

Abstract

Classical theories such as the uniform geometrical theory of diffraction (UTD) utilize analytical expressions for diffraction coefficient for canonical problems such as the infinite perfectly conducting wedge. Although these theories predict the fields accurately in the far-field region for simple problems, it is difficult if not impossible to extend them to wedges composed of dielectric and imperfectly conducting materials. In previous work we presented a numerical approach to this problem using the finite difference time domain (FDTD) method and showed results for the scalar diffraction coefficients of 2-D infinite straight wedges with a 90° wedge angle for incident TM and TE polarization. In this paper we extend this numerical approach using the FDTD method to obtain the general 3-D dyadic diffraction coefficients which can in principle be used to analyze straight wedges of arbitrary shape and composition. In the matrix notation, the dyadic diffraction coefficient can be represented by a 2×2 matrix with two nonvanishing elements when the appropriate ray fixed coordinate system is chosen. The proposed numerical method exploits the temporal causality inherent in FDTD modeling to isolate the diffraction pulse of interest in the time domain. We present results of the dyadic diffraction coefficients in the near field of an infinite perfect electrical conductor (PEC) wedge with a 90° wedge angle illuminated by an arbitrary incident wave in 3-D. The observation points are chosen in the near field due to the large memory requirements of the 3-D FDTD code. We compare our near field FDTD results for the infinite PEC wedge to the well-known analytical solutions obtained using UTD at observation angles that are far away from the incident and reflected transition boundaries, since the near field diffraction coefficients obtained using the UTD theory is most accurate for these observation angles. The good agreement between the FDTD and UTD results indicates the validity of our numerical approach. The power of this approach using FDTD goes well beyond the simple problems dealt with in this paper. It can in principle be extended to calculate near and far field diffraction coefficients for a variety of shape and material discontinuities.

Fast Gaussian Beam Analysis of Ellipsoidal Reflector Antennas

Hsi-tseng Chou* and P.H. Pathak

The Ohio State University ElectroScience Laboratory
1320 Kinnear Road, Columbus, Ohio 43212, USA

Recently a novel Gaussian beam (GB) technique has been developed for the fast analysis of electrically large reflector antennas. In particular, this technique has been successfully employed in the analysis of the scattering (both near and far fields) from a large parabolic reflector illuminated by a single feed antenna(H.T. Chou, P.H. Pathak, G. Zogbi & R.J. Burkholder, 1996 Intl. IEEE AP-S and National URSI Meeting, Baltimore, Md., Vol. 2, AP-S Symp. Digest, pp. 886-889), and the synthesis of a planar feed array consisting of identical antenna elements which illuminates a parabolic reflector to produce a prescribed contoured beam (H.T. Chou, P.H. Pathak, R.J. Burkholder and L.C. Potter, 1997 Intl. IEEE AP-S and National URSI Meeting, Montreal, Canada, URSI Digest, pp. 59) as is often required in communication satellite antenna applications. This paper presents a further validity of the speed and accuracy of the GB method for the analysis of the radiation from a large ellipsoidal reflector. The GB method provides a rapid analysis of electrically large reflector antennas since it requires no time-consuming conventional physical optics (PO) numerical integration over the electrically large reflector surface as is commonly employed in reflector radiation pattern analysis. The advantage of this GB approach stems from the fact that the feed illumination is expanded in a discrete set of a relatively few rotationally symmetric electromagnetic GB's whose fields adequately simulate the radiation field of the feed (in amplitude, phase and polarization). Each GB launched from the feed undergoes reflection from the interior reflector surface as well as diffraction from the reflector edge. Since the expressions for reflected and diffracted fields for each incident GB are available in closed form, this GB analysis of the radiation fields of a large parabolic reflector are evaluated in a matter of a few seconds on a typical workstation; this is in contrast to several hours that are required in the conventional numerical PO integration on such a workstation. In the present analysis, the reflector surface in the neighborhood of the reflection point where the axis of the incident GB axis hits the ellipsoidal reflector surface is locally approximated by a quadratic surface. The closed form solution obtained previously for the scattering of an incident GB from a local quadratic (parabolic) surface is then employed to find the scattering from the actual ellipsoidal reflecting surface illuminated by the same incident GB. The total scattering from the ellipsoidal reflector illuminated by a feed antenna is then obtained by the superposition of the fields scattered by each of the incident GB's in the expansion for feed illumination of the surface. The present work shows that the GB method is not restricted to the analysis of parabolic reflectors alone, but it can also be used for other reflector shapes. It is noted that ellipsoidal surfaces are commonly employed in subreflector designs; also, an offset ellipsoidal main reflector offers an interesting and usefull possibility as an antenna for some ground penetrating radar (GPR) applications.

RADIATION FIELDS EXCITED BY INCIDENT WHISPERING GALLERY MODE OVER CONCAVE-TO-CONVEX BOUNDARY

T. Ishihara*, K. Goto and S. Sayama
Department of Electrical Engineering
National Defense Academy
Hashirimizu, Yokosuka, 239, Japan

Recently, the problems on the scattering cross section by a smooth concave-to-convex body with a concave dent on the part of a body in which the surface shape changes gradually from a convex shape to a concave shape become important. Pathak and Liang [IEEE, Trans. Antennas & Propag. Vol.38 (1990)] and Kempel et al. [IEEE, Trans. Antennas & Propag. Vol.41 (1993)] have used a physical optics (PO) approximation and derived the integral expressions for the scattered fields by a concave-to-convex boundary. By approximately evaluating the integrals, they have derived the asymptotic expressions for the scattered fields.

However, if there is an edge on the concave side of the concave-to-convex boundary, the whispering-gallery (WG) mode is excited in the concave region by the equivalent source by the edge. This WG mode propagates along the concave surface in the form of the field trapped near the concave boundary and is radiated as a beam-shaped field into the free space on the convex region. In the previous study, we investigated the analysis method for the radiation field in the case when the WG mode propagating from the concave side passed through the inflection point and was radiated into the space [K. Goto and T. Ishihara, Electronics and Communications in Japan, Scripta Technica, Inc., Vol.79 (1996)]. A uniform physical optics (UPO) solution has been derived for the radiation field near the caustic by means of the modal rays incident on the concave surface. On the other hand, the UTD solution has been used for the scattered field in the transition region near the shadow boundary appearing when the modal rays are incident on the convex part of the boundary.

In this research, we shall derive the Kirchhoff current on the concave-to-convex boundary using the WG mode on the concave side, the creeping wave on the convex side and the idea of the law of conservation of energy in the transition region near the inflection point. We obtain the radiation field in a wide range from the point near the inflection point to the far distance field by evaluating the Kirchhoff integral by means of various methods. Numerical comparisons with the reference solution reveal the validity and the utility of the present methods.

High-frequency scattering at edges in thin dielectric slabs loaded by periodic strip gratings

A. Armogida, G. Manara*, A. Monorchio, P. Nepa

Department of Information Engineering, University of Pisa,
Via Diotisalvi 2, I-56126 Pisa, Italy

Many theoretical developments have been done over the past several years to analyze the scattering from infinite periodic structures, which are widely utilized in microwave technology to realize frequency selective surfaces (FSS), polarizers, etc. In specific applications, suitable diffraction coefficients are needed to account for the finite dimensions of such structures.

The purpose of this communication is to provide a heuristic diffraction coefficient in the context of the Uniform Geometrical Theory of Diffraction (UTD) to describe the scattering by the edge of a thin dielectric half-plane, loaded by a periodic grating of metallic strips arbitrarily oriented with respect to the edge. The solution procedure is an extension of that proposed in (W.D. Burnside and K.W. Burgener, *IEEE Trans. Antennas Propagat.*, 31, pp. 104-110, 1983) for an isotropic homogeneous dielectric half-plane. First, suitable reflection and transmission coefficients are analytically determined by referring to the corresponding infinite periodic structure, illuminated at oblique incidence by an arbitrarily polarized plane wave. These coefficients are obtained by imposing equivalent boundary conditions at the planar surface containing the strips (R.R. DeLyser and E.F. Kuester, *J. Electromagnetic Waves and Appl.*, 5, pp. 1217-1236, 1991) and the continuity of the tangential components of the fields at the other slab surface. The accuracy of these coefficients as a function of geometrical and electrical parameters of the structure has been checked through comparisons against numerical results obtained by a mode matching technique. Then, the above reflection and transmission coefficients have been attached to the appropriate term out of the four in the standard UTD diffraction coefficient for the perfectly conducting half-plane, to enforce the continuity of the total field at all the shadow boundaries.

Samples of numerical results will be shown at the conference to demonstrate the effectiveness of the heuristic diffraction coefficients proposed and to discuss their limits of applicability.

A Heuristic High-Frequency Formulation for the Diffraction by Dielectric Screens

M. Baroni, F. Mioc, A. Toccafondi and R. Tiberio

*Dept. of Information Engineering, University of Siena,
Via Roma 56, 53100 Siena Italy,
E-mail: albertol@ing.unisi.it*

The Uniform Geometrical Theory of Diffraction (UTD) has been successfully applied to a variety of practical applications involving antennas operating in the presence of environmental structures. Most of the diffraction coefficients that have been developed within the framework of UTD, were obtained from exact solutions relevant to perfectly electric conducting (p.e.c.) canonical configurations. Therefore, they are found very accurate when dealing with diffraction phenomena arising from metallic bodies. However, there are several important practical applications that involve large complex dielectric structures. In these cases, the assumption of p.e.c. boundary conditions (b.c.) results in a lack of accuracy in predicting the actual electromagnetic field. A significant example is found in mobile and wireless communications when describing the electromagnetic propagation in urban and indoor environments. To this end, the high-frequency diffraction from dielectric screens is a useful canonical problem.

Rigorous solutions are available for the case of impenetrable wedges with impedance b.c., that have been developed by applying the method introduced by Maliuzhinets (Maliuzhinets, Sov. Phys. Dokl., 3, 752-755, 1958). However, they led to rather involved formulations that are applicable only to a limited number of canonical configurations; furthermore, they are not suited to treat edges in penetrable panels. Simple high-frequency formulations based on an approximate, heuristic solution are still desirable to provide useful tools to treat several applications, with a degree of accuracy which is satisfactory for most practical purposes. Among the various attempts to provide such tools, one of the most significant and successful contribution was given by Burnside et al. (W. D. Burnside, K. W. Burgener, IEEE Trans. Ant. Prop., 31, 1, 1983).

In this paper, a simple approximate high-frequency expressions of UTD diffraction coefficients for thin dielectric screens are presented. They are heuristically derived from the same background; however, here the formulation is obtained by conveniently modifying the relevant expressions from a Physical Optics approximation. Reciprocity is enforced also introducing an extended reflection coefficient, that was suggested by a suitable formulation of the Maliuzhinets solution. The final dyadic expression in the UTD ray fixed coordinate system rigorously satisfies reciprocity, exhibits the expected discontinuities at the shadow boundaries of the Geometrical Optics field, at the order $k^{-1/2}$ satisfies the b.c. and recovers the known expression for both p.e.c. and p.m.c b.c. Numerical results are presented and compared with the solution for an impedance screen and with Moment Method calculations for a finite dielectric slab. The extension of this solution to junctions between panels of different materials will be discussed during the oral presentation.

Antenna Arrays: Theory and Design

S. R. Rengarajan and J. M. Johnson

Mutual Coupling Between Dielectric-covered Slots	56
<i>F. Nima*, Sensor Systems, USA, S. R. Rengarajan, California State University, USA</i>	
Theoretical Prediction of Frequency Performance Enhancement of Resonant Slotted Waveguide Arrays using Subarrays	57
<i>J. Coetze*, National University of Singapore, Singapore, J. Joubert, University of Pretoria, South Africa</i>	
Genetic Algorithm Optimization in the Design of Slot Arrays	58
<i>S. R. Rengarajan*, California State University, USA</i>	
A Comparison of Fitness Based Selection Operators in Genetic Algorithm Optimization of Arrays	59
<i>J. M. Johnson*, Y. Rahmat-Samii, UCLA, USA</i>	
Lightweight Phased Array Antenna	60
<i>P. K. Kelly*, Ball Aerospace & Technologies Corp., USA, L. Diaz, University of Colorado, USA</i>	
A Parameter Study of the Circularly Symmetric Electronically Scanned Array	61
<i>J. M. Stamm*, J. S. Avestas, Naval Air Warfare Center, USA, J. K. Breakall, Pennsylvania State University, USA</i>	
Applications of MoM and Adaptive FEM Modeling for Printed Array Antennas	62
<i>R. G. Schmier*, E. W. Lucas, T. P. Fontana, Northrop Grumman Corporation, USA</i>	
The Method of Fast Diagnostics and Adaptation of Phased Antenna Arrays	63
<i>Y. S. Shifrin*, Kharkov State University of Radioelectronics, Ukraine, U. R. Liepin, Kharkov Military University, Ukraine</i>	
Reduction of the Pattern Deterioration Produced by the Amplitude and Phase Quantization Error in the Synthesis for Circular Arrays	64
<i>R. Vescovo*, Universita di Trieste, Italy</i>	

Mutual Coupling Between Dielectric-Covered Slots

Fayez Nima*
Sensor Systems
Chatsworth, CA 91311

Sembiam R. Rengarajan
California State University
Northridge, CA 91330-8346
srengarajan@csun.edu

Accurate computation of external mutual coupling is important in the analysis and synthesis of waveguide-fed slot arrays. A number of papers in the literature have addressed the problem of evaluating the mutual coupling between radiating slots cut in rectangular waveguides and radiating into different exterior regions such as half space and baffles. In many practical applications, planar slot arrays contain a protective dielectric cover. There is a need to study the problem of mutual coupling between radiating slots with a dielectric cover. To the best of our knowledge this has been discussed only by Rexberg (Ph.D. Dissertation, Chalmers University of Technology, Sweden, 1988). However, Rexberg provided only limited data on mutual admittance between slots with a dielectric cover, for spacing up to about 1.5 wavelengths in the E-plane. The objective of this paper is to present the results of a systematic investigation of mutual coupling between dielectric-covered slots for spacing in the E-plane, H-plane, and the diagonal plane for different values of the dielectric constant and thickness. Coupling effects have been studied over a longer range of spacing.

We used the spectral domain technique in a manner similar to that of Rexberg. In the computation of the mutual coupling expression, in order to avoid the singularities corresponding to the surface wave poles, we used a deformation of the integration contour in the spectral domain. An efficient technique for calculating the integrals involving highly oscillating functions was employed by the use of the method of weighted averaging (Mosig and Gardiol, *Advances in Electronics and Electron Phys.*, Ch. 6, pp. 195-199, Academic Press, NY 1969). This method is found to be very useful especially for larger values of the spacing between slots. Our results have been validated by comparing them to similar data given in Rexberg's dissertation and the results obtained by other techniques for the special case of no dielectric cover. Numerical results on the mutual coupling will be presented over a wide range of slot spacing in different planes, for a number of values of dielectric thickness and dielectric constant. These results will be useful in the analysis and synthesis of slot arrays containing a dielectric cover.

**Theoretical prediction of frequency performance enhancement
of resonant slotted waveguide arrays using subarrays**

J.C. Coetzee*

Department of Electrical Engineering, National University of Singapore,
Kent Ridge Crescent, Singapore 119260

J. Joubert

Department Electrical & Electronic Engineering, University of Pretoria,
Pretoria 0002, South Africa

Slotted waveguide arrays suffer from severe bandwidth limitations, and useable bandwidths of only a few percent are usually the norm. The reasons for off-centre frequency performance degradation are twofold. The first is the frequency dependence of slot properties, which influences the excitation of the individual radiators. The second reason is the fact that frequency variations cause the peaks of the standing wave to move significantly from the slot locations, resulting in phase differences in the slot fields.

Various efforts have been made to reduce these effects. Techniques to improve the bandwidth of individual radiators include the use of wider slots and special slot geometries, e.g. the so-called dumbbell slots. It has been found though that the phase variations caused by the shifting of the standing wave patterns are the dominant cause of array performance deterioration. This effect becomes more prevalent as the number of slots per waveguide section increases. A widely used method to limit this effect is thus to reduce the number of slots in waveguide sections through the use of subarrays. Guidelines for the expected bandwidth improvements that may be obtained by limiting the number of slots in any waveguide section have been published. However, this data is only approximate and does not take specific array geometries into consideration.

An amended analysis technique, which is based on the procedure proposed by Hamadallah (*IEEE Trans. Antennas Propagat.*, 37, 817-823, 1989) but which includes the effects of higher order internal coupling between slots and the frequency dependence of the waveguide feeds, has been developed. This analysis procedure will be used to assess the advantages of subarraying by applying it to some illustrative case studies.

Genetic Algorithm Optimization in the Design of Slot Arrays

Sembiam R. Rengarajan
California State University
Northridge, CA 91330-8346
srengarajan@csun.edu

Waveguide-fed slot arrays have been used widely in radar and communication applications. Elliott developed a popular technique for the design of linear and planar slot arrays (R. S. Elliott, IEEE Trans. Antennas and Propagat., vol. 31, pp. 48-53, Jan. 1983). Elliott's equations have been rearranged for the purpose of the analysis of a linear array (M. Hamadallah, IEEE Trans. Antennas and Propagat., vol. 37, pp. 817-823, Jul. 1989). Slot arrays have a limited bandwidth because of the resonant nature of each radiating element and the array effects, especially for a standing wave type array. Because of this generally slot arrays are designed to have the optimum performance at the center frequency of the operating band. Consequently the array suffers performance degradation at the band edges.

The objective of this paper is to study the optimization of the slot array antenna performance at a number of frequencies in the operating band. In order to accomplish this we first extended the analysis procedure given by Hamadallah for a linear array to include the case of a planar array consisting of coupling slots between the feed waveguide and each radiating waveguide. We used the genetic algorithm (GA) optimization technique (Goldberg, *Genetic Algorithms*, Addison Wesley, 1989) for this purpose. We investigated the design of a planar array containing a number of sub-arrays. GA optimization was studied first for the design of an isolated sub-array. Later investigation included an infinite array of sub-arrays wherein Floquet mode analysis was used for mutual coupling between elements of various sub-arrays. The parameters that were optimized in our study include the gain of the array and the return loss at a number of frequencies. A method of incorporating the effects of higher-order mode coupling between the coupling slot and a pair of radiating slots in each coupling junction will also be discussed. Some numerical examples will be presented at the symposium.

A Comparison of Fitness Based Selection Operators in Genetic Algorithm Optimization of Arrays

J. Michael Johnson* and Yahya Rahmat-Samii[†]

Department of Electrical Engineering

University of California, Los Angeles

405 Hilgard Ave

Los Angeles, CA 90095-1594

*johnson@ee.ucla.edu, [†]rahmat@ee.ucla.edu

Genetic algorithms (GAs) are flexible, robust, stochastic based search and optimization methods that can handle the common characteristics of a wide variety of electromagnetic optimization problems that are not readily handled by other traditional optimization methods. Owing mainly to their flexibility and robustness, Genetic Algorithms have been shown to be effective in designing antenna arrays, microwave absorbers, and various patch and wire antennas. Effective application of GA optimization to a given problem requires choosing among various GA implementations. Specifically, although the selection operator is a key part of any GA implementation, relative merits and effectiveness of the various types of selection are often not discussed.

The selection operator in GA introduces the influence of the fitness function to the GA optimization process. To do this, selection should be based on a measure of the "goodness" of an individual. However, selection cannot be based solely on choosing the best individual because the best individual may not be close to the optimal solution. Instead, some chance that relatively unfit individuals are selected must be preserved to ensure that genes carried by these unfit individuals are not "lost" prematurely from the population. Among the commonly reported and used selection operators are deterministic ranking, proportionate selection, tournament selection and random selection.

In deterministic selection, also sometimes called population decimation, the individuals are ranked based on their fitness and those with fitness below an arbitrary value are discarded. The remaining individuals are then usually selected randomly from the remaining members of the population. In proportionate selection, also called roulette wheel selection, a probability of selection is assigned to each member of the population based on the relative fitness of the individual. More fit individuals have a better chance of being selected than less fit individuals. Tournament selection involves the choosing a sub-population of N individuals from the population followed by designating the best or most fit individual from the sub-population to becomes the selected individual. The means for choosing the members of the sub-population may be random or may, in-turn, involve a selection operator such as proportionate selection.

The relative performance of these selection schemes described above are compared with respect to the optimization of an array design. Algorithms are compared as well as the average convergence rates and quality of solution when applied to an array design.

Lightweight Phased Array Antenna

P. Keith Kelly*, Leo Diaz
P.O. Box 1538
Broomfield, CO 80038-1538

A unique phased array antenna concept is presented which lends itself to lightweight applications. The array consists of pillbox-fed line source elements arrayed in one dimension, each producing multiple beams in the other dimension for 2-D scan. The pillbox elements consist of array-fed parabolic reflectors constrained in parallel-plate regions fed with a multi-element feed array. The design is capable of low-sidelobe operation and can be made deployable. The pillbox elements produce linear polarization that can be rotated by a twist polarizer or converted with an active lens.

A seven element (63 by 4 inch aperture) phased array was constructed to demonstrate the viability of this approach at X-band. The goal was to prove out the lightweight construction techniques and materials, as well as, to demonstrate good azimuth scanning performance. The antenna has 16 elevation beams covering +/-7.5 degrees of scan centered at boresight. Measured data will be presented showing the azimuth scan performance out to 60 degrees. Measured data will also be presented using a twist polarizer to convert the polarization to vertical.

A PARAMETER STUDY OF THE CIRCULARLY SYMMETRIC ELECTRONICALLY SCANNED ARRAY

James M. Stamm*,†, John S. Avestas†, and James K. Breakall‡

†RF Sensors Branch, Naval Air Warfare Center, Aircraft Division, Patuxent River, MD

‡Pennsylvania State University, Department of Electrical Engineering, University Park, PA

ABSTRACT

Within the last decade, interest in the circular electronically scanned array has grown substantially. For applications where 360° coverage is required, the circular array carries with it a number of benefits: the elimination of mechanical rotation, increased beam agility, the ability to form simultaneous opposing beams, and the reduction in complexity afforded by the symmetry of the configuration. These advantages have led the military to investigate the utility of the circular array for surveillance, communication, and other functions.

In this survey, we perform an analytical and numerical study of the effect of several parameters which affect the array performance; specifically, the antenna diameter, the number of elements, and the element beamwidth. To do so, we consider a circularly symmetric antenna which lies in the horizontal plane, using a number of side-by-side endfire columns (each treated as a unit element) arranged in a ring. A mathematical element pattern is proposed whose beamwidth can be varied with a single parameter. Each column is assigned a phase center removed some distance from the center, and has an associated in-array (embedded) azimuth beamwidth. Eighteen combinations of array size, number of columns, and embedded element beamwidths are studied, and a comparative summary of available gains, beamwidths, and sidelobe/backlobe levels is presented.

Results are given for three types of excitations: 1) a uniform-amplitude excitation with the number of driven columns selected for maximum gain, 2) various low-sidelobe patterns arrived at through a least-squares derived taper, and 3) a globally optimized gain (greater than uniform) obtained using a technique employing Lagrange multipliers. Finally, the pattern sensitivity with respect to small changes in the excitation is examined for each beamwidth, and some comments are made regarding the use of active versus passive endfire arrays.

Applications of MOM and Adaptive FEM Modeling for Printed Array Antennas

Authors: Robert G. Schmier*, Eric W. Lucas, Thomas P. Fontana,
Northrop Grumman Corporation, ESSD, Antenna Department,
Baltimore, MD 21203

Jin-Fa Lee
ECE Department, Worcester Polytechnic Institute
Worcester, MA 01609

Large, doubly periodic arrays are important devices in modern antenna technology both for phased-array radars as well as frequency-selective surfaces. Accurate electromagnetic simulations make the design of these complex devices quite practical for experienced antenna engineers. The idealized infinite periodic array model has proven to be an accurate and useful formulation for most large, real-world planar arrays, while simplifying the computational requirements significantly.

The periodic MOM has been the method of choice for modeling printed array structures. This method requires a highly analytically-based formulation and is known to provide accurate results when sufficiently discretized. Another particularly general and more numerically-based formulation is a combination of the vector finite element method along with some form of periodic MOM or transfinite element method. However, an accurate FEM solution requires an accurate mesh necessitating effective adaptive meshing techniques. This is particularly true for printed arrays which are formed from thin conducting patterns embedded in stratified dielectric media. The dielectric layers are often quite thin with thicknesses perhaps less than $1/100^{\text{th}}$ of the array grid dimensions. Having both MOM and FEM modeling methods for cross-validation results in great confidence for the design's integrity. This provides significant peace of mind during the full array fabrication process. Historically, however, these patch-like arrays have been problematic for 3D FEM methods, even for most of the available adaptive strategies.

In this presentation, we will briefly highlight our formulation and focus some numerical examples on printed patch arrays. We have observed excellent agreement between our periodic MOM and adaptive FEM implementations and thus have achieved several promising cross-validations. We have found our techniques to be robust and efficient.

THE METHOD OF FAST DIAGNOSTICS AND ADAPTATION OF PHASED ANTENNA ARRAYS

Y. S. Shifrin*, U.R. Liepin

*Kharkov State University of Radioelectronics, Ukraine,
Kharkov Military University, Ukraine

In the report a new method of fast diagnostics and adaptation of phased antenna arrays (PAA) to different random factors destabilizing their functioning is considered. The purpose of adaptation is the restoration of initial (undisturbed) amplitude-phase distribution (APD) in the array by the repairing (using electrical methods) of faulty array channels or their replacement. When such complete adaptation of the array is impossible, the adaptive synthesis problem of remained serviceable part of the array (APD in this part) is solving from this or that index of its quality. The method of diagnostics treated in the report is phaseless, basing on power measurement on the array output (receiving PAA) or on the output of control probe located in the far or Fresnel zone of the array (transmitting PAA). Received or radiated by the array power is considered as an index (function) of the array quality. Quality function maximum search is realized by the fast multidimensional algorithm of Newton. Distinctive peculiarities of the proposed method are following:

a) APD in the antenna array is represented by Fourier's series on the basis of Walsh's functions. The direct Fourier-Walsh discrete transform of APD is realized by regular phase shifters (PS) of the array, the inverse one - by the special processor. Representation of APD by a series of Walsh permits:

- to remove restrictions on number of channels in the array N. When using the trigonometric basis, the PS smallest digit is equal to $2\pi/N$. With large N the demands to PS size appear to be impracticable;

- to exclude inherent for Newton's algorithm the necessity of computing

at each step of the iterative process of the second-order derivatives of quality function and inversion of formed from these derivatives matrix; to reduce the volume of other calculations;

b) when searching a quality function extremum, feedback covers at once the whole process of APD calculation. When calculating by other phaseless methods, usually at the beginning the APD spectrum is found and then APD is computed. The latter operation is accompanied by additional unchecked

errors what leads to degradation of the APD diagnostics quality. Specified peculiarities of the proposed method, in addition to short time of diagnostics, also provides its high accuracy and uniqueness, as well as suitability of the method at arbitrary number of the array channels. In the report algorithms of transmitting and receiving array diagnostics are analyzed apart; estimation of necessary time for diagnostics is given. The proposed method has been tested by simulation. Its results have confirmed the high efficiency of the method, which enables to rather quickly restore the artificially distorted APD almost completely. The curves illustrating high quality of restored APD for different classes of initial APD and different types of their distortion are given. In conclusion of the report the application possibilities of the proposed method of phaseless diagnostics and adaptation of PAA at choice of other functions of quality are discussed, as well as specific character of the partially serviceable array synthesis problem solving.

REDUCTION OF THE PATTERN DETERIORATION PRODUCED BY THE AMPLITUDE AND PHASE QUANTIZATION ERROR IN THE SYNTHESIS FOR CIRCULAR ARRAYS

Roberto Vescovo

Dipartimento di Elettrotecnica Elettronica ed Informatica

Università di Trieste

Via A. Valerio, 10 - 34127 Trieste - Italy

A classical problem of pattern synthesis for antenna arrays is to compute the element excitations that produce an array pattern approximating a desired radiation pattern. Several synthesis techniques are available in the literature to solve this problem. However, once the optimal excitations have been computed, they are often quantized to form the array pattern. This produces a quantization error, and therefore a pattern deterioration. We propose a technique to reduce such pattern deterioration, with reference to a problem of pattern synthesis for a circular array of N equally spaced elements. Given a desired radiation pattern $F_0(\phi)$ in the plane of the array, where ϕ is the azimuth angle, the problem consists in finding the excitation vector $a = [a_1, \dots, a_N]$ (where a_1, \dots, a_N are the complex excitations of the array elements) that minimizes the mean-square distance $\rho(a) = \|P(a) - F_0\|$ between the corresponding array pattern $P(a)(\phi)$ and $F_0(\phi)$. A closed form solution to this problem was presented in (R. Vescovo, IEEE Trans. on Antennas and Propagat., 43, 1405-1410, 1995) assuming the absence of the quantization error. Here, we assume that both an amplitude and a phase quantization is introduced to form the array pattern. The amplitude quantization levels are assumed to be A_1, \dots, A_L , and the phase quantization levels are assumed to be Φ_1, \dots, Φ_M . In order to reduce the pattern deterioration produced by the quantization error, we transform the problem by introducing the excitation constraints $a_n \in D_n$ ($n = 1, \dots, N$), where the sets D_n are defined as $D_n = Q_A \leftrightarrow Q_P$, where

$$Q_A = \{z: |z| \in \{A_1, \dots, A_L\}, z \in C\}, \quad Q_P = \{z: \arg(z) \in \{\Phi_1, \dots, \Phi_M\}, z \in C\},$$

where C denotes the set of the complex numbers.

This approach leads to solve the following constrained problem: find the excitation vector $a_e = [a_{e1}, \dots, a_{eN}]$ that minimizes $\rho(a) = \|P(a) - F_0\|$ subject to the excitation constraints $a_n \in D_n$ ($n = 1, \dots, N$).

This problem can be solved using the iterative technique presented in (R. Vescovo, IEEE Trans. on Antennas and Propagat., 43, 1405-1410, 1995). This technique refers to arbitrary constraint sets D_n , and produces a sequence of excitation vectors $\{x_0, x_1, \dots, x_n, \dots\}$, where: x_0 is the excitation vector solving

FDTD Methods

Quantification of Induced EM Fields in a Material Sample in an EM Cavity using FD-TD Method	66
<i>Y. Kan*, K. M. Chen, Michigan State University, USA</i>	
Comparison of the FDTD Method with a New Complex-envelope FDTD Method for the Solution of the Two-dimensional Bandpass-limited Vector Wave Equation	67
<i>J. D. Pursel*, P. M. Goggans, University of Mississippi, USA</i>	
Accuracy of the Complex-envelope FDTD Method	68
<i>J. D. Pursel*, P. M. Goggans, University of Mississippi, USA</i>	
FDTD Computation of Resonant Frequencies for a Cavity Filled with a Collisional Magnetized Plasma	69
<i>G. Marrocco*, L. Tirone, F. Bardati, Università Roma Tor Vergata, Italy, F. D. Marco, ENEA-Frascati, Italy</i>	
Modeling Vibrating Boundaries with the Finite-Difference Time-Domain Method	70
<i>S. Lee*, W. R. Scott, Jr., Georgia Institute of Technology, USA</i>	
Analysis of Truncated Periodic Structures using the FDTD	71
<i>R. Mittra*, V. Bulkin, Penn State University, USA</i>	
Artifacts at Material Boundaries of Lossy Dielectric Bodies in FDTD Simulations	72
<i>M. Burkhardt*, N. Kuster, Swiss Federal Institute of Technology, Switzerland</i>	
Simulation of Wire Antennas Non-conformally Oriented to the FDTD Grid	73
<i>N. Chavannes*, M. Burkhardt, N. Kuster, Swiss Federal Institute of Technology (ETH), Switzerland</i>	
Study of the Effect of the Meshing by Blocks in the Finite Difference - Time Domain Method	74
<i>A. E. Ros*, Laboratoire d'Electronique et Systèmes de Télécommunications, France</i>	
Modeling Nonlinear Devices in FD-TD: the Equivalent Source Method	75
<i>J. Mix*, J. Dixon, Z. Popovic, M. Piket-May, University of Colorado, USA</i>	

Quantification of Induced EM Fields in a Material Sample in an EM Cavity Using FD-TD Method

Yao-Chiang Kan* and K. M. Chen

Department of Electrical Engineering

Michigan State University

East Lansing, MI 48824

Tel:(517)355-6502, Fax:(517)353-1980

E-mail: kan@egr.msu.edu

In the study of the interaction of microwave radiation with non-ionic materials, a material sample is placed in a cylindrical EM cavity which is excited with a fundamental cavity mode. A Finite-Difference Time-Domain (FDTD) method for solving Maxwell's equations in rotationally symmetric geometries is employed to quantify the electric field inside the material sample induced by the cavity mode.

The cylindrical cavities with perfect electrically conducting (PEC) boundary and finite electrically conducting (FEC) boundary are studied in this paper. The FDTD formulation of Maxwell's equations in cylindrical coordinates is first constructed. Blackman-Harris (BH) function is used to produce the excitation source in the cylindrical PEC cavity calculation since the sidelobe of BH function is approximately -92 dB. The excitation probe was assumed to be located at a point on the cylindrical wall. The TM_z , TE_z , and TE_{111} modes of an empty cylindrical PEC cavity are calculated and compared to the analytical solution where z denotes $0x$ and x varies from 1 to 4. The field distributions of TM_{012} and TE_{111} modes in a cylindrical PEC cavity loaded by a small disk of polymer are then calculated. The results are compared with corresponding theoretical predictions. In the cylindrical FEC cavity calculation, the periodic impulse source is used. The field distributions of TM_{012} and TE_{111} modes of an empty cylindrical FEC cavity and that of a cylindrical FEC cavity loaded by a small disk of polymer are calculated. In these calculation, uniform and non-uniform partitioning schemes were used.

After the induced electric field inside the material sample is accurately quantified, the dissipated power density inside the material sample is calculated. This dissipated power density acts as the heating source to raise the temperature of the material sample.

Comparison of the FDTD Method with a New Complex-Envelope FDTD Method for the Solution of the Two-Dimensional Bandpass-Limited Vector Wave Equation

J. D. Pursel* & P. M. Goggans
University of Mississippi
Electrical Engineering
University, MS 38677

Abstract

The majority of systems that make use of the electromagnetic spectrum do not use the entire spectrum. Instead, most systems make use of a band of frequencies that surround some center frequency. These systems are usually referred to as bandpass-limited (BPL) systems. A large number of researchers are currently using the finite-difference time-domain (FDTD) method to analyze and design BPL systems. However, the standard FDTD method uses lowpass-limited (LPL) field quantities and is therefore, a LPL method. Unfortunately, this means that a considerable amount of computational time is wasted on the computation of the response due to frequencies that are outside the bandwidth of interest.

The complex-envelope (CE) representation of BPL signals/systems (Simon S. Haykin, *Communication Systems*, 2nd ed., John Wiley & Sons Inc., 1983) is used to convert a BPL signal/system to a LPL one. Consider a BPL signal as a function of time, $a(t)$, whose frequency spectrum is centered about some frequency, f_0 . The LPL CE representation, $\tilde{a}(t)$, of the BPL signal, $a(t)$, is related to the original signal through the following transformation:

$$a(t) = \Re[\tilde{a}(t) \exp(j\omega_0 t)] \quad (1)$$

where $j = \sqrt{-1}$, $\omega_0 = 2\pi f_0$, and $\tilde{a}(t)$ is a complex-valued function of time.

A new FDTD method that is specific to BPL systems has been developed by the authors (APS/URSI 1997). The CE representation allows for the use of the BPL sampling theorem so that the time step can be chosen based on the bandwidth of the system rather than its maximum frequency. This usually yields a time step that is orders of magnitude larger than the time step in the standard FDTD method.

This presentation begins with the formulation of the classical two-dimensional, transverse-magnetic (TM) vector wave equation with an electric current source, $J_i(\rho, t)$,

$$-\nabla_T^2 \tilde{E}_z(\rho, t) + \tilde{\epsilon} \mu \epsilon(\rho) \tilde{E}_z(\rho, t) + \tilde{\epsilon} \mu j_i(\rho, t) = 0 \quad (2)$$

where $\nabla_T = \nabla - \frac{\partial}{\partial z}$, $E_z(\rho, t)$ is the electric field, $\epsilon(\rho)$ is a spatially varying permittivity, and μ is a constant permeability. A single dot above a quantity signifies a partial derivative with time, two dots represents a second-order partial derivative with time, and boldface type indicates vector quantities. Substituting the CE representation of BPL signals into (2) yields the following CE transformation of (2),

$$\begin{aligned} -\nabla_T^2 \tilde{E}_z(\rho, t) + \tilde{\epsilon} \mu \epsilon(\rho) [\tilde{E}_z(\rho, t) + j2\omega_0 \dot{\tilde{E}}_z(\rho, t) - \omega_0^2 \ddot{\tilde{E}}_z(\rho, t)] \\ + \tilde{\epsilon} \mu [\dot{j}_i(\rho, t) + j\omega_0 \ddot{j}_i(\rho, t)] = 0. \quad (3) \end{aligned}$$

A complete description of this new FDTD algorithm including the discretization scheme for (3) is presented. Results from this new method, the standard FDTD method, and analytic solutions are compared.

Accuracy of the Complex-Envelope FDTD Method

J. D. Pursel & P. M. Goggans*

University of Mississippi
Electrical Engineering
University, MS 38677

The authors (APS/URSI 1997) have developed a new FDTD method that is specific to bandpass-limited (BPL) systems. The new method uses the complex-envelope (CE) representation of BPL systems and signals to convert the usual FDTD method to the complex-envelope FDTD method. In the usual FDTD method, the signal is treated as if it is lowpass-limited and the time step is proportional to the maximum frequency of the electromagnetic source. In the CE FDTD, the time step is proportional to the bandwidth of the electromagnetic source.

If f_{\min} and f_{\max} are the minimum and maximum frequencies of the source, then the source bandwidth and center frequency are given by the following expressions: $B = f_{\max} - f_{\min}$ and $f_c = (f_{\max} + f_{\min})/2$. For both the usual FDTD and the CE FDTD, the selection of the time step proceeds so that the sampling theorem in the time domain is satisfied. The usual FDTD formulation is explicit. As a result, the selection of the time step is tied to the selection of the spatial steps because of the stability requirements imposed by the Courant condition. The CE FDTD is an implicit formulation and as a result, there is no required relationship between the time and spatial steps. For both methods the time step is usually set to be much smaller than the sampling frequency limit requirement so that the error in the finite difference approximations will be low. For the standard FDTD, the sampling theorem requirement can be expressed as

$$\Delta t = \frac{1}{Nf_{\max}} = \frac{1}{N(f_c + B/2)} \quad (1)$$

where N is the number of samples per period. The sampling theorem requires that $N > 2$. To decrease the error in the finite difference approximations, N is usually chosen to be an order of magnitude larger than the minimum. In the usual FDTD method, the minimum value of N may be dictated by the Courant condition rather than by the sampling theorem. For the CE FDTD, the sampling theorem requirement is expressed as

$$\Delta t_{\alpha} = \frac{1}{N_{\alpha}(B/2)}. \quad (2)$$

Combining (1) and (2) yields an expression comparing the required time step in the usual and CE FDTD

$$\Delta t_{\alpha} = \frac{N}{N_{\alpha}} \left(\frac{2f_c}{B} + 1 \right) \Delta t. \quad (3)$$

The expression above can be used to determine the relationship between the time step in the usual method and in the CE method. In general, the time step in the CE method will be much larger than the time step in the usual method for sources with a small percent bandwidth. However, a fair comparison of the time steps requires that N and N_{α} be adjusted so that the numerical accuracy of the two solution methods is the same. This paper presents numerical results that address the time step comparison problem.

FDTD Computation of Resonant Frequencies for a Cavity Filled with a Collisional Magnetized Plasma

G. Marrocco*, L. Tirone, F. Bardati
DISP, Università Roma Tor Vergata, Roma, Italy

F. De Marco, Divisione Fusione, ENEA-Frascati, Italy

In the last few years plasma reactors based on microwave absorption at the Electron Cyclotron Resonance (ECR) were developed for surface processing. One of the research goals in the field of ECR reactors is to improve the method in order to be able to process wafers having larger and/or non planar surfaces. Possible theoretical models are based on the analysis of electromagnetic wave propagation in a collisional plasma confined by a magnetic field in a rectangular or cylindrical cavity. The magnetic field is spatially varying so that the wave propagates along the field lines in regions where the wave frequency is slightly below the cyclotron frequency (whistler wave). The wave approaches the resonance zone where it is absorbed.

In this paper the FDTD method for gyrotropic media (F. Hunsberger, R. Luebbers and K. Kunz, IEEE Trans. Antennas Propagat., 40, 1589-1495, 1992) is presented the formulation of which has been refined to include axial and radial variations of plasma density, and the results of a numerical investigation for a circular axially-symmetric cavity are discussed. For a validation of the computer program, the cavity was homogeneously filled by a collisional axially-magnetized plasma. The roots of the characteristic equation for the resonance problem have been found in the complex frequency plane for comparison with the corresponding resonant frequencies obtained by Fourier transforming the FDTD solution for pulse wide-band excitation (Fig. 1).

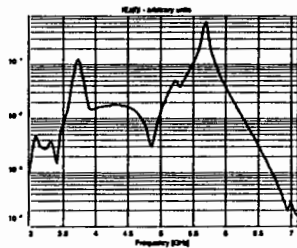


Fig. 1: $|E_z|$ vs. frequency at a point of the plasma filled cavity

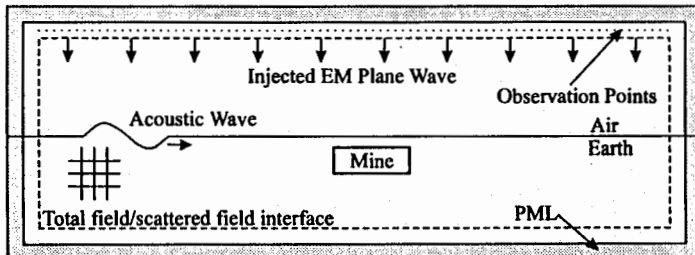
The lower resonant modes have been first calculated for a non gyrotropic plasma, i.e. by zeroing the off-axis components of the dielectric tensor. In such a limit the resonant modes are TE or TM and can be obtained in closed form. Then the resonance frequencies are tracked on the complex plane when the off-axis tensor components are moved from zero to their proper values. The difference between results of closed form and FDTD analysis is about 1% in our numerical computations.

Modeling Vibrating Boundaries with the Finite-Difference Time-Domain Method

Seung-Ho Lee* and Waymond R. Scott, Jr.
School of Electrical and Computer Engineering
Georgia Institute of Technology
Atlanta, GA 30332-0250

Over the past two decades, the finite-difference time-domain (FDTD) method has been widely used to model wave propagation, scattering, antennas, high-speed circuits, ground penetrating radar systems, etc. However, very little discussion has been given to modeling moving or vibrating boundaries. In this work, modeling of vibrating material boundaries is investigated using the FDTD method. This investigation is part of a project in which a land mine detection system that simultaneously uses both acoustic and electromagnetic waves is being studied. The system consists of an electromagnetic radar and an acoustic source. An acoustic wave is induced in the earth that travels through the earth and interacts with the mine; this causes the surface of the earth and the mine to vibrate. These vibrations are different near the mine. The radar is used to detect the vibrations and, thus, the mine. The vibrations are difficult to model with the FDTD method; because they are very small, and their frequency and propagation velocity are many orders of magnitude less than those for the electromagnetic waves.

A two-dimensional FDTD code has been written to study the feasibility of using the FDTD method for modeling the vibrating surfaces. A diagram of the model is shown below. An electromagnetic plane wave is injected and its reflection is recorded at the positions indicated. The acoustic wave travels across the surface and causes the surface to be displaced (vibrate). The reflected electromagnetic waves are recorded both when the acoustic wave is and is not present. The displacements are obtained by comparing the phase of these reflected electromagnetic waves. Displacements as small as 10^{-8} of a FDTD cell have been detected using this method, and displacements have been detected as a function of time and position for acoustic waves traveling across the boundary.



Analysis of Truncated Periodic Structures using the FDTD

Raj Mittra and Vyacheslav Bulkin

EMC Research Lab.

Penn State University, University Park, PA.

The analysis of radar scattering characteristics of periodic structures, *e.g.*, Frequency Selective Surfaces (FSSs) and radar absorbers, is of great practical interest. The Method of Moments (MoM) is well-suited for analyzing these structures when the FSS elements are thin and planar, the dielectric spacers are flat layers, and the screen is doubly-infinite. However, in many applications, the elements are thick, and the FSS elements may themselves have dielectrics inhomogeneities that are not planar. In addition, the FSS is often truncated and inserted into a window in an otherwise conducting screen, or in a screen made of composite material. Structures such as these are difficult to tackle by using the MoM codes, because the associated matrices can become very large and unwieldy. In this paper, we investigate the application of the FDTD to the problems belonging to this category. Although the FDTD has many salutary features, it is not without its difficulties. While it can handle a large number of unknowns — typically far greater than is manageable by using the MoM or even FEM — and can derive the frequency response of a given structure with a single run, numerical experiments show that the results for the scattered field are contaminated by spurious reflections from the mesh truncation boundaries, especially those around the sides. These artifacts, in turn, make it difficult to extract accurate results for the reflection coefficient of the structure, even when a time-gating is employed.

In this paper we show how we can apply a spatial filtering process to suppress the artifacts mentioned above. To validate the filtering process we compare our results, where possible, with those obtained from the MoM code. Fig.1 shows a two-layer truncated FSS structure investigated. Figure 2 presents the FDTD results for the reflection coefficient *vs.* frequency with and without filtering.

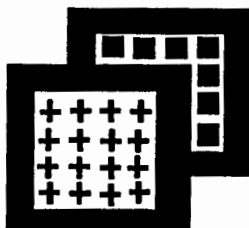


Fig. 1. Two-layer truncated FSS

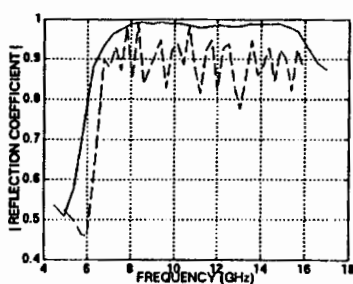


Fig. 2. Stop-band reflection coefficient (—raw data, - filtered)

Artifacts at Material Boundaries of Lossy Dielectric Bodies in FDTD Simulations

Michael Burkhardt* and Niels Kuster

Swiss Federal Institute of Technology (ETH)

8092 Zurich, Switzerland

Phone: +41-1 632 2151, Fax: +41-1 632 1057, e-mail: burkhardt@ish.ee.ethz.ch

Introduction

The Finite-Difference Time-Domain (FDTD) technique has been widely used for exposure assessment of biological tissue since 1975 (A. Taflove and M.E. Brodwin, IEEE-MTT, 11, 888-896, 1975). Due to its facility in handling strongly non-homogeneous objects, it has been successfully used to analyse the exposure of humans to electromagnetic fields as well as to analyse and design *in vitro* and *in vivo* exposure setups (N. Kuster, Mobile Com. Safety, Chap. & Hall, 13-64, 1997). Although the dispersion effect related to the discrete FDTD scheme (A. Taflove, Comp. Electromag., Artech House, 93-106, 1995) and particular uncertainty sources such as boundary conditions (D.T. Prescott and N.V. Shuley, IEEE-MTT, 8, 1162-1178, 1997) have been quite extensively investigated, an estimation of the total error of a particular exposure problem involving lossy bodies can only be assessed through a large set of numerical experiments requiring variation of many parameters. However, one must be aware that the modeling of very fine and complex structures within coarse discretizations and the straight forward assignment of dielectric parameters to voxels may lead to unwanted artifacts.

Objective

Within the discretely staggered scheme of FDTD, material boundaries can only be approximately represented, especially if they are not conformal to the grid. The objective of this study was to assess the errors due to artifacts arising from artificial steps, pixels and ripples on material boundaries when fine geometrical details must be modeled within the conventional Yee grid.

Methods

The main assessment was performed with an inhouse FDTD code and the Finite-Integration Technique using the commercial code MAFIA, whereby different treatment of material boundaries was investigated. For validation purposes the Generalized Multipole Technique (GMT) was used for analytical-type problems, and the near-field assessment system DASY3 was used for the experimental verification of benchmark problems.

Results and Discussion

Errors in integral and local field values due to modeling uncertainties arising from steps, ripples, pixels and staircasing have been assessed depending on the discretization, frequency, material parameters, polarization and type of excitation for homogeneously modeled objects. Concerning non-homogeneously modeled objects, errors due to artificial steps and holes in layers were investigated. Different approaches for representing material boundaries and methods to avoid the described artifacts will be discussed. Artifacts from single voxel steps, ripples and pixels can result in locally enhanced field strengths of several hundred percent in the case of a straightforward assignment of dielectric properties to the voxels of the Yee grid. This must be taken into account when the dielectric body is small and of complicated shape with respect to the grid and when the result parameter is related to a small and local region in space, e.g., when searching for the maximum occurring SAR in a certain tissue type. Globally significant errors, especially for coarse discretizations, were found for objects with focusing effects on an incident electromagnetic field. The results of this study confirm the conclusion from (L.R.A.X.de Menezes and W.J.R.Hoefer, IEEE-MTT, 12, 2512-2517, 1996) that the main source of error when modeling non-homogeneous space with a discrete scheme such as the FDTD method is not the dispersion effect but the numerical representation of material interfaces.

Simulation of Wire Antennas Non-Conformally Oriented to the FDTD Grid

Nicolas Chavanne*, Michael Burkhardt and Niels Kuster
Swiss Federal Institute of Technology (ETH)

8092 Zurich, Switzerland

Phone: +41-1 632 5121, Fax: +41-1 632 1057, e-mail: chavanne@ish.ee.ethz.ch

Introduction

The Finite-Difference Time-Domain (FDTD) technique has been widely used to analyze antenna structures and simple models of handheld transmitters in the near- and far-field, e.g., in (R.Luebbers et. al., IEEE-AP, 12, 1577-1583, 1992). Due to its capabilities, FDTD has gained increasing interest for the simulation of antenna structures in complex environments, e.g., handheld transmitters close to the human head. FDTD has proven to be suitable for accurate determination of near- and far-field parameters for antenna configurations in complex environments. However, certain antenna configurations may not be modeled conformal to the FDTD grid at any position. Straightforward modeling of such antenna configurations will result in a staircased model. The draw-backs for difficult modeling of arbitrarily shaped surfaces has been the subject of many research studies, e.g., introducing *Contour-Path* (T.Jurgens et. al., IEEE-AP, 4, 357-365, 1992) or *Finite-Volume* formulations (V.Shankar et. al., Electromagnetics 10, 127-145, 1990).

A recent study (P.S.Excell et. al., ACES, 2, 55-65, 1996) modeled a rotated phone with a staircased monopole configuration by introducing a correction factor into the field update equations to readjust the staircased physical length to the desired electrical length. In our study different approaches are compared to simulate wire antennas rotated arbitrarily around the major FDTD axes without staircasing.

Objective

The objective of this study was to investigate the performance of arbitrarily oriented wire antennas when simulated with the FDTD method, including the assessment of far- and near-field information such as radiation pattern, near-field distribution and feedpoint impedance.

Methods

A Yee-grid based FDTD algorithm was used to determine the performance of arbitrarily oriented dipole antennas and a previously described generic phone (M.Burkhardt et. al., Proc. Int. Conf. on Appl. Electr. and Comm., 83-86, 1997). Contour-path based modeling and a subgrid approach were compared to straight forward staircase modeling. The results for the generic phone were validated by measurements on a physical model of the generic phone using the near-field scanning system DASY3 (T.Schmid et. al. IEEE-MTT, 1, 105-113, 1996).

Results and Discussion

Standard FDTD modeling of arbitrarily oriented dipole configurations within a rectilinear Yee-grid will lead to staircasing errors. A contour-path model of a thin wire, similar to a published contour-path model for curved surfaces using conformal borrowing (J.Fang and J.Ren, IEEE-MTT, 5, 830-838, 1993) was implemented to simulate a rotated dipole antenna, but still restricted to lie within a FDTD grid plane. The dipole antenna was rotated to different positions. The far-field pattern, the near-field distribution and the feedpoint impedance were analyzed and compared to that of a staircased model. Furthermore, the generic phone, consisting of a simple metallic box and a monopole antenna was rotated around the major FDTD axes, evaluated in the near- and far-field and compared to simulated and measured data of the non-rotated phone. Whereby the feedpoint impedance represents a very sensitive parameter with respect to modeling, very good agreement was found for the far-field patterns.

Study of the Effect of the Meshing by Blocks in the Finite Difference - Time Domain Method

by A.E. ROS

*Laboratoire d'Electronique et Systèmes de Télécommunications
6,Av. Le Gorgeu - BP 809 - Brest Cedex - France
E-mail : Alain.Ros@lesti.gw.univ-brest.fr*

In most of the electromagnetic problems, the study of the evolution of the system in terms of time leads to the solving of integro-differential equations such as Maxwell's equations.

An analytical solution is generally not available but the increasing power of the computers allows the use of numerical methods previously useless on personal computers.

In the field of microwaves, some of them (Transmission Line Matrix Method, Finite Difference-Time Domain Method,...) give a precise description of the electromagnetic field close to the discontinuities and the FD-TD method seems to be the more simple to implement.

An accurate analyze of the variations of the electromagnetic field components in the regions where they have very fast variations requires a smaller spatial discretization of the differential equations.

The introduction of these blocks creates at the interfaces non-physical discontinuities which produce "numerical noise" (or "spurious modes").

In this paper, we shall describe the effects of these changes in the mesh size and we shall propose some original solutions in order to decrease and possibly to cancel these parasitic effects. We also shall be able to discuss how the change in the mesh size have an influence on the electromagnetic field components inside and outside of these regions.

These effects will be discuss in the two case : expanded nodes FD-TD scheme (Yee's formulation) and condensed nodes FD-TD scheme. The comparison will relate not only to the frequency response but also to the numerical aspects : convergence velocity and memory occupation.

Modeling Nonlinear Devices in FD-TD: The Equivalent Source Method

Jason Mix*, Jon Dixon,
Zoya Popovic, and Melinda Piket-May

Department of Electrical Engineering
University of Colorado at Boulder
Boulder, CO 80309-0425
Email: mix@spot.colorado.edu

The most common method to incorporate lumped element devices in FD-TD is the Extended FD-TD Formulation (Allen Taflove, *Computational Electrodynamics: The Finite-Difference Time-Domain Method*, Artech House, 457-465, 1995) in which a current term for the lumped element, J_L , has been added to the differential form of Ampere's Law.

$$\nabla \times \vec{H} = \epsilon \frac{\partial \vec{E}}{\partial t} + \vec{J}_C + \vec{J}_L$$

Algorithms based on this method for simple elements such as the resistor, capacitor, and inductor yield semi-implicit, numerically stable equations. However, the inclusion of a pn junction required by a transistor, results in a set of coupled nonlinear transcendental equations that must be solved at each time step. Thus, an additional procedure for solving nonlinear equations must be employed such as the Newton-Raphson approach.

A new approach, the equivalent source method, substitutes approximately equivalent sources in place of the transistor's ports. This is similar to the method used to link FD-TD and SPICE (ibid. Taflove, 465-469), however, the voltage-current relationships based upon the equations for a general transistor model are finite differenced and incorporated into a regular FD-TD grid. This eliminates the need for additional nonlinear equation solvers and reduces computational cost. In addition, since the equations are based on a general transistor model and the calculations of the nonlinear drain to source current, I_{DS} , is performed in a subroutine, a variety of linear or nonlinear models can be used.

The equivalent source method is applied to a simple common source circuit using a Curtice-Cubic model for the transistor characteristics and compared to a simulation of the circuit using Hewlett Packard's Microwave Design System (MDS). Finally, the transistor is used in an active antenna using the transistor in a 3-port oscillator configuration as an example. The antenna is a printed dipole above a ground plane where the gate and drain terminals are connected to the dipole, and the sources are connected to stubs printed on the same substrate as the dipole. This example is chosen because it displays the capability of the technique by including the nonlinear device, guided waves in the circuit, radiated waves in free space, and possible surface waves in the simulation.

Mesh Truncation Conditions

Extension of the Concurrent Complementary Operators Theory to Numerical Boundary Conditions	78
<i>O. M. Ramahi*, Digital Equipment Corporation, USA</i>	
Comparison of Different Approaches in the Design of Perfectly Matched Absorbers	79
<i>M. Kuzuoglu*, Middle East Technical University, Turkey, R. Mittra, Pennsylvania State University, USA</i>	
Maxwellian Material Based Absorbing Boundary Conditions for Lossy Media in 3D	80
<i>R. W. Ziolkowski*, D. C. Wittwer, University of Arizona, USA</i>	
Trans-impedance / Admittance and their Application to FDTD Grid Truncation	81
<i>S. Malik, R. Kastner*, E. Heyman, Tel-Aviv University, Israel, R. W. Ziolkowski, University of Arizona, USA</i>	
On the Time Domain Discrete Green's Function at the FDTD Grid Boundary	82
<i>R. Holtzman*, R. Kastner, E. Heyman, Tel-Aviv University, Israel, R. W. Ziolkowski, University of Arizona, USA</i>	
An Anisotropic Perfectly Matched Layer (APML) for Mesh Truncation in the Finite Difference Time Domain (FDTD) Analysis.....	83
<i>D. Park*, Chung-Ju National University, Korea, Y. Chen, Hong Kong Polytechnic University, Hong Kong, P. R. China, R. Mittra, Pennsylvania State University, USA</i>	
A New PML Formulation for Anisotropic Media and PSTD Algorithm.....	84
<i>Q. H. Liu*, New Mexico State University, USA</i>	
Absorbing Boundary Conditions for the Path Integral Time-Domain Method.....	85
<i>R. Nevels*, J. Miller, Texas A&M University, USA</i>	
Exploring the Cause of Instabilities Arising from the Application of Higher Order ABCs in FDTD Simulation.....	86
<i>O. M. Ramahi*, Digital Equipment Corporation, USA</i>	
Exact Implementation of Higher-order Bayliss-Turkel Absorbing Boundary Conditions in Finite Element Simulation.....	87
<i>O. M. Ramahi*, Digital Equipment Corporation, USA</i>	

Extension of the Concurrent Complementary Operators Theory to Numerical Boundary Conditions

Omar M. Ramahi
Digital Equipment Corporation
PKO3-1/RII, 129 Parker St.
Maynard, MA 01754, U.S.A.

The introduction of the concurrent complementary operators method (C-COM) [Ramahi, *IEEE Trans. Microwave Guided Wave Lett.*, June 1997] has led to a significant reduction in the non-physical reflections that arise from the termination of the Finite Difference Time Domain (FDTD) mesh. In the C-COM implementation, complementary operators are applied simultaneously in a single simulation, thus allowing for significant suppression of non-physical reflections arising from side and corner regions.

Encouraged by the strong performance of the C-COM in comparison to previously developed mesh-truncation techniques, we extend the construction of complementary operators to encompass numerical boundary conditions that are based, typically, on the behavior of the field in the proximity of the boundary. The motivation behind this effort was the fact that numerical absorbing boundary conditions have certain attractive features that makes them good candidates for mesh termination when the outer boundary is non-rectangular.

As an example involving numerical boundary operators, we demonstrate the application of C-COM on Liao's boundary operators. We present a host of numerical simulations showing that highly accurate solutions can be obtained. In fact, we show that the suppression of non-physical reflections, in the case of numerical operators, to be as effective as applying the C-COM to Higdon type absorbing boundary conditions. However, and for the same attractive features of numerical operators, the flexibility inherent in the complementarization process makes plausible the application of C-COM to non-rectangular or non-regular outer boundaries. These implications will be explored.

Comparison of Different Approaches for Designing Perfectly Matched Absorbers

Mustafa Kuzuoglu*

Department of Electrical Engineering
Middle East Technical University
06531, Ankara TURKEY

Raj Mittra

Pennsylvania State University
319 Electrical Engineering East
University Park, PA 16802-2705 USA

Following the introduction of the concept of a perfectly matched layer (PML) by Berenger for mesh truncation in FDTD, several methods have been developed for designing the PMLs, both for time and frequency domain applications. Berenger's approach is based on the splitting of the field components in a manner that guarantees the decay of the transmitted field within the PML medium. A similar result can be obtained by designing an anisotropic layer having tensor permittivity and permeability. In this case, the need for field splitting is obviated, and the governing equations are Maxwell's equations in the anisotropic medium.

In this work, the properties of the partial differential equations (PDEs) satisfied in the PML regions are discussed. It is shown that although there are different formulations in the FDTD applications, most of these reduce to the same PDE in the frequency domain applications. This result is demonstrated for the PML introduced by Berenger, as well as for the anisotropic PML and its variants. An important consequence of this analysis is the possibility of designing numerical perfectly matched absorbers where the coefficients in the governing PDEs can be chosen to achieve a reflectionless PML-free space interface and rapid decay in the longitudinal direction within the PML medium.

In FEM applications, conformal PMLs can be used to reduce the white space. For this reason, partial differential equations in cylindrical and spherical PMLs are also discussed. The derivation of these equations are based on the absorption of cylindrical and spherical waves without any reflection. The above equations are compared with those satisfied by the field quantities in anisotropic PMLs with curved boundaries. The role played by the electrical radius of curvature of the PML-free-space interface is illustrated for special cases. Finally, the paper discusses the issue of causality, which is important in time domain applications, and also provides an interpretation of the same in the frequency domain.

Maxwellian Material Based Absorbing Boundary Conditions for Lossy Media in 3D

Richard W. Ziolkowski and David C. Wittwer

Electromagnetics Laboratory

Department of Electrical and Computer Engineering

The University of Arizona

Tucson, AZ 85721-0104 USA

Tel: (520) 621-6173 Fax: (520) 621-8076

ziolkowski@ece.arizona.edu

Electromagnetic absorbers have attracted a great deal of attention recently in the computational electromagnetics community. The need to truncate the simulation domain in any finite difference or finite element approach is well-known. Many approaches have been developed to achieve this truncation; they are generally classified now simply as absorbing boundary conditions (ABC's). Like with any real-life absorber, the perfect ABC would absorb perfectly any frequency of electromagnetic radiation incident upon it from any angle of incidence.

It has been shown recently [R. W. Ziolkowski, *IEEE Trans. Antennas and Propagation*, vol. 45(4), pp. 656-671, April 1997 ; R. W. Ziolkowski, *IEEE Trans. Antennas and Propagation*, vol. 45(10), pp. 1530-1535, October 1997] that potentially realizable electromagnetic absorbers can be designed using polarization and magnetization field concepts. A numerical ABC in two dimensions was obtained with this approach by combining an uniaxial material construction and a generalization, the time-derivative Lorentz material (TD-LM) model, of the standard Lorentz dispersion model which is used to characterize lossy dispersive materials. This TD-LM ABC has been shown to have performance characteristics that are comparable to the non-Maxwellian Berenger PML ABC in two dimensional finite-difference time-domain (FDTD) simulations. The advantages of this polarization and magnetization field approach include the close connection of the ABCs and the actual absorber physics associated with Maxwell's equations; the avoidance of the field-equation splitting required by the Berenger PML layers; and reduced memory and operation counts.

The extension of the TD-LM Maxwellian material-based ABC to three dimensional finite-difference time-domain (FDTD) methods will be presented. Its performance will be characterized with comparisons to the Berenger PML ABC for ultrawide bandwidth dipole radiation problems. Further generalizations of the Lorentz material model lead to the 2TD-LM model which includes not only the electric field and one time derivative of the electric field as driving terms (i.e., the TD-LM model), but also two time derivatives of the electric field. It will be demonstrated that this 2TD-LM model leads to an efficient absorber that can be matched to lossy materials. The performance of the resulting lossy material ABC will be characterized in 1D with pulse scattering from a lossy dielectric slab and in 3D with microstrip transmission and radiation problems.

TRANS-IMPEDANCE/ADMITTANCE AND THEIR APPLICATION TO FDTD GRID TRUNCATION

S. Malik[†], R. Kastner^{*†}, E. Heyman[†], and R. W. Ziolkowski[‡]

[†]Department of Electrical Engineering - Physical Electronics
Tel-Aviv University, Tel-Aviv 69978, Israel

^{*}Department of Electrical and Computer Engineering
University of Arizona, Tucson, AZ 85721

The wave impedance is utilized, in general, in the diagonalization of the wave equation into forward- and backward-propagating one-way equations. In the discrete Yee grid, where the electric and magnetic field components occupy alternating locations, the definition of an impedance would depend upon the choice of the location where the impedance is to be defined and the interpolation scheme. Alternatively, a unique trans-impedance (TI) can be defined by substituting a monochromatic plane wave at frequency ω into the discrete Maxwell equations and taking field ratios across two adjacent space-time points. For the 1-D grid, where $t = n\Delta t$ vs. $x = i\Delta x$, the TI is

$$Z, Y = \mp(\mu/\epsilon)^{\pm\frac{1}{2}} \exp j[\omega\Delta t/2 - \sin^{-1}(\gamma^{-1} \sin(\omega\Delta t/2))] \quad (1)$$

A plot of the TI vs. frequency (Fig. 1) shows a bandpass area, where $|Z| = \sqrt{\epsilon}$, with a corresponding phase change, and a bandstop area where the exponent in (1) is real. The TI concept can be used to simulate the free space boundary conditions at a given frequency and angle of incidence, assuming a reflection-free field at the preceding step, by imposing the relationship $E_x^{n+1}(i) = Z H_y^{n+1}(i - \frac{1}{2})$, which applies for the forward-propagating wave constituent. The effectiveness of this condition is compared against Mur's first order boundary condition in Fig. 2, and a significant improvement is achieved in a single layer. This work is extended to the time domain, accounting for all frequencies and incidence angles, in the following paper.

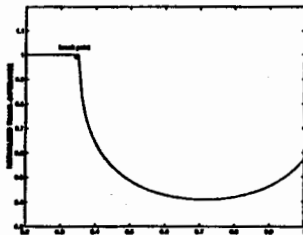


Fig. 1. Normalized trans-impedance/admittance vs. f. $\gamma = 0.7$.

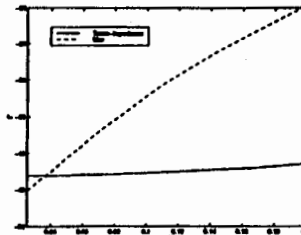


Fig. 2. Γ for this BC (solid) and Mur's 1st order ABC (dashed) vs. f. $\gamma = 0.7$.

ON THE TIME DOMAIN DISCRETE GREEN'S FUNCTION AT THE FDTD GRID BOUNDARY

R. Holtzman[†], R. Kastner^{*†}, E. Heyman[†], and R. W. Ziolkowski[‡]

[†]Department of Electrical Engineering - Physical Electronics
Tel-Aviv University, Tel-Aviv 69978, Israel

[‡]Department of Electrical and Computer Engineering
University of Arizona, Tucson, AZ 85721

A discretized space-time domain Green's function, defined over the boundary of the computational FDTD grid, represents the external medium as a kernel in a discrete convolution summation. It may be applied as a rigorous, quasi-local, single-layer boundary condition. The kernel is calculated independently prior to the actual FDTD calculations, taking into account the shape of the boundary and the composition of the external space. The derivation is carried out in time domain and hence includes the effects of sampling rate and numerical dispersion. The convolution summation is finite to a very good approximation, due to the limited spatial and temporal spreads of the kernel, and as such is a finite impulse response (FIR) filter. In fact, in the 1-D continuous limit, this kernel is impulsive. Accuracy of the solution is controlled by the number of terms retained in the space-time discrete convolution, which can be quite small. For the simplest one dimensional case, where the grid is defined as $t = n\Delta t$ vs. $x = i\Delta x$, our derivation results in the following boundary condition for, say, $E_z^{n+1}(i)$:

$$E_z^{n+1}(i) \approx -\gamma\eta H_y^{n+\frac{1}{2}}(i - \frac{1}{2}) + G(\gamma) * E_z(i); \quad (1)$$

where $E_z(i) = [E_z^1(i), E_z^2(i), \dots]$, $G(\gamma) = [G^1(\gamma), G^2(\gamma), \dots]$ and $*$ is the convolution operator. The Green's function $G(\gamma)$ in (1), is calculated beforehand in the discretized time domain, e.g., the special case of an external free space it takes the form $G(\gamma) = [1 - \gamma^2, -\gamma^2 + \gamma^4, -\gamma^2 + 3\gamma^4 - 2\gamma^6, -\gamma^2 + 6\gamma^4 - 10\gamma^6 + 5\gamma^8, -\gamma^2 + 10\gamma^4 - 30\gamma^6 + 35\gamma^8 - 14\gamma^{10}, \dots]$. Apparently, if $\gamma = 1$, then $G(\gamma) = [0, \dots, 0]$. The same applies, as one may expect, in the the continuous space (i.e., for $\Delta z \rightarrow 0$). If, e.g., $\gamma = 0.7$, then $G = [0.51, -0.2499, -0.0050, 0.0624, \dots]$. Note the rapid temporal decay of G , which indeed renders the convolution integral in (1) a quasi-local operation. A z -transform of (1) results the frequency domain Green's function, as in the preceding paper: $\tilde{G}(\gamma; w) = \frac{1-w \pm \sqrt{(1-w)^2 + 4\gamma^2 w}}{2\gamma w}$ (w is the spectral variable in the z transform). Two dimensional formulation is derived analogously, and is demonstrated by examples that show a significant improvement in reflection errors over traditional Engquist-Majda-Mur type as well as PML type boundary conditions.

An Anisotropic Perfectly Matched Layer(APML) for Mesh Truncation in The Finite Difference Time Domain(FDTD) Analysis

Dong-Hee Park
Department of Electro-
Communication
Engineering
Chung-Ju National
University,
Chung-Buk, Korea

Yinchao Chen
Department of Electrical
Engineering
Hong Kong Polytechnic
University,
Hong Kong

Raj Mittra
Electrical Engineering
Department
Pennsylvania State
University, State College,
PA, USA

This paper describes an anisotropic, perfectly matched layer(APML) for the truncation of the Finite Difference Time Domain(FDTD) mesh. The PML presented in this paper differs from the those published earlier by Gedney [IEEE Trans. Antennas & Propagat., vol.44, 1630-1639, Dec. 1996] and Sullivan [IEEE Microwave Guided Wave Lett., vol. 7, No. 7, July 1997], since the anisotropic PML medium in the present analysis is both Maxwellian and causal. Although the anisotropic PML approach has been used previously in a publication by Chen, *et al.*, [Antennas and Propagation Society International Symposium, vol.2, 1002-1005, 1997], the formulation in this paper is different and, the authors believe, results in update equation that are more convenient to use.

The APML is easily incorporated in the existing FDTD codes. In addition, the truncation of the FDTD mesh is convenient in this approach because it does not require special treatments as does the conventional PML approach.

An important contribution of the paper is a systematic investigation of the FDTD/APML algorithm and show how it depends upon the electrical conductivity σ appearing in the $[\bar{\epsilon}]$ and $[\bar{\mu}]$ tensors of the APML representation. The corner and edge problems are also studied in the context of APML by examining the time domain signatures of the electromagnetic fields, and the performance characteristics, e. g., the input impedance and the radiation pattern of wire antennas.

The APML results are compared with those derived by using PML approach described in a paper by Veihl and Mittra [IEEE Microwave Guided Wave Lett., vol.6, No.2, pp.94-96, July 1996], with Gedney's PML algorithm, and with results derived by using Mur's first order boundary condition.

A NEW PML FORMULATION FOR ANISOTROPIC MEDIA AND PSTD ALGORITHM

QING HUO LIU

KLIPSCH SCHOOL OF ELECTRICAL AND COMPUTER ENGINEERING
NEW MEXICO STATE UNIVERSITY
LAS CRUCES, NM 88003

Email: qhliu@nmsu.edu

The propagation of electromagnetic waves in anisotropic media has attracted much attention since these materials are commonly used in microwave components, microstrip waveguides and antennas, fiber optics, and other areas. Because of multiple wave speeds associate with the anisotropy, conventional absorbing boundary conditions (ABCs) based on one-way wave equation cannot be used for anisotropic media. Other ABCs such as the Liao's, can be used but the performance degrades from that for isotropic media. Recently it was proven by Garcia et al (*Electron. Lett.*, vol. 32, no. 14, pp. 1270-1271, 1996) that Berenger's perfectly matched layer (PML) cannot provide a reflectionless ABC for anisotropic media. An extension of this PML has been made by Perez et al (*IEEE Microwave and Guided Wave Letters*, vol. 7, no. 9, pp. 302-304, 1997) for 2-D lossless anisotropic media so that the PML will be perfectly matched. In this work, we present a new formulation for the true PML in anisotropic media using the concept of complex coordinates (Chew et al, *Int'l. IEEE AP-S Symposium Digest*, Montreal, Canada, July 1997). This PML ABC is reflectionless in the continuous limit, and can provide effective mesh truncation for finite methods.

Using this new PML ABC, we extend the pseudospectral time-domain (PSTD) algorithm for isotropic media (Liu, *Microwave Opt. Tech. Lett.*, vol. 10, pp. 158-165, 1997) to simulating electromagnetic waves in arbitrary anisotropic media. In addition to the high order accuracy associated with the spatial derivatives obtained by FFT, this PSTD algorithm provides an important advantage for anisotropic media: Since a centered grid (instead of a staggered grid) is used in the PSTD method, the undesired requirement for the field and material averaging in the FDTD is eliminated. Numerical examples show the efficacy of this new algorithm.

Absorbing Boundary Conditions for the Path Integral Time-Domain Method

Robert Nevels* and Jeffrey Miller
Department of Electrical Engineering
Texas A&M University
College Station, TX 77843-3128

The path integral time-domain (PITD) method is a new electromagnetic field scattering technique based on a Feynman path integral formulation that gives a propagator solution to the time domain form of Maxwell's differential equations. The essence of the method is that the present time electric and magnetic field components are acted upon by the operator ($\bar{F}\bar{A}\bar{F}^{-1}$), which consist of forward and inverse Fourier transforms (F , F^{-1}) and multiplication by a state transition matrix (\bar{A}) that accomplishes time stepping. Numerically, the Fourier transform is a discrete Fourier transform, which is implemented as a Fast Fourier Transform.

Here we will present a method by which the PITD fields are absorbed at the boundaries of the numerical region. Because a Fourier transform governs the manner in which the fields are manipulated in the numerical space, the propagating and scattered fields are subject to what is known as the 'wrap-around' effect. For example, fields that propagate to the right in the numerical region disappear on the right side of the numerical boundary while simultaneously reappearing on the left side. Originally it was thought that a numerical filter such as a Parzen, Hanning or Welch window could be inserted in the Fourier transform so that waves that approach the numerical boundary would be annihilated. It will be shown that simple filters such as these will give unacceptable errors in the scattered fields and, because the path integral expression is a sequence of nested integrals, the cumulative effect is that of raising any filter to a power equal to the number of time steps.

Our approach therefore has been to develop a modified form of the Berenger boundary condition. Two methods will be described, one in which the Berenger equations are implemented throughout the numerical region and another with only the standard absorbing zone adjacent the numerical border. It will be shown that because stability of the PITD method is insured by the addition of a small amount of loss (σ) throughout the numerical region, the Berenger equations, which require the absorption condition $\sigma/\epsilon = \sigma'/\mu$, appear to be the natural absorbing boundary condition for the PITD method. Examples will be shown illustrating absorption in one and two dimensions.

Exploring the Cause of Instabilities Arising from the Application of Higher Order ABCs in FDTD Simulation

*Omar M. Ramahi
Digital Equipment Corporation
PK03-1/RII, 129 Parker St.
Maynard, MA 01754, U.S.A.*

When using the Finite Difference Time Domain (FDTD) method to solve open-region radiation problems, the application of mesh-truncation techniques becomes an integral part of the simulation. For many problems, the required duration of the simulation need only to extend over enough time steps to capture the bulk of the output energy or pulse at the desired point of observation. For these problems, the stability behavior of mesh-truncation techniques does not pose a serious challenge. However, there are many other applications where the output time signature need to be obtained for a very long duration in order to capture the response of the system over a wide frequency band (via Fourier transformation). For this second class of problems, the issue of stability of mesh-truncation techniques must be carefully addressed.

Mesh-truncation techniques span two classes: This first consists of analytical or numerical Absorbing Boundary Conditions (ABCs), and the second consists of absorptive material. In the latter class, the Perfectly Matched Layer (PML) figures prominently. Few publications have addressed the issue of the stability of PML. More recently, it was found that the split version of PML not to be strongly well-posed [Abarbanel and Gottlieb, *J. Comp. Phys.*, 1997], which merits further investigation into the general stability properties of PML. The study of the instability of ABCs, on the other hand, dates back to the time of their development. In general, it is commonly believed that higher order (ABCs) exhibit instabilities that can be detrimental to many FDTD open-region simulations. Earlier works attributed the cause of instabilities to the intrinsic construction of the ABCs, and, in particular, to the pole-zero distribution of the transfer function that characterizes the boundary condition. Empirical experiments by many researchers found that as the order of the boundary operator increases, the more acute the instabilities become.

In the course of our investigation we found that higher order ABCs, more specifically, those of the Higdon and Liao type, are not intrinsically unstable in their original unmodified forms regardless of their order. We demonstrate, in a conclusive way, this finding through a series of empirical studies. Furthermore, we show that the instabilities that are often reported in the literature are caused by an artifact of the FDTD computational domain. This comes as contrary to previously conjectured hypotheses or theories. These findings, consequently, will have strong implications that can aid in the construction of stable FDTD schemes.

Exact Implementation of Higher-Order Bayliss-Turkel Absorbing Boundary Conditions in Finite Element Simulation

Omar M. Ramahi
Digital Equipment Corporation
PKO3-1/R11, 129 Parker St.
Maynard, MA 01754, U.S.A.

The Absorbing Boundary Conditions (ABCs) introduced in the late 70s by Bayliss and Turkel were perhaps the first operators to terminate a finite element mesh without including excessively high number of elements in the region surrounding the structure. The Bayliss-Turkel (BT) operators acquired a direct appeal because of their simplicity and relatively good accuracy whether the application was in two- or three-dimensional space. Despite the promising performance of the higher-order BT operators, however, only operators of first- or second-order were implemented. This was primarily because of the common understanding that the implementation of third- or higher-order BT operators required the finite-difference approximation of mixed derivatives. Since mixed derivatives posed a complexity when using finite elements, the effort to implement third- or higher BT operators was abandoned. Despite this, however, one can find in the literature several ABC constructions based on the BT operators that extend beyond the second-order. These constructions are typically approximations of higher-order operators where mixed derivatives are either assumed negligible or replaced by simple approximations that vary in accuracy. Unfortunately such approximations give operators that yield unsatisfactory levels of accuracy.

In this work, we revisit the BT operators. We show that these ABCs can be implemented in their original form, having only radial derivatives, in an *exact* fashion. This implementation is fully analogous to the way higher-order Higdon ABCs were originally implemented. More specifically, we implement higher-order partial derivatives by cascading the finite difference approximation of each first-order derivative. We show that such new implementation not only provides an appreciably higher level of accuracy than what was achieved before, but more significantly, it facilitates the exact application of boundary operators to non-circular outer boundaries. Finally, we demonstrate that the exact implementation of higher order BT operators achieves a level of accuracy that surpasses that achieved by perfectly matched layers, while incurring less computational cost.

Hybrid Computational Approaches Involving Finite Methods

T. Cwik and J. M. Jin

Progress in Modeling Complex Conformal Antennas using the Finite Element-boundary Integral Method	90
<i>L. C. Kempel*, K. D. Trott, Mission Research Corporation, USA</i>	
Hybrid FEM with Mesh Refinement for Printed Antenna Modeling.....	91
<i>J. Gong*, S. Wedge, Tanner Research, Inc., USA</i>	
A Hybrid Frontal-FEM/BIE/PO Formulation for Analyzing Scattering from Large and Complex Jet Engine Inlets	92
<i>G. Fan*, J. Jin, University of Illinois, USA</i>	
Improved Accuracy in Microwave Absorber Analysis with a Higher-order Hybrid Finite Element Method	93
<i>Y. Jiang*, A. Q. Martin, Clemson University, USA</i>	
A Hybrid Technique for Axisymmetric Scatterers with Appendages	94
<i>A. D. Greenwood*, J. Jin, University of Illinois, USA</i>	
A Hybrid Method for Computing Zero-sequence Impedance of Underground Three-phase Pipe-type Cables	95
<i>X. Xu*, G. Liu, Clemson University, USA</i>	
Application of MBPE in Conjunction with Hybrid FEM/MoM Technique	96
<i>C. J. Reddy*, Hampton University, USA, M. D. Deshpande, ViGYAN Inc., USA, C. R. Cockrell, F. B. Beck, NASA Langley Research Ctr., USA</i>	
A Hybrid FEM Based Procedure for the Scattering from Photonic Crystals Illuminated by a Gaussian Beam.....	97
<i>G. Pelosi*, A. Cocchi, University of Florence, Italy, A. Monorchio, University of Pisa, Italy</i>	
An Effective Hybrid FDTD-MoM Technique to Predict Radiation from Enclosures	98
<i>O. M. Ramahi*, Digital Equipment Corporation, USA, B. R. Archambeault, International Business Machines, USA</i>	
Analysis of MICs with Curved Surfaces using a Hybrid FDTD-FVTD Algorithm on an Orthogonal Rectangular Grid	99
<i>M. Yang*, Y. Chen, Hong Kong Polytechnic University, Hong Kong, P. R. China, R. Mittra, Penn State University, USA</i>	
Numerical Modeling of Antennas with Nonlinear Lumped Elements via a Hybrid FETD-FDTD Method	100
<i>S. Selleri*, J. Dauvignac, C. Pichot, Université de Nice-Sophia-Antipolis, France, G. Pelosi, University of Florence, Italy</i>	

Progress in Modeling Complex Conformal Antennas Using the Finite Element-Boundary Integral Method

Leo C. Kempel* and Keith D. Trott
Mission Research Corporation
Valparaiso, FL

Significant research has been performed over the past ten years in applying the finite element-boundary integral (FE-BI) method to the problem of modeling conformal antennas. The principal reason for interest in the FE-BI as a means of predicting conformal antenna performance is its ability to model complex antenna shapes with inhomogeneous material properties.

Our research groups as well as colleagues at other organizations have found that achieving acceptable results for such antennas requires more than blindly using general purpose computer programs. Significant effort was required to model the eight-arm, eight section log-periodic antenna (LPA) shown in Figure 1. This LPA could be used as a direction finding (DF) antenna by comparing the phases of mode 1 (360° progressive phase wrap around the ports) and mode 2 (720° progressive phase wrap around the ports).

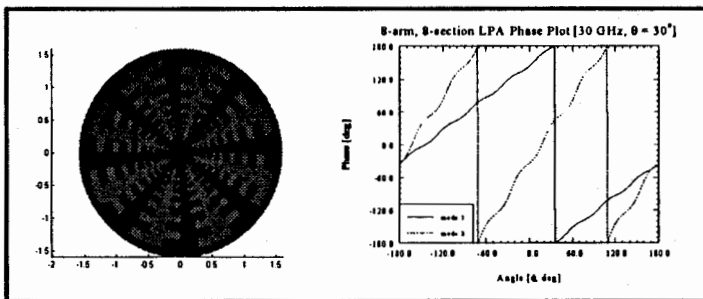


Figure 1. Log-periodic antenna and far-field phase response vs. angle-of-arrival.

The phase of the transmitted signal is shown for modes 1 and 2. The difference between these two mode phases indicates the angle-of-arrival. Note that for mode 1 the slope of the phase response is one while for mode 2 the slope is two.

We will present our latest findings for modeling such complex antennas. This presentation will focus on computational issues, measured data, feeding methods, as well as current and projected capabilities.

Hybrid FEM with Mesh Refinement for Printed Antenna Modeling

Jian Gong* and Scott Wedge

Tanner Research, Inc.

2650 East Foothill Blvd.

Pasadena, CA 91107

jian.gong@tanner.com, scott.wedge@tanner.com

The hybrid finite element method (HFEM) is a powerful approach for modeling printed circuit antennas. By combining finite element and integral equation approaches the hybrid technique allows precision modeling of open antenna configurations that include complex substrates and feeding structures. A difficulty with using the HFEM technique is the lack of an automated mesh refinement procedure that achieves a good balance between accuracy and efficiency. Excellent results can be obtained using manual mesh refinement, but this requires *a priori* knowledge of the physics. Needed is an automated procedure that can guarantee accuracy within pre-defined tolerances.

Automatic mesh refinement is driven by an error estimation scheme. In practice, error estimators are highly problem dependent, and there exists no universal scheme that can be applied to a broad set of physical problems. Our work has been to develop an error estimator for electromagnetic analysis that is particularly well-suited for the hybrid finite element method.

This presentation is concerned with HFEM mesh refinement for printed antennas. We have been investigating the following issues:

- Error estimators suited for hybrid FEM in electromagnetic simulations
- Effect of the BEM global truncation in error estimation on performance
- Proper approaches for error specification in antenna modeling
- Performance comparison of automated versus manual refinement schemes

We will present results of a mesh generation and refinement scheme based on posteriori error estimation. The above error estimation issues will be discussed as they pertain to hybrid FEM analysis of printed antennas. We will also discuss the tradeoff between efficiency and accuracy, and the development of an optimal analysis methodology.

A Hybrid Frontal-FEM/BIE/PO Formulation for Analyzing Scattering from Large and Complex Jet Engine Inlets

Guo-Xin Fan¹ and Jian-Ming Jin

Electromagnetics Laboratory

Department of Electrical and Computer Engineering
University of Illinois at Urbana-Champaign
Urbana, Illinois 61801

Scattering from jet engine inlets contributes significantly to the overall radar cross section (RCS) of an airplane. Accurate and efficient modeling of scattering from engine inlets is one of the most challenging topics in computational electromagnetics. Consequently, a variety of numerical methods have been proposed in recent years. In this work, we present a hybrid formulation which combines the finite element method (FEM), incorporating the frontal algorithm, with the boundary integral equation (BIE) and physical optics (PO) or other high frequency methods to model scattering from large and complex engine inlets.

Through the application of the equivalence principle, the total scattering of an airplane can be divided into two parts: the structural scattering and the inlet scattering. The former is contributed by the surface of the airplane with the front apertures of the inlets covered by a perfect conductor. The latter is contributed by the inlets, which corresponds to the radiated field of the equivalent magnetic currents on the apertures. The structural scattering can be calculated by any of the well-established high frequency methods, such as physical optics (PO) and the shooting and bouncing ray (SBR) method. The inlet scattering is formulated by the FE/BIE method in this work.

The important issue in this work is the application of the frontal algorithm for the solution of the FE/BIE matrix equation, which was first proposed by Jeng (*IEEE Trans. Antennas Propagat.*, vol. 38, pp. 1523-1529, Oct. 1990). In the frontal algorithm, the assembly and elimination of the FEM matrix elements are carried out at same time, and, thus, no global stiffness matrix has to be stored. The maximum computer memory requirement is only for the elements at the front, which corresponds to the elements on each cross-section of the inlet. This greatly reduces the total memory requirement, as well as the computation time, especially for deep inlets.

The algorithm and computer program are carried out for a two-dimensional model using a modified general-purpose frontal computer program. Because of the flexibility of the FEM, as well as the generality of the frontal program, inlets of arbitrary shape coated with any inhomogeneous material can be modeled. The computer codes have been tested for many existing examples, and excellent agreement is obtained for both TE and TM polarizations. Several application examples, including an S-shaped waveguide cavity with a triangular and half-circular termination, are given, together with the specific memory and CPU time requirements. The algorithm can be extended to the modeling of three-dimensional inlets.

¹Guo-Xin Fan is now with Klipsch School of Electrical and Computer Engineering, New Mexico State University, Las Cruces, NM 88003.

Improved Accuracy in Microwave Absorber Analysis with a Higher-Order Hybrid Finite Element Method

Yi-Qun Jiang* and Anthony Q. Martin

Department of Electrical and Computer Engineering
P. O. Box 340915, Clemson University, Clemson, SC 29634
anthony.martin@ces.clemson.edu

A hybrid finite element method (HFEM) for 3D periodic structures, first proposed by Mias et al. (*COMPEL. Int. J. Comput. Math. Electr. Electron. Eng.*, **13**, Suppl. A, 393-398) and by McGrath and Pyati (*Radio Sci.*, **31**, 1173-1179, 1996) has been applied to study the scattering properties of doubly periodic microwave absorbers which are used extensively in electromagnetic anechoic chambers for in-door measurements. As a first step, we have employed the lowest-order vector basis functions defined on tetrahedra in the periodic HFEM formulation (Y-Q. Jiang and A. Q. Martin, *National Radio Science Meeting Digest*, 5-8 January 1998, University of Colorado, Boulder, Colorado, pp. 125). These functions provide a constant tangential and linear normal (CT/LN) representation of the field on mesh edges and require 6 unknowns for a single tetrahedron. As expected, numerical results reveal that the HFEM formulation with CT/LN elements is, without the use of special-purpose meshing, unable to yield accurate results when the reflection from the absorber is very low. While it is generally understood that in such cases accuracy can be improved through the use of mesh refinement techniques, such techniques lead to very complex meshes that are difficult to generate without the aid of an automated mesh generation tool. Savage and Peterson (*IEEE Trans. Microwave Theory Tech.*, vol. 44, No. 6, 1996) have shown that higher-order basis functions applied in the FEM formulation to a rectangular cavity yield improved accuracy and efficiency over the lowest-order CT/LN bases and permit no spurious modes to corrupt the solution. A drawback to using higher-order basis functions is that more unknowns are created for a given mesh. However, a possible advantage to using them is that one may be able to lessen the need for mesh refinement to achieve good accuracy. In this work we investigate the use of the higher-order basis functions which provide a linear tangential and quadratic normal (LT/QN) representation of the field at edges in the mesh. For an individual tetrahedron these functions lead to 20 unknowns, two associated with each of the six edges and two associated with each of the four faces. We describe how the LT/QN elements are employed in the periodic HFEM and present results that show their performance in providing improved accuracy and efficiency for scattering from microwave absorber.

A Hybrid Technique for Axisymmetric Scatterers with Appendages

Andrew D. Greenwood* and Jian-Ming Jin

Center for Computational Electromagnetics

Department of Electrical and Computer Engineering

University of Illinois

Urbana, Illinois 61801

*Also affiliated with Air Force Research Laboratory at Rome/IFSB,
Rome, NY 13441

A hybrid technique is developed to compute scattering from a complex body of revolution (BOR) with appendages. The scattering is computed in two steps. First, the finite element method (FEM) is used to compute the scattering from the BOR with the appendages removed. Then, the method of moments (MoM) is used to compute the scattering from the appendages, and the two methods are combined using the field equivalence principle. Because the appendages need not possess rotational symmetry, the method is more versatile than a BOR method alone.

The complex BOR is composed of perfect conductor and impedance surfaces and arbitrary inhomogeneous materials. The FEM is chosen for this target because it models inhomogeneous materials with less computational complexity than the method of moments (MoM), and it models arbitrary shapes more conveniently than the finite difference method (FDM). Past FEM formulations for BOR scattering use either the coupled azimuth potential (CAP) formulation or the three-component, node-based formulation. The three-component, node-based formulation has the advantage of yielding all components of either the electric field or the magnetic field directly. However, using this formulation it is difficult to enforce the proper boundary conditions at material discontinuities and sharp conductor edges, and the results suffer from spurious modes. To preserve the advantage of finding all components of the electric field or the magnetic field directly, while eliminating spurious modes and the difficulty in enforcing boundary conditions, this new method uses edge-based vector basis functions to expand the transverse field components and node-based scalar basis functions to expand the angular component. The FEM mesh is truncated with a perfectly matched layer (PML) in cylindrical coordinates. The use of PML in cylindrical coordinates avoids the wasted computation which results from a spherical mesh boundary with an elongated scatterer. It also avoids the necessity of placing an approximate absorbing boundary condition far from the scatterer.

The appendages on the BOR are composed of perfect conductor and impedance surfaces, and they need not possess rotational symmetry. The MoM is used to compute equivalent currents on the appendage surfaces based on the incident fields, which are computed by the FEM. The two methods are combined using the field equivalence principle such that all significant interactions are considered.

A Hybrid Method for Computing Zero-Sequence Impedance of Underground Three-Phase Pipe-Type Cables

Xiao-Bang Xu* and Guanghao Liu

Department of Electrical and Computer Engineering

Clemson University

Clemson, SC 29634-0915

Underground three-phase pipe-type cables are widely used in power transmission systems in urban areas. To protect such systems, the utilities engineers need to properly size circuit breakers based on knowledge of the fault currents. For an accurate calculation of the fault currents, it is necessary to know the zero-sequence impedance of the underground pipe-type cable. The method currently most widely used in industry for calculating the zero-sequence impedance is based on a paper by J.H. Neher published in 1964 (J.H. Neher, "The phase sequence impedance of pipe-type cables," IEEE Transactions on Power Apparatus and Systems, Vol. PAS-83, pp. 795-804, August 1964). Neher indicates that in the usual case where the pipe is made of steel, the zero-sequence impedance depend upon the permeability of the steel. It is well known that the permeability of steel changes with the magnetic field intensity. Since the magnetic field intensity varies in the steel pipe, the permeability should be different from point to point in the pipe. But, unfortunately, in Neher's computational model, a *constant* "effective permeability" is used for the *whole* steel pipe and the magnetic field intensity used for calculating the "effective permeability" is obtained from an empirical formula. Neher states, "the difference between the calculated and measured results is within 19% for R and 35% for X".

In this paper, we present an improved method for computing the zero-sequence impedance of a underground three-phase pipe-type cable. The core of such a computation is the determination of magnetic vector potential everywhere within the pipe-type cable. To determine the magnetic vector potential, a numerical technique is developed based on a hybrid finite-element and boundary integral equation formulation (L.W. Pearson, A.F. Peterson, L.J. Bahrmasel, and R.A. Whitaker, IEEE Transactions on Antennas and Propagation, Vol. 40, No. 6, pp. 714-729, June 1992). The finite element method is employed to analyze the region within the pipe-type cable, and the boundary integral equation method is for treating the exterior region. The electromagnetic fields in these two regions are coupled on the outer surface of the pipe. In the development of the numerical technique, special attention is paid to the nonlinear B-H characteristic of the ferromagnetic pipe. An iterative solution procedure is developed for determining the relative permeability in each element of the ferromagnetic pipe. The knowledge of the varying permeability in the pipe is then used to solve for the magnetic vector potential.

Application of MBPE in Conjunction with Hybrid FEM/MoM Technique

C. J. Reddy*

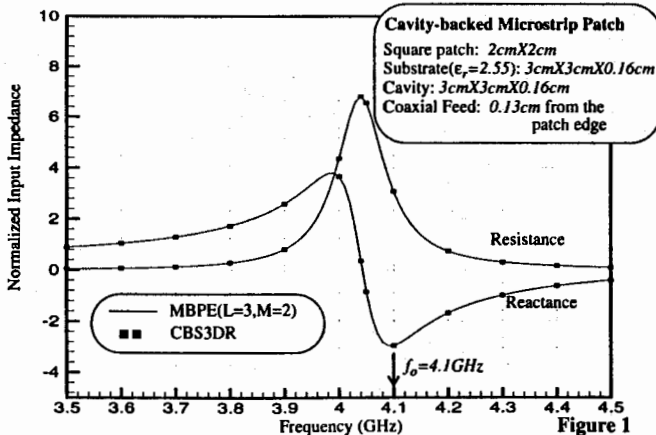
Dept. of Electrical Engg. ViGYAN Inc.
Hampton University Research Drive
Hampton VA 23668 Hampton VA 23666

M.D.Deshpande

C.R.Cockrell and F.B.Beck
Mail Stop 490
NASA Langley Research Ctr.
Hampton VA 23681

ABSTRACT

Hybrid Finite Element Method(FEM)/Method of Moments(MoM) technique has become popular over the last few years due to its flexibility to handle arbitrarily shaped objects with complex materials. One of the disadvantages of this technique is the computational cost involved in obtaining solutions over a frequency range as computations are to be repeated for each frequency over a frequency range. In this paper, application of Model Based Parameter Estimation (MBPE) method (*Burke et al, IEEE Trans. Magn., July 1989*) to hybrid FEM/MoM technique is presented. Hybrid FEM/MoM in conjunction with MBPE is applied to obtain radar cross section of a cavity-backed aperture in an infinite ground plane over a frequency range (*Cockrell et al, NASA TM 110292, 1996, Reddy et al, NASA CR 97-206261, 1997*). MBPE technique is also applied to calculate input characteristics of cavity-backed aperture antennas over a frequency range. In figure 1, normalized input impedance of a cavity-backed square microstrip patch antenna is presented. Comparison of numerical data obtained from MBPE calculations agree well with the values computed at each frequency over the frequency range. More numerical examples will be presented at the conference.



A hybrid FEM based procedure for the scattering from photonic crystals illuminated by a Gaussian beam

G. Pelosi, A. Cocchi

Department of Electronic Engineering, University of Florence
Via C. Lombroso 6/17, I-50134 Florence, Italy

A. Monorchio*

Department of Information Engineering, University of Pisa
Via Diotisalvi 2, I-56126 Pisa, Italy

Recently, interest in photonic crystals has strongly increased due to the possibility of realizing structures with specific frequency selective properties (E. Yablonovitch, *Journal of Modern Optics*, 41, No. 2, 1994). In applied electromagnetics, it is worth mentioning their application for realizing stop-band filters, dielectric waveguides, patch antennas, and planar dielectric reflectors (see for instance M.P. Kasler *et al.*, *Microwave and Opt. Tech. Lett.*, 11, 169-174, 1996). However, we note that several scattering problems presented in the literature on this class of problems have been limited to plane wave illumination conditions.

The purpose of this communication is to provide an efficient numerical procedure for evaluating the field scattered by such structures, when they are illuminated by Gaussian beams. In particular, the incident Gaussian beam is interpreted as a spectrum of both homogeneous and inhomogeneous plane waves. The scattering of each plane wave is analyzed by resorting to a hybrid technique which combines the Finite Element Method (FEM) with a Floquet modal expansion (G. Pelosi *et al.*, *Proc. IEE*, 140, pt. H, 65-70, 1993). Moreover, by applying the Steepest Descent Path (SDP) method, the evaluation of the field at a specific point of the exterior medium, under Gaussian beam illumination, is reduced to the contribution of a single plane wave belonging to the incident spectrum. This strongly increases numerical efficiency.

Extensive numerical results will be shown to demonstrate the effectiveness of the technique, to determine its limits of applicability, and to investigate possible extensions.

An Effective Hybrid FDTD-MoM Technique to Predict Radiation from Enclosures

*Omar M. Ramahi, Digital Equipment Corporation
Bruce R. Archambeault, International Business Machines*

It is evident that the Finite Difference Time Domain (FDTD) method is a viable and highly robust technique capable of addressing a wide variety of radiation problems. However, the FDTD method is a volume-based approach, and this makes it highly inefficient, if not impractical, in addressing structures with electrically large dimensions. Furthermore, when the FDTD is intended for wide-band simulation, the electrical size of the structure can become excessively large to render the simulation impossible, even if a computer with the largest memory is used. On the opposite side of the computational codes spectrum is the Method of Moments (MoM). The MoM is a surface-based technique, and thus it is well suited for simulating electrically large structures. Nevertheless, the MoM can be impractical in addressing inhomogeneous structures and complex excitation sources.

In this work, a hybrid technique is devised such that the FDTD method and MoM are combined in a way to allow for the practical and effective prediction of electromagnetic radiation from enclosures with apertures. The technique consists of two stages. In the first, the FDTD method is used to predict the radiation at the aperture of the enclosure. Here the assumption is made that any external structure to the enclosure does not affect, or-to borrow the terminology of circuit theory—does not *load* the interior. It will be shown that this assumption is valid provided external objects such as wires do not lie in the close proximity to the aperture. The second stage consists of using the aperture field as found in stage one as a source for the MoM that will now characterize the exterior problem.

Results will be provided to show that the proposed hybrid technique can be highly effective, thus permitting the numerical simulation of enclosures that exist in the presence of external wires or other detached structures having electrically large dimensions. A natural, yet very powerful, extension of this technique is then presented to show that perfectly conducting ground planes can be included in the simulation without additional complexity or cost. This extension is proven to be important in the context of numerical modeling encountered in electromagnetic compatibility and interference studies.

Analysis of MICs with Curved Surfaces Using a Hybrid FDTD-FVTD Algorithm on an Orthogonal Rectangular Grid

¹*Mingwu Yang, ¹*Yinchao Chen, and ²*Raj Mittra***

¹*Department of Electronic Engineering*

Hong Kong Polytechnic University, Hong Kong

²*EMC Research Laboratory, 319 EEE, Penn State, University Park, PA*

One of the most significant drawbacks of the conventional Finite Difference Time Domain (FDTD) method is its inability to accurately model curved surfaces that are frequently encountered in practical MIC circuits, and are approximated by using a staircasing approach. Previous attempts to overcoming this difficulty and to reducing the effect of discretization error have resulted in various modified versions of the FDTD, e.g., FDTD on a curvilinear grid, contour-path integral FDTD and the hybrid FDTD-FVTD technique.

In this paper we present a hybridization of the finite difference and finite volume time domain (FDTD-FVTD) algorithms on an orthogonal rectangular grid to analyze MICs with curved surfaces. Our objective is to retain the simplicity of rectangular grid generation, and still maintain the ability to handle curved surfaces accurately. We accomplish this by using the FDTD in the regions where the objects are describable with a rectangular mesh, and switch to the FVTD in the regions where the object surfaces are curved. We note that the electromagnetic fields in the FDTD Yee cells are defined at their edges and normal centers, while those in the FVTD are usually located at the centers of the electric and magnetic cells, respectively. We retain a few overlapping layers between the FDTD and FVTD regions for the purpose of updating the electromagnetic fields in the latter region by using field interpolation. For the cells that contain two or more different material media, we express the fields only in the context of the FVTD by using the interface boundary conditions, and update them by evaluating the volume integral of the Maxwell's equations over a single cell. Experience shows that the proposed FDTD-FVTD algorithm requires only a little increase in CPU time and memory as compared to the conventional FDTD.

To illustrate the application of the method we use it to compute the S-parameters of a dielectric resonator (DR) band-stop filter, comprising a cylindrical dielectric resonator with a circular cross-section, which is coupled to a microstrip line. We show that the hybrid FDTD-FVTD approach yields results for the filter that are more accurate than those derived by using the staircased FDTD approximation.

Numerical Modeling of Antennas with Nonlinear Lumped Elements via a Hybrid FETD-FDTD Method

S. Selleri, J.Y. Dauvignac, Ch. Pichot*

*Laboratoire d'Electronique, Antennes et Télécommunications
Université de Nice-Sophia-Antipolis, CNRS UPRESA 6071
250 Rue A. Einstein, Bât. 4 - 06560 Valbonne, FRANCE*

G. Pelosi

*Electronic Engineering Department, University of Florence
Via C. Lombroso, 6/17 - 50134 Florence, ITALY*

Recently, a hybrid technique combining the Finite Element Time Domain (FETD) and the Finite Difference Time Domain (FDTD) methods has been proposed by (R.B. Wu, T. Itoh, IEEE Trans. Antennas Propagat., 45, 1302-1310, 1997). This hybrid technique is intended to exploit at the same time the different advantages of both methods. In particular, the FDTD technique, besides its inherent implementation simplicity, exhibits very good Absorbing Boundary Conditions (ABC) while presenting serious shortcomings in modeling complex geometries. On the other hand, the FETD method can handle very efficiently complex geometries, but may present high computational costs.

In this contribution, this new technique is extended to treat nonlinear devices. In particular, as a test case, a broadband Vivaldi antenna, connected to various receiving circuit elements, is globally analysed. The antenna, exhibiting a complex geometry, is treated via the FETD technique, thus avoiding the problem of the staircase approximation typical of the FDTD method. The receiving circuit, particularly nonlinear lumped elements, is treated via the FDTD method, because its handling via the FETD method is more complex. The receiving circuit can include a mixer (diode) and local oscillator. This requires to treat an inhomogeneous interface between the two methods, instead of a homogeneous one.

The code validity and its limitations will be presented, showing how the hybrid method allows to use coarser FDTD discretization in the homogeneous area of the domain and how the structure can be globally analysed. Numerical results will be validated with experimental measurements when available.

Efficiency Issues In Integral Equation Computations

Y. Leviatan and E. Michielssen

On the Location of Expansion Centers for the Generalized Multipole Technique for Scattering from Two-dimensional Smooth Scatterers.....	102
<i>F. W. Forest, J. E. Richie*, Marquette University, USA</i>	
Perturbation Formula for the Complex Natural Frequencies of an Object in the Presence of a Layered Medium from an Integral Equation Formulation	103
<i>G. W. Hanson*, University of Wisconsin, USA, C. E. Baum, Phillips Laboratory, USA</i>	
Large-scale, Low-cost Parallel Computers Applied to Reflector Antenna Analysis	104
<i>D. S. Katz*, T. Cwik, California Institute of Technology, USA</i>	
Optimization and Parallelization of GMRES for Very Large Dense and Hybrid Systems.....	105
<i>M. W. Nurnberger*, M. Smelyanskiy, J. Volakis, University of Michigan, USA</i>	
Reduced Matrix Technique	106
<i>M. Waller*, J. Dean, T. Shumpert, Auburn University, USA</i>	
Usage of Hilbert Matrices in the Reduced Expansion and Field Testing (REFT) Method for Matrix Thinning	107
<i>B. Z. Steinberg*, R. Kastner, E. Gershon, Tel-Aviv University, Israel</i>	
Scattering from a Closed Body Above a Rough Surface using the Method of Ordered Multiple Interactions	108
<i>R. J. Adams, B. A. Davis*, G. S. Brown, Virginia Tech, USA</i>	
Efficient Method of Moments Technique for Large 3D Conducting Scattering Problems using High-frequency Current Spectrum Extraction.....	109
<i>D. Kwon*, R. J. Burkholder, P. H. Pathak, Ohio State University, USA</i>	
Two Parameter Generalized Krylov-based Reduced Order Modeling of Multiscreen Frequency Selective Surfaces	110
<i>D. S. Weile*, E. Michielssen, University of Illinois at Urbana-Champaign, USA, K. Gallivan, Florida State University, USA</i>	
Analysis of a Helix Antenna using a Moment Method Approach with Curved Basis and Testing Functions	111
<i>E. D. Caswell*, W. A. Davis, Virginia Polytechnic Institute and State University, USA</i>	
Approximated Closed-form Spatial Anisotropic Microstrip Green's Function	112
<i>B. Popovski*, V. Arnautovski, L. Grcev, B. Spasenovski, Faculty of Electrical Engineering, Macedonia</i>	

On the Location Of Expansion Centers for the Generalized Multipole Technique For Scattering From Two-Dimensional Smooth Scatterers

Francis W. Forest and J. E. Richie*

Department of Electrical and Computer Engineering
Marquette University

P.O. Box 1881, Milwaukee, WI 53201-1881

The generalized multipole technique (GMT) used to compute scattering from homogeneous objects in two and three dimensions is a powerful method that is based on the use of multipole solutions to the Helmholtz wave equation. The multipoles are not required to all be at a single global origin. The use of multiple origins and multipoles of low order is a unique method of improving the convergence of the solution, from that of the classical single origin multipole expansion.

However, the choice of location and order of the multipoles is not clearly understood. Rules for the placement of multipole origins in the vicinity of flat boundaries are available. It is still unclear how the order and placement of multipoles affects or improves the solution for curved bodies.

We have found that the use of monopoles in two-dimensional problems such as scattering from cylinders with smooth cross sections can result in accurate solutions if the origins are chosen

- equally spaced in arc length around the boundary,
- are placed perpendicular to the boundary, and
- are placed a distance away from the boundary that is related to the radius of curvature of the boundary.

In addition, it has been found that the change in the radius of curvature can be used as a measure of the best order for the multipole.

Example solutions to scattering from circular and elliptical cylinders of homogeneous dielectric will be presented to illustrate the aforementioned guidelines. In addition, a boundary consisting of an ellipse over 180 degrees and a circle over the remaining 180 degrees so the symmetry of the cylinder is broken will also be presented to verify the proposed guidelines. Solutions were verified by examination of the boundary condition error along the boundary and the average error in the boundary conditions over the entire interface. It has been found that the monopole solution is often quite accurate, and dipoles were used when the change in the radius of curvature was large, especially near the transitions between the elliptical and circular portions of the combined boundary.

**Perturbation Formula for the Complex Natural Frequencies of an
Object in the Presence of a Layered Medium from an Integral
Equation Formulation**

George W. Hanson

Department of Electrical Engineering and Computer Science

University of Wisconsin-Milwaukee

P.O. Box 784

Milwaukee, Wisconsin 53201

Carl E. Baum

Phillips Laboratory

3550 Aberdeen Avenue SE

Kirtland AFB, NM 87117-5776, USA

It is well known that the natural frequencies of an object are important distinguishing features which can be used in target detection and discrimination schemes, and are generally recognized as aiding in the physical interpretation of electromagnetic interaction data. These natural frequencies are governed by the size, shape, and material composition of the object, as well as the environment in which the object resides. While traditionally natural frequencies have been computed for finite-sized objects in free-space, recently there has been some attention devoted to the determination of the natural frequencies of an object in the presence of a layered medium. Such efforts have been directed towards accounting for realistic environments such as an air-sea or air-ground interface in target detection and identification schemes. Since a given object of interest may reside in many different environments, it is of interest to relate the natural frequencies of an object when in free-space to the natural frequencies of the same object when immersed in a non-homogeneous environment. In this paper a perturbation formula is developed which relates the free-space natural frequencies of an object to those of the same object in the presence of a planarly layered medium. The perturbation formula arises from an exact integral equation formulation for the planarly layered problem, and is valid for intermediate spacing between the object and the nearest planar interface. Numerical results are shown for the natural frequencies of a wire in the presence of a layered medium.

Large-Scale, Low-Cost Parallel Computers Applied to Reflector Antenna Analysis

Daniel S. Katz, Tom Cwik*

*Jet Propulsion Laboratory
California Institute of Technology
4800 Oak Grove Drive, MS 168-522
Pasadena, CA 91109
d.katz@ieee.org*

This paper discusses the use of medium- to large-scale Beowulf-class computers in reflector antenna analysis, based on a discrete approximation of the radiation integral. Beowulf-class computers are defined as piles of PCs running LINUX, using fully mass-market, commercial, off-the-shelf (M²COTS) components. The Beowulf-class systems used in this work consist of Pentium Pro processors and fast Ethernet (100Base-T) networking. Small systems can be purchased for approximately \$1,700 per node as of December 1997. The system used in this work (named Naegling, and located at the California Institute of Technology) has been used in an n-body gravitational simulation with performance of over 10 GFLOPS.

The physical optics (PO) code used in this work (W. A. Imbriale and T. Cwik, "A Simple Physical Optics Algorithm Perfect for Parallel Computing Architecture," *10th Annual Review of Progress in Appl. Comp. Electromag.*, pp. 434-441, 1994) is based on a discrete approximation of the radiation integral (W. A. Imbriale and R. E. Hodges, "The Linear-Phase Triangular Facet Approximation in Physical Optics Analysis of Reflector Antennas," *Appl. Comp. Electromag. Soc. J.*, v. 6, pp. 52-73, 1991). This calculation replaces the actual reflector surface with a triangularly faceted representation so that the reflector resembles a geodesic dome. The PO current is assumed to be constant in magnitude and phase over each facet so the radiation integral is reduced to a simple summation. This program has proven to be surprisingly robust and useful for the analysis of arbitrary reflectors, particularly when the near-field is desired and the surface derivatives are not known.

This paper will include discussion of the parallelization of the PO code, as well as computational results obtained on varying numbers of processors of Naegling, up to the full machine size (currently 140 processors). The computational results will be compared with results obtained from other machines, such as the Intel Paragon and the Cray T3D.

Optimization and Parallelization of GMRES for Very Large Dense and Hybrid Systems

M.W. Nurnberger*, M. Smelyanskiy, and J.L. Volakis

Radiation Laboratory
Dept. of Elec. Engin. & Comp. Sci.
University of Michigan, Ann Arbor, MI 48109-2122

Abstract

As RCS simulations are applied to larger and more complex targets such as airborne vehicles, antennas, circuits, etc., the need for faster and more efficient solvers for both dense and hybrid systems becomes more acute. In the past both direct solvers (LU) and simple iterative solvers (CG, BCG, etc.) have been used. However, these are often limited by memory usage, solution time and convergence difficulties for large and ill-conditioned systems. A solver based on the Generalized Minimum RESidual (GMRES) method offers an attractive compromise between efficiency and robustness for the difficulties mentioned above. As is often the case, a high degree of parallelization is also necessary to achieve the best performance.

The GMRES solver is designed to solve nonsymmetric linear systems using Arnoldi's procedure for the generation of an orthogonal basis in a Krylov space of dimension m . Arnoldi's procedure involves a matrix-vector product, a vector inner product, and an optional preconditioning step, and is the most time-consuming portion of the solver. Optimization and parallelization efforts will thus be focused here, and various modifications to the Arnoldi procedure that emphasize accuracy and/or speed will be examined to determine the most advantageous solution.

A restarted version of GMRES will be used to control storage requirements, and an investigation into the automatic choice of the number of restarts will be made. Parallelization and optimization will be performed on an IBM SP/2 for optimum portability to other distributed- and shared-memory machines. Performance estimates and examples for both dense and highly-sparse systems of varying size (5k – 50k DOF) will be presented, as well as findings regarding the automated choice of the number of restarts.

Reduced Matrix Technique

*M. Waller, J. Dean, and T. Shumpert
Electrical Engineering Dept.
Auburn University, AL 36849-5201

In many antenna and scattering problems where the solution for near-field parameters, such as the induced current distribution, input impedance, etc., is desired in and near the resonance region, the traditional subsectional basis Method of Moments (MoM) still provides one of the most reliable and robust approaches. Unfortunately, this traditional subsectional MoM solution approach usually requires the inversion of extremely large (often prohibitively large), dense, complex number matrices. In addition, when the geometry of the antenna/scatterer changes or the electrical (constitutive) parameters change, appropriate areas of the corresponding (dense) complex MoM matrix change accordingly. Other portions of the original complex MoM matrix remain unchanged. However, since the actual solution (inversion of the MoM impedance/admittance matrix) depends on all matrix elements (changed and unchanged), the inversion of the complete (dense) MoM matrix must be repeated over and over again as the geometrical/electrical changes occur.

In this paper, the authors utilize a little-known matrix inversion relationship to offer a more efficient approach for determining the induced current (and other related near-field parameters) in the resonant frequency regime for antenna/scattering problems. In particular, this reduced matrix technique exhibits significant efficiency for antenna/scattering problems where parts of the geometry change or the electrical parameters of a part of the antenna/scatterer change. Specific illustrations of the reduced matrix technique are applied to several different wire antenna/scatterer geometries to calculate the natural frequencies (Laplace domain poles) and natural modes as the geometrical/electrical parameters change. Although the examples in this paper are limited to wire structures, this reduced matrix technique is equally applicable for surface (polygonal patches) formulations and volume (polyhedral cells) formulations. Finally, this reduced matrix technique often leads to additional physical insight into how geometrical/electrical changes affect the desired or sought-after results for certain near-field, resonant region antenna/scattering parameters.

USAGE OF HILBERT MATRICES IN THE REDUCED EXPANSION AND FIELD TESTING (REFT) METHOD FOR MATRIX THINNING

B. Z. Steinberg, R. Kastner* and E. Gershon

Faculty of Engineering, Tel-Aviv University, Tel-Aviv 69978, Israel

The REFT (Reduced Expansion and Field Testing) method has been recently refined (Steinberg and Kastner, Proc. 1997 URSI meeting, July 13-18, pp. 76), as a systematic procedure, whereby the active number of both testing and basis functions is reduced to a minimum. To facilitate this reduction, both column and row operations are carried out by using the linear transformation $\mathbf{B} \cdot \mathbf{A} \cdot \mathbf{B}^T \cdot \mathbf{V} = \mathbf{B} \cdot \mathbf{E}^{inc}$, where the unknown current distribution is $\mathbf{J} = \mathbf{B}^T \cdot \mathbf{V}$, and \mathbf{B} is a member of the Hilbert matrix family of orthogonal matrices, and whose elements are either 1 or -1. Matrices of higher orders are generated recursively from low orders as follows:

$$H_{2^{n+1}} = H_{2^n} \otimes H_2$$

where \otimes is the Kronecker tensor product. The lowest order matrix is

$$H_2 = \begin{pmatrix} 1 & 1 \\ 1 & -1 \end{pmatrix}, \text{ such that } H_4 = H_2 \otimes H_2 = \begin{pmatrix} 1 & 1 & 1 & 1 \\ 1 & -1 & 1 & -1 \\ 1 & 1 & -1 & -1 \\ 1 & -1 & -1 & 1 \end{pmatrix},$$

$$H_8 = H_4 \otimes H_2 = \begin{pmatrix} 1 & 1 & 1 & 1 & 1 & 1 & 1 & 1 \\ 1 & -1 & 1 & -1 & 1 & -1 & 1 & -1 \\ 1 & 1 & -1 & -1 & 1 & 1 & -1 & -1 \\ 1 & -1 & -1 & 1 & 1 & 1 & -1 & -1 \\ 1 & 1 & 1 & 1 & -1 & -1 & -1 & -1 \\ 1 & -1 & 1 & -1 & -1 & 1 & -1 & 1 \\ 1 & 1 & -1 & -1 & -1 & -1 & 1 & 1 \\ 1 & -1 & -1 & 1 & -1 & 1 & 1 & -1 \end{pmatrix},$$

and so on. Hilbert matrices have the property $H_N \cdot H_N = NI_N$ i.e., the matrix $\frac{1}{\sqrt{N}} H_N$ is unitary. They also form the basis for the Walsh-Hadamard transform. Using this transformation, the matrix $\mathbf{B} \cdot \mathbf{A} \cdot \mathbf{B}^T$ can be thinnned by about 90%, using a suitable threshold. The far field accuracy is excellent in most cases, however the near field has an additive, non-radiating error. This error can be reduced, as preliminary results show.

Scattering from a Closed Body Above a Rough Surface Using the Method of Ordered Multiple Interactions

Robert J. Adams, Bradley A. Davis *, and Gary S. Brown
ElectroMagnetic Interactions Laboratory
Bradley Department of Electrical Engineering
Virginia Tech, Blacksburg, VA 24061-0111

The method of ordered multiple interactions (MOMI) is a robust iterative method proposed by Kapp and Brown (*IEEE A&P*, 44(5), 711-721, 1996) for solving the reduced wave equation in two dimensions in the presence of an extended rough surface having either Neumann or Dirichlet boundary conditions. We have recently extended this method to the case of TE scattering from perfectly conducting elliptical cylinders of infinite extent using a combined field integral equation. An important aspect of this work has involved the determination of an optimal combined field formulation (optimality is determined by the convergence rate of the resultant MOMI series). For an isolated elliptical scatterer, the amount of the EFIE added to the MFIE in forming the optimal CFIE has been found to approach an asymptotically constant value as the size of the scatterer increases.

The problem addressed in this presentation considers the moments of the field scattered from an infinite elliptical cylinder located above a randomly rough, corrugated surface. Numerically, the interaction between the closed body and the rough surface leads to a different optimal combined field formulation than that obtained for either an elliptical body or a rough surface in isolation. Furthermore, as the scatterer is moved closer to the rough surface, the interactions between the two objects become stronger and a reduced rate of convergence is observed. The effect of the ordering of the surface current unknowns in the matrix equation's unknown vector on this rate of convergence will be presented.

Having thus discussed the numerical challenges posed by this scattering geometry, we proceed with an analysis of the statistical moments of the scattered fields. The scattered fields are evaluated using both the exact integral representation discussed above and using the simple superposition approximation whereby all interactions between the cylinder and the rough surface are ignored. Criteria for the evaluation of the scattered field ranging from zero to full interaction are presented based on a given parameter space for the problem. These parameters include the eccentricity of the ellipse, the ratio of the largest dimension of the ellipse to its height above the mean surface, the tilt of the ellipse with respect to the mean surface, and the statistics of the rough surface.

**Efficient Method of Moments technique for large 3D conducting
scattering problems using high-frequency current spectrum
extraction**

D.-H. Kwon*, R. J. Burkholder, and P. H. Pathak

The Ohio State University ElectroScience Laboratory
1320 Kinnear Rd., Columbus, Ohio 43212

A robust and efficient numerical method is presented for analyzing electromagnetic (EM) scattering from three dimensional (3D) conducting bodies using high-frequency current spectrum extraction. Conventional direct-solve integral equation methods for scattering analysis such as the Method of Moments (MM) suffer from storage requirements and computing time of $\mathcal{O}(N^2)$ and $\mathcal{O}(N^3)$, respectively, for N unknown systems, which are not practical for electrically large bodies. Induced currents on large smooth portions of an electrically large scatterer can be represented by a small set of current waves propagating in different directions with corresponding wave numbers, and with slowly varying amplitudes. From a high-frequency point of view, these current directions are almost insensitive to frequency variation. Therefore, if one can obtain the surface wave characteristics of the induced current, it is possible to place a set of smartly chosen basis functions on the smooth portions of the body resulting in significant reduction of the unknowns.

Recently, an efficient numerical treatment of EM scattering problems has received great attention in the literature. Altman and Mittra (*IEEE Trans. Antennas Propagat.*, 44, 548-553, 1996) used an extrapolation technique with MM to analyze scattering from bodies of revolution. They define complex exponential entire domain basis functions over the whole smooth regions of their choice, and extrapolate the frequency dependence of the exponential constants. However, entire domain basis functions are hard to obtain except for special geometries and the extrapolation technique has a limited frequency range. One can overcome this deficiency by dividing the smooth region into a group of large patches of optimally chosen sizes which model the geometric variations of the scatterer surface. In the immediate vicinity of edges or corners, a conventional set of subsectional basis functions needs to be defined to account for singularities of the fields. It is demonstrated that one can reduce the number of unknowns drastically with little degradation in accuracy by choosing smart basis functions and proper testing procedures. It is also noted that this method can be easily incorporated into existing MM codes.

Two Parameter Generalized Krylov-Based Reduced Order Modeling of Multiscreen Frequency Selective Surfaces

D. S. Weile and E. Michielssen*

*Department of Electrical and Computer
Engineering
University of Illinois at Urbana-
Champaign
1406 W. Green St., Urbana IL 61801*

K. Gallivan

*Computer Science Department
Florida State University
203 Love Building, Tallahassee, FL
32306*

Multiscreen Frequency Selective Surfaces (FSSs) have been used in electromagnetic systems as satellite dish antenna subreflectors, radomes, and angular filters over a large portion of the spectrum. While a plethora of methods exists for the numerical simulation of FSSs excited by incident plane waves, the spectral Galerkin derivative of the Method of Moments (MoM) has been used most often because of its accuracy and simplicity (R. Mittra et al., Proc. IEEE, 76, pp. 1593-1615). Unfortunately, iterating the MoM to characterize the reflection coefficient of an FSS over a large band of frequencies and a large range of incident angle can be computationally expensive. A typical multiscreen FSS design may be modeled with hundreds or thousands of basis functions, and for each angle/frequency combination, the solution procedure involves infinite summations in the construction of the MoM matrix, as well as its inversion.

To accelerate the characterization of FSSs, this study introduces a model reduction algorithm based on the notion of a generalized Krylov subspace. Specifically, the method presented here results in a small system that simultaneously approximates the behavior of the FSS over a band of frequencies and a range of incident angles. This is to be contrasted with other model reduction methods, in which the only independent parameter is frequency, and a new model would need to be constructed for each angle of incidence.

The two-parameter model reduction of FSSs proceeds in two steps: linearization and reduction. During the linearization step, the system provided by the MoM is approximated by a polynomial interpolant resulting in a system with linear frequency dependence. During the reduction step, a reduced system is produced that matches the reflection coefficient of the linearized system and its derivatives at several frequency/angle combinations within the frequency band and angular range of interest. The reduction is made possible through the introduction of a generalized Krylov space that can be shown to be intimately related to linear systems that linearly depend on two parameters.

The definition of the generalized Krylov subspace, its relation to model order reduction, and several applications to FSS scattering problems will be presented.

Analysis of a Helix Antenna Using a Moment Method Approach With Curved Basis and Testing Functions

E.D. Caswell* and Dr. W.A. Davis

**The Bradley Department of Electrical and Computer Engineering
Virginia Polytechnic Institute and State University
Blacksburg, VA 24061-0111**

Typically curved wire antenna structures are modeled by approximating curved structures with straight wire segments. The straight wire approximation yields accurate results, but often requires a large number of segments to adequately approximate the antenna geometry. The large number of straight wire segments or unknowns requires a large amount of memory and time to solve for the currents on the antenna. By using curved segments to exactly describe the contour of the antenna geometry the number of unknowns can be reduced, thus allowing for bigger problems to be solved accurately.

This paper focuses on the analysis of a helical antenna. The Method of Moments is used to solve for the currents on the antenna with both triangle basis and pulse testing functions following the contour of the helix precisely. The thin wire approximation is used throughout the analysis. The helix is assumed to be oriented along the z-axis with an optional perfectly conducting ground plane in the x-y plane. For simplicity, a delta gap source model is used. Straight feed wires may be added to the helix and modeled similarly to the helix using the Method of Moments with triangular basis and pulse testing functions.

The primary validation of the curved wire approach is through a comparison with MININEC and NEC. The convergence properties of the antenna input impedance is considered versus the number of unknowns. The convergence tests show that significantly fewer unknowns are needed to accurately predict the input impedance of the helix, particularly for the normal mode helix. This approach is also useful in the analysis of the axial mode helix where the current varies significantly around one turn. The large number of straight wire segments, and thus unknowns, needed to accurately approximate the current around one turn can be greatly reduced by the using this curved segment method.

Approximated Closed-form Spatial Anisotropic Microstrip Green's Function

B.Popovski, V.Arnavovski*, L.Greve, B.Spasenovski

Faculty of Electrical Engineering Karpov II P.O.B. 574 Skopje, Macedonia

e-mail:atvesna@cerera.etf.ukim.edu.mk

In this abstract, a solution of the Sommerfield-type integral when solving the spatial microstrip Green's function due to electric source embedded in anisotropic dielectric layer is presented. By using the spectral theory the electric field due to microstrip structure is expressed in form of spectral Green's function. The examined microstrip structure is characterized by the constitutive parameters ϵ_1 and ϵ_2 . In order to obtain the spatial electric Green's function the integrals to be solved are of the Sommerfield-type form. It is well known that the integral converges very poorly due to the high integrand oscillations when the source and the observer are both on the air-dielectric interface, radially separated.

The approach presented in this abstract is based on the decomposition of the spectral microstrip Green's function in three terms: the quasi-static term dominating in the near-field zone, the contribution from the residue of the poles expressing the surface wave dominating in the far-field zone, and the complex images term dominating in the intermediate zone. Each of the terms obtained by decomposing the spectral electric Green's function has a closed-form solution of its own Sommerfield-type integral.

- For low frequency case the quasi-static term of the spectral Green's function is extracted and solved exactly thus obtaining spatial quasi-static term G_{qs} .
- The influence of the poles of the spectral Green's function is also extracted and solved in closed-form thus obtaining the spatial term of G_{sw} exhibiting the characteristics of the surface wave dominating in the far-field field zone.
- The remaining integrand in the Sommerfield-type integral becomes very smooth, and is approximated in terms of finite sum of complex exponential functions using the Prony's method. In this form it can be solved in closed-form solution thus obtaining the G_{ci} term contributing in the intermediate zone. Thus the final closed-form solution of the spatial electric Green's function takes the form of a sum of three terms: $G_{qs}+G_{sw}+G_{ci}$.

Accuracy of the approximated closed-form solution of the microstrip Green's function for an anisotropic thick dielectric is tested and is proved to be very high for all distances source-observer. The results generally have less than 1% difference between the exact Sommerfield solution and the proposed approach. The proposed approach may be applied for highly efficient moment method solutions drastically reducing the computational time.

Special Session: Antenna Applications of Photonic-Band-Gap Materials
D. H. Yang and K. Agi

Photonic-crystal Antenna Substrates	114
<i>E. R. Brown*, O. B. McMahon, C. D. Parker, MIT, USA</i>	
Theory of Printed Circuits and Antennas on Photonic Band-gap Materials	115
<i>H. Y. D. Yang*, University of Illinois, USA</i>	
Antennas with Photonic Bandgap Structures	116
<i>M. P. Kesler*, J. G. Maloney, Georgia Tech Research Institute, USA, G. Smith, Georgia Institute of Technology, USA</i>	
Dipole Antennas on Three-dimensional Photonic Band Gap Crystals	117
<i>M. M. Sigalas*, R. Biswas, Iowa State University, USA, D. Crouch, Hughes Electronic Corporation, USA, W. Leung, G. Tuttie, K. Ho, Iowa State University, USA</i>	
Electromagnetic Radiation in Photonic Band Gap Materials	118
<i>T. Suzuki*, P. K. L. Yu, University of California San Diego, USA</i>	
Compact Microstrip Patch Antennas on Photonic Crystal Substrates	119
<i>K. Agi*, K. J. Malloy, E. Schamiloglu, M. Mojahedi, University of New Mexico, USA</i>	
Do Two Dimensional Periodic Structures Exhibit Photonic Bandgap Properties?	120
<i>T. Ellis*, J. D. Shumpert, L. P. B. Katehi, G. M. Rebeiz, University of Michigan, USA</i>	
On the Design of Photonic Bandgap Crystal Filters	121
<i>H. J. De Los Santos*, Hughes Space and Communication Co., USA</i>	
Surface Waves Excitation Efficiency for Wave Scattering by Finite Gratings in Dielectric Slab Guide	122
<i>A. S. Andrenko*, M. Ando, Tokyo Institute of Technology, Japan</i>	
Two-dimensional Band-gap Formation in Finite Substrates	123
<i>J. D. Shumpert*, T. Ellis, G. M. Rebeiz, L. P. B. Katehi, University of Michigan, USA</i>	

Photonic-Crystal Antenna Substrates⁺

E. R. Brown, O. B. McMahon, and C. D. Parker
Lincoln Laboratory, Massachusetts Institute of Technology
Lexington, MA 02173-9108

⁺*on leave to the Defense Advanced Research Projects Agency,
Arlington, VA 22203*

A relatively new type of artificial dielectric, called a photonic crystal, offers an elegant and effective solution to the long-standing problem of fabricating high-performance planar antennas on high-permittivity substrates, such as Si or GaAs. The stop band of the photonic crystal rejects the majority of power radiated by an antenna mounted on its surface without shorting out the driving-point impedance. This makes the antenna much more efficient than it would be if mounted on a homogeneous substrate consisting of the same dielectric as the matrix material of the photonic crystal. Antenna characteristics have been measured experimentally for bow-tie and dipole antennas on two types of photonic crystal: (1) conventional (bidielectric) photonic crystals consisting of periodic array of holes filled with air and embedded in a high-dielectric material, and (2) metalodielectric photonic crystals (MDPCs) consisting of a periodic array of metallic spheres embedded in a low-dielectric material. Experiments show that the directive gain can greatly exceed that of the same antenna suspended in free space. For example, a planar $\lambda/2$ dipole yielded a zenithal gain of 10.4 dB at 17.4 GHz with the driving gap mounted in a specific location and orientation on a bidielectric face-centered-cubic (fcc) crystal. Even higher gain was achieved on a fcc MDPC substrate, with the additional benefit of the radiation properties being much less sensitive to the location and orientation of the driving gap. In contrast, the same dipole yielded the typical zenithal gain of approximately 2.0 dB when suspended in free space, and about four times this gain when placed parallel to a metallic plane at a separation of $\lambda/4$. The superior performance of the dipole on photonic crystals can be explained, in part, by a substrate focusing effect, similar to what occurs for feed antennas located at the focal point of reflecting dishes.

Theory of Printed Circuits and Antennas on Photonic Band-Gap Materials

H.Y. David Yang

Department of Electrical Engineering and Computer Science
University of Illinois at Chicago, M/C 154, Chicago, IL 60607-7053

In the last few years, there has been increasing research activities on microwave antenna applications of PBG technology. Printed antennas with controllable PBG material overlay (such as biased ferrites or biased ferroelectric materials) have the potential features of high directivity, high gain, multi-functionality, and beam steering. It has already been demonstrated that a microstrip-element on a dielectric substrate with planar periodic implants has high-gain and high efficiency. High-efficiency is a result of surface-wave elimination by the PBG materials. If the PBG material overlay acts as a frequency selective surface on top of the printed antennas, antenna signatures can be registered in a prescribed way for possible IFF applications, and RCS can be greatly suppressed within the band-gap zone.

This paper presents the fundamental characterization of radiation and scattering properties of integrated antennas (dipoles, patches and slots) with PBG material substrate or overlay. In order to facilitate the analysis, a multi-stage moment method (MSMM) is developed to deal with the problems of antennas and scatterers within periodic structures. This MSMM applies to general periodic structures with anomalies. In the modeling process, there are two vector integral-equations to be solved systematically and sequentially. The first integral equation formulation is to find the electromagnetic fields of an artificial material structure with infinite phased arrays of δ sources. An phased-array matching method transforms the fields due to infinite phased-arrays to those due to a single δ source. Those fields after transformation are dyadic Green's function for the second vector integral equation that is solved to determine the parameters of interest. In this paper, theory that leads to the field solutions of the characteristics of microstrip transmission lines and microstrip dipoles on PBG structure is discussed. The proposed scheme may also apply to more complicated problems such as coplanar waveguides or other types of passive components on PBG structures.

Antennas with Photonic Bandgap Structures

Morris P. Kesler and James G. Maloney

Signature Technology Laboratory
Georgia Tech Research Institute

and

Glenn S. Smith

School of Electrical and Computer Engineering
Georgia Institute of Technology

Atlanta, GA 30332

Photonic Bandgap (PBG) materials have properties that make them attractive for use with antennas. The fact that propagation is not allowed for frequencies in the bandgap region suggests that a PBG material can be useful as a substrate for antennas to enhance the directivity and to suppress the excitation of surface modes in the substrate. Recently, there has been significant interest in this type of application for PBG materials, with theoretical and experimental work involving dipole, slot, microstrip and spiral antennas on PBG substrates appearing in the literature. Much of this work has focused on the field pattern of the antenna-PBG combination.

This thrust of this paper is a more detailed look at the properties of an antenna-PBG combination. In particular, the impact of the PBG material on the impedance and resonance properties of the antenna will be examined. The configuration investigated consists of a strip monopole antenna in front of a three-dimensional PBG crystal. An image plane geometry was used to provide a controlled measurement environment and eliminate the effects of unbalanced excitation. The particular PBG crystal studied was a woodpile structure designed to have a bandgap in the 12-16 GHz frequency region.

Results will be presented of impedance and pattern measurements as a function of monopole length, monopole position, and frequency (both within and outside the bandgap). Selected results will be compared with a full FDTD simulation of the antenna-PBG combination. Comparisons will also be made to predictions based on the reflection plane concept (M. P. Kesler, et al., *Microwave Opt. Technol. Lett.*, 11, pp. 169-174, 1996).

Dipole antennas on three-dimensional photonic band gap crystals

M.M. Sigalas¹, R. Biswas¹, D. Crouch², W. Leung¹, G. Tuttle¹, K-M. Ho¹.

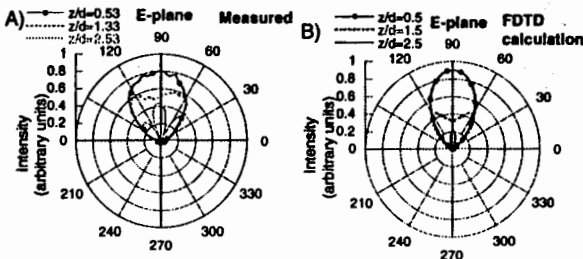
¹Ames Laboratory, Microelectronics Research Center, and
Department of Physics and Astronomy, Iowa State University, Ames IA 50011

²Hughes Electronic Corporation, AET Center,
PO Box 1973, Rancho Cucamonga, CA 91729.

We have measured and calculated the radiation pattern of a dipole antenna on top of and inside a three-dimensional photonic band gap (PBG) crystal. The layer-by-layer PBG crystal, with stacked alumina rods, has a complete stop band between 12 and 14 GHz. We calculated the radiation patterns with the FDTD technique and obtained very good agreement between the FDTD calculations and measurements. The factors affecting the intensity and angular variation of the radiation pattern are the driving frequency, height (or depth), position and orientation of the antenna on the surface.

For our layer-by-layer crystal we find two optimized configurations directly above the dielectric rod to be the most suitable for central lobe patterns. Other configurations have been found to produce narrow lobes of power in the H-plane that could be useful for directional antennas. When the antenna is high above the substrate, the E-field is uniform and the patterns become insensitive to the lateral position. When the dipole is below the surface of the photonic crystal we calculate a strong enhancement of the radiated power. This is due to the decreased impedance of the dipole and increased power input to the dipole.

Within the stop band, the PBG crystal behaves as a perfect reflector and all the power is reflected into the air side. PBG crystals have strong potential in improving antenna performance.



Electromagnetic radiation in photonic band gap materials

Toshio Suzuki^{*} and Paul K. L. Yu

**Department of Electrical and Computer Engineering
University of California, San Diego
La Jolla, California 92093-0407**

Wave propagation in periodic structures exhibit numbers of interesting physical phenomena such as radiation alteration. Inside periodic structures, waves unusually interact with radiators in both frequency and spatial domains, and the process is governed by the *local* behaviors of the electromagnetic modes coupling to the source radiator at the precise radiating frequency in the exact location of the radiator. In this presentation, we demonstrate that this type of irregular radiation, enhancement and suppression of electromagnetic radiation in artificial periodic structures which come to be called "photonic crystals" or "photonic band gap materials".

A source radiator experiences suppression of radiation in photonic crystals if radiation frequencies fall inside photonic band gaps or if the source radiator locates precisely in the node positions where zero amplitude of the coupling modes occurs. Most interestingly, the resulting total radiation power can noticeably exceed the amount in free space or uniform dielectric media, if there are more propagating modes available at the radiation frequency, and/or if those modes couple to the source radiator at their local intensity maxima or at least off-node positions.

Radiation characteristics, for instance, enhancement or suppression factor, pass band or band gap frequencies, source locations and directions, numbers and types of coupling modes and, radiation field pattern, can be all modified by the design of photonic crystals which can be further determined by their geometric, crystallographic, and material configurations. In our presentation, we will discuss radiation spectra and field pattern generated from an electric dipole embedded in photonic crystals, which can be applicable to new antenna designs.

Compact Microstrip Patch Antennas on Photonic Crystal Substrates

K. Agi, * K.J. Malloy, E. Schamiloglu and M. Mojahedi

*Center for High Technology Materials, and
Electrical and Computer Engineering Department*

University of New Mexico
1313 Goddard SE
Albuquerque, NM 87111

Microstrip patch antennas are attractive in communication systems because they are compact. The antennas studied in this work are rectangular patches that are printed on a dielectric substrate backed by a ground plane. The antennas are directly fed with a microstrip line.

There are two issues with patch antennas that are addressed in this paper. The first is bandwidth. Patch antennas, due to their resonant nature, are inherently narrowband. Although various techniques have been shown to effectively increase the bandwidth of the antenna, many of the solutions are complicated or require multi-layer structures. The second issue is antenna size. The most efficient patch antennas are those printed on low dielectric constant, electrically thin substrates, where the thickness of the substrate is much less than the wavelength. A patch can be made compact by printing the antennas on high dielectric constant substrates. The high dielectric constant substrate will increase the electrical thickness of the substrate and reduce the antenna efficiency by allowing for modes in the substrate. On the other hand, the thick substrate will increase the bandwidth. Therefore, a criterion for the proposed antenna structure is to achieve broad bandwidth using simple techniques while maintaining simple fabrication of the antenna.

One method of achieving the desired characteristics is to use a two-dimensional photonic crystal. In this case, the photonic crystal refers to a two-dimensional stop band independent of direction that exists in the substrate where energy is not allowed to propagate. The stop band is achieved by the two-dimensional spatial modulation of the dielectric constant (e.g. air holes in the substrate). The photonic bandgap structures used in this work are two-dimensional arrays of holes that are drilled into the substrate. The two-dimensional array of holes form pass bands and stop bands whose frequencies are determined by the location and size of the holes. For a substrate mode that exists in the stop band (i.e. the frequency of the mode corresponds to a frequency in the stop band), the mode is evanescent.

This talk will describe the details of the implementation of printed antenna structures on a two-dimensional photonic crystal. We will describe the antenna structures studied and present results from experiments as well as calculations using a commercially available finite-difference time-domain package.

Do Two Dimensional Periodic Structures Exhibit Photonic Bandgap Properties ?

Thomas Ellis
J.D. Shumpert
Linda P.B. Katehi
Gabriel M. Rebeiz

The University of Michigan
Ann Arbor, MI 48109-2122

tellis@engin.umich.edu, shumpert@engin.umich.edu
katehi@eecs.umich.edu, rebeiz@engin.umich.edu

The University of Michigan has had a considerable effort in two-dimensional periodic structures for electromagnetic wave shaping and control. Typically, a periodic set of holes are etched into a thick dielectric substrate and microstrip or coplanar-waveguide lines are defined on one side of the dielectric. Also, various tapered-slot antennas have been integrated on such substrates and their performance have been measured between 10 GHz and 100 GHz. The substrates are either Duroid material with a dielectric constant of either 2.2 or 10.5 or the substrates are high-resistivity silicon wafers with a dielectric constant of 12.7. The holes have rectangular, hexagonal, or triangular periodicities varying between $0.2 \lambda_d$ to $0.6 \lambda_d$.

Extensive measurements have been carried out between 1 and 20 GHz on finite thickness substrates using the microstrip and CPW lines. The measurements indicate that the periodic substrate effect results in a sharp cut-off filter which can be explained by simple quasi-static transmission line calculations. Also, for the tapered slot antenna, two mechanisms are at play - the reduction of the effective dielectric constant due to the air-filled holes and the elimination of the TE substrate modes in the dielectric substrate. In both cases, there is no indication of "photonic band gap effects." However, does this necessarily imply that finite thickness substrate two-dimensional periodic structures do not exhibit true photonic bandgap properties?

We have attempted to answer this question by developing a full-wave method-of moment solution for these structures and the results will be shown at the conference.

On The Design of Photonic Bandgap Crystal Filters

H. J. DE LOS SANTOS, Hughes Space and Communications Company, Los Angeles, CA 90009

Photonic Bandgap Crystals (PBC's) are one-, two-, or three-dimensional artificial periodic structures whose transmission properties exhibit frequency bands, called photonic bandgaps, where the propagation of electromagnetic waves is forbidden (E. Yablonovitch, *J. Opt. Soc. Am. B*, 10, 283-295, 1993). Similarly to semiconductors, *impurities* may be introduced in an otherwise periodic PBC to disrupt the periodicity. This results in the introduction of passbands within the photonic bandgaps, thus opening the way for the engineering of novel microwave bandpass filters. Because of the modular properties of PBC's as well as their favorable volume fill fraction, these filters have the potential for being low-cost and extremely lightweight, two features of great importance for application in satellite communications. In this paper we discuss the key aspects PBC filter engineering, namely, PBC physics, electrical design considerations, and fabrication, material, process, and packaging issues.

An intuitive understanding of PBC's may be obtained from an examination of the transmission properties of the unit cell of a one-dimensional periodic structure, Fig. 1. Computation of the unit cell's transmission coefficient yields

$T_{\text{Total}} = \frac{T^2}{1 + R^2 - 2R \cos 2(k_1 d_1 + k_2 d_2)}$, which as a function of frequency exhibits a maximum for $\frac{k_1 d_1 + k_2 d_2}{\pi/2} = \text{even}$, and a minimum for $\frac{k_1 d_1 + k_2 d_2}{\pi/2} = \text{odd}$. These minima,

which result from destructive interference between waves scattered from successive discontinuities in the unit cell, elicit the photonic bandgaps, Fig. 1. The design of PBC's entails designing a unit cell structure, the number of unit cells, and the defect structure that will produce a bandgap in the desired frequency band, and of the desired depth. Experimental results of a two-dimensional PBC filter are shown in Fig. 2.

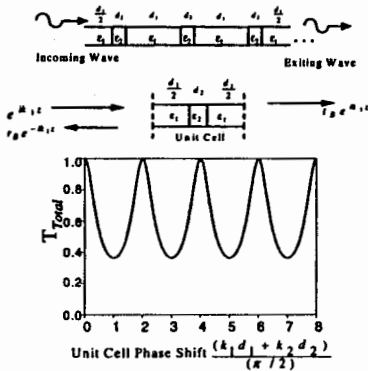


Figure 1

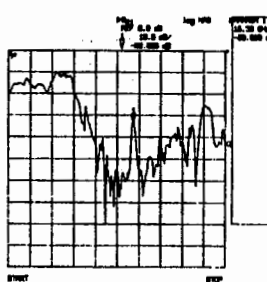


Figure 2

Surface Waves Excitation Efficiency For Wave Scattering By Finite Gratings In Dielectric Slab Guide

Andrey S. Andrenko* and Makoto Ando

Dept. of Electrical and Electrical Engineering

Tokyo Institute of Technology

2-12-1 O-okayama, Meguro-ku

Tokyo 152, Japan

andrey@antenna.pe.titech.ac.jp

An accurate modeling of wave scattering by finite periodic inhomogeneities in open planar waveguides is required for the efficient design of various microwave and mm wave devices. The evaluation of an excitation efficiency of the dielectric slab surface modes is an important part of theoretical study as it provides the data necessary for the operation of space-to-surface wave transformation planar grating couplers or allows one to eliminate undesired dielectric substrate waves along frequency selective surfaces and photonic band gap layers. This work presents the two-dimensional analysis of wave scattering and transformation by finite periodic gratings in open lossless dielectric slab and grounded slab guides and discusses the conditions for the surface modes excitation due to space-to-surface wave transformation.

The problems of plane wave scattering by finite gratings of perfectly conducting rods and strips placed inside or outside the slab waveguide are considered emphasizing on the evaluation of surface waves excitation efficiency. The present study is based on the reciprocity theorem derived for plane wave incidence on the grating in open slab guide and slab's surface mode scattering by the same waveguide inhomogeneity and, therefore, directivity characteristics of the radiation field under the guided wave incidence (A. S. Andrenko and A. I. Nosich, *Microwave and Optical Tech. Lett.*, vol.5, 7, 333-337, 1992) play an important role in the analysis. Since even a few elements grating may produce a highly directive radiation provided that its period equals to that of an infinite grating radiating an outgoing Fourier harmonics, application of reciprocity theorem yields the conclusion that the energy of radiation due to slab's surface mode scattering is equal to the excitation efficiency of the same mode when a plane wave is incident upon the grating in the direction opposite to surface-to-space wave beam radiation. Therefore, it enables one to model the surface waves excitation without solving an entire problem of plane wave or gaussian beam scattering if the rigorous solution of another problem, dielectric slab surface modes scattering and transformation, is available. The conditions of an effective excitation of the surface modes propagating in both directions along the slab have been analyzed as the angle of wave incidence and the period of grating are the key parameters in providing the coupling process while the number of grating elements affect the amplitude of an excited surface mode. Because of high directivity of wave coupling, changing the incidence angle for a few degrees substantially reduces the level of dominant TM-mode being supported by any dielectric layer.

The derivation of reciprocity relations and its application to evaluating the surface modes excitation will be presented and the results obtained for various finite gratings in planar waveguides will be discussed.

Two-dimensional Band-gap Formation in Finite Substrates

J. D. SHUMPERT*, T. ELLIS, G. M. REBEIZ, AND L. P. B. KATEHI
RADIATION LABORATORY

DEPARTMENT OF ELECTRICAL ENGINEERING AND COMPUTER SCIENCE
THE UNIVERSITY OF MICHIGAN, ANN ARBOR, MI 48109-2122 USA

Planar antennas are ideal for high frequency applications being both conformal and easily integrated into thin-film circuits. Unfortunately, they usually have low gain and high ohmic and/or dielectric losses. Since high-density materials are routinely used in the fabrication of these devices, a surface wave suppression technique involving the use of artificial substrates is investigated as a means to increase radiation efficiency. Micromachined substrates, dielectric lenses, and photonic band-gap (PBG) materials are three of the candidate technologies that are currently being investigated at the University of Michigan Radiation Laboratory for use in surface wave suppression. Photonic band-gap structures are found to have unique properties that are advantageous in applications involving semiconductor integrated circuits. Such structures offer the advantage of changing the physical properties of substrates used in fabricating planar circuits. A number of applications for such a structure can be imagined including dielectric mirrors, resonant cavities, high Q filters, isolators, dielectric waveguides, couplers, and frequency selective surfaces (FSS).

Inherently, photonic band-gaps are a large scale phenomena requiring hundreds of periods of alternating dielectric material to achieve the desired frequency gaps. However, it is unclear at the present time whether the mechanisms that exist in finite structures are classical band-gap phenomena. It is also unclear whether the gaps are reproducible for more complicated structures. Our primary goal has been to develop two- and three-dimensional models that can be used to characterize inhomogeneous or periodic substrates. Specifically, we are interested in modeling the effects of dielectric geometry and metalization on substrate properties such as surface wave formation. The band-gap regions of a one-dimensional system one easily be determined for a simple structure. In order to determine the frequencies of interest for a complex two- or three-dimensional structure, a full-wave, doubly periodic, IE/MoM code has been developed to determine the eigenvalues of a two-dimensional, inhomogeneous dielectric unit cell. By using the periodicity of this unit cell, one can model the photonic structure and determine the desired band-gaps.

In parallel to the theoretical modeling, a number of experiments are being designed and fabricated in order to understand the mechanisms of band-gap formation and surface wave suppression involved in more complicated structures. Experimental studies with micromachined dielectrics were carried out to corroborate the theoretical values for the band-gaps. A one-dimensional periodic dielectric substrate has been fabricated and tested to confirm the band-gap predicted by coupled-mode theory exists for microstrip excitation. After establishing the existence of this band-gap in one-dimensional structures at microwave frequencies, many different two-dimensional lattice structures including the square, hexagonal, and rectangular lattices, have been fabricated and tested.

Special Session: Novel Trends in Theoretical Electromagnetics

N. Engheta and R. W. Ziolkowski

Electromagnetic Radiation and Scattering from Elliptical Torus Knots	126
<i>D. H. Werner*, Pennsylvania State University, USA</i>	
Cantor Diffractals and Lacunarity	127
<i>A. D. Jaggard*, Wheaton College, USA, D. L. Jaggard, Univ. of Pennsylvania, USA</i>	
Cantor Ring Arrays	128
<i>D. L. Jaggard*, Univ. of Pennsylvania, USA, A. D. Jaggard, Wheaton College, USA</i>	
Exact Geometrical Optics Scattering by an Isorefractive Wedge Structure	AP
<i>P. L. E. Uslenghi*, University of Illinois at Chicago, U.S.A</i>	
A Multiresolution Approach for Homogenization and Effective Properties -Propagation in Complex Ducts.....	129
<i>B. Z. Steinberg*, J. Oz, Tel-Aviv University, Israel</i>	
EM Characterization of Photonic Band Gap (PBG) Structures: An Overview.....	130
<i>Y. Rahmat-Samii*, UCLA, USA</i>	
Finite Photonic Band Gap Material Based Waveguides, Power Splitters and Switches.....	131
<i>R. W. Ziolkowski*, University of Arizona, USA</i>	
Multilevel Techniques in Solving Electromagnetic Scattering Problems.....	132
<i>W. C. Chew*, E. Michielssen, J. M. Song, University of Illinois, USA</i>	
Rotation in Electromagnetic Field Equations: A Discussion, Interpretation and Application.....	133
<i>R. Nevels*, J. Miller, R. Miller, Texas A&M University, USA</i>	
Fractional Kernels and Intermediate Zones in Electromagnetism: Planar Geometries.....	134
<i>N. Engheta*, University of Pennsylvania, U.S.A</i>	

ELECTROMAGNETIC RADIATION AND SCATTERING FROM ELLIPTICAL TORUS KNOTS

Douglas H. Werner
The Pennsylvania State University
Applied Research Laboratory
P.O. Box 30
State College, PA 16804-0030

The electromagnetic scattering properties of perfectly conducting thin knotted wires were first considered by (O. Manuar and D. L. Jaggard, *Optics Letters*, 20 (2), 115-117, 1995). The particular emphasis of this work was on an investigation of the backscattering properties of threefold rotationally symmetric trefoil knots. More recently, the electromagnetic characteristics of a special class of knots, known as (p,q)-torus knots, were studied by (D. H. Werner, *IEEE Antennas and Propagation Society International Symposium Digest*, 2, 1468-1471, 1997). It was demonstrated that the well-known trefoil originally considered by Manuar and Jaggard is one important example of a (p,q)-torus knot. A convenient set of parametric representations was developed for this particular family of knots by making use of the fact that they may be constructed on the surface of a standard circular torus. These parameterizations were then used in combination with Maxwell's equations to derive vector potential and corresponding electromagnetic field expressions which describe the radiation and scattering from circular (p,q)-torus knots. In particular, closed form expressions were derived for the radiation integrals associated with electrically small circular (p,q)-torus knots. The derivation of a new knotted wire Electric Field Integral Equation (EFIE) was also outlined.

The constructions considered above were restricted to knots that reside on the surface of a torus which has a circular cross-section. In this paper a more general set of parameterizations is developed which are valid not only for circular but also for elliptical (p,q)-torus knots. From a geometrical point of view, circular torus knots may be considered as a special case of the more general elliptical torus knots, even though topologically speaking they are equivalent. This is a subtle yet important distinction since the introduction of one additional parameter allows the electromagnetic characteristics to be studied for a much wider class of knot geometries. Another important property of elliptical torus knots is the fact that the standard circular loop as well as linear dipole geometries may both be obtained as special cases by making the appropriate choice of parameters.

Cantor Diffractals and Lacunarity

Aaron D. Jaggard* and Dwight L. Jaggard

Department of Mathematics
Wheaton College
Wheaton, IL 60187
adj@pender.ee.upenn.edu

Moore School of Electrical Engineering
Complex Media Lab., Univ. of Pennsylvania
Philadelphia, PA 19104-6390
jaggard@seas.upenn.edu

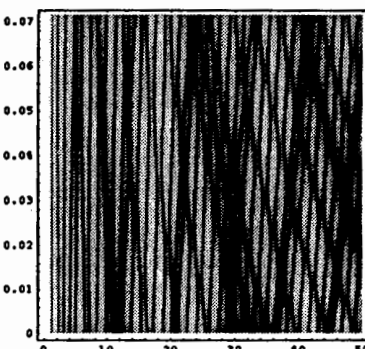
Introduction

Diffractals denotes fractals that diffract waves. Here we investigate diffraction by Cantor apertures (*Cantor diffractals*) including a new class of Cantor targets based on a polyadic Cantor set described by several fractal descriptors. We find scaling properties characteristic of these apertures and examine their radiation patterns through the introduction of *twist plots* which allows one to find windows of lacunarity for which these apertures exhibit desired behavior such as low sidelobes. We find these diffractals have *subfractal*, *fractal* and *superfractal* radiation regimes that provide distinctive diffraction patterns.

Cantor Diffractals

As an example, we consider diffraction by Cantor targets or apertures described by one- and two-dimensional Cantor sets and their generalizations. Such targets are multi-scale and, for certain configurations, these apertures are associated with iterative methods of solution. These apertures also display symmetries in their diffraction patterns. For example, there is an inherent symmetry with respect to stage of growth that is connected to their iterative solutions. Likewise, these apertures have scaled symmetry with respect to sidelobe structure.

One aperture of particular interest is a generalization of the triadic Cantor targets examined previously [Jaggard and Spielman, *Microwave Opt. Tech. Lett.* 5, 460-466 (1992)]. For this generalization, we vary the texture or lacunarity of the target and relate these changes to changes in the radiation pattern. Optimal lacunarity can be obtained from radiation patterns such as that displayed in the twist plot on the right where cuts of the radiation pattern are stacked upon each other as the lacunarity is varied. We find "windows" of operation where for particular fractal dimension and lacunarity the posses relatively low sidelobes. Furthermore, features in the twist plot are directly related to geometric features in the diffractal.



Cantor Ring Arrays

Dwight L. Jaggard* and Aaron D. Jaggard

Moore School of Electrical Engineering
Complex Media Lab., Univ. of Pennsylvania
Philadelphia, PA 19104-6390
jaggard@seas.upenn.edu

Department of Mathematics
Wheaton College
Wheaton, IL 60187
adj@pender.ee.upenn.edu

Introduction

We present a new class of fractal ring arrays we denote *Cantor ring arrays* based on a polyadic Cantor set with a number of design variables. When thinned, these arrays have performance that is superior to their periodic counterparts and similar to or better than their random counterparts for a moderate number of elements. Cantor ring arrays have distinctive *subfractal*, *fractal* and *superfractal* radiation regimes whose boundaries are predictable by the array geometry.

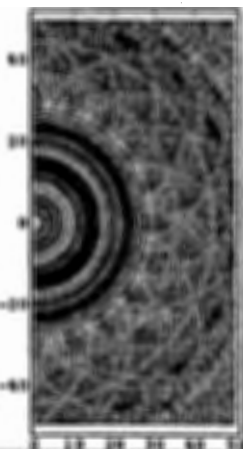
Fractals and Arrays

Fractal electrodynamics has covered the analysis and synthesis of several discrete and aperture arrays including random linear arrays [Kim and Jaggard, *Proc. IEEE* 74, 1278-1280 (1986)], Cantor target aperture arrays, large lacunar arrays, planar arrays, uniform and tapered linear arrays, and most recently, Weierstrass ring arrays. The related area of fractal antenna elements is of interest for broadband or multiband radiation and for compact antennas. Here we investigate a class of discrete arrays in which variations in both fractal dimension and lacunarity can be examined.

Cantor Ring Arrays

For Cantor ring arrays, the radiation pattern is expressed in closed-form in terms of a continuous ring contribution plus higher-order residual terms that take into account the azimuthal variation due to the gaps between array elements on each ring. The design parameters include fractal dimension, lacunarity, number of gaps, stage of growth, number of elements, and number of rings.

This work suggests that certain fractals may provide the right mix of order and disorder to provide an alternative to the periodic (very ordered) and random (very disordered) methods typically used. A sample radiation pattern, as a function of spatial frequency, is shown on the right. The pattern is symmetric with respect to rotations of 180 degrees.



A Multiresolution Approach for Homogenization and Effective Properties - Propagation in Complex Ducts

Ben Zion Steinberg¹ and Jasmin Oz
Department of Interdisciplinary Studies
Faculty of Engineering
Tel-Aviv University
Ramat-Aviv, Tel-Aviv
69978 Israel

Multiresolution techniques can be used to study the effective properties of propagation and scattering in complex (finely structured) environments. As a case study, a new formulation that governs the propagation of the smoothed (large scale) component of the field in complex ducts is derived and compared to the generic formulation governing the propagation of the complete field. The former and the latter are termed here the "effective formulation" and the "complete formulation", respectively. The relation between the small scale structure of the system heterogeneity (the structure defined over length scales much smaller than the wavelength) and the large scale field (the component of the field defined over length scales of the order of the wavelength) are investigated. In particular, we use multiresolution and wavelet expansion to derive effective measures for the system heterogeneity. These measures are heterogeneity functions that are simpler (smoother) than the heterogeneity associated with the complete propagation formulation, but can still reproduce the correct large scale behavior of the field, and hence the correct far field as well, when used in conjunction with the new formulation.

Few fundamental issues must be addressed in such a study. The first concerns the existence of the effective measure in boundary value propagation problems and its properties. Thus, we show that while the mapping of a heterogeneity to its effective measure is unique, the converse is generally not true. Furthermore, we show that the effective measures introduce an *effective anisotropy* into the propagation problem, even if the generic complete formulation is isotropic. The second fundamental issue concerns the boundary conditions and the associated modes. Recall that the boundary values are usually given as auxiliary conditions that apply to the complete field and not to its large scale component. Thus, the question of the relevant boundary conditions that apply to the effective formulation arises. We discuss the role of the boundary conditions and its manifestation in the large scale effective formulation and study the relation between the modes and propagation coefficients of the complete and of the effective formulation. In particular, the modal expansion of wavefields associated with the effective representation and the resulting Green function is derived and compared to their complete counterparts. It is shown that while a ad-hoc smoothing operation results in a Green function that is not reciprocal (loss of self adjointness), the systematic approach of the present study yields a self-adjoint effective formulation, and hence a reciprocal effective Green function. The manifestation of the effective anisotropy in the modal representation of wavefields associated with the effective formulation is demonstrated. The third fundamental issue concerns the efficacy of ray theories. Since the medium heterogeneity in the complete formulation is described over length scale much smaller than the wavelength, ray theories are not valid on the level of the complete field description. However, the effective measures of the complex heterogeneity are much smoother, and asymptotic "high frequency" techniques are formally valid on the level of the effective formulation. The resulting "effective ray theory" is discussed and an attempt is made to explore its physical interpretations.

¹Corresponding author, e-mail: steinber@eng.tau.ac.il

EM Characterization of Photonic Band Gap (PBG) Structures: An Overview

Yahya Rahmat-Samii

Department of Electrical Engineering
University of California, Los Angeles
Los Angles, CA 90095-1594
rahmat@ee.ucla.edu

What are PBG's: PBG's are synthesized 2-D or 3-D multi-layered periodic structures that effectively prevent the propagation of electromagnetic waves in a specified band of frequency. Generally speaking, it is desired that this property be held for any incidence angles and polarizations of electromagnetic waves in the prevention band.

PBG Structures: PBG's may be constructed in a variety of ways either through periodic perforations of multi-layered substrates or through the development of properly stacked 2-D or 3-D periodic metallic or dielectric structures.

PBG Applications: Because of the wide-bandwidth of the propagation prevention band gap, PBG's may be used in various microwave/millimeter wave devices and antennas. Potential applications of PBG's may be found in antenna gain enhancement, miniaturization of antenna dimensions, ground planes, cavities, waveguide structures, etc.

EM Characterization of PBG's: In the recent past, most of the activities were directed towards the design and experimental performance evaluation of PBG's. More recently attention has been focused on the EM theoretical/numerical modeling and performance characterization of these complex structures. In this presentation, an overview of the application of modern numerical techniques will be presented. Among these techniques special emphasis will be given to the application of FDTD and periodic method of moments. The performance of several candidate PBG structures will be evaluated to critically examine the EM properties of PBG's and their potential utilization in various applications. Attempts will be made to provide physical and engineering insights into PBG's in microwave and millimeter wave regime.

Finite Photonic Band Gap Material Based Waveguides, Power Splitters and Switches

Richard W. Ziolkowski

Electromagnetics Laboratory

Department of Electrical and Computer Engineering
The University of Arizona, Tucson, AZ 85721

Tel: (520) 621-6173

Fax: (520) 621-8076

E-mail: ziolkowski@ece.arizona.edu

Abstract

Photonic bandgap waveguide structures have been modeled successfully with a FDTD full-wave, vector Maxwell equation simulator. These nanometer sized waveguides and the extension of these geometries to power splitters (T-junctions) and switches (Y-junctions with a defect) will be described.

Summary

Nanometer and micron sized optical devices are currently being explored for their applications in variety systems associated with communications, data storage, optical computing, etc. However, as the size of optical devices is pushed to the size of an optical wavelength and less, the need for more exact materials and response models is tantamount to the successful design and fabrication of those devices. Moreover, the time scales for many of these devices is rapidly approaching the femtosecond regime. For this reason the finite-difference time-domain (FDTD) method is receiving intensive study (see, for example, [1-6]).

Additionally, most current simulation models are based on known macroscopic, phenomenological models that avoid issues dealing with specific microscopic behavior of the materials in such devices. Inaccuracies in the simulation results are then exacerbated as the device sizes shrink to subwavelength sizes and the response times of the excitation signals surpass the response times of the material. Phenomenological models lose their ability to describe the physics in this parameter regime; hence, they lose their accuracy there. Quantum mechanical effects begin to manifest themselves; the simulation models must incorporate this behavior to be relevant. As discussed in [7,8], this leads to a semiclassical Maxwell-Bloch model, i.e., a careful marriage between microscopic (quantum mechanical) material models of the resonant material systems and the macroscopic Maxwell's equations solver.

It has been further demonstrated that photonic bandgap (PBG) structures can be used to form nanometer sized waveguiding structures [9]. The ability of the FDTD approach to model finite-sized PBG structures with defects and to recover known behaviors in one and two dimensions has been demonstrated [10]. The Maxwell-Bloch FDTD simulator has been applied to the modeling of several vertical cavity surface emitting lasers (VCSELs) based upon PBG structures [11].

This paper summarizes preliminary efforts to model nanometer sized waveguiding structures that have resonant linear and nonlinear materials built into them. Results for the basic sub-wavelength

MULTILEVEL TECHNIQUES IN SOLVING ELECTROMAGNETIC SCATTERING PROBLEMS

W. C. CHEW*, E. MICHELSSEN, AND J. M. SONG

CENTER FOR COMPUTATIONAL ELECTROMAGNETICS
ELECTROMAGNETICS LABORATORY

DEPARTMENT OF ELECTRICAL AND COMPUTER ENGINEERING

UNIVERSITY OF ILLINOIS, URBANA, IL 61801, USA

PHONE: (217)333-7309, FAX: (217)244-7345, EMAIL: W-CHEW@UIUC.EDU

Numerical solutions of integral equations usually involve a dense matrix, which is computationally intensive to solve. As a result, differential equation solvers like FEM (finite element method) and FDTD (finite difference time domain) have become quite popular. Recently, there has been renewed interest on solving integral equations, due to the advent of various fast multilevel techniques in solving these equations. These fast solvers exploit the special structure of the matrices that arise from the numerical approximation of the integral equation. The kernel of the integral equations is usually related to the Green's function which is translationally invariant. This property manifests itself in the numerical approximations of the Green's operator: the matrix has an inherent Toeplitz-like structure, or that the matrix can be factored by translational matrices. As a result, an otherwise dense-matrix vector multiply can be performed in $O(N \log N)$ operations.

In this presentation, we will review these methods and relate them to communication of N telephones, group theory, and fast Fourier transforms of nonuniformly spaced data, and so on.

The existence of the diagonal form of translation matrices is related to group theory representation theorem. Matrix representations of group operators are diagonal when the representations are irreducible. When plane waves are used as a basis, the translation operators are diagonal as they form the irreducible representation of the translation group.

The calculations in the multilevel fast multipole algorithm is often related to the radiation pattern calculation of a group of sources. If N radiation points are to be calculated with N source points, this is generally an N^2 process. When the N source points are aligned uniformly on a line, classical FFTs can be used to find the radiation pattern in $N \log N$ operations. However, when the N source points are arbitrarily distributed in space, classical FFTs cannot be used, and the multilevel techniques are a fast way to find the radiation pattern in $O(N \log N)$ operations.

Rotation in Electromagnetic Field Equations: A Discussion, Interpretation and Application

Robert Nevels*, Jeffrey Miller and Richard Miller
Department of Electrical Engineering
Texas A&M University
College Station, TX 77843-3128

Rotation in physical space is a linear orthogonal transformation of the coordinates of a point such that the sum of the squares of the coordinates remains invariant. A general two component vector \mathbf{F}' in physical space is rotated through an angle θ by the simple transformation

$$\mathbf{F} = \bar{\mathbf{A}} \mathbf{F}'$$

where $\bar{\mathbf{A}}'$ is the rotation matrix

$$\bar{\mathbf{A}}' = \begin{bmatrix} \cos \theta & \sin \theta \\ -\sin \theta & \cos \theta \end{bmatrix}$$

A matrix analogous to $\bar{\mathbf{A}}'$ occurs in a number of instances in electromagnetic field analysis and is also described as a rotation. Its form is

$$\bar{\mathbf{A}} = \begin{bmatrix} \cos \phi & jZ \sin \phi \\ \frac{j}{Z} \sin \phi & \cos \phi \end{bmatrix}$$

where ϕ is a combination of terms that do not represent a physical angle and Z is an impedance. Examples include the duality transformation, the ABCD matrix for a lossless transmission line and the transition matrix in the time domain path integral equation (R. Nevels, J. Miller, and R. Miller, "The Path Integral Time-Domain Method: A New Numerical Method for Electromagnetic Scattering", APS/URSI International Symposium, Montreal, Canada, July 1997, p. 263) for 1-D propagation in an inhomogeneous region. It appears that a general 'rule of thumb' is that a rotation matrix can occur in the solution of any set of coupled hyperbolic equations with two or more independent variables. In this paper we will give an interpretation of rotation in electromagnetic propagation, scattering and transmission line analysis and show a simple powerful transmission line numerical method that arises from the path integral equations.

Fractional Kernels and Intermediate Zones in Electromagnetism: Planar Geometries

Nader Engheta

Moore School of Electrical Engineering

University of Pennsylvania

Philadelphia, Pennsylvania 19104, U.S.A

Tel: (215) 898-9777, Fax: (215) 573-2068

E-mail: engheta@pender.ee.upenn.edu

Fractional derivatives and fractional integrals are interesting mathematical operators addressed and analyzed in a branch of mathematics known as fractional calculus [see e.g., K. B. Oldham and J. Spanier, *The Fractional Calculus*, Academic Press, New York, 1974] We have been interested in bringing together the tools of fractional operators and the electromagnetic theory, and to search for potential applications and physical interpretations of such fractional operators in electromagnetics [see e.g., the review article: N. Engheta, "On the Role of Fractional Calculus in Electromagnetic Theory," in *IEEE Antennas and Propagation Magazine*, Vol. 39, No. 4, pp. 35-46, August 1997.] Our interest in general is to see how fractional derivatives/integrals and some other fractionalized operators can play a role in addressing the "intermediate-zone" problems in electromagnetism, and to develop an area which we are naming "fractional paradigm in electromagnetism."

One of the interesting problems to address is the following: since fractional derivatives and integrals effectively address the "intermediate behavior" for such operators, can fractionalization of some appropriate operators provide us with proper tools to tackle certain electromagnetic problems involving intermediate zones? Specifically, it is clear that for a given charge and/or current distributions in a finite-size volume, whether it is a static or dynamic case, the quantities of interest such as electric fields or potentials resulted from such a source may be expressed in terms of integrals involving the Green functions and the given source. Furthermore, it is also well known that in order to find some simpler expressions for the quantity of interest, usually more attention has been paid to the analysis of the far-zone and the near-zone fields while less attention has been aimed at the intermediate zones. In our recent study, we have been able to show that if the appropriate kernels, which relate quantities of interest in the near zone to the quantities in the far-zone region, are found and then such kernels are properly "fractionalized", these new "fractionalized kernels" can provide us with the new kernels that "link" the near-zone quantities with the quantities at the intermediate zones.

In this talk, the results of our study of such fractionalization of kernels and their roles in treating the intermediate zones in the planar geometries will be presented and the physical interpretation and justification behind the results will be provided.

Scattering and Imaging from the Surface, Ground and Buried Objects

B. J. Kooij and W. R. Scott

Ocean Altimetry and Scatterometry with GPS: Feasibility Study..... 136
C. Zuffada, G. Hajj, L. Young, J. Thomas, California Institute of Technology, USA*

Modeling and Measurement of Scattering from Rough Asphalt Surfaces at Millimeter-wave
Frequencies..... AP
E. S. Li, K. Sarabandi, University of Michigan, USA*

An Experimental Model of a Acousto-electromagnetic Sensor for Detecting Land Mines..... AP
W. R. Scott, Jr, J. S. Martin, Georgia Institute of Technology, USA*

Efficient Method for the Near-field Electromagnetic Scattering by Buried Objects AP
T. J. Cui, W. C. Chew, Dept of Electrical and Computer Engineering*

Focused Synthetic Phased Array for Subsurface Imaging..... AP
W. J. Graham, Lockheed Martin Corporation, USA*

Efficient One Dimensional Inversion of Induction Log Data AP
S. Y. Chen, W. C. Chew, University of Illinois, USA, W. D. Kennedy, Mobil Exploration and
Producing Technical Center, USA*

Iterative Scattering by a Conducting Sphere Partially Buried in a Ground Plane..... AP
A. Hamid, King Fahd University of Petroleum and Minerals, Saudi Arabia*

Ocean Altimetry and Scatterometry with GPS: Feasibility Study

Cinzia Zuffada*, George Hajj, Larry Young and J.B. Thomas

Jet Propulsion Laboratory
California Institute of Technology
Pasadena, CA 91109

ABSTRACT

The feasibility of a new low-cost space flight instrument named GPS-based Oceanographic and Atmospheric Low-Earth Orbiting Sensor (GOALS) is currently under investigation. This instrument would consist of a new generation of JPL receivers called Turbo Rogue Space GPS Receiver 3, connected to several antennas, one upward-looking (toward zenith) for the purpose of doing precise orbit determination, one or more antennas oriented toward the Earth's limb for the purpose of atmospheric occultations, and one or more down-looking (toward nadir) to track GPS signals reflected off the ocean surface. While the first two of these applications have been demonstrated on existing missions such as TOPEX/Poseidon and GPS/MET, the latter is an entirely new application of GPS whose feasibility is currently being investigated.

Tracking signals reflected off the ocean can have two different modes of operation. The first mode is to track the specularly reflected, phase coherent signal for both L1 and L2. This signal would come from a well defined area on the ocean surface around the reflection point determined by geometrical optics, with a diameter of about 1 km as determined by the first Fresnel zone. This mode provides the L1 and L2 group and possibly phase delays along the reflected raypath. Given sufficient accuracy and knowledge of the precise positions of the transmitting and receiving satellites, one can use these measurements to determine (1) the total electron content along the indicated reflected raypath, (2) delay induced by the atmosphere and (3) ocean height at the reflection point. Our presentation will discuss the effects of the ocean roughness on the specularly reflected part of the signal, the corresponding frequency spread, and the accuracy with which phase and range can be measured.

The second mode of operation corresponds to tracking the diffuse part of the signal scattered from a much larger area on the ocean (of order tens to hundreds of kilometers) surrounding the specular reflection points. In this case, the signal received does not have coherent phase, and the receiver measures the reflected power if it exceeds the receiver's thermal noise. In this mode, the GPS receiver would function in a manner similar to traditional scatterometers, where the surface would be subdivided by means of iso-range and iso-doppler contours, and the receiver would track the signal from defined range/doppler cells. Our presentation will address the power level of the scattered signal as a function of surface conditions such as wind velocity and surface capillary waves. We will discuss the expected received signal-to-noise ratio and provide quantitative estimates of pixel sizes of the portion of the ocean surface mapped by the instrument.

Mobile Propagation Studies for Outdoor and Indoor Scenarios

W. Vogel and G. S. Brown

Discussion on the Applicability of Employing Ray Tracing Technique to Predict Outdoor Channel Characteristics.....	138
<i>H. Li*, H. Lin, C. Chen, T. Liu, National Taiwan University, Taiwan R.O.C.</i>	
Use wideband Measurements to Determine Propagation Mechanisms	139
<i>H. Li*, T. Liu, C. Chen, H. Lin, National Taiwan University, Taiwan R.O.C.</i>	
ISI Simulation for Indoor Wireless Communications	140
<i>H. Li*, M. Lee, R. Lane, National Taiwan University, Taiwan R.O.C.</i>	
Using the Reflection Coefficient to Characterise a Wall of a Building	141
<i>Y. Huang*, University of Liverpool, UK</i>	
Field Performance Measurements of Multiple Helmet-mounted Antennas.....	142
<i>C. Espinoza*, M. Luevano, A. Medina, S. Sudanthi, J. McLean, H. Foltz, G. Crook, University of Texas - Pan American, USA</i>	
Low Grazing Angle Bistatic Terrain Scattering Measurements.....	143
<i>W. G. Stevens*, M. J. Sowa, B. Weijers, Air Force Research Laboratory, USA, D. J. McLaughlin, Northeastern University, USA</i>	
Propagation Analysis in Container Terminals.....	144
<i>K. S. Huang*, H. S. Chiang, J. K. Chung, Chunghwa Telecom Co., Taiwan, J. F. Kiang, National Chung-Hsing University, Taiwan</i>	
Investigation of Base-station Polarization Diversity in Personal Communication Systems	145
<i>X. Tian*, H. Ling, W. J. Vogel, University of Texas, USA</i>	
Comparison of Ray Tracing, 3D and 2D FDTD Simulations of Propagation Models for Wireless Communications	146
<i>Z. Yun, M. J. White, M. F. Iskander*, University of Utah, USA</i>	

Discussion on the Applicability of Employing Ray tracing Technique to Predict Outdoor Channel Characteristics.

Hsueh-Jyh Li, Han-Chiang Lin, Cheng-Chung Chen and Ta-Yung Liu

Department of Electrical Engineering

National Taiwan University

Taipei, Taiwan R.O.C.

The channel characteristics of outdoor environment is very complicated. All scatterers such as buildings, vehicles, pedestrians, light poles, trees, curbs and ground etc, will contribute to the total field. The ray-tracing technique is an effective numerical method for studying site-specific channel properties. Some important characteristics such as the power fading and delay spread can be derived from the simulation results.

To proceed the ray-tracing simulation, one has to key-in parameters such as the layout of streets and buildings, dielectric constant of buildings, roughness factors of walls, and geometries of important scatterers. However, physical environments are usually very complicated and it is difficult to describe the environment and the parameters accurately. In general, the input parameters are much simplified, for example, buildings along a street are modeled as a smooth long wall and the roughness of the building is modeled by a rough factor.

Power fading is a result of multipath interference. However, each path wave cannot be differentiated from power fading measurement. Delay profile provides information about amplitude and delay time of multipath waves. By comparing the measured delay profile with the physical environment, certain important propagation mechanisms can be identified.

In this paper we will employ the ray-tracing technique with simplified input layout to simulate outdoor radio channel and compare the simulation results with those obtained by wideband measurements. The parameters to be compared include the delay profile, the average power, and the root mean square delay spread etc. We will demonstrate the comparison results, analyze the difference, and discuss the applicability of the simulation tool to predict outdoor channel characteristics. It was found that the respective delay profiles could look very different, which indicates that the scattering mechanisms in the real environment are different from those considered in simulations. However, the respective average propagation losses can match very well. Nevertheless, the root mean square delay spreads obtained by simulations and measurements can be very different especially when the line of sight between the transmitting and receiving antennas is obstructed.

Use wideband Measurements to Determine Propagation Mechanisms

Hsueh-Jyh Li,Ta-Yung Liu,Cheng-Chung Chen and Han-Chiang Lin

Department of Electrical Engineering

National Taiwan University

Taipei, Taiwan R.O.C.

Channel characteristics measurements can be divided into narrowband measurements and wideband measurements. Narrowband measurements only measure the power level, but contributions from different paths cannot be differentiated. Wideband measurements can measure delay profiles, which provides information about amplitude and time delay of each path wave. A network analyzer system has very wide bandwidth and therefore can give very fine range resolution or time-delay resolution. It is a powerful tool for analyzing wave propagation mechanisms.

In the literature, reflection coefficients or diffraction coefficients were usually derived from CW measurements. However it is very difficult to isolate each single propagation mechanism because the measured field is the superposition of all path waves. In this paper we will use the network analyzer system to measure delay profiles and by isolating each path component to determine the reflection and diffraction coefficients.

In the presentation we will discuss factors which may affect measurement accuracy and propose a calibration procedure to acquire reliable measurements. We have found that, to avoid ambiguity in the total path lengths traveled by multipath waves, the sampled frequency increment should be finely sampled. We also found that zero padding should be used in the FFT if the peak values sampled would be used to represent contribution of certain mechanisms. We have proposed wideband measurement methods to determine reflection and edge diffraction coefficients. The ray-tracing technique has been employed to calculate outdoor channel characteristics, which are then compared with those obtained by measurements. Consistency between the experimental and simulation results show the effectiveness of the proposed methods.

ISI Simulation for Indoor Wireless Communications

Hsueh-Jyh Li, Ming-Lun Lee, and Rong-Yuan Lane
Department of Electrical Engineering
National Taiwan University
Taipei, Taiwan
R.O.C.

Due to the difference in time delay of the multipath waves, the wireless channel usually suffers with power fading and intersymbol interference (ISI). Serious ISI can result in bit transmission error and degrade transmission performance.

ISI is related to factors such as the filter, the modulation schemes, the demodulation circuitry as well as the channel impulse response. In this paper we will use the ray-tracing technique to obtain the impulse response and take into consideration factors of filtering, carrier recovery and timing recovery to evaluate transmission performance under different data rates for specific environments.

To calculate outage probability for a certain environment, one has to obtain impulse responses of many positions (e.g. thousands or tens of thousands of positions). However, a great deal of calculation time and memory space would be required if the impulse response of every position is calculated. We have proposed an approximation method which can save a large amount of computing time and storage space in the calculation of many impulse response in a given environment. This approximation method is then used to simulate ISI for several indoor environments, including a room furnished with metal shelves and rooms separated by walls with and without windows on top of the walls. Results show that the existence of windows on the walls can raise the average level of received power. However, due to a more dispersion of multipath waves, the allowable data transmission rate is reduced instead.

Using the Reflection Coefficient to Characterise a Wall of a Building

Y. Huang (Yi.Huang@liv.ac.uk)

University of Liverpool, Liverpool, L69 3GJ, UK

The radio channel characterisation is important for the system design and planning. The dielectric properties and thickness of the walls and ceilings are required for the calculation of the wave reflection and transmission so as to accurately predict the radio channel performance in the desired indoor/picocell environment. Direct measurements of the thickness of the walls and ceilings are not normally possible and the dielectric measurement cannot be made destructively, thus a non-destructive methods to characterise such a layered medium is required. Unfortunately, none of the existing methods is suitable for this application, because they measure either the dielectric properties or the thickness of the material, not both at the same time. Therefore a novel approach based on the free space method is introduced in this paper to obtain both the dielectric properties and the thickness of a wall.

As the first order approximation, the wall can be assumed as a homogeneous one-layer medium with thickness d and an effective dielectric permittivity ϵ ($= \epsilon_0 \epsilon_r$) and conductivity σ . Let the incident wave to the wall be a plane wave, then the total reflected waves are actually superpositions of infinite number of reflected rays on the wall, the total reflection coefficient takes the form of

$$\Gamma(\omega) = \frac{1 - e^{-2\gamma d / \cos \theta_i}}{1 - \Gamma_{01}^2 e^{-2\gamma d / \cos \theta_i}} \Gamma_{01}$$

This expression is compact but not explicit enough to reveal the linkage between the reflection coefficient and the dielectric properties. Let us define:

$$x = \sqrt{(\epsilon_r - j\sigma/\omega\epsilon_0)}, \text{ and } B(\omega) = 2\omega\sqrt{\mu_0\epsilon_0}$$

The equation can then be re-written as

$$\frac{(\Gamma(\omega) + 1) \cdot x^2 + 2 \cdot \Gamma(\omega) \cdot x + \Gamma(\omega) - 1}{(\Gamma(\omega) + 1) \cdot x^2 - 2 \cdot \Gamma(\omega) \cdot x + \Gamma(\omega) - 1} = e^{-jB(\omega) \cdot d \cdot x} \quad (1)$$

for the normal incidence case.

It is apparent that B is a constant for a given frequency and x is the only variable related to the dielectric properties of the unknown medium in this equation. The question shows explicitly the relations among three important parameters: reflection coefficient Γ , dielectric property x and the thickness d of the medium. Once any two of the three are given, the third parameter can be obtained using this equation. For example, if the complex reflection coefficient Γ and the thickness d are measured, Eq. (1) can be used directly to obtain the dielectric properties of the medium. It is not difficult to verify that this solution is unique. However, it is worth pointing out that the solution for d is not unique when both Γ and x are given; for this case, the general solution is $d = d_0 + 2\pi n / (B(\omega)x)$, and n is an integer.

Because the dielectric properties (permittivity and conductivity) of a medium change slowly with the frequency, hence they can be considered as constants over a small range of frequency. However, the reflection coefficient is sensitive to the change of frequency. This means if we replace Γ in Eq. (1) with the measured reflection coefficients at two slightly different frequencies, a system of equations can be formed to obtain both electric properties x and the thickness of the wall d uniquely. Measurement results have demonstrated the effectiveness of this approach.

Field Performance Measurements of Multiple Helmet-Mounted Antennas

C.Espinoza, M.Luevano, A.Medina, S.Sudanhi, J.McLean, H.Foltz, G.Crook
Electrical Engineering, University of Texas - Pan American
1201 W. University Drive, Edinburg, TX 78539

Multiple antennas combined with diversity communication schemes offer improved performance for mobile systems. In particular, multiple personnel-mounted antennas selected with an adaptive switching algorithm can compensate for changes in body position, orientation, and surroundings. In this work, measurements are made on one such system: a multiple patch helmet antenna system in a variety of environments.

A number of special circumstances apply to helmet mounted antennas. The helmet structure itself affects the electromagnetic properties of the antenna elements and the interaction between them. Furthermore, the system must operate with the helmet both in a normal upright configuration as well as prone and crouching positions, and may be required to operate with one or more elements in contact with earth or other lossy materials.

It is difficult to make analytical or numerical predictions of performance under all these possible conditions. Thus, in this work, we will present measurements of received signal strength performance in base-to-helmet, helmet-to-base, and helmet-to-helmet communication scenarios, and comparisons of the adaptive system with conventional antennas. These measurements cover the widely-used 2.45 GHz ISM band for a variety of propagation environments including both open, urban, and indoor. In particular, the effect of ground proximity for prone positions over dry soil, moist soil, and a number of construction materials is studied.

LOW GRAZING ANGLE BISTATIC TERRAIN SCATTERING MEASUREMENTS

William G. Stevens¹, Michael J. Sowa, Bertus Weijers
Electromagnetic Scattering Branch
Sensors Directorate
Air Force Research Laboratory
Hanscom AFB, MA 01731

David J. McLaughlin
ECE Department
Northeastern University
Boston, MA

Fully-polarimetric measurements of bistatic scattering from suburban, foliage-covered terrain were conducted, and normalized cross section results are presented. The measurement system consisted of a 2.71 GHz pulsed radar using a ground-based transmitter and receiver. Transmitter and receiver antennas were 110 meters and 200 meters, respectively, above the local terrain to produce incidence and scattering angles near grazing. Baseline separation of transmitter and receiver was approximately 8 kilometers. The 0.5 millisecond transmitter pulsedwidth and 1 degree half-power beamwidth of the transmit antenna defined the bistatic resolution cell, generally producing cells having area between 10^4 and 1.4×10^4 square meters. The collection of cells this size and in this region consists of both homogeneous elements, mainly trees, and heterogeneous components, where parts of fields and some buildings also may be present within a cell along with foliage. The transmitted pulse was switched between vertical and horizontal polarization at alternate repetition intervals while vertical and horizontal components of the scattered signal are recorded simultaneously. With a pulse repetition frequency of 400 Hz, the scattering scene is sufficiently stationary between successive pulses that the complete polarization scattering matrix can be represented.

Propagation Analysis in Container Terminals

*King-Shih Huang, *Hung-Sheng Chiang, *Jin-Kung Chung, and *Jean-Fu Kiang

*Telecommunication Lab.

Chunghwa Telecom Co., Ltd.

Yang-Mei, Taoyuan, Taiwan 326, ROC

*Department of Electrical Engineering

National Chung-Hsing University

Taichung, Taiwan 402, ROC

Propagation studies in outdoor and indoor environments are important issues in the planning and installation of personal communication systems. Measurement data have been collected at many different locations, and statistical methods are usually used to characterize the properties of the subject channels. Typical parameters extracted from measurements are decaying rate with distance, time delay, time delay spread, and so on. Semi-analytical models like mode-matching method and ray-tracing technique have also been proposed to identify the key factors that affect the channel properties. In general, the propagation environments are simplified to regular shapes so that the analytical models can be applied. If the geometry becomes more complicated, these methods may take too much computation time.

In this work, we develop a ray-tracing approach with diffraction correction to study the propagation properties in container terminals. Due to the standard size of containers and regular deposit in the terminals, corridors are formed at regular intervals. It is required to set a steady communication link between the base stations and the users walking in the corridors. The container walls cause multiple reflections when a ray trace is confined within the corridor. The upper edge of the container sitting at the top of the pile causes diffraction to the incident ray, and the diffracted ray is confined within the corridor in the form of multiple reflections.

Image theory is used to list two sets of traces between the base station and the user terminal. The first set consists of all possible traces that experience multiple reflections from the container wall. The second set consists of all possible traces that are diffracted by the upper edge of the top container and then multiply reflected by the container walls. A simulation program which combines a ray-tracing approach and image theory is developed to study the effects of the geometrical parameters like corridor width, height, and length. Measurements are also conducted at several terminal sites to verify the accuracy of this model.

Investigation of Base-Station Polarization Diversity in Personal Communication Systems

Xin Tian, Hao Ling, Wolfhard J. Vogel

The University of Texas at Austin
10100 Burnet Road, Austin, TX 78758

Achieving both reliable uplink performance and long battery life for handsets in personal communications are conflicting requirements. Diversity operation of the base-station can help overcome the deepest fades and thus reduce the power demands made on the mobile handset. However, space diversity reception at typical elevated base-station locations requires separation of 30λ for broadside incidence and even more for in-line incidence and is therefore difficult to implement from an environmental point-of-view. Polarization diversity for mobile radio systems can offer both reduced real-estate impact and improvements in performance. This comes about because polarization diversity implements 2-branch receiver diversity with the advantage that base-station antennas can be spaced as closely as desired.

An experiment was carried out to assess the benefits of polarization diversity over space diversity. Measurements were made with three sets of antennas, including a conventional vertically polarized, horizontal space diversity arrangement, a dually polarized antenna with vertical and horizontal polarization and a dually polarized antenna with two slant 45° polarizations. The signals received with each antenna/polarization were recorded while a 1.9 GHz CW transmitter was driven in a suburban environment. The transmitter antenna was alternately roof-mounted vertically, roof-mounted at a 45° angle, and mounted inside the vehicle at 45° .

Of all the cases analyzed, the base-station with the vertical/horizontal polarization diversity had the lowest correlation between the two branches for the fast fading. This case also exhibited the best log-normal distribution for the local mean and Rayleigh distribution for the fast fading. Detailed results of the diversity data analysis, including the properties of the phase difference between the two branches, will be discussed.

separate sheet

Comparison of Ray Tracing, 3D and 2D FDTD Simulations of Propagation Models for Wireless Communications

Z. Yun, M. J White, and Magdy F. Iskander*

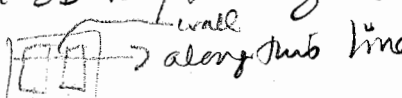
Electrical Engineering Department
University of Utah, Salt Lake City, UT 84112

Abstract

Propagation modeling is critically important in providing overall evaluation and guiding needed improvements in wireless communication systems. Radio propagation in the micro- or pico-cells is specially complex due to presence of a large number of randomly distributed reflectors and scatterers. The detailed knowledge of the field distributions is, therefore, essential and identifying avenues for achieving desirable distributions in most valuable. Ray tracing technique is one of the most commonly used methods in characterizing the propagation of radio wave in wireless communications. Ray tracing, however, is not very efficient in handling situations when complex and closely spaced multiple structures are present. In this case FDTD method may help due to its capability in modeling arbitrary geometries with complicated electric properties. 3D FDTD code requires significant computational resources, and hence the three dimensional FDTD algorithm can only used to simulate electrically small areas. It is then evident to use two dimensional FDTD method so as to model larger propagation sites.

In this paper we present a comparative study of simulation results based on the ray tracing, 3D FDTD, and 2D FDTD methods applied to propagation models in wireless communication. Advantages and limitations of these methods will be described and the accuracy of the 2D FDTD simulations particularly when used in a one floor model will be emphasized. It is shown that a combination of these techniques will give more accurate, reliable, and efficient simulation procedure for modeling propagation characteristics in wireless communication systems.

2D FDTD and 2D ray tracing compared
well



3D FDTD and 3D ray tracing
agreed well

Compared to AP Trans Ray Tracing
propagation paper that had
measurements

Electronics and Photonics

M. Piket-May and S. C. Hagness

An FEM Based Method on Full Wave Characterization of Distributed Circuits Including Linear and Nonlinear Elements	148
<i>E. Yasan*, L. P. B. Katehi, University of Michigan, USA</i>	
Optimized Waveguide-coupled Microcavity Ring and Disk Resonators.....	149
<i>S. C. Hagness*, A. Taflove, Northwestern University, USA</i>	
Microstrip and Stripline Design Study	150
<i>A. Byers*, B. Boots, M. Niyompong, M. Piket-May, University of Colorado, USA</i>	
Design of 20 and 30 GHz Tapered Power Dividers with Distributed Film Resistor	151
<i>K. Ayyildiz*, E. Arvas, Syracuse University, USA, S. Rehnmark, ANAREN Microwave Inc., USA</i>	
Thermal Conduction Analysis on Microwave IC Packages.....	152
<i>J. F. Kiang*, National Chung Hsing University, Taiwan, S. P. Liu, W. T. Lo, Industrial Technology Research Institute, Taiwan</i>	
A Green's Function Approach for Modeling Semiconductor Lasers and Optical Waveguides	153
<i>M. A. Jensen*, R. H. Selfridge, Brigham Young University, USA</i>	
Rough Surface Gratings for Quantum Well Infrared Photodetectors.....	154
<i>V. Jandhyala*, University of Illinois at Urbana-Champaign, USA, D. Sengupta, Jet Propulsion Laboratory, USA, E. Michielssen, B. Shanker, M. Feng, G. Stillman, University of Illinois at Urbana-Champaign, USA</i>	
Light Coupling In Quantum Well Infrared Photodetectors.....	155
<i>T. Cwik*, A. Borgioli, D. Wilson, California Institute of Technology, USA</i>	
Dispersive Properties in Phase-shifted Bragg Grating Filters	AP
<i>Q. Zeng*, Concordia University, Canada</i>	

An FEM Based Method on Full Wave Characterization of Distributed Circuits Including Linear and Nonlinear Elements

Eray Yasan* and Linda P. Katehi
Radiation Laboratory

Dept. of Electrical Engineering and Computer Sci.
The University of Michigan, Ann Arbor, MI 48109-2122, U.S.A.
Tel: 313-764-0502, Fax: 313-747-2106, Email: eray@engin.umich.edu

Theoretical characterization of microwave circuits including linear and nonlinear elements has been an interest in many ways using numerical techniques including Finite Element Method (FEM). Since the lengths of elements connected to the microwave circuit are very short so that Kirchoff's laws can be applied, the conventional scheme to find S parameters by adding extra line lengths is no more applicable. In this case the circuit is treated as a combination of inner (internal) ports where the linear or nonlinear elements are connected and the outer (external) ports where the input and output of the circuit are taken. Work has been done in time domain using "Compression Approach"(J. Kunish,M. Rittweger, S. Heinen and I. Wolff, Proc. 21st European Microwave Conf.,1296-1301,1991).

The linear passive part of the circuit is analyzed using the FEM. The ports are excited one at a time while the others are left open to derive the appropriate voltages and currents at all ports. The linear part of the circuit is thus characterized by the impedance matrix (Z-matrix). To reduce the computational cost, circuit symmetries are used and assuming circuit lossless, S parameters can be found using the simple relation

$$([Z] + [I])^{-1} ([Z] - [I]) = [S].$$

Following the computation of scattering matrix, a simulation software such as HP EEsof Libra and connecting the linear or nonlinear elements to the inner ports yields the input and output S-parameters of the microwave circuit.

As an example a microstrip line with a gap where a lumped element is connected has been analyzed. Simple lumped elements like resistors, capacitors and inductors have been connected and the resulting circuits have been modeled successfully. A diode mixer on a coplanar waveguide (cpw) designed for higher power handling capability has been analyzed using the above method in connection with Harmonic Balance Method (HBM). Results from these studies will be presented and discussed extensively.

Optimized Waveguide-Coupled Microcavity Ring and Disk Resonators

Susan C. Hagness* and Allen Taflove

Department of Electrical and Computer Engineering
McCormick School of Engineering and Applied Science
Northwestern University
2145 Sheridan Road, Evanston, IL 60208
s-hagness@nwu.edu

Waveguide-coupled microcavity ring and disk resonators have shown promise as versatile elements for photonic integrated circuits. The key advantages of these compact resonators are the wide free spectral range and the potential for high-density integration. These devices may serve as micron-size narrow-band tunable filters, frequency-domain switches, or intensity/phase modulators in optical communications and computing applications. An important step towards practical fabrication and commercialization of these devices is the exploration of designs that might reduce sensitivity to fabrication variations. In this paper, the FDTD method is used to investigate various designs of ring and disk resonators.

The coupling of light between the adjacent waveguides and the ring or disk is controlled by the width of the air gap and the coupling interaction length. To achieve the desired level of coupling, previous designs have required air gaps on the order of 0.1 nm. Since designs which permit wider air gaps are desirable from a fabrication point of view, we have explored designs in which the coupling length is increased in order to compensate for the increased gap width. FDTD simulations illustrate that elongated resonator geometries achieve this goal.

In comparison to single-mode microring resonators, microcavity disk resonators have the advantage of lower side-wall scattering loss. However, higher-order whispering-gallery modes may propagate without the presence of the inner rim. The higher-order modes must be suppressed in order to use microdisk resonators in WDM applications where low crosstalk across a wide spectrum is required. FDTD simulations reveal that by optimizing the width of the adjacent waveguides, the coupling between the waveguide mode and the higher-order modes of the disk can be minimized. Thus the optimized microdisk resonator offers a higher Q than the corresponding microring resonator as well as the desirable single-mode transmission characteristics.

Microstrip and Stripline Design Study

A. Byers*, B. Boots, M. Niyompong, M. Piket-May

University of Colorado at Boulder

Electrical and Computer Engineering Department

Boulder, CO, 80309-0425

mjp@colorado.edu 303-492-7448 fax:303-492-2758

Understanding interconnect behavior in electronic packages is of critical importance to successful package level and system level design and performance. Rapidly increasing clock speeds require that analog effects must be understood in order to optimize packaging without threatening the integrity of the electronics inside. Physical and electrical tradeoffs can be understood and optimal performance can be achieved if the performance characteristics for various structures are numerically studied before commitment to hardware is made. The application of Maxwell's equations with in a finite-difference time-domain engine fully accounts for the structures electrical behavior. The results presented in this paper will help to determine the optimal physical parameters of a given system while staying within electrically and physically dictated thresholds that accompany a variety of case studies.

We will first present some initial results for novel transmission line structures along with their performance characteristics. We will present a systematic study of microstrips and striplines over meshed ground planes. There are a number of reasons a meshed ground plane may exist. Sometimes the structures are periodic and can even exhibit photonic band gap like behavior, other times there are simply reasons that there needs to be a slot in the ground plane, again changing the performance of the line. [Piket-May et. al., APS/URSI Proceedings, June, 1995, p260] We will present some ground rules and suggestions for optimal design for a number of packaging and signal integrity specifications. This work will expand the study done by A. Mathis. [URSI Proceedings, Jan 8 1998, p314]

It has been shown that microstrip photonic band gap (PBG) structures may be designed to minimize unwanted harmonic propagation. [Radisic et. al., URSI Proceedings, Jan 7, 1998, p192]. We will present initial conclusions for using photonic band gap dielectrics in microstrip and stripline structures. We will compare these results to those obtained using a periodic meshed ground plane. Once again we will present a systematic study for a number of packaging and signal integrity specifications.

Results of case studies using other numerical techniques as well as measured data will be used for verification wherever possible.

DESIGN OF 20 AND 30 GHZ TAPERED POWER DIVIDERS WITH DISTRIBUTED FILM RESISTOR

Kasim AYYILDIZ*, Ercument ARVAS
Dept. of EECS, Syracuse University, Syracuse, NY 13244

Stig REHNMARK
ANAREN Microwave Inc., Syracuse, NY 13057

At lower frequencies, mostly stepped power dividers are used in microwave circuits. They are built with quarter-wave transformers and output port match and isolation are achieved with chip resistors. At higher frequencies, step discontinuities and chip resistors introduce undesired capacitive reactances. The chip resistor shows additional problems: a small displacement from its optimum location or a small difference in its value or dimensions causes poor match, isolation and unequal power split. To solve these problems, a tapered stripline power divider is designed. The goal is not to achieve a very large bandwidth but a component that is "forgiving" for manufacturing tolerances. The design process is based on the "even-odd" mode splitting of the circuit. A tapered transmission line is used to match the 100Ω line at the power splitting point to the standard 50Ω . The space between the matching sections is filled with a printed distributed film resistor for output port match and isolation. The purpose is to determine the optimum matching section, the optimum separation between the matching sections and the optimum resistivity of the film resistor such that the input and output mismatch is below a certain level over a band of frequencies. Hecken's near optimum taper is used as the matching section. A MINIMAX optimization process is performed to find the optimum separation and the optimum resistivity of the film resistor. With this new power divider the film resistor can vary $\pm 30\%$ in its resistivity or the gap between the lines can change by ± 2 mils without significant performance degradation. Furthermore, since the tapered power divider has no step discontinuities, it does not suffer from capacitive reactances existing in the stepped power dividers. The performance has been simulated using HFSS and the results for the 20 GHz power divider are shown in the figure below. We are in the process of obtaining experimental results.

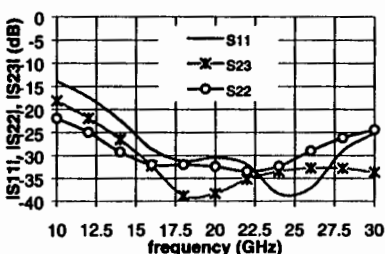


Figure 1: HFSS Simulation.

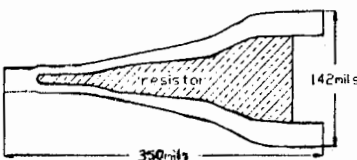


Figure 2: The power divider.

Thermal Conduction Analysis on Microwave IC Packages

*Jean-Fu Kiang, *Shih-Ping Liu, *Wen-Teng Lo

*Department of Electrical Engineering

National Chung-Hsing University

Taichung, Taiwan 402, ROC

*Computer and Communication Research Laboratories
Industrial Technology Research Institute

Chutung, Hsinchu, Taiwan 310, ROC

Heat conduction is an important issue in designing integrated circuits where heat dissipation may raise the temperature of certain components above their operating range and cause malfunction. Materials with high heat conductivity can be used to build heat sinks so that the heat generated by active components are guided away from the whole circuit. Due to the tight package in a monolithic integrated circuit, the heat generated by the active components may accidentally affect other temperature-sensitive components. One possible solution is to use the ground planes inside the circuits as heat shields. Additional heat conduction paths should be designed to bypass the internal heat. Several conduction paths may form a heat shield to partially enclose the sensitive components, hopefully to reduce their ambient temperature.

In this work, a two-dimensional model is proposed to analyze the heat conduction characteristics in a microwave integrated circuit package. A Laplace equation of temperature distribution is derived from the power conservation law and the Fourier's law which relates the heat flow density to the temperature gradient. The normal components of the heat flow density are continuous across the interface between two adjacent materials. A finite difference (FD) scheme is then developed to solve the Laplace equation in a finite region for the temperature distribution from which the power flow pattern and other parameters can be derived. A mode-matching method is also derived to check the accuracy of the FD approach under special circumstances.

Several heat paths and shields are studied by using this approach to check their effectiveness in reducing the temperature of the enclosed area. Factors analyzed include the path geometry, the shield size, and how the paths are connected to the heat sink.

A Green's Function Approach for Modeling Semiconductor Lasers and Optical Waveguides

Michael A. Jensen* and Richard H. Selfridge
Department of Electrical and Computer Engineering
Brigham Young University
Provo, UT 84602

The important role played by optical technology in today's technical marketplace has motivated the development of a wide variety of integrated optical devices based upon semiconductor and dielectric materials. Distributed Feedback (DFB) lasers, integrated optic switches and modulators, and in-fiber gratings are just a few examples of devices which have been developed over the years. Because of the complexity associated with these devices, the use of numerical and analytical simulation tools can greatly facilitate design optimization. Such tools must be able to accommodate the large electrical domains, the material inhomogeneities, and the solid state physics associated with most optical devices.

Recently, a new technique has been developed, known as the Recursive Green's Function Method (RGFM), which has proved very useful in the analysis of photonic and optical structures. The method models arbitrarily inhomogeneous media by dividing the domain of interest into small unit cells in which the material properties are assumed to be homogeneous. The Green's function satisfying the generalized Helmholtz equation is then obtained for each unit cell, and these Green's functions are combined using a recursive formulation to obtain the Green's function for the entire inhomogeneous domain. Surface integral equations are then solved to obtain the optical fields within or external to the structure. This approach leads to excellent computational efficiency, with storage requirements of $O(N)$ and computational requirements of $O(N^{3/2})$ for two-dimensional domains, where N is the number of unit cells used to discretize the region. This efficiency allows the analysis of relatively large structures. When the technique is solved in conjunction with the rate equations appropriate for active carriers in a semiconductor medium, then the analysis tool becomes an excellent candidate for predicting such parameters as side mode gain margin, threshold current density, and spatial hole burning in semiconductor DFB lasers.

This presentation will focus on the underlying theory of the RGFM technique, with particular emphasis given to its application to optical structures. The incorporation of active carrier rate equations into the solution approach will also be highlighted. The computational accuracy and efficiency of the technique will be demonstrated using comparisons to closed-form or previously solved example problems. The methodology will then be applied to several representative one- and two-dimensional optical structures, including DFB lasers and end-coupled optical waveguides, to illustrate the utility of the method in the design of practical optical devices.

Rough Surface Gratings for Quantum Well Infrared Photodetectors

Vikram Jandhyala^{++†}, Deepak Sengupta⁺⁺⁺, Eric Michielssen[†],
Balasubramaniam Shanker[†], Milton Feng^{++†}, and Greg Stillman⁺⁺

[†]Center for Computational Electromagnetics
and ⁺⁺Microelectronics Laboratory
Dept. of Electrical and Computer Engineering

1406 West Green St.

University of Illinois at Urbana-Champaign
Urbana IL 61801

and

⁺⁺⁺Mail Stop 302-306
Jet Propulsion Laboratory
4800 Oak Grove Drive
Pasadena, CA 91109

Quantum well infrared photodetectors (QWIPs) with AlGaAs/GaAs quantum wells exhibit great potential for use in large infrared imaging arrays. Quantum mechanical selection rules dictate that n-type unstrained QWIPs respond only to the component of the optical field along the growth direction. To facilitate detection of normally incident radiation by such imaging arrays, grating couplers are necessitated. These gratings diffract the incident optical field in directions favorable to intersubband absorption.

In the past, both periodic and quasi-random QWIP gratings have received attention. Periodic gratings have been studied extensively, through both experiment and numerical analysis. The use of quasi-random gratings as opposed to periodic ones has experimentally been shown to result in larger absorption over broad spectral ranges. Unfortunately, the computational analysis of scattering from such gratings has been restricted to one-dimensional profiles because of the large computational costs associated with the electromagnetic analysis of optically large, arbitrarily shaped, two-dimensional surfaces.

A recently developed integral-equation based electromagnetic analysis technique, the steepest descent fast multipole method (SDFMM), permits the rapid and accurate solution of the electric field integral equation governing scattering from quasi-planar structures. The SDFMM relies on an alternative representation of the homogeneous medium Green's function through a steepest descent integration and an inhomogeneous plane wave expansion. Previously, we have applied this technique to the analysis of scattering from two-dimensional quasi-random gratings interfacing with GaAs and have observed improved spectral behavior over that due to periodic gratings. In this work, rough surface gratings are proposed as a new class of optical couplers for QWIPs. Using the SDFMM, we have analyzed the scattering produced by these gratings. It should be emphasized that this is an extremely large-scale electromagnetic problem, involving 10^4 or 10^5 method of moment basis functions. The SDFMM, a multilevel fast solver, exploits the quasi-planar nature of rough surface gratings to obtain an accurate solution with minimal CPU time and memory usage. Rough surface QWIP couplers are seen to possess remarkable absorption and spectral properties. They offer larger absorption than periodic gratings, and exhibit an extremely flat spectral response.

Several numerical examples, comparing the absorptions profiles of periodic, quasi-random, and rough surface gratings, will be presented. The effect of rough surface grating parameters (mean square height and correlation length) on absorption and spectral behavior will also be demonstrated. It is expected that the use of rough surface gratings will result in a substantial enhancement in sensitivity and spectral response of QWIP-based imaging arrays. We anticipate that the *a priori* analysis of rough surface couplers using the SDFMM will provide designers with appropriate rough surface designs and parameters for improved QWIP performance.

LIGHT COUPLING IN QUANTUM WELL INFRARED PHOTODETECTORS

Tom Cwik*, Andrea Borgioli and Dan Wilson
Jet Propulsion Laboratory
California Institute of Technology
Pasadena California, 91109
cwik@jpl.nasa.gov

Detectors for long-wavelength infrared radiation are under development for a wide range of applications. Over this band (3-18 μm) applications range from spaceborne sensors used in the examination of absorption spectra to ground based hand-held digital cameras. Using device processing techniques, multiple gallium arsenide quantum well layers are designed into imaging focal plane arrays. The quantum well structures are engineered to absorb energy in the desired band when the electric field of the incident light is polarized perpendicular to the quantum well layers. Since the infrared radiation is incident normal to the quantum well layers in the design of a focal plane array, methods for coupling the incident radiation to modes that have the electric field polarized perpendicular to the layers (and in the direction of incidence) are needed. This requires a light coupling device imbedded into the focal plane array that will convert the incident energy into the correct polarization (S. Gunapala, et al, IEEE Trans. Elect. Dev., Vol. 44, No.1, Jan 97).

Light coupling can be accomplished by placing a periodic grating at a location below the multiple quantum well structure. The grating is designed to cause the reflected zero'th harmonic to be minimized while coupling energy into the +/- first harmonic propagating parallel to the multiple quantum wells. This design causes the reflected electric field to be polarized properly and to be absorbed by the quantum wells. In this paper, modeling and optimization of the light coupling grating using finite element methods will be discussed. The total electric field integrated over the quantum well volume will be used as a figure of merit for the detectivity of the quantum well infrared photodetector. The effect of planewave incidence as well as the effects of a light collecting lens will also be examined.

Electromagnetic Theory

R. J. Pogorzelski and D. L. Jaggard

Excitability and Power Characteristics of Nonreciprocal Complex Modes in Ferrite Loaded Boxed Microstrip Lines.....	158
<i>M. J. Freire*, F. Mesa, M. Horno, University of Sevilla, Spain</i>	
Conditions for the Appearance of Complex Modes in Strictly Bidirectional Waveguides	159
<i>M. Mrozowski*, Technical University of Gdansk, Poland</i>	
Einstein Needle-radiation Revisited: Highly Directive Currents on Large Closed Loops.....	160
<i>D. Margetis*, Harvard University, USA, G. Fikioris, Rome Laboratory, USA</i>	
An Analysis of Mode Coupling on Waveguiding Structures from the Theory of Universal Unfoldings.....	161
<i>G. Hanson*, University of Wisconsin-Milwaukee, USA</i>	
Symmetry Relations of the Translation Coefficients of the Scalar and Vector Multipole Fields.....	162
<i>K. T. Kim*, Air Force Research Laboratory, USA</i>	
Complex-order Fractional Curl in Electromagnetism	163
<i>N. Engheta*, University of Pennsylvania, USA</i>	
Exact Formulation of Electromagnetic Fields from Maxwell Equations with Current Distribution	164
<i>F. C. Chang*, TRW Space & Electronics Group, USA</i>	

Excitability and power characteristics of nonreciprocal complex modes in ferrite loaded boxed microstrip lines.

Manuel J. Freire, Francisco Mesa, Manuel Horno
Microwave Group, Dept. of Electronics and Electromagnetism
Avda. Reina Mercedes s/n, 41012, Sevilla (Spain)
Phone: 34-54552891; Fax: #34-54239434; e-mail: mesa@cica.es.

Many reports in the literature have analyzed the existence of complex modes in the dispersion relations of different reciprocal/nonreciprocal microwave guiding structures. In reciprocal structures, the study of the power associated with complex modes has shown that reciprocal complex modes do not carry power separately whereas the power associated with the superposition of a pair of complex modes having the same attenuation constant (α) and opposed phase constants ($\pm\beta$) is purely reactive [A. Omar, K. Schünemann, IEEE-MTT, 33, 1313-1322, 1985], [T. Rozzi, L. Pierantoni, M. Farina, IEEE-MTT, 45, 345-353, 1997]. Therefore, complex modes in reciprocal structures are strongly coupled and cannot exist separately. In addition, the analysis of the current density excited by practical feeds in infinite-length boxed reciprocal microstrip lines has shown that reciprocal complex modes are always excited in pairs of modes with $\pm\beta-j\alpha$ complex propagation constants, the superposition of this pair of modes giving place to a modulated evanescent mode [M. J. Freire, F. Mesa, M. Horno, Proc. of 27th EUMC, 1142-1147, 1997].

It is also well known that, in nonreciprocal transversely magnetized waveguides, evanescent modes cannot exist and all the modes that do not carry net average active power must be complex in these structures [R. Marqués, F. Mesa, M. Horno, IEEE-MGWL, 2, 278-280, 1992]. However, the physical significance of these modes has not been yet clearly established. In order to get a clear insight into the nature and role of complex modes in nonreciprocal structures, the authors have analyzed the power characteristics and the degree of excitability of complex modes in an infinite-length ferrite loaded boxed microstrip. Thus, an algorithm has been developed to compute the power carried by complex modes through the cross section of the structure. Explicit data and power profiles show that nonreciprocal complex modes store net average reactive power and do not carry net average active power, although an active power flux density exist. Therefore, nonreciprocal complex modes are purely reactive in the same way as occurs in transversely magnetized waveguides [R. Marqués, F. Mesa, M. Horno, IEEE-MTT, 41, 1409-1418, 1993]. Moreover, the modal decomposition of the current density excited by a delta-gap voltage source on the strip conductor of the boxed microstrip has shown that nonreciprocal complex modes are excited individually, in agreement with their reactive nature. In consequence, complex modes set up the reactive part of the modal spectrum in nonreciprocal structures, playing the same role of evanescent modes in reciprocal structures.

Conditions for the Appearance of Complex Modes in Strictly Bidirectional Waveguides

Michał Mrozowski,

Technical University of Gdańsk,
Department of Electronics, Narutowicza 11/12
80-956 Gdańsk, Poland

Complex modes are the least known type of waves which may exist in lossless waveguiding structures. A single complex wave can not exist because it always gives rise to a second complex wave having a complex conjugate propagation constant. Such a pair stores reactive energy. These basic facts about complex modes have been established by many researchers. It has also been shown that complex waves above cutoff are a result of the degeneracy between forward and backward waves. However, the circumstances accompanying the appearance of complex waves below cutoff have not been explained. Recently, (Mrozowski, "Guided Electromagnetic Waves", Research Studies Press, 1997) a comprehensive theory of complex waves has been developed. In this contribution the results of this theory will be presented for the wide class of inhomogeneously loaded strictly bidirectional waveguides. The analysis is based on the generalized telegraphist equations, the theory of symmetric matrix pencil and the general orthogonality and energy relations for modes in inhomogeneous anisotropic waveguides. The new theory, valid for arbitrary strong inhomogeneities, predicts that the complex waves below cutoff result from the coupling of nearly degenerate pair of waves, each having different energy properties. The energy stored in electric field of one wave taking part in the interaction has to exceed the energy stored in the magnetic field and the opposite must be true for the second wave. A new fact which was established for a complex wave is that while it cannot transport energy the average value of electromagnetic momentum is nonzero. The theory explains which guide geometries are prone to complex waves and allows one to predict the approximate frequency range of the complex wave pair. These theoretical findings will be illustrated at the conference by the numerical investigation of energy relations in several waveguiding structures.

**"EINSTEIN NEEDLE-RADIATION" REVISITED:
HIGHLY DIRECTIVE CURRENTS ON LARGE CLOSED LOOPS**

Dionisios Margetis*

Gordon McKay Laboratory, Harvard University, Cambridge, MA 02138-2901
and

George Fikioris

Rome Laboratory, Electromagnetics & Reliability Directorate,
Hanscom AFB, MA 01731

In 1922, Oseen (*Ann. Phys.* **69**, 202, 1926) demonstrated that an arbitrarily small current-carrying region can give rise to an arbitrarily narrow radiation pattern. Oseen termed this extreme theoretical possibility "Einstein needle-radiation," referring to a 1909 paper by Einstein on the quantum nature of radiation (*Phys. Ztschr.* **10**, 817, 1909). Today it is well known that there is no upper limit to the directivity of an idealized current distribution.

It is the purpose of this analysis to study simple models of highly directive, electrically large closed loops of currents via the solution of a constrained optimization problem. The starting point is the Fredholm integral equation of the second kind, satisfied by an optimum current that maximizes the directivity D in the far field under a fixed ratio $C = N/T$, where N is proportional to the ohmic losses and T is the total radiated power. For a circular loop of size ka , the optimum current is found to be

$$J(\phi) = \sum_{n=-\infty}^{\infty} \frac{J_n(ka)}{1 + \alpha g_n(ka)} e^{in\phi}, \quad (1)$$

where $g_n(ka) = J_n(ka)^2$ in two dimensions and of more complicated structure in three dimensions, and α is a positive Lagrange multiplier signifying the dependence on C . For large ka , (1) is treated approximately for moderately large values of C up to $C \rightarrow \infty$, where the "Einstein needle-radiation" obtains.

A generalization of the analysis to other convex loops is attempted, with emphasis on the derivation of universal asymptotic forms. For example, the universal form

$$D \sim \frac{\ln(C \ln C)}{\ln \ln C} \quad \text{as } C \rightarrow \infty$$

is studied in some detail.

**An Analysis of Mode Coupling on Waveguiding Structures
From the Theory of Universal Unfoldings**

George W. Hanson
Department of Electrical Engineering and Computer Science
University of Wisconsin-Milwaukee
P.O. Box 784
Milwaukee, Wisconsin 53201

The singularity theory concept of a universal unfolding is applied to the problem of coupling of modes on longitudinally invariant waveguides. Starting with an unperturbed waveguide which exhibits sufficient symmetry such that orthogonal modes may propagate, functional conditions are provided for points of modal degeneracy. These points are obtained as degenerate Morse points, and result in a normal form which provides for the orthogonal nature of the modes. When a small perturbation is introduced to break structural symmetry, the normal form admits a unity-codimension universal unfolding which characterizes the hyperbolic behavior of coupled (non-orthogonal) modes. This procedure can be connected to traditional coupled-mode theory, where the Morse point represents the minimum of the coupling coefficient. This theory is useful for the rapid identification of regions of mode-interaction by specifying necessary and sufficient functional characteristics for mode coupling to occur. Results will be shown for a variety of guided-wave structures which exhibit mode coupling, including asymmetric coupled microstrips, shielded microstrip lines, and bianisotropic slab waveguides.

SYMMETRY RELATIONS OF THE TRANSLATION COEFFICIENTS OF THE SCALAR AND VECTOR MULTIPOLE FIELDS

Kristopher T. Kim
Electromagnetics Technology Division
Sensors Directorate
Air Force Research Laboratory
31 Grenier Street
Hanscom AFB, MA 01731-3010

The translation addition formulas of multipole fields express the multipole field of one coordinate system in terms of the multipole fields of another coordinate system that is related to the former by a pure translation. They have been useful analytic tools in many areas of electromagnetic research such as the theoretical study of scattering from multiple spheres, probe correction in spherical near-field scanning, and modeling of wave propagation through a discrete random medium, to name a few. More recently, fast scattering algorithms were proposed that use the translation formulas to reduce the computational complexities of solving surface and volume integral equations. The interest in these algorithms has, in turn, brought about renewed interest in the formulas as well as efficient ways to compute the translation coefficients (K.T. Kim, *IEEE Trans. Propagat.*, Vol. 44, No. 11, pp. 1482-1487, 1996).

While applying the translation formulas to solve a volume integral equation efficiently, we observed certain symmetry properties of the translation coefficients. Since symmetry relations can be used to check the accuracy of computed values of translation coefficients as well as to further reduce the computational cost of evaluating them for the aforementioned applications, we were motivated to investigate their symmetry relations. The translation coefficients of scalar and vector spherical multipoles are of the form, $\Gamma_{l,m}^{l',m'}(k, \vec{R})$, where (l, m) and (l', m') are, respectively, the modal indices of the original and the translated multipole fields, while k and \vec{R} are, respectively, the wavenumber and the translation vector. Specifically, we investigate the respective symmetry relations of the translation coefficients of the scalar and vector multipole fields under (i) spatial inversion of the translation vector, $\vec{R} \rightarrow -\vec{R}$, (ii) interchange of modal indices, $\{(l, m), (l', m')\} \rightarrow \{(l', m'), (l, m)\}$ and (iii) simultaneous change of the signs of the azimuthal indices, m and m' , $\{(l, m), (l', m')\} \rightarrow \{(l, -m), (l', -m')\}$. In order to remain general, the wavenumber, k , is assumed to be complex corresponding to wave propagation through a lossy medium. We further show that when k becomes real, the symmetry relations reported here reduce to those reported earlier.

Complex-Order Fractional Curl in Electromagnetism

Nader Engheta

Moore School of Electrical Engineering

University of Pennsylvania

Philadelphia, Pennsylvania 19104, U.S.A

Tel: (215) 898-9777, Fax: (215) 573-2068

E-mail: engheta@pender.ee.upenn.edu

The idea of fractionalization of the curl operator in electromagnetics was recently introduced by us [N. Engheta, "Fractionalization of the Curl Operator and Its Electromagnetic Application," a talk presented in the 1997 *IEEE Antennas and Propagation International Symposium/North America Radio Science (URSI) Meeting*, Montreal, Québec, Canada, July 13-18, 1997. The summary appeared in the Digest of the IEEE AP-S Symposium, Vol. 2, pp. 1480-1483; and N. Engheta, "Fractional Curl Operator in Electromagnetics," *Microwave and Optical Technology Letters*, Vol. 17, Issue 2, February 5, 1998. In press] We showed that a new operator, which we called fractional curl operator denoted as curl^α , can, in general, be defined from a conventional curl operator in such a way that when the non-integer parameter α takes the value zero this operator becomes the identity operator and when α becomes unity the operator acts as a conventional curl operator. For all non-integer real values of α between zero and unity, this fractional curl operator provides the "intermediate" situations. Using this operator we were also able to "fractionalize" the concept of duality in electromagnetics [N. Engheta, "Fractional Derivative and Its Role in Fractionalization of Duality Principle in Electromagnetism," a talk in *USNC/URSI National Radio Science Meeting*, Boulder, CO, Jan. 5-8, 1998, abstract in page 308; and N. Engheta, "Fractional Duality in Electromagnetic Theory" a talk in the 1998 *URSI International Symposium on EM Theory*, Thessaloniki, Greece, May 25-28, 1998.]

An interesting issue to raise is the following: What would happen if the fractional parameter α in the new operator curl^α took a complex quantity? What implications would this complexification have for such an operator? It turns out that allowing the parameter α to have complex values would bring some interesting additional features for the fractional curl operator. For instance, one would be able to extend the standard problem of reflection of electromagnetic plane wave normally incident on a perfectly conducting plate to the case of normal reflection from an impedance wall with surface impedance having complex values. Some other properties can also be attributed to this complexification of parameter α .

In this talk, the results of our theoretical study of complexification of parameter α in the fractional curl operator will be presented and the physical meanings behind these results will be discussed.

EXACT FORMULATION OF ELECTROMAGNETIC FIELDS FROM MAXWELL EQUATIONS WITH CURRENT DISTRIBUTION

Feng Cheng Chang *
Antenna Products Center
TRW Space & Electronics Group
Redondo Beach, California

In the usual approach to solving Maxwell's equations with given current distributions, the vector potential function is first calculated, and the desired electromagnetic fields are then obtained by vector differential operations upon this vector potential. A vector differential operation is an operation which contains the vector differential operator ∇ , such as the gradient, divergent, curl, and Laplacian. By using the free-space Dyadic Green's function, one may bypass the vector potential function, and thereby establish a direct relation between the current source and the resulting electromagnetic fields. However, the solutions to Maxwell's equations are still quite involved, because of the vector differential operations in addition to the integration. In numerical computation, the evaluation is usually much easier for the integration than for the differentiation, since the integration can always be approximately using summation.

Convenient formulas for the electromagnetic fields in solving the Maxwell's equations with given current distributions are derived and presented herein. These formulas remove the complicated vector differential operations and replace them with simple vector algebraic operations. A vector algebraic operation is an operation which contains only the dot product and cross product of vectors. The resulting field solutions are exact and can be explicitly written in matrix formulation. Both the current source and the resulting fields can also be expressed in terms of any desired coordinate systems.

If the electromagnetic fields either in the near field (Fresnel's region) or in the far field (Fraunhofer's region) are of primary interest, the formulation can be greatly simplified. The electromagnetic fields are easily derived by simple matrix multiplication whenever the radiation vector is determined.

* Formally with National Space Program Office, Hsinchu, Taiwan, R.O.C.

Transient Fields, Effects, and Systems

E. Heyman and E. Miller

On Chaotic Electromagnetic Wave Propagation.....	166
<i>T. X. Wu*, D. L. Jaggard, University of Pennsylvania, USA</i>	
Short-pulse Scattering from a Dielectric BOR Buried in a Lossy Layered Medium	167
<i>N. Geng*, L. Carin, Duke University, USA</i>	
Resonances of a Dielectric BOR Buried in a Lossy, Dispersive Layered Medium	168
<i>N. Geng*, L. Carin, Duke University, USA</i>	
The Effects of Transients due to Element Switching on SS Frequency Hop Communication Systems.....	169
<i>F. A. Pisano, III*, C. M. Butler, Clemson University, USA</i>	
Spectral Alternatives for the Synthesis of Short-pulse Wavefields in Waveguides.....	170
<i>B. P. de Hon*, Eindhoven University of Technology, The Netherlands, E. Heyman, Tel-Aviv University, Israel, L. B. Felsen, Boston University, USA</i>	
Transient Radiation and Reception Involving the Resistively Loaded Dipole	171
<i>S. N. Smadar*, E. Mokole, Naval Research Laboratory, USA</i>	
Robust Target Identification in White Gaussian Noise for Ultra-wideband Radar Systems	172
<i>J. Mooney*, Z. Ding, L. S. Riggs, Auburn University, USA</i>	
An Internal Problem Solution for a Transient Inhomogeneous Conducting Half-space.....	173
<i>I. Y. Vorgul*, Kharkov State University, Ukraine.</i>	
Approximation Method for the Transient Scattering of an Object above Infinite PEC Plane	174
<i>D. B. Ge*, Y. B. Yan, Xidian University, P.R.China</i>	

On Chaotic Electromagnetic Wave Propagation

Thomas Xinzhang Wu* and Dwight L. Jaggard

Moore School of Electrical Engineering

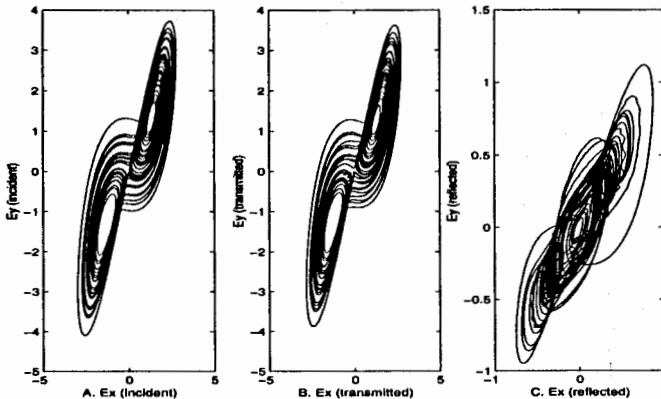
University of Pennsylvania

Philadelphia, PA 19104-6390

Recently, chaotic communication has caught the attention of many researchers [see e.g., S. Hayes, *Physical Review Letters* **70**, 3031(1993)]. Chaos in mathematical equations and in physical systems was originally thought to be a form of noise or random disturbance. It is now well known that chaos is not noise but rather an intricate pattern that arises in the behavior of non-linear systems that are extremely sensitive to changes in initial condition. Because of this sensitivity, controlling chaos was originally thought to be difficult. However, it has recently been demonstrated that chaos can be controlled [E. Ott, C. Grebogi and A. Yorke, *Physical Review Letters* **64**, 1196(1990)]. This has piqued interest in new, non-linear devices and systems for communications. In such systems, chaotic electromagnetic wave propagation becomes crucial in the system design.

Here, we explore a new area, chaotic electromagnetic wave propagation, in electromagnetic research. We review basic concepts associated with chaos (e.g. stability of dynamical system, strange attractor, fractal dimension, phase diagram, Lyapunov exponent, basin of attraction, bifurcation diagram and Poincaré map). We then show our results concerning chaotic electromagnetic wave scattering.

As an example of our work, we consider wideband chaotic waves scattered by a dielectric slab. Here, we use a Lorenz system to generate a chaotically polarized plane wave. The trajectory of the electric field traces the strange attractor shown in Figure A. For the normal incidence case, it is interesting to note that the transmitted wave has almost the same attractor (Figure B) as the incident wave, but the reflected wave may be rather different (Figure C) and so gives the *chaotic signature* of the slab. Both normal and oblique incidence are investigated.



wu-jaggard1.ps

Short-Pulse Scattering from a Dielectric BOR Buried in a Lossy Layered Medium

Norbert Geng* and Lawrence Carin

Department of Electrical and Computer Engineering

Duke University

Durham, NC 27708-0291

Electromagnetic scattering from bodies of revolution has been a subject of interest for nearly three decades. This research has been motivated by the fact that a body of revolution (BOR) can be used to simulate many man-made targets (*e.g.*, missiles). Most previous such research has focused on targets in free space, representative of scattering from airborne BORs. However, there has recently been significant interest in using electromagnetic scattering (radar) for the detection of underground targets. In the work presented here, we are interested in buried mines. It is well known that such targets often closely resemble BORs. A principal challenge in mine detection involves plastic mines, with such targets generally composed of only trace metallic content (usually the tiny firing pin, often representing only a few grams of metal). In the work presented here, we therefore consider dielectric BORs buried in a layered medium, with the lossy, dispersive layers representing the typical layered character of many soils (and/or a snow layer).

While scattering from a plastic mine can be solved via a three-dimensional finite-difference time-domain (FDTD) algorithm, such requires solution of the fields at all points in the computational domain. Though ceding some generality, the MoM formulation only requires solution of the fields along the BOR generating arc, from which the scattered fields can be determined at any point. Moreover, a modified version of the BOR-MoM code can be used to study the properties of dielectric-mine resonances, something that is difficult to perform via FDTD, since mines are generally characterized by low-Q resonances.

The BOR-MoM analysis developed here uses a mixed-potential integral-equation formulation. To effect such, one requires the space-domain dyadic Green's function for a general layered medium, here considering loss and dispersion as well. As is well known, closed-form representation of the dyadic Green's function components is only possible in the spectral domain, while the Sommerfeld integrals required for conversion to the space domain must be evaluated approximately. Most electromagnetic mine-detection systems are of an ultra-wideband nature, and therefore it is essential that the Green's function components (which are frequency dependent) be computed as efficiently as possible. To this end, we exploit here the method of complex images.

In addition to describing the above formulation, with a focus on computational efficiency for wideband applications, we examine the phenomenology associated with scattering from buried dielectric and conducting targets. Of particular interest are the effects of target and soil properties on the subsequent target signature, as a function of operating frequency. Moreover, the use of a layered-media Green's function, rather than the simplified half-space Green's function, allows us to examine several important and realistic scattering problems of interest. For example, one may be interested in detecting small mines buried in soil, with the soil covered by a snow layer. The phenomenology of this problem is examined in detail, as a function of snow type (wetness) and snow depth.

Resonances of a Dielectric BOR Buried in a Lossy, Dispersive Layered Medium

Norbert Geng* and Lawrence Carin

Department of Electrical and Computer Engineering

Duke University

Durham, NC 27708-0291

If a target is excited by a short pulse of electromagnetic energy, fields are diffracted initially at localized scattering centers in and on the target. Subsequently, after the incident wave has departed (at what is termed "late time"), multiple diffractions occur *between* scattering centers and, for a penetrable target, energy reverberates inside as well. Each such multiple diffraction or reverberation is accompanied by energy that radiates away from the scatterer. Consequently, the late-time energy in and on the target decays, as do the associated late-time radiated fields. This late-time phenomenon has been parametrized rigorously in terms of the well-known singularity expansion method (SEM).

In the work presented here, we are interested in dielectric targets (*e.g.*, plastic land mines) buried in a lossy, dispersive layered medium (simulating soil). Modeling of a target's natural modes requires solution of the source-free target response. Therefore, here we utilize the method of moments (MoM), with restriction to targets that can be simulated as a body of revolution (BOR). While the restriction to BOR targets is clearly a simplification, most land mines are accurately so modeled.

The MoM analysis of targets buried in a lossy layered medium requires accurate computation of the layered-medium Green's function, with such necessitating the efficient analysis of Sommerfeld spectral integrals. Numerous techniques have been developed for the analysis of these ubiquitous integrals, with the recently developed method of complex images constituting a particularly attractive option. Target resonances are characterized by *complex* frequencies, introducing complications with regard to branch-cut and pole locations, with such impacting the path of integration for the Sommerfeld integrals. We address these issues in detail and demonstrate how such are handled within the context of the method of complex images.

In addition to discussing the algorithm itself, we present several numerical results on the resonances of buried plastic targets, as a function of soil type and target depth. As a comparison, we also show results for buried conducting targets of the same shape. Finally, to assess the practicality of resonance-based detection of buried plastic targets, we consider the Cramer-Rao lower bounds for the resonant frequencies of such targets.

The Effects of Transients Due to Element Switching on SS Frequency Hop Communication Systems

Frank A. Pisano III* and **Chalmers M. Butler**

Department of Electrical and Computer Engineering

Clemson University

Clemson, SC 29634-0915

In a frequency hopping spread spectrum communication system, one needs an antenna that can radiate and receive effectively at different frequencies. For a small/compact, robust, omni-directional antenna to be practicable in this application, it must have a modest radiation resistance at the frequencies at which radiation and reception are to take place. To this end we consider the feasibility of a scheme involving switching different lengths of wire into and out of a wire antenna structure. The structure is tuned to resonate at the center frequency of the frequency slot in which the transmitter operates momentarily. When the transmitter "hops" to the next frequency slot, antenna elements are switched in or out so that the structure now resonates at the center frequency of the new frequency slot. Therefore, in each frequency slot the structure resonates at the frequency of operation or near thereto, thus assuring an adequate level of radiation resistance. The antenna doesn't have wide bandwidth in general but during any hop epoch radiation resistance is adequate, causing the effective bandwidth to appear broad.

However, in this scheme a setup time is required for the currents to settle after each frequency hop. As the hop occurs, the element configuration state of the antenna structure is switched, creating transients in the antenna's currents. (Transients also occur from a shift in frequency alone.) These transients must be allowed to settle down before data can be processed reliably by a receiver. Otherwise data errors are introduced in a digital communication system.

To analyze data errors that can arise due to the physical constraints of a wire antenna operating in a mode involving element switching and to determine other characteristics of transients created by switching structural configuration and frequency, the authors have developed a method to determine currents and radiation based on a time domain integral equation applicable to an antenna structure comprising switched, curved-wire elements. The integral equation solution technique developed for this application is very stable and accurate, as it must be in order to be able to treat switched time-harmonic signals of many cycles.

By means of the time-domain analysis, the authors evaluate the performance of a noncoherent receiver and illustrate the use of a switched antenna in a frequency hop communication system. Also, the authors will demonstrate the use of multiple antenna configurations under switched conditions and discuss the effects of settling times and pulse lengths required to prevent the introduction of errors into the communication system.

Spectral Alternatives for the Synthesis of Short-pulse Wavefields in Waveguides

B. P. de Hon¹, E. Heyman¹ and L. B. Felsen²

¹ Department of Electrical Engineering, Eindhoven University of Technology, Eindhoven, The Netherlands

¹ Department of Electrical Engineering - Physical Electronics, Tel-Aviv University, Israel

² Department of Aerospace and Mechanical Engineering and Department of Electrical and Computer Engineering, Boston University, Boston, MA

The canonical two-dimensional problem of synthesis of short-pulse wavefields in a simple waveguiding configuration is addressed, focusing attention on various alternative spectral synthesis options. Specifically, the non-dispersive generalized-ray representation is set against the dispersive collective description of the spectral wavefield. For the collective representation, two different synthesis options are considered, viz., a conventional summation of modes, versus what we shall refer to as a non-conventional summation of spectral resonances. In the conventional approach the field is synthesized in terms of a time-harmonic spectrum of modes. In the non-conventional approach the time-harmonic integration is performed prior to the integration over the spatial spectrum, leaving the field expressed as a plane-wave spectrum of resonances.

Each representation bears a distinct physical interpretation and has different convergence properties. We explore the trade-off between the alternative representations with respect to the space-time observation regime, the frequency content of the excited pulse and the spatial directivity. An asymptotic analysis is shown to lead to a synthesis of the wavefield constituents in terms of instantaneous frequencies and instantaneous normalized slownesses (normalized wavenumbers), through which a cogent description of space-time-domain wave phenomena is obtained. Configuration and pulse-dependent characteristic parameters are extracted through which the near-zone and far-zone regimes are delineated. Numerical results are presented to elucidate the underlying principles.

TRANSIENT RADIATION AND RECEPTION INVOLVING THE RESISTIVELY LOADED DIPOLE

Suren N. Samaddar*

Eric L. Mokole

Radar Division (Code 5340)

Naval Research Laboratory

Washington, DC 20375-5336

Based on the frequency-domain results of Wu and King (T.T. Wu and R.W.P. King, *IEEE Trans. Antennas Propagat.*, AP-13, May 1965, 369-373), an analytical representation of the transient radiated field from a resistively loaded dipole that is excited by an arbitrary pulsed voltage $V(t)$ is derived. The field is then expressed in terms of various differential and integral operations on $V(t)$, allowing one to identify the points on the antenna from which radiation occurs. In particular, the transient field from the antenna at an observation point (r, θ) can be written as the sum of four distinct contributions: two pulses from the feed point of the dipole and one pulse from each of its endpoints. With respect to the contributions from the feed point, the two pulses emanate simultaneously. One pulse is a retarded replica of the input voltage, where the retardation time is r/c and c is the speed of light. The other pulse is a time integral of $V(t)$ and an attenuation factor that depends on the transit time h/c , where $2h$ is the length of the dipole. The attenuation factor appears to be a consequence of the resistive loading. The pulses from the ends of the dipole are also time integrals of $V(t)$ with the same attenuation factor; however, they emanate at two later times. Because previous work on transient radiation from this resistively loaded dipole considered specific forms of $V(t)$, such as the gaussian pulse, the aforementioned interpretation was not apparent. Analogously, the behavior of the received open-circuit voltage by the same resistively loaded dipole can be interpreted similarly.

Robust Target Identification in White Gaussian Noise for Ultra-Wideband Radar Systems

Jon Mooney*, Zhi Ding, and Lloyd S. Riggs

Department of Electrical Engineering
200 Broun Hall • Auburn University, Alabama 36849

Radar target identification, as witnessed by the plethora of the literature on the topic, is an important problem of considerable interest to many civilian and military agencies. The number of signatures even for a small target library can become quite large, since, in general, a unique return is produced for each new target aspect. Any robust target identification algorithm must adequately address this issue. The extinction pulse (E-pulse) and other related techniques, which are based on a singularity expansion method description of the radar return, indeed boast an aspect independent identification algorithm. However, as demonstrated in this paper, the performance of these techniques in white Gaussian noise is inferior to the method described here.

In this paper, we develop a new method based on a generalized likelihood ratio test (GLRT) to perform target identification in the presence of white Gaussian noise. As with the E-pulse technique, our method takes advantage of the parsimonious singularity expansion representation of the radar return. In general, the SEM representation of the late-time radar return of the k th target in the presence of noise can be modeled as

$$y(t) = \sum_i a_i^{(k)} \exp(s_i^{(k)} t) + n(t) \quad t > T_L \quad (1)$$

where $n(t)$ is additive white Gaussian noise with zero mean variance σ^2 . The parameters $a_i^{(k)}$ and $s_i^{(k)}$ denote the coupling coefficient and pole (resonant frequency and decay rate) of the i th mode, respectively, of the k th target. The coupling coefficient a_i is an aspect dependent parameter which means its value depends on the orientation of the target with respect to the source of wideband illumination. In contrast, the pole s_i is aspect independent. The poles are strictly dependent only on the geometry of the target. Assuming that the poles of each target in the "target library" have been determined, then a likelihood function for each target can be developed using the model structure in (1) and the probability density function of the noise. These likelihood functions, each of which are a function of the unknown coupling coefficients (a_i), can then be used in a generalized likelihood ratio test (GLRT) to develop a decision rule (or detector) as to which target in the "target library" is present.

In addition to the development of a GLRT, sufficient statistics and simple practical implementations of the GLRT are presented. Simulation results using various thin wire targets are presented contrasting the performance of the GLRT to the E-pulse technique as a function of signal-to-noise ratio.

ON INTERNAL PROBLEM SOLUTION FOR A TRANSIENT INHOMOGENEOUS CONDUCTING HALF-SPACE

Irena Yu. Vorgul

Applied Electrodynamics Dept., Kharkov State University, 4 Svoboda Sq., Kharkov 310077, Ukraine. e-mail: ira@unicom.kharkov.ua

Scattering objects, especially natural ones, often are nonstationary. It can result in essential transformation of the scattered field.

The present work is devoted to solving the problems of internal field determination in a half-space with temporal and spatial (along the longitudinal coordinate) variation of the medium conductivity, when an external field is known. For arbitrary temporal and spatial conductivity dependences one constructs the method which can be called an analog of "embedding" method (used for random layered media) for transient media.

The problem is solved analitically. Mathematically it is formulated in terms of the Volterra integral equation for the internal and internal fields obtained by the Green's function of corresponding wave equation. The medium with transient conductivity is assumed to be inhomogeneous only along x axis, and the fields are considered to have only those components which are normal to the x - axis being independent on the y - and z -coordinates. It allows to solve one-space-dimensional problems. In this case the equation for the external field shows that this field can be determined by the function of only one variable and by an incident field. It is due to the assumed homogeneity of the external medium.

The integral equations for the external and internal fields are solved jointly being reduced to a first-order partial differential equation for a new function which determines the internal field in shifted time moments. Its right part is an infinite row of x powers with coefficients which are algebraic expression consisted of the conductivity time-dependence on the half-space boundary and the function of one variable determined by the external field. The exact solution for the internal field is then obtained by this row integration. For the field analysis we confine it considering a finite number of the terms, dependent on the desired accuracy. The more is x , the more terms must be taking into account to provide the required accuracy, so the developed technics is by its application an analog of "embedding" method applying to transient media.

Some examples of this technics usage with field analysis is also made.

Approximation Method for the Transient Scattering of an Object above Infinite PEC Plane

D.B.Ge and Y.B.Yan

Department of Physics, Xidian University

710071, Xi'an, P.R.China

email: dbge@xidian.edu.cn

Consider an object above the infinite perfectly conducting (PEC) ground with height of H , illuminated by a plane wave of electric field perpendicular to the PEC plane. This problem can directly be dealt with by the FDTD (P.B.Wang, G.L.Leonard, J.E.Baron, E.M.Gurrola, and R.A.Simpson, IEEE Trans. AP-44, 504-514, April, 1996) when the object is quite close to the PEC plane. However, the FDTD computation region will be too large to afford if the object goes far from the PEC plane. Here we present an approximation technique on the basis of free-space solution to treat this problem.

The transient scattering can physically be seen as the following process: the incident pulse first interacts with the object producing the first-order scattered field. This scattered field is propagating and reflected by the PEC plane back to the object. The interaction will further result in the second-order scattered field. The higher-order scattered fields will come out because of the multi-reflection, that however can usually be neglected if the object is not so close to the PEC plane. For far-field observation point, the first-order scattered field coming directly from the object and through the reflection of the PEC plane can be calculated by using the free-space FDTD computation and the image principle. To evaluate the second-order contribution, we first calculate the near-field for the observation point located downward below the object at a distance of $2H$. This field, which can be seen as the one reflected from the PEC ground, then impinges upward upon the object as an incident wave. The scattered field can again be computed by the free-space FDTD. The summation of these two parts, in which the time delay of the second-order with respect to the first-order scattering should be considered, gives rise to the transient scattered fields. The transient scattering for some simple objects are computed to exemplify this scheme. The proposed approximation method can be applied to the RCS estimate of an object located above the PEC plane.

Random Media Effects on Propagation and Scattering

G. S. Brown and A. Ishimaru

Dispersion-like Random Effects in Ultrashort Pulsed Beam Propagating through Nondispersive Random Media	176
<i>J. Gozani*, University of Colorado, USA</i>	
Statistical Moments of the Mutual Coherence Function Propagating through Intermittently Random Media	177
<i>J. Gozani*, University of Colorado, USA</i>	
Correlation Imaging of Objects in a Random Medium	178
<i>A. Ishimaru*, Y. Kuga, T. K. Chan, J. D. Rockway, J. J. Liu, University of Washington, USA</i>	
Electromagnetic Models and Measurement of Random Dielectric -Metallic Media: Model Comparison to Coaxial and Free Space Measurements	179
<i>R. Moore*, Georgia Institute of Technology, USA</i>	
Numerically Computed Effective Permittivity of a Composite Material Formed from Spherical Inclusions	180
<i>K. W. Whites*, F. Wu, University of Kentucky, USA</i>	
Scattering Cross Sections of a Random Medium Layer	181
<i>S. Mudaliar*, ARCON Corporation, USA</i>	
An Enhanced Steepest Descent Fast Multipole Method for the Analysis of Scattering from Two Dimensional Multilayered Rough Surfaces	182
<i>M. El-Shenawee*, V. Jandhyala, E. Michielssen, W. C. Chew, University of Illinois at Urbana-Champaign, USA</i>	
Ducting Effects on LGA Backscatter from 1-D Randomly Rough Perfectly Conducting Surfaces	183
<i>R. S. Awadallah*, G. S. Brown, Virginia Tech, USA</i>	
Optimal Time-Domain Detection of Targets Buried Under a Rough Air-ground Interface	184
<i>T. Dogaru*, L. Carin, Duke University, USA</i>	
On the Use of the Tapered Plane Wave Incident Field in Scattering and Propagation Simulations	185
<i>J. V. Toporkov*, R. S. Awadallah, G. S. Brown, Virginia Tech</i>	
Numerical Solutions of Wave Scattering from a Lossy Dielectric Random Rough Surface at Low Grazing Incidence using a Physics-based Two-grid Method Combined with the Banded-matrix Iterative Approach/Canonical Grid Method	186
<i>Q. Li*, L. Tsang, University of Washington, USA, C. H. Chan, City University of Hong Kong, Hong Kong, P. R. China</i>	

DISPERSION-LIKE RANDOM EFFECTS IN ULTRASHORT PULSED BEAM PROPAGATING THROUGH NONSIPERSIVE RANDOM MEDIA

Joseph Gozani

Cooperative Institute for Research of Environmental Sciences
University of Colorado at Boulder,
Boulder, Colorado 80309-0449

The propagation of an ultrashort pulsed beam through a nonsipersive random media is addressed via the time-domain moment equations derived by Gozani (Opt. Lett., Vol. 21, 1712, 1996). By a short pulse of a length T we mean that $vT \ll \ell$ is 1–100 times the wavelength, where v is the wave speed in the medium, and ℓ is the smallest scale of the turbulent fluid, and pulsed beams are localized space-time solutions of the wave equation that propagate unchanged along the ray trajectories (E. Heyman, IEEE Trans. Antennas Propag., Vol. AP-42, 311, 1994.). This formulation produced already the time-domain partial differential equations for the evolution of the first- second- and fourth-order statistical moment through random media with inhomogeneous background. In this case, locally orthogonal coordinate system along the rays of geometrical optics rather than the cartesian coordinate system is adopted and statistical closure of the moments is obtained along these rays.

The time-domain moment equations are much more complicated than the moment equations in the frequency domain, however they allow the analysis of unmodulated temporal waveform. This mode of operation is suitable for ultra-wideband communication, radar and energy channeling systems. Also, the scattering potentials of these equations are strongly coupled in space-time, thus a simplification is required. To this end, we examine the evolution of the second statistical moment through a band-limited non-dispersive random medium. This assumption leads to a partial differential equation that is easy to compare with the two-frequency equation. The latter equation is currently used for pulse propagation through random media [A. Ishimaru, *Wave Propagation and Scattering in Random Media* (Academic, New York 1978)]. The comparison shows that the resulting time-domain equation exhibits dispersion-like multiple forward scattering even for a non-dispersive medium. The source of this dispersion and its implications are discussed.

STATISTICAL MOMENTS OF THE MUTUAL COHERENCE FUNCTION PROPAGATING THROUGH INTERMITTENTLY RANDOM MEDIA

Joseph Gozani

Cooperative Institute for Research of Environmental Sciences
University of Colorado at Boulder,
Boulder, Colorado 80309-0449

Large-scale fluctuations of light propagating through an intermittently random medium, such as the stratosphere or the nighttime troposphere are associated with a large-scale variability due to the patchy turbulence. Whereas by definition, we expect the averages to be stable quantities, repeated experiment exhibit a physical variability larger than those predicted for statistically stationary medium. Longer averages to stabilize the results are met with a difficulty because of a geophysical, e.g., diurnal, variation. The meaning of these longer averages is dubious because the external factor of the variation is not universal, e.g., in one place it can be the cloudiness and in the other the orography.

In particular, as we measure the Mutual Coherence Function (MCF) that determines the resolution limit of the optical system, the MCF is fluctuating on scales that prohibit us from reducing the estimation error. Local (moving) averages are a partial solution, however they suffer from arbitrariness of the size of the local scale. Pooling data from different temporal time-frames can also be done but depends on the specific conditional algorithm used. Finally we note that a discrepancy is bound to happen because, often, the large-scale variability is not included in the theoretical model.

To overcome these limitations, the theory of wave propagation through intermittently random media was recently developed (J. Gozani, *Phys. Rev. E*, 53, 6486-6491, 1996). This theory produced observables averaged over the large-scale fluctuations, e.g. averaged MCF. Next we are interested in the spread of the measured MCF about its average. The MCF should be considered a non-Gaussian random process. For this reason it is insufficient to consider only its variance, but higher moments are required as well. We obtain equations and solutions describing the evolution of the statistical moments of the MCF. If time will allow we will also expound on the probability density function of the MCF for wave propagation through intermittently random medium.

Correlation Imaging of Objects in a Random Medium

Akira Ishimaru,* Yasuo Kuga, Tsz-King Chan, John D. Rockway and Jun J. Liu

Department of Electrical Engineering
University of Washington, Box 352500
Seattle, Washington, 98195-2500
Tel: 206-543-2169; Fax: 206-543-3842
Email: ishimaru@ee.washington.edu

The imaging of objects in a random clutter environment is an important problem today. Examples are the detection of land mines and the imaging of tissues surrounded by a scattering medium. We have been conducting studies on the correlation of scattered waves from a random medium and a phenomenon called "memory effect" which shows strong correlation under certain conditions based on stochastic invariance of the scattered wave. We have also been conducting studies on confocal imaging of objects by making use of space-time focusing which is an extension of the conventional linear path SAR (Synthetic Aperture Radar) to an arbitrary path. We have studied circular SAR to obtain an image with transverse resolution of the order of the wavelength and the axial resolution determined by the bandwidth. This paper combines these two techniques to achieve correlation confocal imaging of objects in a clutter environment.

We take the correlation of two signals. One is the coherent sum of signals from each antenna with a matched filter focused on a given point. The other is the coherent sum of signals from antennas with different frequencies and angles focused on the same point. For a random medium, the correlation is considerably reduced mainly because of the frequency difference. However, for deterministic objects, the correlation is not reduced, thus obtaining an enhanced image in the presence of clutter. General formulations are given as the coherent sum of the output in terms of the incident spectrum, two-way Green's functions, scattering amplitudes, and matched filter focusing functions. General formulations are applied to the circular SAR geometry where antennas are located on a ring or several rings, and an object is located in a random medium with a given spectrum. It is shown that for a random medium, the correlation of the output from two different frequencies and angles is reduced while the correlation for a deterministic target is not affected. Microwave experiments are conducted to verify the theoretical calculations.

Electromagnetic Models and Measurement of Random Dielectric -Metallic Media: Model Comparison to Coaxial and Free Space Measurements

Rick Moore, Signature Technology Laboratory, Georgia Tech Research Institute, Georgia Institute of Technology, Atlanta, GA 30332 (ricky.moore@gtri.gatech.edu)

The validation of electromagnetic models for dielectric-conducting mixtures has relied on various measurement techniques for comparison of data. Discrepancies between measurement-model and measurement technique to measurement technique are especially evident for materials where the metallic concentration is near a critical concentration threshold. Electromagnetic transmission line measurement techniques have been the preferred methods to perform constitutive parameter measurements (ϵ, μ, σ) of iso or anisotropic scale invariant homogeneous materials for frequencies from 50 MHz to 18 GHz. However, for material mixtures constitutive parameter measurements are found to depend on the dimensionality of the test fixture, sample (sample thickness and/or sample-test fixture cross sectional dimensions) and electromagnetic wavelength when transmission line techniques are applied in the measurement of artificial materials (see figure below). The sources of observed measurement variation derive from a critical electrical percolation threshold and relative electrical conductor correlation, $\xi(f) = \sqrt{\epsilon_r(f)\mu_r(f)a_0|p - p_c|^{-\nu}} / \lambda_0$, within the material. Here a_0 is the conducting inclusion size; p is the inclusion volumetric concentration; p_c is the electrical percolation threshold; $\epsilon_r(f)\mu_r(f)$ are permittivity and permeability of the media surrounding the inclusion at the frequency f with free space wavelength λ_0 and ν is the characteristic critical exponent (4/3 in 2D and 0.88 in 3D). Sources of measurement differences include: (1) measurement variations deriving from sample finite thickness, 2 vs 3 dimensionality, (2) measurement variations deriving from sample and sample-test fixture cross section and (3) cross sectional scale of electrical conductivity for a conductor concentration near the critical volume threshold. These error sources impact model validation. This paper presents comparisons a renormalized effective medium theory and method of moment model simulation of electromagnetic properties of random media and compare their predictions to measured data taken from coaxial and focussed beam measurements for identical material compositions (see below). Agreement between the models and measurement is achieved when focussed beam measurement techniques are utilized. These produce planar wave-fronts whose extent is 3-4 freespace wavelengths when incident on the sample.

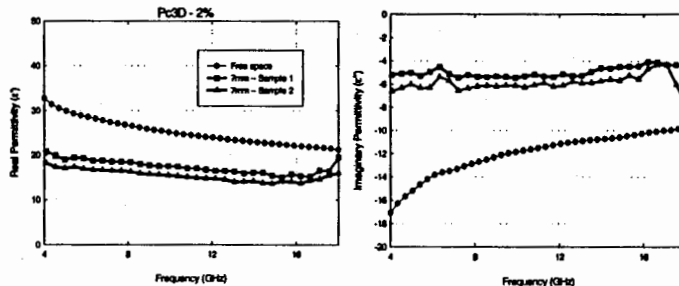


Figure 1 Permittivity measurements of identical materials with free space and coaxial line.

Numerically Computed Effective Permittivity of a Composite Material Formed from Spherical Inclusions

Keith W. Whites* and Feng Wu

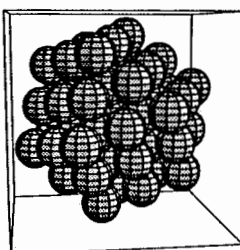
Department of Electrical Engineering
University of Kentucky
453 Anderson Hall
Lexington, KY 40506-0046

The effective permittivity, ϵ_{eff} , of a composite material comprised of discrete and randomly located spherical particles can be computed using a number of methods. In the long wavelength limit, examples of these methods include the Maxwell Garnett equation, mixing formulas such as the Polder-van Santen and the QCA-CP methods and a host of others (A. H. Sihvola and J. A. Kong, *IEEE Trans. Geosci. Remote Sensing*, vol. 26, no. 4, pp. 420-429, 1988). These methods all yield simple expressions for ϵ_{eff} but are only approximations that are restricted to small volume concentrations and/or small inclusion permittivity.

An accurate analysis for the effective constitutive parameters of such a composite material requires the use of numerical methods to compute the electromagnetic scattering by the particles. For mixtures of spheres, such an analysis for ϵ_{eff} in the long wavelength limit was given in W. C. Chew et. al., *IEEE Trans. Geosci. Remote Sensing*, vol. 28, no. 2, pp. 207-214, 1990.

In this paper, we will discuss the computation of the effective constitutive parameters for composites of spherical inclusions using a numerical methodology that has been successfully applied to chiral and uniaxial bianisotropic chiral materials (K. W. Whites, *IEEE Trans. Antennas Propagat.*, vol. 43, no. 4, pp. 376-384, 1995; K. W. Whites and C. Y. Chung, *J. Electromagn. Waves Appl.*, vol. 11, pp. 371-394, 1997). Applying this method here, an ensemble of material spheres is distributed within an imaginary spherical region in space as for the 55 scatterers shown below. The scattered fields are then computed using a numerical method. Since we are concerned here with spherical scatterers, the generalized RATMA algorithm is applied for computational efficiency (W. C. Chew, et. al., *IEEE Trans. Microwave Theory Tech.*, vol. 40, no. 4, pp. 716-723, 1992.)

Finally, to compute the effective material parameters, simulated annealing is used to minimize an appropriately chosen functional that involves the numerically computed scattered fields and the analytical expression of these same fields scattered by a single, solid material sphere. Results will be shown for the computation of the effective constitutive parameters for material spheres both in the long wavelength limit and at finite frequency.



SCATTERING CROSS SECTIONS OF A RANDOM MEDIUM LAYER

S Mudaliar
ARCON Corporation
260 Bear Hill Road
Waltham, MA 02154

Electromagnetic wave scattering from a layer of random medium is studied using a multiple scattering theory. The layer is modelled as a random continuum with plane parallel boundaries. The media above and below the layer are homogeneous. The fluctuations of permittivity of the layer are assumed to be small, stationary and obey Gaussian statistics. The correlation function is assumed to be exponential in the elevation and Gaussian in the azimuth. Our interest in this paper is the derivation of the normalized radar cross sections (NRCS) of the random medium.

Multiple scattering processes in this random medium are adequately described by the modified radiative transfer (MRT) equations [Zuniga & Kong, *J. Appl. Phys.* 51, 5228-5244, 1980]. These equations are derived from the Bethe-Salpeter equation under the ladder approximation and the Dyson equation under the nonlinear approximation. Thus the basic essential multiple scattering processes are taken into consideration including some of the processes ignored in the conventional radiative transfer theory. The MRT equations are a pair of coupled integro-differential equations for the up and down travelling Stokes vectors. In addition there is a pair of boundary conditions on the upper and lower boundaries of the layer. The task of obtaining analytical solution for this system appears impossible. However, in the first order approximation the MRT equations become decoupled and can be solved readily. This leads to explicit expressions for the NRCS. We have arranged the expressions in such a way that the various scattering processes may be readily identified for study. We find that there are four distinct scattering processes involved in any general bistatic situation. But in the cases for forward and backward scattering there are additional scattering processes, due to coherence between waves travelling in opposite directions. They exist only in the copolarized NRCS and can be significant in certain situations.

The theory described above is used to interpret the measured NRCS from foliage-covered terrain [McLaughlin et al., *Electron Lett.* 21, 1291-1292, 1995]. This experiment was conducted at S-band over forested terrain of Massachusetts. We chose parameters appropriate for that experiment and found that the theory is fairly good in explaining the behavior of the measured results.

An Enhanced Steepest Descent Fast Multipole Method for the Analysis of Scattering from Two Dimensional Multilayered Rough Surfaces

M. El-Shenawee*, V. Jandhyala, E. Michielssen, and W.C. Chew

Center for Computational Electromagnetics

Department of Electrical and Computer Engineering

University of Illinois at Urbana-Champaign

1406 W. Green St., Urbana IL 61801

The analysis of scattering of electromagnetic waves from rough surfaces is a problem that continues to attract investigators from many disciplines due to its wide range of applications. The numerical solution of scattering problems involving realistic two-dimensional random rough surfaces requires fast and memory efficient computational techniques. The Steepest Descent Fast Multipole Method (SDFMM) (V.Jandhyala, B.Shanker, E.Michielssen, and W.Cheow, Proc. IEEE APS, 2308-11, 1997) is an integral equation based multilevel algorithm for efficiently analyzing scattering from two-dimensional rough surfaces. The SDFMM dramatically accelerates the iterative solution of the moment method equations for rough surfaces. In this work, several enhancements to the original SDFMM technique are presented to render the method highly suitable for analyzing scattering from extremely large, rough, and complex surfaces.

Key to the SDFMM is the use of accurate and efficient numerical steepest descent path (SDP) integration rules for representing the Green's function. These rules are required to function in conjunction with a multilevel fast multipole method (FMM). In this work, a highly optimized numerical integration technique is presented for this purpose. A minimal number of quadrature points lying along the exact SDP are determined such that the tails of decaying integrands arising in the SDFMM equations are truncated in an optimal manner. To efficiently and accurately simulate scattering from large scale rough surfaces, error estimates associated with the SDFMM are necessitated. These estimates are essential for an *a priori* selection of parameters associated with the SDFMM, including number and location of SDP integration points, interpolation orders, and number of FMM harmonics. In this work, detailed theoretical and numerical error estimates and complexity analyses are presented. Tradeoffs between accuracy and efficiency are discussed.

In several remote sensing applications, multilayered and multiregion rough surfaces are encountered. Such applications include the estimation of sea ice depth, the detection of oil spills on oceans, and the characterization of scattering from conglomerates of ice, water, and soil. As will be shown, the enhanced SDFMM permits the rapid simulation of scattering from such large and complex surfaces.

Ducting Effects on LGA Backscatter from 1-D Randomly Rough Perfectly Conducting Surfaces

Ra'id S. Awadallah and Gary S. Brown.

Electromagnetic Interactions Laboratory

The Bradley Department of Electrical Engineering

Virginia Tech, Blacksburg, Virginia 24061

The problem of electromagnetic wave scattering by a randomly rough surface is usually formulated in two steps. The first step involving setting up an integral equation (the magnetic field integral equation, MFIE, or the electric field integral equation EFIE) governing currents induced on the surface by the incident field and solving for these currents numerically. The currents are then used in the appropriate radiation integral to calculate the field scattered by the surface.

In homogeneous media, the implementation of the above two steps is straightforward since the kernel (Green's function or its normal derivative) which appears in the integral equation is well known. This is not the case, however, in inhomogeneous media (ducting environment) where the Green's function is not readily known and can be determined only approximately using asymptotic techniques. For a ducting environment created by the presence of a linear-square refractivity profile ($n^2(z) = a - bz$, where a and b are constants), we obtained a closed-form approximation of the Green's function and used it in studying forward propagation at low grazing angles over rough surfaces. The numerical method we used to solve the MFIE is MOMI, a very robust and efficient method D. Kapp and G. Brown (1995) developed which does not require matrix storage or inversion. Our calculations were meant to be a benchmark for people studying forward propagation using the parabolic wave equation.

Unlike the parabolic wave equation technique, our approach can also be used to calculate LGA backscatter in a ducting environment, an issue which, to our knowledge, has never been addressed before. Using our approach, we have observed that the power calculated as a function of distance in the backscattering direction does not have the simple inverse distance dependence but exhibits an oscillatory pattern on a realization by realization basis and reaches a certain pattern upon averaging. This is obviously a ducting effect as will be discussed fully in this paper. Analysis was carried out mainly for the TM or vertical polarization for an ocean-like Pierson-Moskowitz surface. In our talk we focus on the TM case because the backscattering amplitudes are typically much larger than those observed for the TE (horizontal) case.

Optimal Time-Domain Detection of Targets Buried Under a Rough Air-Ground Interface

Traian Dogaru* and Lawrence Carin

Department of Electrical and Computer Engineering

Duke University

Box 90291

Durham, NC 27708-0291

We consider short-pulse electromagnetic detection of a target buried under a rough surface. The most commonly used scheme for detection of transient signals is the matched filter, in which the target signature is assumed known exactly. However, the fields transmitted through a penetrable rough surface constitute a random process, and therefore the fields that impinge upon a buried target are in turn random. Therefore, even if the buried target is known exactly, its scattered fields must be treated as a random process. This is complicated by the fact that the rough surface introduces clutter, with statistics generally different from those of the buried target. In this paper, we consider implementation of an optimal detector that properly accounts for the random target signature and background clutter.

An optimal scheme for detection of a random signature requires integration over the signature's density function. This is implemented approximately via Monte Carlo integration, through consideration of multiple realizations of the target signature (each for a particular rough surface, from an ensemble). Therefore, instead of requiring the statistics of the target response, *per se*, we require access to a set of target signatures representative of said statistics.

To efficiently compute the statistical target signature and as well as the statistics of the clutter, we have developed a stochastic scattering-matrix formulation. In this scheme, the scattering-matrix that characterizes propagation through and scattering from the penetrable rough surface is parametrized statistically. The statistics of the scattering matrix are computed once, off line, using a finite-difference time-domain (FDTD) formulation. Propagation through the soil, after penetrating the surface, is a deterministic process which is easily handled via a transmission matrix. Moreover, a deterministic scattering matrix is used to handle scattering from the buried target, as a function of target orientation. These scattering matrices are combined to provide an efficient means of computing the stochastic target signature and clutter statistics, and are integral elements in the optimal detector. Detector performance is quantified in the form of the receiver operating characteristic (ROC), with results demonstrated as a function of the target type and interface roughness.

On the Use of the Tapered Plane Wave Incident Field in Scattering and Propagation Simulations

Jakov V. Toporkov, Ra'id S. Awadallah and Gary S. Brown

Electromagnetic Interactions Laboratory

The Bradley Department of Electrical Engineering

Virginia Tech, Blacksburg, Virginia 24061-0111

Numerical studies of surface scattering and propagation over rough surfaces usually require tapering the incident field. Probably, the simplest and most popular "incident beam" is the Gaussian-tapered plane wave. The fact that such incident field does not exactly satisfy the Helmholtz equation prompted E. Thorsos (1988) to derive a modified approximate Gaussian taper that satisfies it more closely. This form of tapered field has found a broad application within the electromagnetic community.

For surface scattering problems, it is known that as the angle of incidence approaches grazing, the beam waist should be made larger. Several criteria that relate the angle of incidence to the beam waist have been proposed both for Gaussian (H. Ngo and C. Rino, 1994) and Thorsos (D. Kapp, 1995) tapers. In our scattering simulations with the ocean-like Pierson-Moskowitz surfaces we saw a distinctive signature of the Thorsos and Gaussian taper failure for the horizontal polarization (TE case): as the incident angle approaches grazing, the backscattered cross section consistently exhibits an anomalous jump. From our observations, we determine the value of an arbitrary constant involved in the Kapp's criterion and show that this criterion is very robust. Once the incident angle is in the region where the taper fails, the surface current, which is the solution to the magnetic field integral equation (MFIE), also displays quite distinctive features. We find that Gaussian and Thorsos tapers with the same waist fail at about the same incident angle, with the Thorsos taper being somehow more robust.

While studying propagation over a rough surface in a homogeneous medium, we found some discrepancy between the incident field given by defining the Thorsos taper directly on the surface and that given by propagating the same Thorsos taper from a certain vertical plane to the rough surface. This discrepancy is again attributed to the approximate nature of the Thorsos taper. This effect, not appreciated before, may be of importance when rough surface effects are incorporated in propagation problems. Finally, in our presentation we will outline the derivation of the Thorsos taper and point out all approximations involved and the resulting limitations.

Numerical Solutions of Wave Scattering from a Lossy Dielectric Random Rough Surface at Low Grazing Incidence Using a Physics-Based Two-grid Method Combined with the Banded-Matrix Iterative Approach/Canonical Grid Method

Qin Li*, Leung Tsang, and Chi Hou Chan†
Electromagnetics and Remote Sensing Laboratory
Department of Electrical Engineering, Box 352500
University of Washington
Seattle, Washington 98195-2500, USA
Tel: (206) 685-7537, Fax: (206) 543-3842
Email: tsang@ee.washington.edu
†Applied Electromagnetics Laboratory
Department of Electronic Engineering
City University of Hong Kong
83 Tat Chee Avenue
Kowloon, Hong Kong

To solve wave scattering by a lossy dielectric rough surface with a large dielectric constant, usually a single dense grid (SDG) of 20 to 50 points per wavelength is required for accurate results. A single coarse grid (SCG) of 10 points per wavelength does not give accurate results. However, the CPU and memory requirements of SDG are much larger than that of SCG. In a physics-based two-grid method (PBTG), two grids are used: a dense grid and a coarse grid. Because of the Kramer-Kronig relation, a large real part of the dielectric constant is usually associated with a large imaginary part. The PBTG method is based on two observations: (1) Green's function of the lossy dielectric is attenuative and (2) the free-space Green's function is slowly varying on the dense grid. The first property lossy dielectric gives a banded submatrix for the Green's function of the lossy dielectric. The second property allows us, when using the free-space Green's function on the dense grid, to first average the values of surface unknowns on the dense grid and then place them on the coarse grid. After finishing multiplication of matrix and vector, the products are placed on the dense grid by using linear interpolation. By combining PBTG with the banded-matrix iterative approach/canonical grid (BMIA/CAG) method, the new algorithm can solve a large rough surface scattering problem for both TE and TM cases and also for near grazing incidence. Using this method, we calculate the variation of backscattering coefficients with dielectric permittivities from $(5.56 + i0.6)\epsilon_0$ to $(31.5 + i4.11)\epsilon_0$, and incidence angles from 80° to 85° for both TE and TM waves. Salient features of the numerical results are: (1) A single coarse grid (SCG) has poorer accuracy for the TM case than the TE case. (2) PBTG-BMIA/CAG speeds up CPU and preserves the accuracy. It has accuracy comparable to a single dense grid and yet has CPU comparable to a single coarse grid. (3) PBTG-BMIA/CAG gives accurate results for emissivity calculations and also for low-grazing backscattering problems (LBGA).

Biological Effects of Electromagnetic Fields

M. F. Iskander and M. A. Stuchly

Human Dosimetry in 60 Hz Magnetic Fields: Effect of Muscle Anisotropy	188
<i>T. W. Dawson, M. A. Stuchly*, University of Victoria, Canada</i>	
Potential Effects of 60 Hz Magnetic Fields on Cell Differentiation in Vitro.....	189
<i>E. J. Rothwell*, K. M. Chen, J. Zhang, J. Suk, C. C. Chang, J. E. Trosko, G. Chen, B. L. Upham, Michigan State University, USA</i>	
RF Electromagnetic and Thermal Analysis of an Exposure Equipment for Planar Lipid Bilayer Membranes	190
<i>V. W. Hansen*, M. Alaydrus, T. F. Eibert, F. Wilczewski, Bergische University, Germany</i>	
Electromagnetic Influences Monitoring System on Humans Near Power Transmission Lines Based on Virtual Reality	191
<i>M. Kacarska*, S. Loskovska, L. Ololoska, L. Grcev, University Sv. Kiril i Metodij, Macedonia</i>	
Exposure to E-field of Power Lines Should Not be Ignored.....	192
<i>R. W. P. King*, Harvard University, USA</i>	
The Influence of the Non-heating Doses of the Millimeter Wave Radiation on the Immune Status of Cattle	193
<i>V. V. Murav'ev*, A. A. Tamelo, Belarusian State University of Informatics and Radioelectronics, Belarus, N. H. Fedosova, Belarusian Agricultural Academy, Belarus, U. M. Byahun, Belarusian State University of Informatics and Radioelectronics, Belarus</i>	
High Resolution Dosimetry for Live Line Workers	194
<i>T. W. Dawson, M. A. Stuchly*, K. Caputa, University of Victoria, Canada</i>	
Microwave Power Feeding to Divided Chambers	195
<i>J. F. Kiang*, D. S. Yu, National Chung-Hsing University, Taiwan</i>	
High Precision Near-field Scanner for Analysis of Handheld Transmitters	196
<i>K. Pokovic*, T. Schmid, O. Egger, N. Kuster, Swiss Federal Institute of Technology (ETH), Switzerland</i>	
An Algorithm for Computations	197
<i>K. Caputa, M. Okoniewski*, M. A. Stuchly, University of Victoria, Canada</i>	

Human Dosimetry in 60 Hz Magnetic Fields: Effect of Muscle Anisotropy

Trevor W. Dawson and Maria A. Stuchly*

Department of Electrical and Computer Engineering
University of Victoria, Victoria, B.C., V8W 3P6, Canada

The recent development of MRI-derived, anatomically realistic voxel model of the human body suitable for electromagnetic modeling, and of effective methods for computations of induced electric fields, has resulted in numerical estimates of organ-specific dosimetry for human exposure to low frequency magnetic fields (Dawson et. al., Bioelectromagnetics, vol. 18, pp. 478-490, 1997). However, these estimates have used isotropic conductivities for all tissues, while it is well known that muscle is anisotropic at low frequencies.

In this work a high resolution (3.6 mm), voxel model of the human body is used. Some 30 tissues and organs are identified among them the anisotropic muscle. One major difficulty in implementation of muscle conductivity anisotropy in numerical modeling schemes is the assignment of the orientation of muscle fibers. In human limbs higher conductivity can be assumed for the longitudinal direction (vertical for a standing posture), but in other body parts the fibers are oriented at various angles. Proper orientations of the muscle fibers are not discernible from the MRI images used in deriving the voxel model. To overcome this problem the computations for five scenarios covering the range of possible limiting cases are performed. They include: the isotropic case of a muscle conductivity of 0.35 S/m, also used in previous computations, two sets of conductivity values with longitudinal conductivities of {0.35, 0.2} and transverse conductivities of {0.7, 0.2}, for contrast ratios of 1.75:1 and 3.5:1, and two sets with the longitudinal and transverse conductivity allocations swapped.

Computations are performed using the scalar potential finite-difference (SPFD) method, in which the current densities in each voxel are equal to the conductivities represented the tensor multiplied by the electric field. The SPFD method is efficient, and a seven-band, diagonally dominant, symmetric and definite (after imposing an additional condition) matrix is solved using the conjugate gradient method.

The inclusion of the muscle anisotropic properties changes the average and maximum induced electric fields and current densities in practically all organs and tissues despite the unchanged isotropic properties of other tissues. The average electric field and current density levels in various body organs and tissues other than muscle vary by factors of up to 1.76 and 1.7, respectively, for at least one magnetic field orientation with respect to the body. The change in the average current density for muscle is up to a factor of 3.0, but the changes in the average electric field are not more than 10 % for muscle. Similarly, the maximum variations in the maximum current density are up to 2.43 for other tissues and up to 5.43 for muscle. Although realistic incorporation of anisotropy of muscle into a numerical scheme is an exceedingly complex problem, accounting for muscle anisotropy is clearly of importance in the accurate numerical modeling of low frequency induction in humans.

Potential Effects of 60 Hz Magnetic Fields on Cell Differentiation in Vitro

E.J. Rothwell¹, K.M. Chen, J. Zhang, and J. Suk

Department of Electrical Engineering

C.C. Chang, J.E. Trosko, G. Chen, and B.L. Upham

Department of Pediatrics and Human Development

Michigan State University

East Lansing, MI 48824

Epidemiological studies have suggested a link between exposure to low-frequency electromagnetic fields and the development of Leukemia, a disease resulting from the blocking of the maturing process of blood cells. Thus, one possible mechanistic link between EM fields and cancer is through an interference with the cell differentiation process.

To investigate this hypothesis, Friend Leukemia cells (normal hematopoietic cells transformed into leukemia cells by the Friend leukemia virus) were treated with Dimethylsulfoxide (DMSO) or hexamethylene bis-acetamide (HMBA) and exposed to 60 Hz magnetic fields at a strength of 1 G for four days. Under normal circumstances, treatment with DMSO or HMBA causes Friend Leukemia cells to differentiate into normal red blood cells. Any reduction of differentiation in the exposed cells would suggest that the EM fields are interfering with the chemical-induced signal transduction mechanism causing cell differentiation.

Experiments were performed by placing samples in both sham and exposure chambers. In a double-blind scenario, the processed cells were stained for hemoglobin (present only in the differentiated red blood cells) and counted using a hemocytometer. After the results were compiled, the identity of the exposed samples was revealed. Results show that exposure to EM fields inhibits differentiation of chemically-treated Friend Leukemia cells. Differentiation of DMSO-treated cells was decreased by 36% under exposure to EM fields; for HMBA treatment, the reduction was 26%. This suggests that EM field exposure interferes with the mechanism that ultimately turns on the hemoglobin gene. Experiments to determine whether exposure to EM fields blocks differentiation of human breast stem cells or human neuron stem cells are currently being performed.

In establishing a mechanistic connection between tumor promotion and magnetic field exposure, it is necessary to accurately determine the intracellular exposure level, as well as the nature and strength of the currents induced within each cell. To this end, numerical techniques such as the finite element method have been employed to solve Maxwell's equations within simple models of biological cells. Results from these studies will also be presented.

RF Electromagnetic and Thermal Analysis of an Exposure Equipment for Planar Lipid Bilayer Membranes

V. W. Hansen*, M. Alaydrus, T. F. Eibert, F. Wilczewski

Department of Theoretical Electrical Engineering
Bergische Universität-GHS Wuppertal, D-42097 Wuppertal, Germany

Planar lipid bilayers can be used to model biological cell membranes without the need of handling complicated cell structures and the properties of the lipid bilayers can directly be investigated. The exposure of lipid bilayers to pulsed RF fields (900 MHz) revealed significant effects on the low frequency electric behavior of the bilayers (G. H. Boheim et al., 2nd World Congr. Electr. and Magn. in Biology and Medicine, p. 30, 1997). However, an objective judgment of these effects is only possible if the exposure conditions of the lipid bilayer are known sufficiently accurate. First of all, it has to be clarified whether the effects occur in the thermal or athermal range. In a second step further interaction mechanisms of the pulsed RF fields with the lipid bilayer can be analyzed. For these purposes a detailed knowledge of the RF field distribution in the exposure device and especially in the very vicinity of the lipid bilayer is of importance. The most challenging problem of the electromagnetic analysis is that of modeling the very thin lipid bilayer (≈ 5 nm) within the exposure device with geometric dimensions that are orders of magnitude larger than the thickness of the lipid bilayer. To alleviate this difficulty the electromagnetic analysis was broken into several steps. First, the exposure setup was analyzed using a finite difference time domain (FDTD) code based on an approximate consideration of the lipid bilayer. Subsequently, a high-resolution modeling of the bilayer in its local environment as part of an infinite planar multi-layered structure was performed using a finite element/boundary element hybrid approach having the advantage that the lipid bilayer can be described analytically as one layer of the multi-layered structure. Finally, the fields obtained by the high-resolution analysis were related to the approximate results of the FDTD calculations.

The obtained data were used to calculate the power loss distribution in the vicinity of the lipid bilayer where the highest losses occur. The power loss distribution then was used as source of a thermal analysis in the vicinity of the lipid bilayer utilizing a finite element code simulating the heat conduction equation.

Our analysis shows that the used exposure equipment is capable to produce relatively high voltages at the lipid bilayer of up to some mV for applied RF powers of 1 W. However, there are also relatively high electric field strengths in the electrolyte near the lipid bilayer of up to 3000 V/m. The performed thermal analysis gave maximum temperature oscillations of some mK for typical GSM signals (pulse width 0.577 msec, period 4.6 msec). Both, the electromagnetic and the thermal analysis were performed for various exposure conditions and lipid bilayer parameters. However, in all cases the overall temperature increase was less than 0.2 K and the temperature oscillations due to the pulsed RF signals crucial for the judgement of the experiments were even orders of magnitude lower. Therefore, we can state that experiments with applied powers of up to at least 10 W are clearly performed in the athermal range. Also, the measured effects seem to confirm this conclusion.

Electromagnetic Influences Monitoring System on Humans Near Power Transmission Lines Based on Virtual Reality

Kacarska M., *Loskovska S., Ololoska L., Grcev L.

University "Sv. Kiril i Metodij", Faculty of Electrical Engineering,
Karpov II bb, 9100 Skopje, Macedonia
e-mail: mkacar@cerera.eif.ukim.edu.mk

For the past twenty years there has been apprehension that the electric and magnetic fields (EMF) arising from the supply and use of electricity may have adverse effects on health. However, in spite of great number of large-scale studies, the scientific evidence to date is not conclusive in assessment of the risk associated with low frequency EMF exposure (CIGRE Working group 36.06, Electra, 161,131-141,1995). To support the better understanding of EM influences, a system for monitoring EM influences on humans in living and working environments is underdevelopment. The system based on virtual reality (VR) offers to user to create and to investigate working and living environments, and to make judgments about the functional characteristics of devices placed in them. Additionally it considers the influences of EM processes to humans, synthesizing performances of 3D graphics interfaces with mathematical methods for determination of human's exposure parameters to EM fields.

The paper will present the visualization of electromagnetic influences on a lineman during a live line-work on a high voltage transmission line. A fundamental parameter when discussing the health risks of EM power absorption in the human body is the specific absorption rate (SAR). The SAR is the mass-normalized rate of EM energy absorbed by the body. At a specific location (x,y,z) SAR may be defined by: $SAR = \sigma |E|^2 / \rho$ [W/g], where σ is the tissue conductivity, ρ is the tissue mass density, E is the RMS value of the total field strength in the body.

The electric field distribution around the power transmission lines of 400 KV voltage, 50 Hz frequency, is calculated including influence of the ground. The method of moments (MOM) has been used to calculate the SAR distribution into the human body. To reduce the requirements for resource memory of the MOM, the sparse matrix technic combined with parallel processing is used.

The Figure 1 shows the obtained SAR distribution on a 3-D model of the lineman. The human body is divided on the nonuniform block cells with inhomogeneous dielectric constant and conductivity. The calculations have proved that under the high voltage power lines the value of electric field intensity exceeds 1 KV/m, and SAR values in some points are beyond 1.6 mW/g (which are the protection values for the ANSI/IEEE standards).

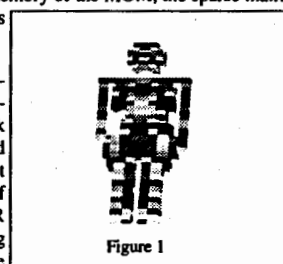


Figure 1

EXPOSURE TO E-FIELD OF POWER LINES SHOULD NOT BE IGNORED

Ronald W. P. King

Gordon McKay Laboratory, Harvard University, Cambridge, MA 02138-2901

As reported by *Science* (277, 29, 1997): "the results of the most carefully controlled study yet (Linet et al., *New Engl. J. Med.* 337, 1, 1997): a \$5 million, 5-year investigation into the possible link between magnetic field exposure and childhood leukemia ... are negative." These results are consistent with recent analytical work that shows that it is the electric field, not the magnetic field that may have a significant link with childhood leukemia. The current density $J_z(z)$ and electric field $E_z(z)$ induced in the human body by an incident 50-60 Hz electric field E_z^{inc} are given by $J_z(z) = \sigma E_z(z) = I_z(z)/A(z)$, where $\sigma \sim 0.5 \text{ S/m}$ is the mean conductivity of the body, $A(z)$ is its cross-sectional area at the distance z from its center, and

$$I_z(z) = \frac{j2\pi k_0 h^2 E_z^{\text{inc}}}{\zeta_0 \Psi} \left(1 - \frac{z^2}{h^2}\right) \quad (1)$$

is the total current across $A(z)$. Here, $k_0 = \omega/c$, $\zeta_0 = 120\pi \Omega$, $h \sim 0.875 \text{ m}$ is the half-length of the body, and $\Psi = 2\ln(2h/a_0) - 3$, with $a_0 = [A(0)/\pi]^{1/2}$. This formula applies with the arms in contact with the body when this is far from the earth. It is in King and Wu (*J. Appl. Phys.* 78, 668, 1995). Generalizations of (1) to a body standing on the earth barefooted or with rubber-soled shoes are also given. Formulas for $J_z(z)$ and $E_z(z)$ in specific organs are in King and Sandler (*Radio Sci.* 31, 1153, 1996), and in all parts of the body when the arms are raised in King (*J. Appl. Phys.* 81, 7116, 1997). The additional circulating current and electric field induced by the magnetic field B_y^{inc} are given in King and Wu. They are very small in the interior of the body. The ratio of circulating to axial current at $z = 0$ where both have their maxima is $I_z^{\text{circ}}(0)/I_z^{\text{axial}}(0) = 0.065$. Hence, the effect of exposure to the magnetic field is insignificant compared to that due to the electric field.

The study by Linet et al. involved exposure to the fields of low-voltage distribution lines in urban areas and high-voltage transmission lines in suburban and rural areas. Only the fields of 220 kV to 1 MV transmission lines are potentially hazardous. For these, $E_z^{\text{inc}} = cB_y^{\text{inc}}$, $E_y^{\text{inc}} = -cB_z^{\text{inc}}$. Typically, for a 440 kV line,

	$y = 10 \text{ m}$	$y = 30 \text{ m}$	$y = 50 \text{ m}$	$y = 100 \text{ m}$	$y = 200 \text{ m}$
$ E_z \text{ (V/m)}$	2140	560	61.6	21.6	2.8
$ B_y \text{ (\mu T)}$	7.12	1.88	0.20	0.072	0.009

Epidemiological studies assume that only exposure to the magnetic field is involved in the incidence of leukemia. The electric field is ignored. Since the power lines involved are of unspecified types and voltages, the electric field associated with the magnetic field cannot be determined. There is one exception, the outstanding investigation by Feychtung and Ahlbom (*Amer. J. Epidemiol.* 138, 467, 1993) which involved only 220-400 kV transmission lines and an accurately calculated magnetic field from which the electric field can be determined. Hence, the statistical risk of childhood leukemia related by Feychtung and Ahlbom to the incident magnetic field can be correctly related to the incident electric field. This shows a risk ratio of 3 to 4 for children living within 50 m of the 220-400 kV transmission lines where the incident electric field is $E_z^{\text{inc}} \geq 61.6 \text{ V/m}$.

The Influence of the Non-heating Doses of the Millimeter Wave Radiation on the Immune Status of Cattle

Valentin V. Murav'ev¹, Alexander A. Tamelo¹,
Nina H. Fedosova², Uladzimir M. Byahun¹

¹ Belarusian State University of Informatics and Radioelectronics,
vul. Petrusya Broўki 6, BLR-220027 Minsk, Republic of Belarus

² Belarusian Agricultural Academy,
BLR-223015 Gorky, Republic of Belarus

In this report the conclusion concerning the efficiency of the combined spectrum influence is made. This influence concerns the electromagnetic wave's oscillations of low frequency waves of the extremely high and infrared frequencies. The experimental results concerning non-heating doses influence on the cow's embryos are given

At present experimental dates of influence millimeter low levels efficiency on the immune status of cattle brought out. An important issue belongs to the recurrence of the carried out experimental results in the research *in vivo*. In the periodical literature the influence efficiency of the millimeter waves non-heating doses (power density $P < 10 \text{ mW} / \text{sm}^2$) is widely discussed.

The immunoglobulin and hormone concentration constancy in the blood during 3 years, that means that the influence takes place on the cell level.

The research direction are:

- a) following during 3 years the immune status of the born cows, embryos of which have been irradiated;
- b) results have been in the notice such illnesses as stomach diseases, mastitis and others.

Experimental results of the non-heating millimetrewave influence at cow's embryos transplantation are described.

By studying the transplanted calves' physiological state the albumin's exchange was analysed. It was found out, that the full albumin's concentration of the experimental group calves which was processed by the combined spectrum averaged 74.83 g/l at the age of the 4 weeks and significantly increased to the point 75.4 g/l at the age of the 2 months while the albumin's concentration of the control groups calves decreased to the point 64 g/l to the end of the second months. This fact shows that there are breach processes of the bowels function in the control groups calves' organism. These breach processes are accompanied by the hyperhydremous. The gamma-globulin's concentration of the control group calves' blood significantly exceeded the same concentration of the experimental group. This fact shows that the experimental group calves have the higher level of the natural resistibility. By the calves' age increasing the appointed differences between the control and experimental groups calves are preserved.

The ways of the transplanted calves' organism immunological tolerance were investigated. During the first 2 hours after the birth 60% transplanted calves which embryos were processed by the electromagnetic waves got from the first group receptors has immunoglobulins' G content exceeding 10 g/l and 40% has immunoglobulins' content between 8.8...10.0 g/l. The immunoglobulins' G content of the calves' blood got from the second group receptors without process of the electromagnetic waves has averaged $6.8 \pm 1.7 \text{ g/l}$, the majority of the calves has immunoglobulins' G content not exceeding 7.0 g/l. Sickness rate of the first and second groups calves averaged accordingly 10.0 and 40.9%.

Discuss the process of influence on so named MHC complex, which are situated on the surface of limfotuziit and its connection with the process on the surface of membranes of cells.

References

1. V.Murav'ev, A.Tamelo, U.Byahun etc. Investigation of Action of the Non-heating Millimeter Wave Radiation on Animals// 1997 IEEE AP-S International Symposium and URSI Radio Science Meeting, Montreal, Canada, July 13-18 1997, p.660.

High Resolution Dosimetry for Live Line Workers

T. W. Dawson, M. A. Stuchly * and K. Caputa
Department of Electrical and Computer Engineering
University of Victoria, Victoria, BC, V8W 3P6, Canada

Live-line utility workers are exposed to strong 60 Hz (50 Hz in Europe) magnetic fields. While there is no convincing scientific evidence that weak magnetic fields of the order of $1\mu\text{T}$ cause harmful health effects, there is still a need to ensure that occupational exposures to strong non-uniform magnetic fields do not result in excessively large electric fields and current densities induced in tissues. A level of the induced current density of 10 mA/m^2 is used as a benchmark in various guidelines. However, the levels of induced electric fields that may interfere with cardiac pacemakers are only recently being evaluated.

Numerical evaluations of the induced fields and currents resulting in high resolution (3.6 mm) dosimetric data for various organs and tissues for an upright human body have previously been performed (e.g. Dawson, et. al., *Bioelectromagnetics*, 18:478-490, 1997). The same numerical method, namely the efficient scalar-potential finite-difference method, is used for the modeling of live-line exposures.

One of the essential factors in accurate dosimetric computations is the quality of the models representing the human body. This is a particularly challenging problem for live-line utility workers, since their postures are different from that obtained from segmentation or a CT or MRI scan of the human body. The models with representative postures, shown in Fig. 1, are obtained from an MRI based model of an upright human body by tissue segmentation, followed by rotation of limbs using computer programs developed for this purpose. To maintain the anatomical integrity of the limbs and joints, a visualization software (Data Explorer, IBM) and manual editing is used.

Dosimetric data have been obtained for over 20 organs and tissues for typical work postures, examples of which are shown in Fig. 1, for typical line currents for high voltage transmission lines from 135 kV to 550 kV. The results are given in terms of maximum, mean, rms and variance of the electric field and current density.

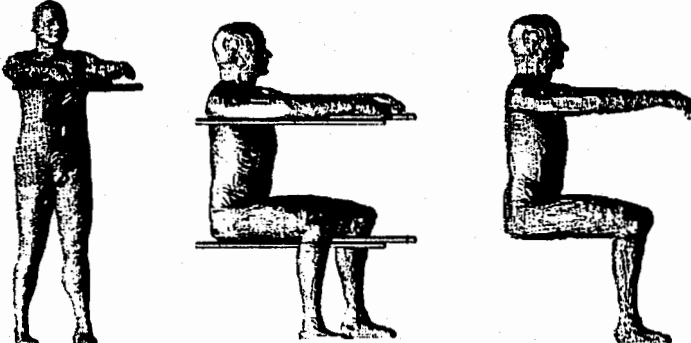


Fig. 1. Examples of typical postures of live-line workers.

Microwave Power Feeding to Divided Chambers

*Jean-Fu Kiang and Dong Shiao Yu
Department of Electrical Engineering
National Chung-Hsing University
Taichung, Taiwan 402, ROC

Microwave ovens are so popular that almost every household owns at least one. Microwave heating have also been widely used in manufacturing industries and agriculture to dehydrate papers, woods, to cook foods, to melt wax from molding ceramics, and so on. For the latter applications, a conveying belt system is usually applied so that the heated components or materials can be successively heated and allowed time for the heat distribution to become uniform. The heated materials are put in chambers lying above the conveying belt. The chamber walls and the belt itself are made of good conductor to shield the microwave power from leaking out to the surrounding environments. As the chamber walls (dividers) pass by the feeding aperture, part of the incoming power is reflected back to the source via the feeding waveguide. Nonreciprocal devices are usually used to absorb such reflected power to reduce the possibility of damaging the microwave source.

The main contribution of this work is to develop a rigorous full wave solution to analyze the power heating efficiency in such a conveying system. Layered medium is assumed in the chambers to represent the heated materials. The fields in each of the chamber and the waveguide regions are expanded in terms of the guided modes in each respective region. Equivalence principle is applied to replace the waveguide opening by a perfect electric conductor and effective magnetic surface currents. By imposing the continuity conditions between contiguous layers inside each chamber and across the waveguide aperture, a set of integral equations are obtained in terms of the magnetic surface currents.

The method of moments is then applied by first choosing a set of basis functions to expand the magnetic surface currents. Then the same set of basis functions are used as the weighting functions to test the resulting integral equations. Results of an aperture feeding a chamber are also used for comparison under special circumstances. Different geometrical and electrical parameters of the chambers and the waveguide are used in the numerical computation to analyze their effects.

High Precision Near-Field Scanner for Analysis of Handheld Transmitters

Katja Pokovic*, Thomas Schmid, Oliver Egger and Niels Kuster

Swiss Federal Institute of Technology (ETH)

8092 Zurich, Switzerland

Phone: +41-1 632 6459, Fax: +41-1 632 1057, e-mail: pokovic@ish.ee.ethz.ch

Introduction

Antenna designers of wireless communications systems face tough challenges, with a highly competitive market constantly demanding cheaper, smaller and lighter devices that operate longer on a single battery load and have excellent radiation performance. Most recently the exposure of the user has also become an issue which is closely related to radiation performance. To evaluate and optimize the performance of transmitters operating in such a complex environment, tools for analyzing the close near-field of these transmitters is required.

Objectives

The objectives were to develop the new generation of improved E- and H-field probes for compliance testing of mobile communications equipment and to integrate them into a scanning system enabling complex scanning and flexible and sophisticated data evaluation.

Materials and Methods

Most of the scientific investigations have been carried out simultaneously using both experimental and numerical tools. Basic studies included investigations on secondary modes of reception, mutual coupling and spherical probe isotropy. A new sandwich construction of the lines on epoxy substrates was developed, which solved three problems at once: 1) the interlead capacitance was greatly increased, decreasing the RF signal pickup by more than 20 dB; 2) the width of the substrate was reduced by almost a factor of two, which is essential for smaller probes; 3) ceramic substrates were replaced by epoxy substrates, improving the robustness of the probes and permitting thinner substrates (<0.1 mm). This new technology also enabled increase of the spatial resolution without impairing the sensitivity by reducing the spatial distance of the dipole centers (0.6 mm). E-field probes for free space and measurements in tissue simulating liquid have been realized. The fine tuning of the dipole angle in order to achieve spherical isotropy of $< \pm 0.3$ dB, which was first determined by numerical simulations, has been done experimentally. The newly developed isotropic H-field probe consists of three concentric loop sensors, each with a diameter of 3.8 mm. The shunt resistance and the layout have been optimized to achieve excellent isotropy ($< \pm 0.2$ dB) and minimal E-field sensitivity in the bandwidth of greatest interest, i.e., 300 MHz up to 2.5 GHz. The DASY scanner and software have been redesigned to integrate the new probes and to provide sufficient flexibility for accurate and efficient scanning. The calibration procedures have also been improved to ensure maximum measurement precision in the near field.

Conclusion

The developed scanner equipped with the latest probe designs enables efficient assessment of the extreme near-fields, which has proven to be highly valuable for optimization of transmitters embedded in complex environments, as will be demonstrated with various examples.

An Algorithm for Computations of the Power Deposition In Human Tissue with the FDTD Method

Kris Caputa, Michal Okoniewski* and Maria A. Stuchly,
Department of Electrical and Computer Engineering,
University of Victoria, Victoria, BC, V8W 3P6, Canada

With the proliferation of mobile wireless communication devices, a well defined and accurate evaluation of the so called specific absorption rate (SAR) is critical in view of recently introduced regulations in the U.S. and guidelines in Europe. For compliance, SAR averaged over 1 g or 10 g of tissue mass in a shape of a cube must not exceed a specified value. While the SAR has been used previously for mobile devices, such as cellular telephones, no specific information has been given of how 1 g or 10 g values have been evaluated. The spatial distribution of the electric field and the corresponding power distribution within the human tissue, typically in the head, is most frequently determined with the finite difference time domain method (FDTD). The transformation from the distribution of the dissipated power into the distribution of 1 g (or 10 g) averaged SAR is not a trivial task. The following has to be accounted for by a successful algorithm: (i) numerical methods, including the FDTD use staggered meshes, (ii) tissues vary in specific gravity, therefore the size of a tissue cube of required weight varies from one point to another, (iii) various mesh sizes along the axis and graded meshes are often utilized, and (iv) in a mesh with unequal spacing along x, y, z building a cubical volume using whole voxels is not feasible.

We present three possible ways of computing the power dissipated in the voxel, as based on 3, 6 or 12 electric field components, and comment on their merit and compare the results for various mesh resolutions. The core of the contribution is the development and evaluation of two efficient algorithms for computations of 1 g (10 g) average SAR. One of the algorithms applies to uniform in all directional meshes and the other to non-uniform meshes. The technique is based on the concept of a low pass adaptive 3D spatial filter with a cube shaped mask, that changes its volume via an adoption mechanism responding to changes in the tissue specific gravity.

In the case of a uniform mesh, the key parts of the algorithm are: (i) Cubes are built and weighted. The largest cube of mass less than required is considered the core of the sought cubic volume. (ii) An additional layer of voxels is added to the core. The masses of the sides, edges and corners of that layer are evaluated. (iii) A cubic equation is solved to compute the fraction $f = dx/dx$ of the external layer that needs to be added to the core to obtain the required averaging mass. This equation is $cf^3 + cf^2 + sf - k = 0$, where c is the total mass of 8 corners, e is the total mass of 12 edges, s is the total mass of 6 sides, and k is the required fraction of the outer layer mass. (iv) Add up the power of core elements and weighted power of the sides, edges and corners using appropriate powers of f as weights. A similar but more complicated algorithm based on the same principle is also developed for graded meshes.

A detailed evaluation is performed for both algorithms and the three schemes of averaging of the field components. The tests are done at 835 MHz for a 50 mm thin dipole at two distances (5 and 15 mm) from the surface of a two-layer sphere, with the outer layer 5 mm thick and having the bone properties and the inner sphere having the brain properties. Two different mesh sizes are used to illustrate various sources of errors and demonstrate the correct operation of both algorithms.

Issues In Differential Equation Based Methods

S. Gedney and R. Lee

A Critical Look at Implicit Moment-matching Methods for Reduced-order Modeling of Distributed Electromagnetic Systems	200
<i>A. C. Cangellaris*, University of Illinois, USA</i>	
Scattering of Electromagnetic Waves by a Metallic Object Partially Immersed in a Semi-infinite Dielectric Medium.....	201
<i>R. T. Ling*, P. Ufimtsev, Northrop Grumman Corp., USA</i>	
Error Reduction using Richardson Extrapolation in the Finite Element Solution of Partial Differential Equations using Wavelet-like Basis Functions.....	202
<i>W. E. Hutchcraft*, Worcester Polytechnic Institute, USA, L. A. Harrison, R. K. Gordon, University of Mississippi, USA, J. Lee, Worcester Polytechnic Institute, USA</i>	
Convergence Improvements of Iterative Solvers for Poorly Conditioned Antenna Applications.....	203
<i>Y. Y. Botros*, J. L. Volakis, University of Michigan, USA</i>	
Software Tools for Diagnostics and Repair of CAD Generated Aircraft Models Used in Electromagnetic Computations	204
<i>E. Oliker*, L. Prussner, Matis, Inc., USA, V. Oliker, Emory University, USA, J. Romanovsky, St. Petersburg State University, Russia</i>	
Finite Element and Finite Volume Formulations of Time-harmonic Scattering Problems over a Uniform Mesh	205
<i>M. Kuzuoglu*, Middle East Technical University, Turkey, R. Mittra, Pennsylvania State University, USA</i>	
Application of P-refinement Techniques to Vector Finite Elements	206
<i>R. S. Preisig*, A. F. Peterson, Georgia Institute of Technology, USA</i>	
Higher Order Interpolatory Vector Functions on Pyramidal Elements	207
<i>R. D. Graglia*, I. Cheema, Politecnico di Torino, Italy</i>	
Finite Element Method Determination of the Loss of Bandpass Filters using Skin Elements	208
<i>G. P. Riblet*, Microwave Development Labs., Inc., USA</i>	
Application of the Cross-section Method to the Analysis of Waveguide Transitions Including Cut-off Cross-sections.....	209
<i>I. Ederra*, M. Sorolla, Universidad Pública de Navarra, Spain, M. Thumm, University of Karlsruhe, Germany, B. Katsenelenbaum, Russian Academy of Sciences, Russia</i>	

A CRITICAL LOOK AT IMPLICIT MOMENT-MATCHING METHODS FOR REDUCED-ORDER MODELING OF DISTRIBUTED ELECTROMAGNETIC SYSTEMS

Andreas C. Cangellaris

Department of Electrical and Computer Engineering
University of Illinois at Urbana-Champaign
Urbana, IL 61801-2991, U.S.A.
E-mail: cangella@uiuc.edu

Following the successful application of model-order reduction techniques in complex electronic circuit simulation, electromagnetic simulation researchers are currently investigating the opportunities that such methods provide in conjunction with rapid analysis of distributed electromagnetic systems. As a result, several researchers have demonstrated the use of Padé approximations of the response of electromagnetic systems to effect the so-called *fast frequency sweep*, where the system response over a broad range of frequencies is obtained at approximately the cost of factoring the approximating matrix at only a few frequency points. In addition to rapid broadband calculation of the frequency response of an individual electromagnetic component, such Padé approximations of electromagnetic responses provide for efficient macromodeling of electromagnetic multiports. Such multiport macromodels, described in terms of reduced-order (Padé) approximations of the elements of either their scattering parameter or admittance matrix, can be incorporated in network-oriented circuit simulators for the purposes of large scale, efficient simulation of complex electronic systems.

In this paper, recent advances in electromagnetic model order reduction are reviewed and evaluated critically. The emphasis is placed on *implicit moment matching* techniques because of their capability to generate high-order Padé approximations of high accuracy. This capability is critically important for reduced-order modeling of distributed electromagnetic systems which, in their continuous form, are of infinite order. These implicit moment matching methodologies utilize either the Lanczos or the Arnoldi algorithm to generate the moment vectors in such a way that they are orthogonal to each other. This way, every new moment vector generated provides new information about the system, thus leading to the robust development of Padé approximations of order as high as needed to capture the response of the system under study over the frequency bandwidth of interest. Furthermore, instead of extracting the poles and residues of the approximated response via a moment-matching procedure, the generated set of orthogonal moments may be used directly to produce a reduced set of state equations for the system in hand. This is done by projecting the original system into the subspace spanned by the generated set of moment vectors.

Discrete approximations of electromagnetic systems of practical interest often involve hundreds of thousands, or even millions, of state equations. Consequently, from the available implicit moment matching methodologies, those that do not require any matrix inversion are of greatest interest. Such a methodology has been proposed by Remis and van den Berg (Remis and van den Berg, IEEE Trans. Microwave Theory Tech., 45, 2139-2149, 1997). However, because it relies, essentially, on moment matching about the point at infinity, its use in the model-order reduction of electromagnetic systems with rich low-frequency information raises some questions. On the other hand, it is clearly very appropriate for systems for which the early-time response is of interest. Alternative implementations of the Lanczos algorithm utilize moment matching about a finite frequency point, dictated by the anticipated useful bandwidth of interest (Zhao and Cangellaris, Microwave and Optical Letters, Jan. 1998). Using this methodology, Padé approximations that capture accurately the response of the system over the entire bandwidth of interest can be generated. The possibility of complementing the two approaches is of interest, and its feasibility will be discussed. In addition to contrasting these implicit moment-matching methodologies, the presentation will examine also

Scattering of Electromagnetic Waves by a Metallic Object Partially Immersed in a Semi-Infinite Dielectric Medium

R.T. Ling* and P.Ya. Ufimtsev+

Northrop Grumman Corp.

8900 E. Washington Blvd.

Pico Rivera, CA. 90660-3783

+Also with

Electrical Engineering Department

University of California, Los Angeles

Los Angeles, CA 90095-1594

The concept of the generalized scattering amplitude is applied to the electromagnetic scatterings of arbitrarily shaped, perfectly conducting objects partially immersed in a planar semi-infinite homogeneous dielectric medium. The incident field enters in the free half space. Thus the total field in the free half space is composed of the incident field, the reflected field, and the scattered field while it consists of the transmitted (or refracted) field and the scattered field in the dielectric half space. In a 2-D formulation, after the outgoing cylindrical wave is factored out from the scattered field, the remaining component is defined as the generalized scattering amplitude. The transformed Helmholtz equation in terms of the generalized scattering amplitude can be solved numerically using a finite-difference method over the entire scattering domain including both the semi-infinite free space and the semi-infinite dielectric medium. The dielectric medium can have arbitrary complex permittivity and permeability. The arbitrary shapes of metallic obstacles are treated with numerically generated body-fitted grids. Example problems of scatterings by infinitely long, perfectly conducting circular cylinders and cylinders of ship-shaped geometric cross section partially buried in imperfectly conducting planar earth and ocean water are solved to demonstrate the theoretical formulation and numerical method. The far-field solutions for the monostatic and bistatic radar cross sections and the induced current density on the obstacle's surface for both E-field and H-field polarizations are computed. The radial profiles of the generalized scattering amplitude and the total field over the entire scattering region are also presented and their properties are discussed.

Error Reduction Using Richardson Extrapolation in the Finite Element Solution of Partial Differential Equations Using Wavelet-Like Basis Functions

W. Elliott Hutchcraft(*), Lee A. Harrison, Richard K. Gordon, Jin-Fa Lee(*)

Department of Electrical Engineering
University of Mississippi
University, MS 38677

Department of Electrical Engineering (*)
Worcester Polytechnic Institute
Worcester, MA 01609

In recent years, error analysis has become increasingly important in the computational sciences and error estimation techniques have received abundant attention in the scientific literature. These estimation techniques have only rather recently been applied in computational electromagnetics. For example, error estimation has been employed in the finite element determination of the magnetic field in a two-dimensional region using edge-based elements (G. Drago, P. Molfino, M. Nervi and M. Repetto, *IEEE Transactions on Magnetics*, vol. 28, no. 2, pp. 1743-1746, March, 1992); and Richardson extrapolation has been used in conjunction with the finite difference analysis of both one and two-dimensional electrostatics problems (W. Elliott Hutchcraft, Richard K. Gordon, *Proceedings of the 28th IEEE Southeastern Symposium on System Theory*, Baton Rouge, LA, April, 1996).

Another topic that has recently become increasingly important in computational electromagnetics is wavelet analysis. For instance, wavelet basis functions have been employed in an integral equation technique for the solution of scattering problems (J. C. Goswami, A. K. Chan, and C. K. Chui, *1994 Digest of the IEEE Antennas and Propagation Society International Symposium*, vol. 1, p. 2, June 1994); and wavelet-like basis functions have been employed in a finite element analysis of electrostatics problems (Lee A. Harrison, Richard K. Gordon, *Proceedings of IEEE Southeastcon '96*, Tampa, FL, April, 1996).

In this paper, both wavelet-like functions and error analysis will be employed in an efficient technique to solve partial differential equations. Wavelet-like basis functions and Richardson extrapolation will be used in the finite element solution of two-dimensional electrostatics problems. An advantage of using wavelet-like basis functions rather than traditional finite element basis functions is that when wavelet-like basis functions and simple diagonal preconditioning are used in conjunction with an iterative solution technique the rate of convergence is much faster than is the case when the traditional basis functions are used. One advantage of the use of error analysis is that it can help lead to calculation of solutions that are quite accurate but don't require extremely long compute time or substantial computer memory capacity.

In this paper, the construction of the wavelet-like basis functions will be discussed. Then, several sample problems will be studied in which these basis functions are used to solve electrostatics problems with both Neumann and Dirichlet boundary conditions. From these solutions, the implementation of Richardson extrapolation to reduce the numerical error will be discussed. Comparisons will be made with solutions obtained using the traditional basis functions and with solutions obtained before the error analysis process.

Convergence Improvements of Iterative Solvers for Poorly Conditioned Antenna Applications

Youssry Y. Botros, and John L. Volakis

Radiation Laboratory

Department of Electrical Engineering

and Computer Science,

The University of Michigan

Ann Arbor, MI 48109-2212

Abstract

Poorly conditioned systems may be generated in several cases when modeling FEM problems. An example is the Perfectly Matched Layer (PML) truncation scheme which utilizes active anisotropic material to terminate the computational domain. Using such material within the computational domain dramatically degrades the system condition. Similar situation occurs when ferrite materials are used to control the frequency response of some antennas. Moreover, for large antennas or microwave circuits with small geometrical details, non uniform meshing results in significant deterioration of the matrix condition. Therefore, when iterative solvers are employed to solve such systems, the overall convergence is poor and it may be necessary to employ robust iterative schemes with strong preconditioners. The Generalized Minimal Residual (GMRES) solver is a good candidate since it guarantees convergence even for poorly conditioned indefinite systems. Preconditioners which vary from the simplest Diagonal Preconditioner (DPC) to the most expensive Approximate Inverse Preconditioner (AIPC) can be readily employed as part of the solver. The CPU cost of the GMRES solver is $O(m^2n)$ where m denotes the number of basis functions or search vectors associated with the GMRES iterations and n is the matrix size (number of unknowns). Typically, $m \ll n$ and its value depends on several factors including the system condition, specified tolerance and FEM size. The CPU cost of the AIPC is $O(p^2n)$ where p is the bandwidth of the FEM matrix. Regarding memory cost, the GMRES solver requires $O(mn)$ storage and the AIPC storage requirement varies from n to n^2 when the AIPC is represented by a full matrix storage. A Flexible version of the GMRES (FGMRES) will be also presented. This version permits modifications of the preconditioner within the iteration for optimizing memory and CPU resources. Several examples including truncation applications, spiral antennas and ferrite loaded resonators are presented to demonstrate the superior performance of the iterative FGMRES scheme with the adapted AIPC.

Software Tools for Diagnostics and Repair of CAD Generated Aircraft Models Used in Electromagnetic Computations

Elena Oliker, Laird Prussner
Matis, Inc., Atlanta, Georgia 30329
e-mail: matis@netcom.com

Vladimir Oliker
Emory University, Atlanta, Georgia 30322
Joseph Romanovsky
St. Petersburg State University, St. Petersburg, Russia

Building a high-quality realistic aircraft model suitable for high-accuracy electromagnetic (EM) or computational fluid dynamics (CFD) calculations is an expensive and time-consuming task. Consequently, it is highly desirable to develop capabilities to transform existing aircraft models into models suitable for EM or CFD calculations. The requirements to the geometry of the model for EM and CFD calculations have a substantial overlap and the same transformation tools can be utilized by both fields.

The purpose of this talk is to describe the recent progress made in the development of a software system, "GeomFix", which is a general purpose system built to perform such transformations and produce topologically and geometrically consistent surface models satisfying specific requirements. GeomFix works with triangular faceted files but can import files in various formats, including IGES files. Among the tasks that GeomFix can deal with are: analysis of the surface file and its parts, removal of irrelevant parts, combining parts into assemblies based on relationships between parts, identification of disjoint sub-parts, translating parts that are far apart in order to enable join, re-scaling parts, checking and correcting orientation of facets, cutting large parts into more manageable (smaller) surfaces (cutting is performed either by planes (slicing) or along curves (cutouts)), building curves (including surface geodesics), extending surfaces, finding intersections of components, re-building triangulation along the intersection curves, sewing parts together, removing duplicate/unreferenced points, removing degenerate facets, filling cracks on the surface, repairing triangulations that include overlaps, have more than two triangles sharing an edge, or have T-junctions, improving aspect ratio of the mesh, building convex hulls, building symmetric images of parts of a surface, identification of boundaries, folds, triplets, duplicates, degenerate facets, etc. The GeomFix has a graphics user interface that allows easy and intuitive navigation among different diagnostics and repair tools.

Finite Element and Finite Volume Formulations of Time-harmonic Scattering Problems solved on a Uniform Mesh

*Mustafa Kuzuoglu**

Department of Electrical Engineering Raj Mittra
Middle East Technical University Pennsylvania State University
06531, Ankara TURKEY 319 Electrical Engineering East
University Park, PA 16802-2705 USA

In finite methods, an important first step in the solution of scattering problems involving complex objects is the generation of a non-uniform mesh. The mesh generation algorithm must be able to handle the geometric complexity by generating a mesh of tetrahedra or hexahedra over the computational domain. In order to avoid ill-conditioning in the resulting matrix equation, special care should be taken not to generate elements with large aspect ratios. In discretizing a domain, consideration must be given to an accurate representation of material and geometric discontinuities.

In this work, an alternative approach, which avoids the difficult mesh generation phase, is proposed. A uniform hexahedral mesh is generated over the computational domain (which is taken as a rectangular prism) and special care is devoted to elements that contain part of the free space-scatterer interface. In the FEM formulation, integrals in the weak variational form are modified in these elements. Similarly, in the finite volume (FV) approach, differentiation formulas are modified for elements containing an interface, *i.e.*, for the case where the constitutive parameters are discontinuous. Another major advantage of this approach is the reduction in storage and computational time as a result of the tabulation of a single local matrix for identical elements.

In this paper, the performance of the FEM and FV approaches are compared for specific scattering problems and the conditioning of the matrix equations are discussed for these two approaches. The partitioning of the computational domain into smaller prisms is also examined from the point of view of designing an effective pre-conditioner based on a non-overlapping domain decomposition procedure.

Application of p-refinement techniques to vector finite elements

R. Stephen Preissig and Andrew F. Peterson
School of Electrical & Computer Engineering
Georgia Institute of Technology
Atlanta, GA 30332-0250*

Over the years, there have been many extensions and variations on the classical scalar finite element method. The recent development of vector finite elements has promoted similar extensions. One aspect of finite elements is the possibility of adaptive refinement of the finite element mesh, such as the h -refinement process where portions of the mesh are refined to achieve smaller cells and higher accuracy where required, and the p -refinement strategy, where the polynomial order of the representation is selectively increased throughout portions of the mesh. Based on work in scalar finite element analysis, it is generally thought that improved convergence can be obtained with p -refinement or a mixture of h -refinement and p -refinement strategies. This presentation will consider several aspects of p -refinement applied to vector finite elements.

Interpolatory vector basis functions of arbitrary order on triangles, quadrilaterals, tetrahedra, etc. can be developed based on a recent article (Graglia, Wilton, Peterson, *IEEE Trans. Antennas Propagat.*, March 1997), making it relatively easy to implement higher-order representations. To implement a p -refinement strategy, it is necessary to augment the existing bases with special vector functions that provide a transition from one polynomial order to another in adjacent cells. These functions must maintain tangential continuity between cells, to achieve a curl-conforming representation. One possibility is to employ hierarchical vector basis functions, so that the representation can be refined without changing the original basis functions and repeating the calculations. A new set of hierarchical functions, whose highest-order members at each level satisfy the Nedelec conditions, will be presented for triangular cells. It appears that hierarchical functions may improve the computational efficiency of the implementation at the expense of introducing more poorly conditioned intermediate matrices. An alternative approach is to work with interpolatory vector functions, and replace all the functions within certain cells during p -refinement. This approach will be described.

Numerical results will be presented that illustrate the performance of mixed polynomial representations for several canonical structures.

Higher Order Interpolatory Vector Functions on Pyramidal Elements

R. D. Graglia*, I.-L. Gheorma

Dipartimento di Elettronica, Politecnico di Torino
10129 Torino, ITALY

New developments on higher order interpolatory vector elements for the numerical solution of integral and differential equations have been reported recently (R.D. Graglia, D.R. Wilton and A.F. Peterson, *IEEE Trans. Antennas Propagat.*, vol. 45, no. 3, 329-342, 1997). Higher order triangular and quadrilateral elements are commonly used to solve 2D problems while tetrahedrons, bricks and, to some extent, triangular prisms are used to solve 3D problems. By this work we intend to address few problems which are still open. The first problem is encountered when one wants to change the mesh size of a brick mesh by introducing one layer of pyramidal elements having quadrilateral base, or when one wants to mix different elements to discretize a given 3D volume; this latter case could be of some importance in hybrid approaches because one may work with a tetrahedral mesh in the inner volume region by still discretizing the external surface with a quadrilateral mesh.

The second problem is to define higher order interpolatory vector bases on pyramidal elements so to guarantee the continuity of the tangent or normal components across two adjacent elements where, in this case, the elements attached to the pyramid can either be tetrahedrons, bricks or pyramids. From a strictly geometrical point of view, all the problems one has here are related to the presence of the tip of the pyramid, i.e. the point in common to four faces of the pyramid. Notice that for all the other volume elements (brick, tetrahedron and prism) only three faces join at a corner.

At the conference we will present higher order interpolatory vector functions on pyramidal elements, prove their completeness and discuss all their properties. The results will then be extended to deal with the case of distorted (curved) pyramids. Numerical results for a rectangular cavity solved by using pyramidal elements will also be presented.

Finite Element Method Determination of the Loss of Bandpass Filters Using Skin Elements

G.P.Riblet
Microwave Development Labs., Inc.
Needham Heights, MA 02194

This approach was motivated by an interest in finding a simple way to determine the theoretical resistive loss of microwave bandpass and bandstop filters which were already being analyzed by the finite element method. Typically such an FEM analysis is performed for the lossless case. However insertion loss resulting from finite conductivity is also an important parameter. It has been found that by including additional thin skin elements adjacent to conducting surfaces, the loss of such filters can also be evaluated simultaneously. The basic finite element program structure remains unchanged. More elements are required, however. In the case of a five section waveguide bandpass filter, only 20 percent more elements are needed. The skin elements should be thin enough that the magnetic field vector within them is effectively tangential to the adjacent conducting surface. The method is an extension of the well known technique for calculating the attenuation per unit length of a transmission line with known E and H fields such as rectangular waveguide or coax.

The accuracy of the approach based on skin elements was confirmed by determining the attenuation per unit length of silver plated WR42 waveguide using this method. Taking the microwave surface resistivity of silver plating to be 3 $\mu\Omega/cm$ and the skin elements to have the thickness of the skin depth, the attenuation was found to be .1396dB/ft at 23.0 GHZ. This is within one part per thousand of the result of .1397dB/ft calculated from the standard formula for the attenuation of rectangular waveguide. A five section WR42 waveguide bandpass filter has also been analyzed. It consists of six thin centered irises .029" wide. Starting from the end of the filter the lengths of the irises are .0382" , .1786" and .2079" respectively. They are separated by gaps of .2555" , .2572" , and .2573" respectively. The skin elements were all .010" thick. The theoretical mid-band insertion loss of the filter is .43 dB. The experimental minimum insertion loss of an actual silver plated unit is .47 dB. The unit was tuned slightly to obtain five nearly equal spaced ripples within the passband of 22.8 to 23.2 GHZ. In agreement with the experimental curve, the theoretical loss increases more rapidly at the low end of the passband.

APPLICATION OF THE CROSS-SECTION METHOD TO THE ANALYSIS OF WAVEGUIDE TRANSITIONS INCLUDING CUT-OFF CROSS-SECTIONS.

Ederra, I.¹, Sorolla, M.¹, Thumm, M.² and Kaisenelenbaum, B.³

¹ Departamento de Ingeniería Eléctrica y Electrónica

Universidad Pública de Navarra

Campus Arrosadia s/n, 31006, Pamplona, Spain

email: ederra@zeus.tsc.upna.es

² Forschungszentrum Karlsruhe

Institute of Technical Physics

P. O. Box 3640, D-76021 Karlsruhe, Germany

and Institute of Microwaves and Electronics, University of Karlsruhe

³ Institute of Radio-Engineering and Electronics

Russian Academy of Sciences

11 Mokhovaya, 103907 Moscow, Russia

This paper is devoted to the numerical test of some equations obtained analyzing nonuniform waveguides that include cut-off cross-sections with the cross-section method. This is one of the mathematical methods employed to solve a certain class of electrodynamic problems, considering nonuniform tubular waveguides.

The basic idea of the cross-section method ("Theory of nonuniform waveguides: The cross-section method", Kaisenelenbaum et al., 1998), is that the electromagnetic fields in an arbitrary non-uniform waveguide cross-section are represented as a superposition of the waves of different modes propagating in forward and backward directions along an auxiliary straight uniform waveguide of the same cross-section and with the identical distribution of ϵ and μ . The coefficients of this superposition satisfy first order ordinary differential equations. The general problem of the field derivation in an non-uniform waveguide is reduced in such a way to the problem of the fields in a uniform waveguide and to the solution of coupled-wave ordinary differential equations.

In our case, this method has been used to analyze some transitions in circular waveguides including cut-off cross-sections, i.e. sections of waveguide where a mode goes below cut-off. First, the case when the propagating mode goes below cut-off has been considered. Then, the reflection coefficient value is one, and its phase depends on the portion of waveguide where the mode is below cut-off. This dependence is given by a parameter named δ_0 . In the second case, cut-off cross-sections of the main parasitic mode have been analyzed. When the transition is smooth enough, a simple formula gives the reflected power in this mode. The results obtained using this method have been compared in both cases with those obtained with a Mode Matching and Generalized Scattering Matrix code and, as can be seen in figures 1 and 2, are in good agreement.

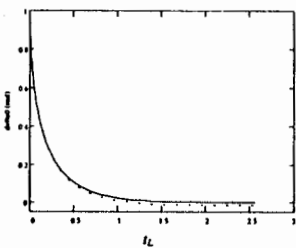


Fig. 1: δ_0 (parameter that gives the dependence of the phase of the reflection coefficient) vs t_L (parameter related with the length of the transition). Comparison between the theoretical values (solid line) and the Mode Matching and GSM results (dotted line).

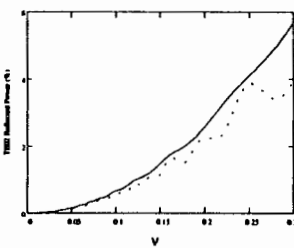


Fig. 2: Reflected power in the TE_0 mode vs slope of the transition. Comparison between the theoretical values (solid line) and the Mode Matching and GSM results (dotted line).

EM Scattering from Finite and Extended Bodies

R. J. Marhefka and S. Maci

Calculation and Analysis of Electromagnetic Scattering from a Helicopter Rotor.....	212
<i>P. Pouliquen*, Centre d'Electronique de l'ARmement, France</i>	
Electromagnetic Scattering Analysis of Sample Objects within the Near-field of a Subwavelength Aperture Utilizing FDTD Methods.....	213
<i>W. C. Symons*, D. R. A. Lodder, University of Kentucky, USA</i>	
Spurious Interior Resonances in Differential-equation-based Solutions of Scattering Problems.....	214
<i>C. M. Butler*, Clemson University, USA</i>	
The Partial Representation of the Fields Scattered by Large Objects	215
<i>R. Zaridze*, G. Bit-Babik, K. Tavzashvili, Tbilisi State Univ., Georgia, N. Uzunoglu, D. Economou, Technical Univ. of Athens, Greece</i>	
Analytical-numerical Approach for the Solution of the Diffraction by a Thin Dielectric Strip.....	216
<i>E. I. Veltov, Ukrainian Academy of Sciences, Ukraine, K. Kobayashi*, Chuo University, Japan, S. Koshikawa, Antenna Giken Co., Ltd., Japan, K. Takagi, N. Motoi, Chuo University, Japan</i>	
On the Born Approximation for Scattering from Buried Plastic Targets.....	217
<i>T. Dogaru*, N. Geng, L. Carin, Duke University, USA</i>	
Electromagnetic Scattering by a Uniaxial Chiral Cylinder with Arbitrary Cross Section: Generalized Mode-matching Method.....	218
<i>D. Cheng*, Y. M. M. Antar, Royal Military College of Canada, Canada</i>	
Time-Domain, Point Source Excitation of a Dielectric Wedge: Perturbation for Nearly Equal Wave Speeds	219
<i>A. M. Davis*, R. W. Scharstein, University of Alabama, USA</i>	
Study of Interaction between an Object and Infinite PEC Plane by MoM.....	220
<i>Q. L. Li, D. B. Ge*, S. Y. Shi, Xidian University, P.R.China</i>	

CALCULATION AND ANALYSIS OF ELECTROMAGNETIC SCATTERING FROM A HELICOPTER ROTOR

P. POULIGUEN

Centre d'ELectronique de l'ARmement (CELAR), Division GEOS,
35170 Bruz, FRANCE

ABSTRACT

A high frequency model, using Physical Optics (P.O.) and the Method of Equivalent Currents (M.E.C.), is proposed to estimate the Radar Cross Section (R.C.S.) and the spectral response from a helicopter rotor. The rotor is made of N rotating blades positionned symmetrically with equal spacing angles.

The problem is treated by using the quasi-stationary approach, since the rotating velocity is much less than the velocity of light and the angular frequency of rotation is very small compared to the angular frequency of the radar wave (*J. Van Bladel, Proc. IEEE, Vol. 64, No. 3, 1976*). At each instant, in the presence of a linearly polarized time harmonic incident spherical wave, the electromagnetic field scattering by the rotor is calculated by assuming that the blades are frozen in their tracks.

The model proposed in this paper is new to the author knowledge and very general. It furnishes the time-dependent monostatic or bistatic scattered electromagnetic field of the rotating blades. The calculation can be accomplish versus the range between the Radar and the rotor centre of symetry ; giving the possibility of a near field simulation. This last characteristic can be very useful if one consider, for example that for a 15 m diameter rotor at 10 GHz, the Fraunhofer far field range is equal to 30 km. The blades geometry is exactly taken into account with the aid of a triangular meshing generated by the software I-DEAS. It is also possible to consider the characteristics (conductivity, permittivity, permeability) of the materials which constitute the blades coating.

Then, two methods are used to calculate the spectral response of the rotor. Firstly, Fast Fourier Transform (FFT) is performed on a period of the time dependent scattered field to produce the R.C.S. spectrum. Secondly, a three dimensional "time - Doppler" map, or "time - Doppler" image, is accomplished by segmenting the time domain data into windows of N_{FFT} points and transforming these windows into the frequency domain (*J. Pentalone, Conference paper, NIST, Boulder, Co., USA, pp. 2-43 to 2-46, 1992*). Finally, examples are given where the temporal and spectral characteristics of a generic rotor are studied versus the blades number, the Radar frequency, the viewing aspect angle and the range separating the Radar and the rotor. The effects of near field on these characteristics are particularly analysed.

Electromagnetic Scattering Analysis of Sample Objects Within the Near-Field of a Subwavelength Aperture Utilizing FDTD Methods.

W. C. Symons* and Dr. R. A. Lodder

Department of Electrical Engineering and College of Pharmacy
University of Kentucky
A123 ASTeCC Building
Lexington, KY 40517-0286

Currently, Near-Field Scanning Optical Microscopes (NSOMs) are becoming increasingly popular analytical instruments. This popularity can be attributed to their ability to resolve images beyond the diffraction limit of conventional optical microscopes. Furthermore, NSOMs achieve this resolution while maintaining such important nondestructive characteristics of their conventional counterparts as the ability to gather spectral information of the sample. This subwavelength resolution is achieved by raster scanning a subwavelength aperture within a wavelength distance of a sample. Thus, the image resolution is determined by the aperture size, aperture/sample separation distance, and the step size of the raster scan.

In order to accurately interpret the image data of NSOM instruments, it is important to fully understand the near-field optical phenomena involving the electromagnetic scattering characteristics of sample objects illuminated within the near-field of a subwavelength aperture. To this end, a finite-difference time-domain (FDTD) model was derived and implemented according to the physical attributes of an NSOM instrument. Specifically, the NSOM instrument was modeled as a subwavelength aperture located within an infinite PEC plane which was then illuminated by an incident plane wave. Absorbing boundary conditions were then utilized to simulate the free space surroundings of the instrument. Furthermore, a near-field to far-field transformation was required to simulate radiation incident upon a detector located in the far-field. Once the basic model is implemented, it can then be utilized to simulate various samples of interest including thin PEC wires, PEC plates, and dielectric slabs. For example, thin PEC wire samples can be compared to closely spaced PEC plates. In this manner, it is possible to gain a better understanding of NSOM effects such as polarization, aperture/sample separation distance, and aperture size.

Spurious Interior Resonances in Differential-Equation-Based Solutions of Scattering Problems

Chalmers M. Butler

Department of Electrical and Computer Engineering
Clemson University
Clemson, SC 29634-0915

There is an abundance of literature in which spurious solutions of scattering problems at the so-called interior resonances of the scatterer are attributed to failure of the integral equation at frequencies corresponding to these resonances. It has been demonstrated for perfectly conducting scatterers that the interior resonance failure manifests itself also in solutions obtained exclusively by differential equation methods (C. M. Butler, Digest, URSI National Radio Science Meeting, p. 305, Boulder, CO, 5-8 Jan. 1998). It is shown analytically that the failure actually rests with the formulation of the boundary value problem, not with the technique used to solve the formulated equations, be they differential equations or integral equations. Is the same true of dielectric scatterers, even though it is well known that no true resonance can exist in the case of a cavity whose walls are penetrable as is true of any cavity that one might fashion from a dielectric body? The answer is a clear "Yes" as is illustrated in this paper by means of a differential-equation-based analytic solution of the problem of scattering by a dielectric cylinder.

In this paper the equivalence principle and eigenfunction expansion methods are employed to determine the equivalent currents that enable one to express the field which is scattered by a dielectric cylinder and that which penetrates the cylinder. Though this solution procedure is entirely analytic and is unrelated to integral equation methods, it clearly fails at interior resonances. The internal resonance frequencies are found explicitly in analytical form for both the TM- and TE-excitation dielectric cylinder scattering problems. Different formulations – based on the equivalence principle – lead to solutions which fail in different ways, all of which are predictable analytically.

Evidence is offered to support the claim that the internal resonance difficulty lies deeper than a failure of an integral equation at discrete frequencies. It is corroborated that these failures are associated with the fundamental formulation. And it is demonstrated, again analytically, that the problems can be cured by the standard procedures commonly called combined field and combined source techniques. In the present cases the combined field and combined source remedies are called upon to render differential equation methods unique at all frequencies, even in the case of the dielectric cylinder problem.

The Partial Representation of the Fields Scattered by Large Objects

R. Zaridze, G. Bit-Babik, K. Tavzarashvili. Tbilisi State Univ., Georgia. iae@resonan.ge
N. Uzunoglu, D. Economou. Technical Univ. of Athens, Greece. deco@esd.ece.ntua.gr

This paper attempts to expand the possibilities of the Method of Auxiliary Sources (MAS) for large-body scattering problems or high frequencies. Emphasis is given on approximate solutions by considering the basic phenomena and effects which are responsible for the creation of the scattered field (SF). Such approach will allow to get the solution of diffraction problems with minimum computer resources. Paper focuses on investigations of the scattered fields singularities (SFS) which are the bright spots in the area of caustic. The efficient utilization of the MAS in applied electrodynamics is shown. Besides, the investigation of the SFS localization, their behavior for various frequencies and different shapes of the scatterers and finally how they turn into caustic for optics, when wavelength goes to zero, is a matter of theoretical interest.

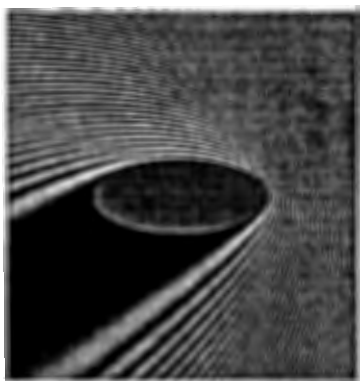


Fig. 1 The absolute value of the full field.
(Incident plus scattered)

Investigations have shown that: 1) SFS may be localized from the geometry of scatterer and the incident field; 2) the prior knowledge of SFS localization sharply simplifies the solution of diffraction problem. In this work the holographic method for SFS localization is presented. It is based also on MAS. The SFS are used as radiating bright spots, which form the scattered field partially, each in correspondent sector. The localization of singularities is given for the field scattered by perfectly conducting elliptical cylinder and strips.

Another approach for SFS localization coming from

Fresnel's zones and caustic consideration is also discussed. As an example Fig. 1 illustrates the solution of scattering problem on large perfectly conducting elliptical cylinder ($ka=100$), taking into account all these peculiarities. The number of unknowns in this case is the whole number of $N=2ka/\pi$, while the accuracy of solution is within 1%. The wavenumber can be easily increased but the resolution of picture is limited so we restricted ourselves with $ka=100$.

Analytical-Numerical Approach for the Solution of the Diffraction by a Thin Dielectric Strip

Eldar I. Veliev 1), Kazuya Kobayashi 2), Shoichi Koshikawa 3), Kazuhiko Takagi 2), and Norio Motoi 2)

- 1) Institute of Radiophysics and Electronics, Ukrainian Academy of Sciences,
Ulitsa Proskury 12, Kharkov 310085, Ukraine
- 2) Department of Electrical and Electronic Engineering, Chuo University,
1-13-27 Kasuga, Bunkyo-ku, Tokyo 112, Japan
- 3) Antenna Giken Co., Ltd., 4-72 Miyagayato, Omiya 330, Japan

Approximate boundary conditions are often used to simplify solutions of scattering problems involving complicated structures. The simplest conditions are the standard impedance boundary condition applicable at the surface of a lossy dielectric and the related transition conditions modeling a thin dielectric layer as a current sheet. Recently it was suggested by Senior and Volakis (Approximate Boundary Conditions in Electromagnetics, IEE, London, 1995) that a thin dielectric layer can be effectively modeled by a pair of modified resistive and conductive sheets each satisfying given boundary conditions. In this paper, we shall consider the model of a thin dielectric strip formed by the combination sheets and analyze the plane wave diffraction by means of the analytical-numerical approach (E. I. Veliev and V. V. Veremey, Analytical and Numerical Methods in Electromagnetic Wave Theory, Chap. 10, M. Hashimoto, M. Idemen, and O. A. Tretyakov, Eds., Science House, Tokyo, 1993).

We consider a planar dielectric strip of width $2a$ and thickness t , illuminated by an H-polarized plane wave. The H polarization implies that the incident magnetic field is parallel to the edge of the strip. The geometry can be approximately replaced by the strip of zero thickness, where the total field satisfies the boundary condition of coincident resistive and modified conductive sheets on the surface of the strip. Applying the boundary condition to an integral

representation of the scattered field, the problem is formulated as two integral equations satisfied by the unknown current density functions. Expanding the current density functions in terms of the Chebyshev polynomials by taking into account the edge condition, our problem is reduced to the solution of two infinite systems of linear algebraic equations (SLAE) satisfied by the unknown expansion coefficients. These coefficients are determined numerically with high accuracy via truncation of the SLAE. The scattered field is evaluated asymptotically and a far field expression is derived. Numerical examples on the radar cross section are presented for various physical parameters and the far field scattering characteristics are discussed in detail. Some comparisons with the results in the paper by Volakis (Radio Sci., 23, 3, 450-462, 1988) are also given to validate the present method.

On the Born Approximation for Scattering from Buried Plastic Targets

Traian Dogaru*, Norbert Geng and Lawrence Carin

Department of Electrical and Computer Engineering

Duke University

Durham, NC 27708-0291

There are many problems in which one may use radar for the sensing of subsurface (buried) dielectric targets. For example, the electromagnetic sensing of plastic land mines constitutes a difficult problem of current interest. In such problems one is often interested in imaging the target, for which a fast forward-scattering solver is essential. Moreover, in the context of buried-target detection, one needs to efficiently compute the signature of a given target, as a function of target depth, orientation, and background (soil) properties. A fast forward solver is therefore also important for such problems. The Born approximation is a very attractive option for the efficient modeling of scattering from dielectric targets, resulting in linear inverse-scattering algorithms and quick computation of target signatures for detection and identification. To test the accuracy of the Born approximation, benchmark signatures are required, based on a rigorous solution of Maxwell's equations. In the work presented here, we utilize a rigorous forward solver to test the accuracy of the Born approximation, for three-dimensional dielectric targets embedded in a layered medium, with application to scattering from plastic land mines.

Our rigorous forward solver employs the Method of Moments (MoM), for dielectric targets embedded in a lossy, dispersive layered medium. To make such an analysis tractable, we restrict the MoM analysis to targets that can be simulated as a body of revolution (BOR). Therefore, the accuracy of the Born approximation will be tested for the case of BOR targets, but it can be applied subsequently to more general scatterers.

It is well known that the Born approximation assumes a weak contrast between the electrical properties of the target and background. However, for the case of a target buried in a layered medium, of interest here, there are additional simplifications inherent to the Born approximation. In particular, all reverberations between the target and the surrounding layers are unaccounted for. This phenomenon may constitute an important part of the target signature in some scenarios. Therefore, in the context of this work, we present a detailed numerical examination of the accuracy of the Born approximation for plastic targets buried in a lossy layered medium. In this context, we provide a detailed accounting of where the Born approximation is appropriate for such problems, and where it fails.

Electromagnetic scattering by a uniaxial chiral cylinder with arbitrary cross section: generalized mode-matching method

Dajun Cheng* and Yahia M. M. Antar

Department of Electrical and Computer Engineering

Royal Military College of Canada

Kingston, Ont. K7K 5L0, Canada

Recently, Lindell and co-workers proposed a uniaxial chiral medium and investigated the polarization transformation of this material (e.g., I. V. Lindell and A. H. Sihvola, IEEE Trans. Antennas Propagat., 43, 1397-1404, 1995). From a phenomenological point of view, the constitutive relations of this medium can be written as $D = [\epsilon] \cdot E - [\xi] \cdot H$ and $B = [\mu] \cdot H + [\xi] \cdot E$, where the permittivity dyadic $[\epsilon] = \epsilon_c [I]_c + \epsilon_{\perp} \bullet_z \bullet_z$, the permeability dyadic $[\mu] = \mu_c [I]_c + \mu_z \bullet_z \bullet_z$, and the cross-coupling dyadic $[\xi] = \xi_c \bullet_z \bullet_z$. In the present work, electromagnetic waves in a uniaxial chiral medium are represented in terms of the cylindrical vector wave functions, and a generalized mode-matching method is proposed to study the two-dimensional electromagnetic boundary value problem of the uniaxial chiral medium.

The formulations of the cylindrical vector wave functions in a uniaxial chiral medium are considerably facilitated by using the concept of characteristic waves in the Fourier transform spectral domain and the method of angular spectrum expansion where the amplitudes of the spectral longitudinal components of the electrical field are assumed to be continuous and separable with respect to their variables. For the cylindrical structure which is bounded by the surface $\rho = f(\phi)$ with $f'(\phi)$ being a single valued and assumed function of the azimuthal angle ϕ , the incident, internal, and scattered waves are expanded in terms of the cylindrical vector wave functions. The generalized mode-matching method is applied by taking the integration of the azimuthal variable from 0 to 2π so that the continuity of the tangential fields is satisfied at the global boundary interface. To numerically evaluate the expansion coefficients of the scattered wave, the infinite summation involved is such truncated that the series is taken to be summed up from $-N$ to N . To validate these formulations, numerical results for a deviated circular cylinder have been computed and compared with those calculated by the conventional mode-matching method. Excellent agreement between the results is obtained. Further numerical results indicate that the bistatic echo width of the cylindrical structure with arbitrary cross section computed by using the cylindrical vector wave functions in conjunction with the generalized mode-matching method has excellent convergence property (i.e., the computed results for the bistatic echo width are stable with respect to N), which establishes the reliability and applicability of the present formulations.

TIME-DOMAIN, POINT SOURCE EXCITATION OF A DIELECTRIC WEDGE: PERTURBATION FOR NEARLY EQUAL WAVE SPEEDS

ANTHONY M.J. DAVIS*, Mathematics Department
ROBERT W. SCHARSTEIN, Electrical Engineering Department

University of Alabama, Tuscaloosa, AL 35487

The propagation of electromagnetic energy into and out of a wedge-shaped region having different permittivity and permeability (distinct wave speed and impedance) is a phenomenon that defies rigorous analysis because the wave speed contrast precludes an eigenfunction approach. In the Biot-Tolstoy extension (A.M.J. Davis and R.W. Scharstein, *J.Acoust.Soc.Am.*, 101, 1821-1835, 1997) the scalar field generated by an impulsive point source in the presence of a penetrable wedge with the same wave speed, both the 'geometric optics' and diffracted fields are expressed as residue series that cannot, in general, be summed in closed form. However, when the wedge angle is a rational multiple of π , these series become periodic in some sense and summation is achievable when the number of terms per 'period' is low enough. The 'geometrical optics' field in the summable cases is the expected combination of impulsive (delta) functions but the diffracted field for general wedge angles cannot be similarly inferred.

The corresponding electromagnetic problem involves both a scalar and a vector potential, related by a Lorentz gauge and satisfying the same boundary value problem as in the acoustic case. This exact isovelocity solution is regarded as a first step toward effective modeling of scattering by penetrable surfaces that separate media with similar wave speeds. It is used here to construct a first order perturbation of the exterior field with respect to a small relative difference in refractive indices. In the time domain, the point source must be smoothly switched on and off and then, by interchanging the roles of the interior and exterior regions, the perturbation of the exterior field is generated by the isovelocity interior field and appears as a convolution integral that symmetrically involves the illumination of the whole wedge by impulsive sources at the source and field points. The limited time duration of the applied point source can reduce the region of integration within the wedge. In the frequency domain, stationary phase techniques applied to the far field demonstrate that the largest possible contribution arises from a ray passing through the wedge, possibly with internal reflection, and the next largest contribution is restricted to the reflection zone where it provides the expected correction for wave scattering at a plane interface.

Typeset by *AMS-TeX*

Study of Interaction between an Object and Infinite PEC Plane by MoM

Q.L.Li, D.B.Ge and S.Y.Shi

Department Of Physics, Xidian University

710071, Xi'an, P.R.China

Email: dbge@xidian.Edu.Cn

The study of the interaction between an object and the infinite PEC ground is motivated by the RCS estimate for the over-the-horizon radar. Suppose the object is located at a distance of h above the PEC plane and its dimension is within the resonant region. The interaction between the object and PEC plane results in, on one hand, the redistribution of currents on the object compared with the free-space case. On the other hand, the scattered field at observation point is the summation of the fields coming from the object and PEC plane. The later problem can be easily evaluated by the image principle if the current distribution on the object was known. In this report, by using the MoM we analyze the former problem and derive a rule of thumb for the free-space approximation to the current distribution on the object.

Considering the object above an infinite PEC plane, we first build up a magnetic integral equation. Then we apply the MoM to discretize it and obtain a matrix equation. The solution gives the current distribution on the object that includes the interaction between the object and PEC plane. This current distribution is, in principle, different from the case when the object is in free space. Two examples are analyzed for the frequency range of 3-30 MHz. One is a rectangular plate of 12×8 meters. The second example is a finite cylinder with radius of 2 meters and length of 20 meters. The backscattered fields at far region observation point on the PEC plane oscillate first with increasing the distance of h and then tend to be smooth while h is greater than 50 meters. We may conjecture that the influence on the current distribution on object by the PEC plane can be negligible when h is greater than a critical distance that is 50 meters in these examples. The critical distance is dependent on the monostatic RCS and bistatic RCS downwards to the PEC ground from the object in free space. Therefore, we may evaluate the current distribution by free space approximation providing the object is located beyond the critical distance. The scattered field is then computed by the image principle considering the contribution from the PEC plane. Based on this free space approximation, the evaluation of RCS for a complex object above the PEC ground becomes far more easily treated.

Adaptive and Configurable Antenna Arrays

R. L. Haupt and T. K. Sarkar

Beam Broadening through Pure Phase Control.....	222
<i>J. A. Grzesik*, B. Toland, TRW Electronics Systems Group, USA</i>	
Design of Low-cost Multi-band Squint-free Phased Array Antenna using TTD Subarray Technique	223
<i>R. M. Najafabadi*, J. J. H. Wang, Wang Electro-Opto Corporation, USA</i>	
Null Formation by Phase-only Modification in the Pattern of a Linear Array.....	224
<i>R. Vescovo*, Universita di Trieste, Italy</i>	
Amplitude and Phase Adaptive Nulling with a Genetic Algorithm.....	225
<i>Y. Chung*, R. L. Haupt, University of Nevada, USA</i>	
Adaptive Unequally Spaced Phased Arrays	226
<i>S. Nagraj*, S. Park, T. K. Sarkar, Syracuse University, USA</i>	

BEAM BROADENING THROUGH PURE PHASE CONTROL

J. A. Grzesik* and B. Toland

TRW Electronics Systems Group
One Space Park
Redondo Beach, CA 90278

Broad array beams have evident value in contexts such as wide area broadcast or else dispersed target acquisition. Beam broadening can always be achieved by subjecting the element amplitudes to a taper of sufficient severity, but only at the expense of an undesirable gradation in the underlying power delivery network. The question which naturally arises then is whether, in conjunction with a uniform amplitude, one can broaden an array beam through the exercise of phase control alone.

A provocative inroad on this question appeared during the 1997 AP-S/URSI Montréal Symposium [Bryan Cleaveland, "Flat-Topped Beams from a Uniform Amplitude Rectangular Aperture," Volume 2, Paper 35.1, pp. 686-689]. The particular phase pattern adopted there took the form of a quadratic saddle function having its principal directions along the diagonals of a uniform-amplitude rectangular aperture. Flat-topped beams of excellent quality were indeed attained.

We proceeded to explore this issue of beam broadening through pure phase control by examining a hierarchy of simple, linear array models, beginning with population level six and restricted always by mirror symmetry about their midpoints. The symmetry constraint assures for the array (Schelkunoff) polynomial (of odd order one less than the element count) an exact palindromic form having its roots deployed as inverse pairs, and with one further root always fixed at $w = \exp(ik\cos(0)) = -1$. At population level six, in particular, these roots pairs are easily ascertained in fully explicit form on the strength of mere quadratic equations. The root orbits are then easily tracked so as to reveal those preferred phase ranges which maintain all four roots at substantial remove from the unit circle. And, with such separation duly assured, the array pattern settles down to a broad ripple altogether free from nulls. Graphical examples are given of the broad, rippled array patterns thus attained.

The residual pattern ripple can evidently be flattened below any desired coarseness level by increasing the array population. Schelkunoff polynomial dissection of the type described, when undertaken for a symmetric array of next higher population eight, hinges already around a cubic resolvent just prior to the final quadratics for the three inverse root pairs. A level ten array has the cubic replaced by a quartic. While analytic root formulae (respectively associated with the Renaissance names Tartaglia/Cardano and Ferrari) are still available for both these cases, symmetric arrays beginning with level twelve demand in general a numerical solution for their resolvents.

With a view to retaining as far as possible the control of analytic root formulae, we are in the process of exploring the possibility that some sort of degradation of the array symmetry into subordinate element blocks may splinter the array polynomial into lower-order factors having all of their resolvents accessible to the classical root machinery just now suggested. Furthermore, regardless of how it is that one determines these roots, it is clear that the process of root displacement away from the unit circle, a removal designed to smoothe one's array pattern and to evade the peril of nulls, is open to computer-based phase optimization. We are in the process of examining this issue as well, and hope to report on some additional results thus gained.

Design of Low-Cost Multi-Band Squint-Free Phased Array Antenna Using TTD Subarray Technique

Reza M. Najafabadi* and Johnson J. H. Wang
Wang Electro-Opto Corporation
1335 Capital Circle
Marietta, GA 30067

Traditional phased array antennas are narrowband and suffer from beam squint as the frequency of operation changes. To overcome the beam squint problem in a wideband or multi-band operation, time shifters instead of phase shifters are generally employed to achieve true-time-delay (TTD) for the array elements. However, TTD arrays suffer from severe complexity, high cost, and low performance. Therefore, practical TTD arrays have been limited to those using the subarray technique. In this paper, it is shown that by using the subarray technique we have developed a low-cost squint-free multi-band phased array antenna using a smaller number of photonic TTD lines.

In a design for a 32-element linear array, we use 8 subarrays fed with 3-bit time shifters for gross scan up to 50° off boresight. For phase shifters in each element, we employ the newly developed 3-bit integrated SMM antenna/phase-shifters (Wang et al, IEEE International Symposium on Phased Arrays and Technology, October 1996). The integrated SMM antenna/phase-shifter has a 10:1 bandwidth, and is low-profile, conformable, and low-cost in production quantities. The phase shifters, in conjunction with the time shifters and using a special beam-steering scheme, enable the array to have adequate beam coverage over the entire scan volume with adequate crossover between adjacent beams.

Computer simulation of this antenna array shows a practical design that offers significant advantages in overcoming the high cost and complexity of TTD arrays, including those using the subarray technique. These achievements would have been impossible if not for the special SMM antenna/phase-shifters and the specific subarray architecture employed.

NULL FORMATION BY PHASE-ONLY MODIFICATION IN THE PATTERN OF A LINEAR ARRAY

Roberto Vescovo

Dipartimento di Elettrotecnica Elettronica ed Informatica
Università di Trieste
Via A. Valerio, 10 - 34127 Trieste - Italy

We examine the problem of modifying the array pattern of a linear array in such a way as to form nulls at assigned directions, by modifying only the phases of the excitations of the array elements. With reference to a linear uniform array of $N+1$ isotropic elements, consider the pattern

$$P(a_0)(u) = \sum_{n=0}^N a_{0n} \exp(jn\beta du),$$

where $a_0 = [a_{01}, \dots, a_{0N}]^T$ is the column vector of the complex element excitations, $\beta = 2\pi\lambda^{-1}$ with λ the wavelength, d is the distance between two consecutive elements, and $u = \sin\theta$, where θ is the angle from broadside. A modification ϕ_n of the phase of the n th excitation a_{0n} (for every $n = 1, \dots, N$) yields the excitation vector $a = [a_1, \dots, a_N]^T$ where $a_n = a_{0n} \exp(j\phi_n)$, and the corresponding pattern is therefore $P(a)(u) = \Re_n a_{0n} \exp(j\phi_n) \exp(jn\beta du)$. We want to find a vector $\Phi = [\phi_0, \dots, \phi_N]$ such that:

$$(a) \Re_n \phi_n^2 = \|\Phi\|_E^2 = \text{minimum}$$

$$(b) P(a)(u_m) = 0, \quad m = 1, \dots, M$$

where $\|\Phi\|_E$ is the Euclidean norm of Φ and u_1, \dots, u_M denote M assigned directions (we assume that $2M < N+1$). This problem is nonlinear, and should be solved iteratively. However, we linearize the problem assuming that the phase variations ϕ_n are small, so that $\exp(j\phi_n) \approx 1+j\phi_n$ (note that this assumption is consistent with the above condition (a)). When imposing condition (b), this linearization process leads, after some manipulations, to the matrix equation $U\Phi = v$, where U is a real $2M \times (N+1)$ matrix and v is a real vector of length $N+1$. The problem reduces then to minimize $\|\Phi\|_E$ (condition (a)) while satisfying the condition $U\Phi = v$. This problem has the solution $\Phi = U^+v$, where U^+ is the generalized inverse matrix of U . This method allowed to achieve quite satisfactory results.

A linearization approach to solve the same problem is proposed also in (H. Steyskal, *IEEE Trans. Antennas Propagat.*, 31, 163-166, 1983). However, in the latter work the pattern $P(a_0)(u)$ to be modified is assumed to be real. In the

Amplitude and Phase Adaptive Nulling with a Genetic Algorithm

You Chung*

Randy L. Haupt

University of Nevada

Department of Electrical Engineering/260

Reno, NV 89557-0153

Email:haupt@ee.unr.edu

702-784-6927

fax:702-784-6627

The genetic algorithm has proved to be useful in a wide range of antenna designs. From wire antennas to thinned arrays, these algorithms have proven to be powerful alternatives to traditional numerical optimization approaches. A genetic algorithm has also proven useful as a phase-only adaptive nulling algorithm. This approach resulted in relatively fast placement of nulls using only the beam steering phase shifters.

This presentation takes the results in extends the phase-only adaptive nulling results one step further by introducing adjustable amplitude weights as well. The added amplitude weight could be in the form of an attenuator but could also be implemented in the software of a digital beamforming antenna array. In the examples presented, we use a continuous parameter genetic algorithm rather than the traditional binary form of the algorithm. Both phase shifters and attenuators take away power from the main beam of the antenna. Therefore, it is imperative to limit the range of amplitude and phase values for placing the nulls. This inherent main beam constraint will be explained and outlined in the talk.

We present results of convergence speed of the algorithm, signal to noise ratios, and null depths for linear arrays of various sizes. The use of amplitude weights as well as phase weights in the adaptation process overcomes some of the series detrimental side effects of phase-only nulling, such as placing a null in quantization lobes and at symmetric locations about the main beam. Convergence speed of this algorithm is far superior to random searches and gradient approaches. Results between phase and amplitude and phase-only nulling are compared. In addition, these results are compared with those from random search and gradient methods.

ADAPTIVE UNEQUALLY SPACED PHASED ARRAYS

Srikanth Nagraj, Sheeyun Park and Tapan K. Sarkar
Department of Electrical and Computer Engineering
Syracuse University, Syracuse, New York 13244-1240

ABSTRACT: The objective of the presentation is to illustrate how to process data in the presence of strong jammer and clutter utilizing non-uniformly spaced phased arrays. Typically, one can use a circular, hexagonal or a cross for more efficient utilization of the aperture. The second possibility is that one may be dealing with a non planar phased array not by choice but due to vibration of the aircraft structure or the sonobuoys bobbing up and down in the ocean or a towed phased array. In these situations it is desirable to perform adaptive processing to enhance the signal in the presence of strong clutter and jammers. Conventionally, the analysis procedures primarily deal with uniformly spaced linear phased arrays and practically nothing is available in the published literature on how to perform adaptive processing utilizing non-planar and non-uniformly spaced arrays. The talk will outline a direct data domain approach for the extraction of the desired signal adaptively in the presence of strong signal and clutter. Since it is a least squares approach the adaptive procedure provides the best estimate. The adaptive process is carried out utilizing the conjugate gradient method and hence it is possible to implement the algorithm on a signal processing chip to adaptively enhance signals received by a non-uniformly spaced array in the presence of strong jammer, clutter and thermal noise. In contrast to a covariance based approach the direct data domain approach is fast and accurate. In addition, for a covariance based statistical methods which is the current state of the art, it is difficult if not impossible to handle signals from non-uniform arrays as it is difficult to form an estimate of a uniformly sampled covariance matrix from an unequally spaced data sets. Results will be presented utilizing a circular, hexagonal and a sinusoidally modulated array.

Electromagnetic Measurement Techniques

D. A. Hill and C. C. Courtney

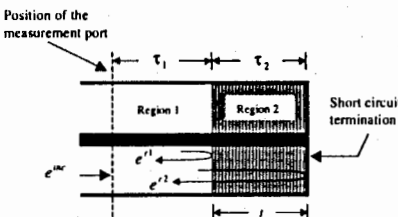
One-port, Time Domain Measurement of the Permittivity and Permeability of Materials.....	228
<i>C. Courtney*, W. Motil, Voss Scientific, USA</i>	
Analysis of Sample-to-wall Gaps in the Electromagnetic Characterization of Materials in Rectangular Waveguide Field Applicator Measurements.....	229
<i>M. J. Havrilla*, D. P. Nyquist, Michigan State University, USA</i>	
Error Analysis of the Open-structure Resonant Technique for Measuring Dielectric Properties	230
<i>W. R. Humber*, Air Force Research Laboratory, USA, W. R. Scott, Jr., Georgia Institute of Technology, USA</i>	
Radiated Field Coupling to Signal Cables	231
<i>Z. Pantic-Tanner*, M. Mack, M. Wilson, San Francisco State University, USA</i>	
Synthesis of Wideband Antenna Patterns from Narrowband Measurements	AP
<i>M. A. Mitchell*, R. L. Howard, R. G. Hemphill, Georgia Tech Research Institute, USA, J. K. Mulcahey, Raytheon Company, USA</i>	
Rapid Diagnostic Imaging Applications of Advanced MST Probe Arrays.....	232
<i>B. Cown*, SATIMO, Inc., USA, P. Garreau, E. Beaumont, SATIMO (SARL), France, J. Estrada, SATIMO, Inc., USA</i>	
A Plane-wave Integral Representation for Fields in Reverberation Chambers.....	233
<i>D. A. Hill*, National Institute of Standards and Technology, USA</i>	
Field Distribution in the Microwave Processing of a Ceramic Fiber.....	234
<i>N. D. Terril*, W. A. Davis, Virginia Polytechnic Institute and State University, USA</i>	
A System for Unobtrusive Measurement of Surface Currents	AP
<i>P. H. Harms*, J. G. Maloney, M. P. Kesler, E. J. Kuster, Georgia Tech Research Institute, USA, G. S. Smith, Georgia Institute of Technology, USA</i>	
Charged Beam Excitation and Pulsed RF Coupling in the Dielectric Wakefield Accelerator	235
<i>M. E. Conde, W. Gai, R. S. Konecny, J. G. Power, P. Schoessow, P. Zou, Argonne National Laboratory, USA, T. Won*, Illinois Institute of Technology, USA</i>	

One-port, Time Domain Measurement of the Permittivity and Permeability of Materials

Clifton Courtney * and William Motil
Voss Scientific
418 Washington St. SE
Albuquerque, NM 87108
(505) 255-4201
e-mail: vosssci@vosssci.com

Single port, frequency domain measurements to determine the electrical characteristics of a material are often made for liquids or amorphous solids (dirt, biological material) that will not maintain a definite shape. Before yielding the desired property, the corresponding data reduction procedure requires an assumption of the value of either the permittivity or permeability (often one chooses $\mu_r = 1$). To recover the complete material characteristic (ϵ_r, μ_r), a pair of two-port, frequency domain measurements are needed, s_{11} and s_{21} . This can involve intricate sample and test cell preparation. This paper describes a one-port, time domain measurement technique that can yield the broadband, frequency dependent, complex values of permittivity and permeability of a sample material. The measurement procedure is accomplished as follows.

A coaxial line, possibly oriented vertically, is depicted in the figure. The line is loaded with a sample material (Region 2) and terminated with a short circuit. A signal input terminal is located at one end, and a measurement port is located between the input terminal and the front interface of the sample.



A pulse is introduced at the excitation port and allowed to propagate to the interface. The pulse is partially reflected at the sample material interface, and partially transmitted. The transmitted portion travels to the end of the line and is reflected by the terminating short circuit. This waveform travels back toward the interface and is partially transmitted forming the second observed reflection, and partially reflected back toward the short circuit. The incident ($e^{inc}(t)$), first reflected ($e^{r1}(t)$) and second reflected ($e^{r2}(t)$) waveforms are recorded at the measurement port. A formulation of the frequency domain parameters s_{11} and s_{21} for the "virtual" two-port system (the original line and its image) is computed from the time domain partial returns. A description of the data processing procedure is given, the governing equations are presented, and the associated waveforms and resulting material values for an example are presented.

Analysis of Sample-to-Wall Gaps in the Electromagnetic Characterization of Materials in Rectangular Waveguide Field Applicator Measurements

Michael J. Havrilla* and Dennis P. Nyquist

Department of Electrical Engineering
Michigan State University
East Lansing, Michigan 48824

In rectangular waveguide materials characterization measurements, gaps commonly occur between the sample and waveguide walls as a result of imprecise machining of the sample material. These gaps can influence the accuracy of measured constitutive parameters because higher order modes are excited, thereby changing the ideal wave impedance and interfacial reflection and transmission coefficients. The purpose of this investigation is to accommodate these errors under small gap conditions.

Sample-to-wall gaps are studied by regarding the waveguide as inhomogeneously filled in the cross-sectional plane with LSE (left/right gaps) or LSM (bottom/top gaps) propagation modes supported in the sample/gap region. Resulting characteristic equations for the corresponding propagation constants are solved numerically to determine shifts from the ideal TE_{10} propagation constant of a uniformly filled guide. A modal analysis is used to obtain (under small gap conditions) approximate expressions for the wave impedance and interfacial reflection and transmission coefficients. This is done by considering a single TE_{10} mode incident upon, and reflected from, the sample and only a single LSE or LSM mode inside the sample region. Expressions for the scattering parameters are obtained using a wave-processing (or wave matrices) approach, and are found to be

$$S_{11} = \frac{R(1-P^2)}{1-R^2P^2} \quad , \quad S_{21} = \frac{P(1-R^2)}{1-R^2P^2} \quad , \quad P = e^{-\gamma l}$$

where P is the one way phase delay and attenuation through the sample region, γ is the propagation constant of the lowest order LSE or LSM propagating mode, and l is the thickness of the sample. The interfacial reflection and transmission coefficients, R and T , are obtained through continuity of the tangential components of the electric and magnetic fields across the interface and by applying an appropriate testing function, resulting in the following set of equations

$$1+R = T \frac{\int_{cs} ds e_y^{Iselm}(x,y) e_y^{10}(x)}{\int_{cs} ds e_y^{10}(x) e_y^{10}(x)} \quad , \quad 1-R = T \frac{\int_{cs} ds \frac{e_y^{Iselm}(x,y)}{Z_{Iselm}(x,y)} e_y^{10}(x)}{\frac{1}{Z_{10}} \int_{cs} ds e_y^{10}(x) e_y^{10}(x)} \quad (LSE/LSM MODE)$$

Theoretical and experimental results will be given for materials having both low and high permittivities and permeabilities for several gap geometries. These results will be compared with other gap models.

Error Analysis of the Open-Structure Resonant Technique for Measuring Dielectric Properties

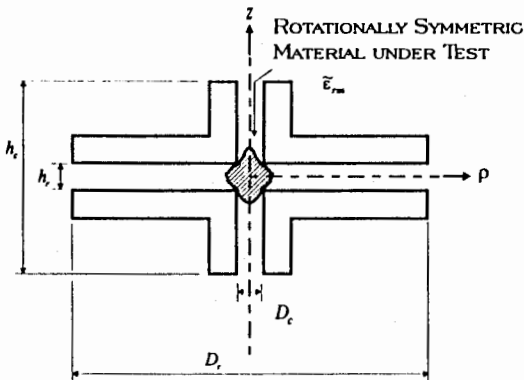
William R. Humbert*

Air Force Research Laboratory
Electromagnetics Technology
Hanscom AFB, MA. 01731

Waymond R. Scott, Jr.

Georgia Institute of Technology
School of Electrical and Computer Engineering
Atlanta, GA. 30332

Various errors that may occur in dielectric measurements using the open-structure resonant technique are presented. The measurement fixture used in this technique is rotationally symmetric and is shown in the figure below (cross section in $\rho - z$ plane). The fixture consists of two metallic plates placed opposite each other, where each plate has a center opening leading to a tubular section. In this configuration, the fixture has both circular and radial waveguide regions. At the junction of these waveguide regions is the core of the resonator. The material or a portion of the material to be measured is positioned within the core of the resonator. The resonant frequency and quality factor are measured. Using these measurements along with a finite-element model of the fixture containing the material under test, the relative permittivity and loss tangent of rotationally symmetric materials can be determined. The technique has been successfully used to measure a wide range of materials in both dielectric properties and material geometry. Measured results show the technique to be very accurate.



A sensitivity analysis will be presented which quantifies the errors associated with inaccurate measurements of the critical dimensions, h_r and D_c . Also, an investigation of the effect of air gaps on measured results will be presented. Finally, results will be presented which support the treatment of the right-angle metallic corner and the open-ended waveguide regions in the finite-element model.

RADIATED FIELD COUPLING TO SIGNAL CABLES

Z. Pantic-Tanner, M. Mack, and M. Wilson*

San Francisco State University

San Francisco, CA 94132

(zpt@sfsu.edu)

F. Gisin

Silicon Graphics

Mountain View, CA 94039

M. Salazar-Palma

Polytechnic University of Madrid

Madrid, Spain 28040

Electric and magnetic fields produced by electrostatic discharge, sparking, RF transmitters, and other sources, can cause significant susceptibility problems in computer, airline or automotive industry, and in sensitive electronics equipment. One of the main mechanisms of coupling is through signal and power cables that act as pick up probes. Coupling of electromagnetic fields to parallel wire transmission lines has been studied by a number of authors both in the frequency and in the time domain (C. R. Paul, EMC-18, 183-190, 1976; A. K. Agrawal et al., EMC-22, 119-129, 1980; E. S. M. Mok, and G. I. Costache, Proc. IEEE Int. Sym. on EMC, 80-84, 1990; P. Naylor and C. Christopoulos, Int. J. Num. Modelling, 227-240, 1990).

In this paper we revisit the coupling problem from the point of view of the emerging susceptibility measurement technique based on a GTEM cell use. Equipment under test (EUT) is rotated through three orthogonal positions and the corresponding measurement data are taken. In order to relate these data to the open area test site (OATS) measurements, the contributions of the portions of the signal and power cables that rotate with the EUT as well as those that stay fixed have to be evaluated. Accordingly, we examine endfire, sidefire, and broadside excitations. A comprehensive study of different mechanisms of coupling of a uniform plane EM wave to signal cables, such as twin-pair and twisted pair lines is performed. Contributions of the normal magnetic, transverse electric, and longitudinal electric fields to the induced voltages at the near and far end of the line are evaluated. Three different models are employed for numerical analysis: lumped-parameter, distributed-parameter, and antenna model. A lumped parameter model, based on L, Γ , or Π configuration, is valid for lower frequencies and yields a simple analytical solution that is suitable for estimation purposes. For somewhat higher frequencies a cascade of lumped-parameter cells is used to more accurately represent resonant behavior of the cable. The effect of the basic lumped cell configuration (L, Γ , or Π) on the induced voltages is determined. For high frequencies a distributed-parameter model is used; the analysis is performed by implementing distributed voltage and current sources into a conventional transmission line model. For very high frequencies an antenna model is employed; numerical analysis is accomplished by MOM and FEM. Finally, actual measurements are performed in a GTEM cell for all three orthogonal excitations and the data compared with the obtained numerical results.

RAPID DIAGNOSTIC IMAGING APPLICATIONS OF ADVANCED MST PROBE ARRAYS

B. Cown*, Ph. Garreau**, E. Beaumont**, and J. Estrada*

*SATIMO, Inc., Suite E-116, 1318 Chandler Court, Acworth, GA, 30102 USA

**SATIMO (SARL), "Le Pin", rue de la Terre de Feu, Z. A. de Courtabœuf, 91952, Les Ulis, France

This paper describes applications of probe arrays based on the Advanced Modulated Scattering Technique (A-MST) to accomplish rapid diagnostic imaging of 1) anechoic chambers, 2) microwave antennas, 3) subsurface objects, and 4) penetrable materials.

The technical feasibility of performing fast diagnostic testing of large anechoic chambers by using A-MST probe arrays in conjunction with the MUSIC imaging algorithm was demonstrated based on the outcome of experiments conducted at the compact range/anechoic chamber facility at the Centre Nationale de Recherches Spatiales (CNES) in Toulouse, France, under the sponsorship of the U.S. Air Force. In particular, a wideband (1.5 GHz-6.0 GHz) linear array of 64 dual-polarized modulated scattering probes was installed on the 7-axis positioner located in the quiet zone of the CNES compact range reflector, and the complex electric field existing at the location of each of the 64 probes along the 5.7-foot length of the array was measured in less than 10 milliseconds. A special version of the MUSIC code was developed and utilized to obtain high resolution images of the chamber. An Automated Field Probe System employing A-MST probe arrays is under development for installation at the Benefield Anechoic Facility at Edwards, AFB, California.

The A-MST probe array described has also been used to perform rapid diagnostic testing of a panel of the ERS-2 satellite antenna. (ERS-2 panel furnished courtesy of the European Space Agency and the Ericsson Company). The ERS-2 antenna panel is composed of slotted wave guides distributed on a surface of 1 meter wide by 1 meter high, and it operates in C-band. The requisite near-field (NF) measurements were conducted in 15 seconds at the SATIMO NF test facility in Courtabœuf, France. FFTs were utilized to perform the back projection onto the aperture plane of the ERS-2 panel.

A variety of subsurface objects have been successfully imaged in nearly-real time by a "Microwave Camera" employing a linear array of 32 dual-polarized modulated scattering probes operating over the 0.4 GHz to 1.2 GHz frequency range. The range of applications has included water channels in snow as well as buried metallic and plastic objects.

MST probe arrays have been used to perform NF imaging measurements to detect and image defects in penetrable microwave composite materials, paper, and wood, and to determine moisture content in paper and food products.

The A-MST probe array measurement systems, measurement protocols, validation results, and on-going research and development activities will be presented and discussed at the symposium

A Plane-Wave Integral Representation for Fields in Reverberation Chambers

David A. Hill
Electromagnetic Fields Division
National Institute of Standards and Technology
Boulder, CO 80303
USA
dhill@boulder.nist.gov

Reverberation chambers (also called mode-stirred chambers) are experiencing increased use for radiated emissions and immunity measurements. They are electrically large, multimoded cavities that use either mechanical stirring (P. Corona, G. Latmiral, and E. Paolini, *IEEE Trans. Electromag. Compat.*, 22, 2-5, 1980) or frequency stirring (D. Hill, *IEEE Trans. Electromag. Compat.*, 36, 294-299, 1994) to create a statistically uniform field. Deterministic and statistical mode theories have been used to analyze reverberation chambers, but they are not convenient for predicting the response of a reference antenna or a test object in the chamber environment.

The purpose of this paper is to present a plane-wave, integral representation for the fields that satisfies Maxwell's equations and also includes the statistical properties expected for a well-stirred field. The statistical nature of the fields is introduced through the plane-wave coefficients that are taken to be random variables with fairly simple statistical properties. The representation uses only propagating plane waves (for all real angles); so it is fairly easy to calculate the responses of test objects or reference antennas. Ensemble averages can be derived, and these averages can be used to predict measured values averaged over stirrer position. For positive quantities, such as received power, ensemble (stirrer) averages are typically equivalent to averages over plane-wave incidence and polarization. Comparisons of calculated and measured responses will be shown for several test objects.

The same integral representation can be used to derive probability density functions of several field quantities and antenna and test-object responses. Starting with the simple statistical properties of the plane-wave coefficients, the maximum-entropy method (which yields the least-biased results) is used to derive the probability density functions of the electric and magnetic fields and antenna and test object responses. The probability density functions are in agreement with previous results for field magnitude and received power based on the central limit theorem (J.G. Kostas and B. Boverie, *IEEE Trans. Electromag. Compat.*, 33, 366-370, 1991), but are more general in scope.

FIELD DISTRIBUTION IN THE MICROWAVE PROCESSING OF A CERAMIC FIBER

N.D. Terril* and Prof. W.A. Davis

The Bradley Department of Electrical Engineering
Virginia Polytechnic Institute and State University
Blacksburg, VA 24061-0111

Microwave processing of ceramics can lead to thermal runaway in materials having a temperature dependent dielectric constant. Controlled heating of the material may be achieved by manipulating the field to which it is exposed. Recent experiments at the Los Alamos National Laboratory observed thermal runaway while investigating the heating of a ceramic fiber fed continuously through a TE_{101} mode cavity. Microwave energy was coupled to the cavity from a fundamental TE mode waveguide through a rectangular aperture.

The purpose of this paper is to model the field interaction effects in the microwave heating of a ceramic fiber to investigate possible ways of controlling thermal runaway. Maxwell's equations for the fields within the cavity will be solved, including the interaction of the fiber and an arbitrarily shaped aperture. We will explore any potential distribution effects on the field caused by shaping the aperture. The thermal coupling effects due to the temperature dependent dielectric constant of the fiber will also be discussed.

To determine the interaction effect with the fiber and potential runaway control, we investigate the interaction of the aperture, fiber, and cavity properties in the field solution. The mathematical model consists of a truncated set of TE and TM modes related at the aperture and fiber interfaces. The fields are solved at the aperture interface using a Green's function type approach. The electric field in the aperture is expressed as an independent set of truncated aperture modes found from a numerical Green's function formulation. These aperture modes are matched to the cavity and incident modes in the vicinity of the aperture. The fiber is assumed to be a cylindrical rod with a sufficiently small cross-section, allowing us to approximate the tangential electric fields as continuous. The rod is then treated as a line source with a current proportional to the equivalent volume current density and the cross-sectional area. This equivalent line source is used to relate the fields at the fiber interface. The relationship of this work to the parallel heat transfer effort will be discussed.

CHARGED BEAM EXCITATION AND PULSED RF COUPLING IN THE
DIELECTRIC WAKEFIELD ACCELERATOR

M.E. Conde, W.Gai, R.S.Konecny, J.G.Power, P.Schoessow, P. Zou
Argonne National Laboratory
Argonne, Illinois 60439

T. Wong*
Illinois Institute of Technology
Chicago, Illinois 60616

We report on a novel RF source capable of producing high peak power, short duration RF pulses to be used for particle acceleration. An acceleration experiment currently underway at the Argonne Wakefield Accelerator (AWA) uses an electron beam that is both short in duration (20 ps FWHM) and high in charge (65 nC) to excite an acceleration compatible mode (TM 01) in a dielectric lined, cylindrical waveguide. The RF pulse excited by this electron beam is termed a wakefield and is used at the AWA to accelerate a second electron beam in either a collinear method or a parallel method. In the collinear method, the second electron beam trails directly behind the first beam and can either be accelerated or decelerated depending on its phase in relation to the RF pulse. In the parallel method, the RF pulse is coupled out of the dielectric lined waveguide and transported through a metallic rectangular waveguide into a second structure specifically designed to optimize the acceleration gradient for the second electron beam.

The parallel method of acceleration is also of interest as a novel RF source since once the energy is coupled into the rectangular waveguide it can be used for purposes other than particle acceleration. The excited RF pulse is magnetically coupled out of the cylindrical dielectric lined waveguide through a slot on its sidewall into a metallic rectangular waveguide operating in the TE 10 mode. The characteristics of the RF pulse generated in the dielectric lined waveguide is controlled through its geometry, the dielectric constant of the lining and the structure of the electron beam. Analytic calculations showed that this method to be capable of producing short RF pulses (1-10 ns) at high peak power (10MW - 1GW) for the range of parameters under study. Bench top, CW measurements characterizing the coupling between the dielectric lined waveguide and the metallic rectangular waveguide using a network analyzer as well as proof of principle results using charged particle beam excitation of the high power short RF pulse will be presented.

Medical Applications of Electromagnetic Fields

K. S. Nikita and R. W. Scharstein

Blackbody Radiation from a Stratified, Lossy Dielectric Sphere..... 238
R. W. Scharstein, University of Alabama, USA*

Using FDTD in the Design of Body-implanted Devices that Radiate Radio-frequency Energy 239
R. Luebbers, Pennsylvania State University, USA, J. Schuster, Remcom Inc., USA*

Modeling of a New Generation of Planar Applicators Used for Medical Applications 240
C. Vanoverschelde, V. Thomy, L. Dubois, M. Chive, J. Pribetich, I.E.M.N. , France*

Model of Influence Electromagnetic Signal on the Oscillator Neural Network 241
V. G. Spitsyn, N. Spitsyna, Tomsk State University, Russia*

Incoherent Power Feeding of the Array Applicator Composed of Coaxial-slot Antennas for
Interstitial Microwave Hypothermia 242
L. Hamada, I. Dean, K. Saito, K. Ito, Chiba University, Japan*

BLACKBODY RADIATION FROM A STRATIFIED, LOSSY DIELECTRIC SPHERE

ROBERT W. SCHARSTEIN

Electrical Engineering Department
University of Alabama
Tuscaloosa, AL 35487-0286
phone 205-348-1761, fax 205-348-6959
e-mail rscharst@ualvm.ua.edu

An engineering model of the blackbody radiation from piecewise homogeneous, lossy dielectrics is implemented for the canonical spherical geometry. The mean-square electric field external to a three-layered ball (or head model) is computed via the usual fluctuation dissipation theorem, in combination with a simplifying use of reciprocity and Poynting's theorem. At a fixed, narrow frequency band, the complex dielectric constant and absolute temperature of each layer are input parameters, as are the electrical radii of the layers. The resultant second-order statistics are given in terms of convergent series of spherical wave functions. One advantage of this model for a finite body, in contrast to planar stratifications that are necessarily of infinite extent, is its natural incorporation of realistic proximity effects between the distributed source and receiver.

Two limiting cases are examined and serve as a partial check on the accuracy of the calculations. The far field mean-square value, which is proportional to the radiometric measure of brightness temperature, is compared with published data for a homogeneous sphere. A separate treatment of the high loss case, where the dominant diffusive nature of the internal fields can be exploited, is expected to agree with the full wave solution in some "transition region" of intermediate loss. This simple geometry serves as a model to study such radiation and shielding effects between the various layers of skin, muscle, fat, and bone that may be at different temperatures in a living organism.

Typeset by *AMS-TEX*

Using FDTD in the Design of Body-Implanted Devices that Radiate Radio-Frequency Energy

Raymond Luebbers* and Joseph Schuster

Department of Electrical Engineering

The Pennsylvania State University

University Park, PA 16802

and

H. Scott. Langdon

Remcom Inc.

Calder Square Box 10023

State College, PA 16805

Implantable devices such as pacemakers have traditionally been designed for input/output of data using very low frequencies. For the pacemaker, re-programming of the device may be necessary, and stored data relating to cardiac events may be communicated to the physician. Other applications include implanted drug delivery devices and biological monitoring devices.

The exterior-interior communication is often accomplished using magnetic coils at low frequencies. While this provides basic function, the data rate is very slow. Also, the magnetic coil must be placed on the skin while data is being transferred. Communication at radio frequencies would allow much higher data rates and remote location of the external communication antenna/device.

Design considerations include the frequency of operation, antenna, and location inside the body. The interaction of the antenna with the enclosing biological tissue is complicated. Determining an optimum frequency for a given device size and location within the body is not straightforward.

There is an extensive literature on the application of The Finite Difference Time Domain (FDTD) method to the determination of Specific Absorption Rate (SAR) and antenna radiation characteristics for transmitting devices located external to the body. In particular, numerous papers have been published on applying FDTD to determine SAR levels for cellular phones and other personal communication devices.

However, there has been little published on applying FDTD to implantable devices, which is the topic of this paper. In particular, effects of frequency, antenna shape, insulation, and location within the body on the input impedance, efficiency, and radiation gain patterns will be presented.

MODELING OF A NEW GENERATION OF PLANAR APPLICATORS USED FOR MEDICAL APPLICATIONS.

C. VANOVERSCHELDE, V. THOMY, L. DUBOIS, M. CHIVE, J. PRIBETICH*.
I.E.M.N. - Avenue Poincaré - B.P. 69 -
59652 VILLENEUVE D'ASCQ CEDEX - FRANCE

A large number of microwave devices have been designed and tested for medical applications (and more particularly hyperthermia). Among these devices, we are interesting since more than a decade, in the study of external planar applicators. We present in this paper the results concerning the last generation of planar applicators we have developped in order to heat large areas.

The first kind of structure consists of a planar applicator with several parallel patches (length 6.25 cm, width 3 mm, spacing between each patch 10 mm). The feeding of the patches is obtained by use of coaxial cables through a power divider. We have the possibility to feed in phase the different patches either all together or in alternate mode : only the odd patches are fed during a short time, then the even patches are fed during the following period and this technique is started again. So, it is possible to heat either a large area or to heat preferentially a given zone and so, to control the depth and the width of the heated zone.

The next studied structure is the planar microstrip-microslot applicator : it consists of annular aperture (average radius R_m and a width W) opened in the ground plane of a microstrip line. Different structures have been realized variing the radius R_m and a width W of the aperture and also the length of the microstrip. This applicator will be used to make a adjustable bees' nest array in order to heat in depth large tumoral areas of any shape. Both kinds of applicators are constructed on a substrate of relative permittivity $\epsilon_r = 4.9$ and of thickness $h_1 = 1.58$ mm.

The modeling of the studied structures is based on the Spectral Domain Approach (S.D.A.). In fact, this model allows to determine in a short time the dimensions of the applicator in order to obtain the expected heating and the S_{11} parameter which gives a good level of adaptation of the applicator. Experimental measurements have also been carried out on phantom (polyacrylamide gel) models of human tissues: measurement of the return loss (S_{11} parameter), determination of the energy distribution and of the thermal mapping.

The experimental measurements obtained at the heating frequency $F = 915$ MHz are according at the wanted effects. With these new applicators, we observe an increase of the power deposition diagram (as compared to previous applicators with a single patch) involving an increase of the therapeutic heated zone.

Model of Influence Electromagnetic Signal on the Oscillator Neural Network

V.G. Spitsyn, N.V. Spitsyna

Siberian Physical and Technical Institute Tomsk State University,
Revolution square, 1, Tomsk, 634050, Russia,
E-mail: spic@elefot.tsu.tomsk.su

1. Introduction. The purpose of this work is development of a numerical model of interaction of electromagnetic signals with oscillator neural networks and investigation of the mechanisms this interaction.

2. Method. The method of stochastic modeling is applied for the solve of this task (V.G. Spitsyn, Electromagnetic Waves and Electronic Systems, 2, 45-49, 1997). Every act interaction of signal with oscillator is accompanied by displacement the frequency of signal and of oscillators vibrations. The model is suggested, which describe transfer of signals in three dimensional oscillator neural network with stochastic connections. Every oscillator has possibility connection with all another oscillators. It agrees with Brindly's and Marr's idea (D. Marr, Proc. Roy. Soc. Lond., B176, 161-234, 1970) about chance disposition inter - neural networks. The process of interaction of signals with oscillators, disposed in spherical region is investigated.

3. The results of calculation interaction electromagnetic signals with oscillator neural network. The results of calculaton demonstrate, that after interaction of harmonic signal with oscillators, having monochromatic spectrum of vibrations, additional harmonics appear in spectrum of oscillators' vibrations. The amplitude of this harmonics is decreased with growth number of acts interaction.

Influence of harmonic signal on the oscillator neural network with disperse of frequency oscillators' vibrations leads to decreasing of width of frequency spectrum of oscillators' vibrations and in the limit to monochromatization its form. Therefore we may do the conclusion about then that in process of function oscillator neural network with external electromagnetic influence the synchronization of oscillators, taking part in process stochastic transfer of signals, takes place.

4. Conclusion. In this work a model interaction of electromagnetic signals with oscillator neural network is offered. The results of modeling influence of harmonic signal on the oscillator neural network show that decreasing of width of frequency spectrum of oscillators' vibrations and monochromatization its form takes place.

Incoherent Power Feeding of the Array Applicator Composed of Coaxial-Slot Antennas for Interstitial Microwave Hyperthermia

*Lira HAMADA†, Irena DEAN†, Kazuyuki SAITO†
and Koichi ITO‡

†Graduate School of Science & Technology,
‡Department of Electrical & Electronics, Faculty of Engineering
Chiba University
1-33 Yayoi-cho, Inage-ku, Chiba-shi, 263-8522 Japan
TEL: 81-43-290-3326 FAX: 81-43-290-3327
e-mail: hamada@antenna.nd.chiba-u.ac.jp

Hyperthermia is one of the modalities for cancer treatment, which heat the tumor or target cancer cell up to the therapeutic temperature (over 42-43 deg. C.) without damaging surrounding normal tissues. In the past few decades, combination to another well-established modalities such as the radiotherapy or the chemotherapy have been successfully studied from both sides of the medicine and the engineering.

The authors have been studying on the coaxial-slot antenna for interstitial microwave hyperthermia. This antenna is designed for the regional heating of large-volumed and deep-seated tumors that can not be controlled by another cancer treatment only. The antenna is consisted of a very thin semi-rigid coaxial cable which outer diameter is approximately 1 mm, to reduce the burden on the patient under treatment. The tip of the cable is short-circuited and several numbers of ring slots are cut on the outer conductor. Changing the number and location of these slots can vary the heating patterns of the antenna. The antenna is embedded into the catheter, a thin plastic tube for medical safety, and is usually applied as an array applicator inserting several antennas into the tumor.

So far the authors have revealed the characteristics of the antenna and the array applicator fed coherently from single power generator through power divider. In this paper, to obtain more uniform and enlarged heating region, the incoherent power feeding from multiple power generators to the array elements is examined by both experimental and theoretical studies. The comparison of the incoherent operation with the coherent one will be made in the SAR (Specific Absorption Rate) and the simulated temperature distributions inside the human body.

Wavelet Methods

D. R. Wilton and R. D. Nevels

Recovery of Signal from Transient Responses Contaminated by Gaussian White Noise Based on Orthogonal Bases of Compactly Supported Wavelets in Frequency Domain.....	AP
<i>J. Dan*, X. Shanjia, Univ. of Science and Technology of China, China, W. Xianliang, L. Shixiong, Anhui University, China</i>	
Analysis of Truncated Periodic Array using Two-stage Wavelet-packet Transforms for Impedance Matrix Compression	244
<i>Y. Shifman*, Z. Baharav, Y. Leviatan, Israel Institute of Technology, Israel</i>	
Impedance Matrices Generated by Discrete Wavelet Transformations with Semi-orthogonal Wavelets	245
<i>R. Miller*, R. Nevels, Texas A&M University, USA</i>	
Application of Adaptive Wavelet Packet Basis to Solving Electromagnetic Integral Equations.....	AP
<i>H. Deng*, H. Ling, University of Texas at Austin, USA</i>	
Moment Method Analysis of a Loop Array using Wavelet Expansions.....	AP
<i>Y. Ojiro*, K. Hirasawa, University of Tsukuba, Japan</i>	

Analysis of Truncated Periodic Array Using Two-Stage Wavelet-Packet Transforms for Impedance Matrix Compression

Y. Shifman, Z. Baharav and Y. Levitan

Department of Electrical Engineering

Technion - Israel Institute of Technology

Haifa 32000, Israel.

e-mail: levitan@ee.technion.ac.il

A novel method of moments procedure is applied to the problem of scattering by metallic truncated periodic arrays. In such problems, the induced current shows localized behavior within the unit cell and at the same time exhibits cell-to-cell periodicity. In order to select a set of expansion functions that may account for such a behavior, a two-stage basis transformation has been applied to a pulse basis which is used for expanding the current over the scatterer. At the first stage of this transformation, the pulse functions within each of the unit cells are independently transformed to an ordinary wavelet basis. Respective wavelet functions belonging to different unit cells are, in turn, grouped together and re-transformed to reveal the periodicity of their coefficients. The desirable expansion functions are then iteratively selected from this newly constructed basis to form a compressed impedance matrix, via the IMC method (Z. Baharav and Y. Levitan, "Impedance Matrix Compression with the Use of Wavelet Expansions", *Microwave and Optical Technology Letters*, Vol. 12, No. 3, pp. 268-272, August 1996; Z. Baharav and Y. Levitan, "Impedance matrix compression (IMC) using iteratively selected wavelet basis for MFIE formulations", *Microwave and Optical Technology Letters*, Vol. 12, No. 3, pp. 145-150, June 1996).

The new approach has been successfully applied to the problem of TM two-dimensional scattering by a truncated periodic array of conducting strips. The compression ratios obtained in this manner are higher than those achieved using a basis constructed via an ordinary single-stage wavelet transform. An even higher compression is attained by considering, in addition, functions that reveal array-end related features and iteratively selecting the expansion from an overcomplete dictionary. The advantages of using this overcomplete dictionary of wavelet-packet expansion functions are demonstrated as well.

Impedance Matrices Generated by Discrete Wavelet Transformations with Semi-Orthogonal Wavelets.

Richard E. Miller* and Robert D. Nevels
Department of Electrical Engineering
Texas A&M University
College Station, Texas 77843-3128

It has previously been shown that by using wavelets as the basis set for the moment method solution of electromagnetic integral equations, the moment impedance matrix can be made more sparse than it is with the classical pulse basis. Sparsity of the wavelet impedance matrix is obtained by selecting an error criterion whereby any elements below a fixed threshold are set to zero. The majority of previous research has focused on orthogonal wavelet sets and the semi-orthogonal spline wavelet. In this paper, it will be shown that the dual semi-orthogonal wavelet yields a remarkably sparse moment impedance matrix.

The moment method matrix equation is given by

$$Zi = v \quad (1)$$

where Z is the pulse impedance matrix, i is the unknown current vector and v is the source vector. The wavelet impedance matrix is generated by the Discrete Wavelet Transform (DWT) which can be incorporated into (1), giving

$$TZT^T(T^T)^{-1}i = Tv \quad (2)$$

where T is the wavelet transformation matrix and T^T is the transpose operator. The semi-orthogonal wavelet transform matrix is not an orthogonal matrix, $T^{-1} \neq T^T$, therefore, the solution vector i is not found by performing an inverse DWT. Instead the transpose of the wavelet transformation matrix is used, which gives

$$i = T^T(TZT^T)^{-1}Tv \quad (3)$$

This becomes important for semi-orthogonal wavelets, since the reconstruction and decomposition sequences have different lengths, as opposed to orthogonal wavelets that have equal length sequences. The use of short sequences decreases the numerical execution time. The semi-orthogonal wavelet has an infinite set of decomposition coefficients and a finite set of reconstruction coefficients. The dual semi-orthogonal wavelet uses the finite set of coefficients for decomposition and the infinite set of coefficients for reconstruction.

As given in equation (3), if the DWT is used with the dual semi-orthogonal wavelet, only the finite coefficient set is needed. The impedance matrices generated for plane wave excitation of a two-dimensional finite width flat plate scatterer by the semi-orthogonal wavelet, dual semi-orthogonal wavelet and orthogonal wavelet will be compared.

Special Session: Microelectromechanical Systems, MEMS

P. L. E. Uslenghi

MEMS Technologies for Low Power Radio-on-a-chip	248
<i>A. P. Pisano*, DARPA / ETO</i>	
Micromachining Techniques for High-frequency Circuits	249
<i>L. P. B. Katchi*, G. M. Rebeiz, University of Michigan, USA</i>	
Study of High Frequency Circuits on Micromachined Reconfigured Substrates.....	250
<i>R. F. Drayton*, J. Wang, University of Illinois, USA</i>	
An Efficient Field Solver for Micro-electromechanical Systems (MEMS)	251
<i>V. Veremey*, R. Mittra, Pennsylvania State University, USA</i>	
Submillimeter Cylindrical Filters and Antennas Fabricated with Cylindrical LIGA	252
<i>A. D. Feinerman*, University of Illinois, USA, Y. W. Kang, D. C. Mancini, Argonne National Laboratory, USA</i>	
Biological Microchips: Properties and Applications.....	253
<i>A. Mirzabekov*, Engelhart Institute of Molecular Biology, Russia</i>	

MEMS TECHNOLOGIES FOR LOW POWER RADIO-ON-A-CHIP

Albert P. Pisano
MEMS Program Manager, DARPA/ETO
Arlington, VA 22203-1714, U.S.A.

Beginning with a brief review of MEMS fabrication technologies, this talk will show how MEMS may replace not only discrete passive components of radios, but also complete sub-circuits. In so doing, the radio designer may achieve performance improvement, power reduction, and weight reduction all simultaneously. Combined with recent results from the microwave analog front-end technology program (MAFET) and with integrated, low-power, non-volatile data storage, MEMS technology is poised to revolutionize RF communication as well as telemetry systems.

MICROMACHINING TECHNIQUES FOR HIGH-FREQUENCY CIRCUITS

Linda P. B. Katehi, Gabriel M. Rebeiz

Department of Electrical Engineering and Computer Science
The University of Michigan, Ann Arbor, MI 48109-2122, U.S.A.

High frequency applications impose very strict requirements on circuit performance including low loss, low dispersion and negligible parasitics. Presented herein are micromachining approaches that offer flexibility to the design of circuits and antennas by allowing for on-wafer packaging and locally reduced substrate thickness to achieve excellent electrical performance. The fabrication of these circuits is based on conventional Si/GaAs/InP fabrication techniques and, as such, they preserve their monolithic character while at the same time allowing for high density and three-dimensional integration.

Micromachined high-frequency circuits with integrated packaging offer light weight and controllable parasitics, which makes them appropriate for hand-held communication systems and miniature intelligent millimeter-wave sensors where system requirements impose strict limits on electrical performance. Recent advances in semiconductor processing techniques allow for integration in all of the directions of the three dimensional space. The capability to incorporate one more dimension, and a few more parameters, in the circuit design, leads to revolutionary shapes and integration schemes. These circuit topologies have reduced ohmic loss and are free of parasitic radiation or parasitic cavity resonances without losing their monolithic character. Integration capabilities are thereby extended and performance is optimized. The evolution of micromachined circuits and antennas for operation at microwave and millimeter-wave frequencies is still in its infancy. However, presented here is a description of recent accomplishments in this area, with emphasis on the effort performed at the University of Michigan. There are two techniques which have shown promise for use, and which extensively use micromachining to realize novel circuits. The first utilized dielectric membranes to support transmission line and antenna configurations and emphasizes optimization of circuit performance. The second technique introduces new concepts in packaging such as adaptive or conformal packaging and, in addition to improvement in performance, it emphasizes size/volume/cost reduction. The merits of each approach, in relation to electrical performance, fabrication, and compatibility, will be presented, and the impact of the newborn technologies to the state of the art will be discussed.

Study of High Frequency Circuits on Micromachined Reconfigured Substrates

Rhonda Franklin Drayton* and Jianpei Wang

Electromagnetics Laboratory and Microfabrication Laboratory

EECS Department

University of Illinois at Chicago

Chicago, IL 60607

At microwave frequencies and above, the challenge to develop high performance planar circuits with very low loss demands the exploration of diverse fabrication technologies. Micromachining offers tremendous enhancement to standard MMIC design and fabrication techniques. The incorporation of micromachining with MMIC fabrication techniques has produced a tremendous number of flexible solutions in both high frequency circuit and antenna designs. For example, novel monolithic self-packages, developed for planar transmission lines, offer superior isolation between circuits in high density packaging environments. Additionally, significant performance improvements have been achieved for planar microstrip antennas in large ($\epsilon_r=11.7$ or 12.9) index environments that result in performance that is comparable to similar designs on low-index substrates.

Research to date mainly relies on the use of Si micromachining to selectively reconfigure specific regions of a semiconductor substrate. This is done to achieve a desired mechanical configuration that improves and in some cases optimizes the electrical performance of a planar circuit or antenna design. In the packaging case, cavities are etched above and below a transmission line; whereas in the antenna/circuit case, material is partially or completely removed in a specified region. Despite the past advancements, basic circuit components have not been evaluated for high frequency designs based on reconfigured substrates.

This paper will evaluate the performance of several passive circuit components as well as fundamental circuit elements that have been developed on micromachined reconfigured substrates. These reconfigured substrates will consist of either mixed thickness or mixed dielectric constants regions and will be used to evaluate basic circuit elements commonly required to develop high frequency planar circuit components. The presentation will briefly highlight the fabrication and design methodology, as well as the measurement and characterization techniques used to evaluate circuit performance. The electrical and electromagnetic wave properties of the designs will be evaluated and compared to traditional planar lines on regular "non-etched" substrates.

An Efficient Field Solver for Micro-electromechanical Systems (MEMS)

Vladimir Veremey and Raj Mittra

Electromagnetic Communication Research Laboratory
Pennsylvania State University, 319 Electrical Engineering East
University Park, PA 16802-2705

e-mail: RIMECE@engr.psu.edu or vvy2@psu.edu

The modeling of micro-electromechanical systems, or MEMS, is an important problem that requires the coupling of several disciplines to simulate the forces generated by a variety of mechanisms, including electrical and mechanical types. An example of such a structure is a comb drive which experiences a deformation when a positive potential is applied on the drive structure.

In this paper we concentrate on the problem of efficient solution of electrostatic fields in complex three-dimensional structures. The knowledge of these fields enables us to predict the electrostatic forces and to estimate the mechanical deformation of the structure.

The field solver discussed in this paper is based on the well-known Finite Difference (FD) method. It has many salutary features, including the ability to handle arbitrary geometries and inhomogeneous structures with relative ease, and it generates sparse matrices that can be solved efficiently via iterative techniques. One drawback of the finite methods is the need to truncate the mesh accurately and efficiently. In this paper we devise a novel technique for mesh truncation that utilizes a combination of the Berenger Perfectly Matched Layer (PML) concept generalized to the static case, coupled with an impedance boundary condition. The method employs dielectric layers with anisotropic properties to reduce the influence of mesh truncation on the computation of the capacitance matrix of interconnect configurations. In addition, at points near the boundary, we replace the conventional FD equations with those based on the premise that the potential decreases in an exponential fashion in the asymptotic region as we recede away from the structure in the direction of the boundary.

To further enhance the efficiency of the field computation using the FD/PML approach, we introduce a two-step mesh refinement procedure. As a first step, we compute the electric potential at the nodes of a coarse grid, used to discretize the computational domain that includes the PMLs. Next, we recalculate the electric potential at the nodes of the refined grid, whose cell size is smaller by a factor of 2 (or more) as compared to that of the coarse grid. The computational domain for the refined calculation includes only the points in the close vicinity of the structure. The initial values of the potential at the grid points on the FD boundary are calculated by using a spline interpolation of the results obtained in the first step.

The above technique has been applied to the field computation problem in a number of complex structures to validate the accuracy of the method and demonstrate its numerical efficiency.

Illustrative numerical examples will be included in the presentation of the paper.

SUBMILLIMETER CYLINDRICAL FILTERS AND ANTENNAS FABRICATED WITH CYLINDRICAL LIGA

A. D. Feinerman

Microfabrication Applications Laboratory, Dept. of EECS
University of Illinois at Chicago, U.S.A.

Y. W. Kang and D. C. Mancini

Advanced Photon Source, Argonne National Laboratory, U.S.A.

An x-ray lithography lathe has been developed that can pattern cylindrical, ellipsoidal, and other non-planar objects. This lathe is capable of patterning on a micron scale a wide variety of shapes including shapes impossible to achieve with a conventional lathe. This lathe allows the creation of a variety of high frequency one and two conductor filters and antennas.

Using this technique, we have investigated coaxial and cylindrical waveguide filters and antennas for millimeter frequencies. An R-band filter being implemented has a one-millimeter center conductor surrounded by a corrugated metal shell that ranges from four to two millimeters in diameter. Corrugations are 0.2 mm wide with a 2.2 mm period. HFSS modeling of this filter predicts good performance in the 20-40 GHz range. The PMMA is assumed to have a dielectric constant of 2.6 and a loss tangent of 0.001. The copper thickness is assumed to be greater than three skin depths, which is about 0.4 microns at 40 Ghz. Removal of the PMMA after metal deposition will significantly improve the filter performance. This technique can also open up slots in the outer conductor of the cylindrical waveguides to make efficient radiators in this frequency range. The technique can be scaled up and down to create high performance precision antennas and filters over an extremely wide range of frequencies. The coaxial design will facilitate incorporating these components into integrated RF circuits.

BIOLOGICAL MICROCHIPS: PROPERTIES AND APPLICATIONS

Andrei Mirzabekov

Argonne National Laboratory, U.S.A.

and Engelhardt Institute of Molecular Biology, Moscow, Russia

Microarrays of gel-immobilized compounds on a chip (MAGICChips) are polyacrylamide gel micropads fixed on a glass slide. They may contain chemically immobilized oligonucleotides, DNA, antibodies, proteins, or other compounds.

Oligonucleotide chips have been used for mutation and sequence polymorphism screening; gene expression monitoring; detection of microorganisms; HLA allotyping; DNA chemical modification, fractionation, replication, and ligation; and thermodynamic analysis of DNA duplexes. Generic microchips containing all 4,096 possible 6mers have been tested for DNA sequence analysis.

Reflectors and Broadband Antenna Design

W. A. Imbriale and A. Kishk

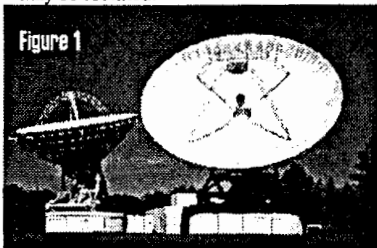
Performance and Potential Applications of Refurbished 30 Meter Former Satellite Communications Facilities.....	256
<i>D. R. DeBoer*, P. G. Steffes, Georgia Institute of Technology, USA</i>	
Efficient Algorithm for Beam Shaping Technique	257
<i>G. G. Cheng*, S. H. Huynh, Antcom Corporation, USA</i>	
Reflector Antenna Shaping from Feed Field Intensity Measurements.....	258
<i>D. Denison*, M. Shapiro, R. Temkin, Massachusetts Institute of Technology, USA</i>	
Fields at the Focal Point of a Reflector Antenna Surface due to Laser-light Illumination	259
<i>C. Ozzaim*, C. M. Butler, Clemson University, USA</i>	
On the Design of Luneburg Multi-beam Antenna.....	260
<i>G. G. Cheng*, S. H. Huynh, M. Sanchez, Antcom Corporation, USA</i>	
Design and Experimental Investigation of a Wideband Polarization Filter.....	261
<i>J. Shaker*, M. Cuhaci, Communications Research Centre, Canada</i>	
Singly- and Multiply-folded Broadband Conical Antennas	262
<i>J. S. McLean*, H. D. Foltz, E. Guzman, University of Texas - Pan American, USA</i>	
Development of Integrated Double-discone Antenna	263
<i>Y. Enyao*, Guilin Institute of Electric Technology, China, Y. Shaohua, C. Xinke, Guangzhou Communication Research Institute, China</i>	
Dielectric Resonator Antenna Elements with Enhanced Bandwidth	264
<i>G. P. Junker, A. A. Kishk*, A. W. Glisson, University of Mississippi, USA</i>	
Analysis of Arbitrarily Shaped Dielectric Resonator Antenna Structures	265
<i>A. J. Movahedi, A. W. Glisson*, A. A. Kishk, University of Mississippi, USA</i>	

Performance and Potential Applications of Refurbished 30 Meter Former Satellite Communications Facilities

David R. DeBoer and Paul G. Steffes
School of Electrical and Computer Engineering
Georgia Institute of Technology

A class of large satellite communication antennas built in the mid-1970's comprise a potential set of large antennas available for research or commercial satellite communications or radio astronomy upon upgrade. With the advent of low-noise electronics, facilities of this size with the associated maintenance costs were largely abandoned. Although many have sat idle and decaying over the intervening years, these facilities remain a potential resource for research and education. The Georgia Institute of Technology acquired one such facility located south of Atlanta in Woodbury, GA (Figure 1). This facility consists of a pair of 30 meter antennas built in the mid-1970's and used by AT&T through the early 1980's for satellite communications. Initially as a set of small-scale student projects and later as a full-scale project funded by the SETI Institute, one of the 30 meter antennas has recently been fully renovated. The structure was completely stripped and new electrical, mechanical and feed/RF systems were installed.

One concern with a "vintage" facility is the achievable performance for a reasonable cost, since the years of disuse take a toll on the antenna superstructure and surface performance. Detailed inspection of the superstructure and measurements taken with the refurbished Woodbury facility indicate that this facility survived these years quite well and reasonable efficiencies are achievable in the 1-6 GHz frequency range. The hybrid-mode ultra-wideband feed/orthomode transducer (OMT) assembly has been described previously (IEEE AP-S 1997 International Symposium Digest, vol. 3, p. 1634) and allows full 1-6 GHz band use with a single feed. With this new feed/OMT in place illumination efficiencies on the order of unity were measured, with overall efficiencies on the order of 30-40% across the L and S microwave bands (1-3 GHz). Microwave holography will be performed in the near future to further characterize the surface and see if any gross misalignments may be rectified.



Efficient Algorithm for Beam Shaping Technique

*Cheng, Guan G., Huynh, Son H.
Antcom Corporation
21515 Hawthorne Blvd.
Torrance, CA 90503

Future satellite communication requires re-configurable multiple beams in certain regions. For example, the beam pattern can be re-shaped to enhance the coverage gain during the raining season. In light of the generally computational-intensive nature of the optimization schemes, the capability of rapid beam re-configuration is critical, particularly for the multi-beam antenna (MBA) applications. We propose an efficient algorithm for rapid beam shaping. The shaped beam antenna of interest is the parabolic-type reflector with an adjustable array feed, or a phased array. The antenna far-field beam pattern can be re-configured by varying amplitude and/or phase of each feed element.

Three representative examples are given. Example 1 presents contour beams covering some geographical coast lines. The antenna is a parabolic reflector fed by multi-horn with uniform weights. Example 1 shows that an uniform-weight MBA design which provides the required beam coverage is achieved directly via the algorithm. The MBA design which includes the geometry configurations of the parabolic reflector and the array feed, are given along with the predicted beam performance.

Example 2 is similar to Example 1 except the feed is weighted with variable amplitude and phase. Example 2 demonstrates that the contour beam can be efficiently re-configured by adjusting the amplitude and phase at each feed element. Numerical results for several cases are shown as well.

Finally, Example 3 is a parabolic MBA for spot beams coverage. The beam shapes are re-shaped such that the antenna gains are changed accordingly. The beam shape is also controlled by the weights of the feed elements. The design of the beamforming network and the simulation results are presented.

Reflector Antenna Shaping from Feed Field Intensity Measurements

Douglas Denison, Michael Shapiro, Richard Temkin
Plasma Science and Fusion Center, Waves and Beams Division
Massachusetts Institute of Technology

In the problem of antenna radiation pattern synthesis, one solution is to use a set of shaped reflectors to transform a given feed pattern into the desired radiated field. In this presentation we demonstrate a new approach to designing a quasi-optical, off-set shaped reflector antenna system from measured feed field intensities in order to fully account for the actual field structure, thus ensuring the desired radiated field. The method may be used to design quasi-optical mode converters, transmission line components, and phase correctors for radio telescopes.

In microwave and mm-wave applications (> 100 GHz), we often find it difficult to measure phase, yet we need both the field amplitude and phase to shape the reflectors. We consider the case of near-field intensity measurements of the feed pattern over two or more planes. We further stipulate that the beam be quasi-optical - paraxial, spatially compact, no reactive power, and all reflectors are large in terms of a wavelength. Katsenelenbaum and Semenov (B.Z. Katsenelenbaum and V.V. Semenov, Radio Eng. and Electronic Phys., 12, 223-231, 1967) proposed an iterative algorithm for phase retrieval that is directly applicable to quasi-optical beams and can be conveniently implemented numerically. We use the phase retrieval algorithm to both recover the phase of the feed system and to shape the reflectors by treating them as phase correctors. We will present some results of our extensive numerical simulations which elucidate the accuracy of the approach.

We have used the present method to design a pair of reflectors to transform a 110 GHz microwave beam into an ideal Gaussian beam as part of an internal mode converter for use in a high-power gyrotron. The feed pattern is complicated, and is sensitive to machining and alignment errors in the feed structure. We measured the electric field intensity over several consecutive planes in the near field of the feed, and we used the phase retrieval algorithm to recover the phase of the beam and to design the shaped reflectors. The reflectors were machined from solid aluminum and tested on the feed structure. We will present analysis of the measured radiated field and show it is indeed a Gaussian beam with parameters that match those of the theoretical design, demonstrating the validity of our approach.

Fields at the Focal Point of a Reflector Antenna Surface due to Laser-Light Illumination

Cengiz Ozzaim* and Chalmers M. Butler

Department of Electrical and Computer Engineering
105 Riggs Hall, Clemson University, Clemson SC 29634

When a properly modulated laser beam illuminates a conducting surface it may cause electrons to be emitted in such a way that the resulting electromagnetic radiation is equivalent to that from a distribution of electric dipoles on and normal to the surface. The distribution of these dipoles over the illuminated spot is dictated by the laser light intensity distribution and their spatial oscillation is controlled by the laser modulation. This "spot" of dipoles radiates in the presence of the illuminated surface at a frequency dependent upon the modulation. For a vanishingly small spot of laser light on the conducting surface, the radiating source is modeled as an electric dipole, while, for a larger spot, it is taken to be an ensemble of normal dipoles whose amplitude and phase are dictated by the characteristics of the laser light and the spot.

A conducting parabolic reflector, illuminated by a laser, is illustrated in Figure 1. With the addition of a feed or collector at the focal point of the paraboloid, one has a standard reflector antenna. The laser excited dipoles radiate in the presence of the reflector antenna and create a field everywhere. It is the field at the focal point, as a function of the modulated laser beam characteristics, that one wishes to determine. Since one needs to know the field only at the focal point, one can obtain the desired information by solving a radiation problem and then employing the reciprocity theorem. This indirect but efficient reciprocity-based technique for determining the field is carried out in two steps. First, a rotationally symmetric source is impressed at the focal point and the resulting radiation is determined from zero order BOR theory. From knowledge of this radiated electric field and the value of the impressed source, one determines the field at the focal point by invoking the reciprocity theorem. This technique, though simpler than more direct methods, is completely rigorous and involves no approximations not employed in direct procedures. Data are presented to illustrate the results of this analysis.

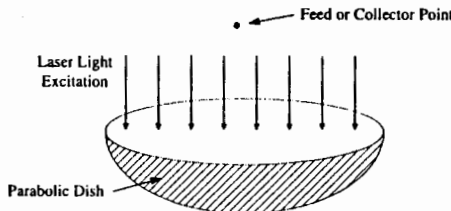


Figure 1. Reflector antenna surface illuminated by modulated laser light.

On the Design of Luneburg Multi-Beam Antenna

*Cheng, Guan G., Huynh, Son H., and Sanchez, Marco
Antcom Corporation
21515 Hawthorne Blvd.
Torrance, CA 90503

The increasing demand of Low Earth Orbit (LEO) satellite constellation is evident in future and emerging global personal communication systems. LEO satellite is normally required to provide large number of beams for wide-angle global coverage. The design of multi-beam antenna (MBA) is therefore essential for low cost and high performance. We propose the Luneburg lens for MBA applications for global communications. The main advantage of the Luneburg lens MBA is that all its beams are identical with no scan loss.

A practical design of layered Luneburg lens MBA is presented. We propose an optimization scheme which determines the antenna configuration including the number of shells, the dielectric constant for each shell, the size of the lens, feed layout, and beamforming network. A computer model is developed for the prediction of far-field performance, and the numerical results for discrete shells are also shown.

Three types of Luneburg lens MBAs are given for comparison. They are: a) single-aperture MBA, b) multi-aperture MBA, and c) single-aperture with shared feed elements. First of all, the single-aperture MBA presents a simple antenna configuration which provides 3-dB contiguous, multiple beams, yet with the drawback of significant feed spillover loss. Secondly, the multi-aperture MBA produces higher gain by trading the feed spillover with excess hardware. However, the use of multiple apertures results in weight and mechanical alignment problems. Finally, the MBA with shared feed poses another way of reducing feed spillover by sharing the adjacent feed elements at the expense of beamforming network complexity. Antenna configurations and numerical results of all three types of MBA are evaluated, along with practical design issues.

Design and experimental investigation of a wideband polarization filter

Jafar Shaker* and Michel Cuhaci
Communications Research Centre
3701 Carling Ave., Box 11490, Station H
Ottawa, Ontario, Canada, K2H 8S2

The advent of various schemes of wireless communications (such as mobile and LMCS) has placed stringent requirements on available frequency bands. These constraints can be alleviated to a certain extent by frequency reuse through polarization diversity. Polarization filters are crucial to the implementation of such schemes. Therefore, a study was undertaken to investigate the characteristics of a perforated screen polarization filter and its effect on the performance of an antenna that employs such a filter.

Strip gratings have been used in the past as polarization filters, and various computational and analytical tools have been devised for the calculation of their reflective characteristics. The two dimensional grid structure introduced in this paper maintains the same level of polarization isolation as a strip grating filter while being superior in terms of mechanical strength.

There have been various publications on the frequency dependence of the reflective characteristics of two dimensional grids of slots. However, the polarization selectivity of these structures has not been thoroughly investigated. This paper is an attempt to fill this gap and discuss the intricacies in the utilization of a two dimensional perforated screen, such as the effect of the spacing between grid and the antenna on performance, and measurement techniques.

The design and experimental verification of a wideband polarization filter composed of a perforated metallic screen is presented in this paper. The filter was used to suppress the cross-polarization of both a horn antenna and a large array of dielectric resonators. Effective suppression of the cross-polarization (in the order of 25 dB) was observed for both cases. The insertion loss was in the order of 1 dB in the case of the horn and 0.5 dB in the case of the array antenna. The 10 dB return loss bandwidth was measured to be 20%. It was demonstrated that the filter can be installed in close proximity of the antenna radiating aperture without any significant degradation in its insertion loss or polarization isolation performance. Therefore, the utilization of such filters does not violate the compact nature of planar arrays.

The radiation pattern of the antenna in conjunction with the filter was measured in the major planes for both co- and cross-polarization. A reduction in the beamwidth of the antenna was observed as the filter is mounted on the radiating aperture. The modification of the antenna radiation pattern was caused by the angular sensitivity of the polarization filter.

Singly- and Multiply-folded Broadband Conical Antennas

J. S. McLean, H. D. Foltz, G. E. Crook

Electrical Engineering, The University of Texas - Pan American
1201 West University Drive, Edinburg, TX 78539

Electrically-small, broadband antennas have numerous useful attributes among which is the ability to replace sets of multiple antennas with a single, compact package.

Conical and biconical antennas exhibit low radiation quality factors and hence have the potential to provide broad band operation. However, they require external tuning and matching elements for operation over a frequency range in which they are electrically-small. These matching elements increase overall package size and complexity and often limit efficiency. The folding of monopole and dipole antennas provides impedance transformation as well as reactance/susceptance compensation thus providing broadband operation in a small package without the need for external tuning elements.

Here, a folding scheme combined with dielectric loading is used to produce broadband, electrically-small, singly- and multiply-folded conical and biconical antennas. Because conical and biconical radiating elements exhibit intrinsically lower radiation quality factors than do wire elements, these antennas provide superior performance over conventional folded antennas. They provide bandwidth approaching the fundamental physical limit for a given volume, require no external tuning or matching elements and are very efficient.

The operation of these antennas will be discussed and measured data will be presented for input impedance, radiation efficiency, and radiation patterns. Finally, the performance of these antennas will be compared with fundamental physical limits.

Development of Integrated Double-discone Antenna

Yang Enyao

Guilin Institute of Electric Technology, China

Yang Shaohua, Chen Xink

Guangzhou Communication Research Institute, China

Traditional discone antenna is characterized by broadband and low gain. It is worth discussing to construct an array with discone as the element. The ordinary array excitation which usually leads to the fork structure is impractical in application. This investigation actualizes the integration of double-discone by using a coaxial branch-pipe unit. The structure is shown in fig.

Starting from the rigid cable, the radius of the outside conductor is gradually extended, then via the coaxial branch-pipe, the internal and external coaxial cable are formed. They excite discone 1 and 2 separately. To make the two discones to be in phase, it is necessary to stuff some medium in the interior of the external cable and, in the meantime, to meet the following equation:

$$\Delta\Phi = \Phi_1 - \Phi_2 = \frac{2\pi}{\lambda_0} (l + d) - \frac{2\pi\sqrt{\epsilon_r}}{\lambda_0} l = 0$$

Hence we have $l = d / (\sqrt{\epsilon_r} - 1)$. Using MM, computing are made in the case of integrated double-discone system with $d=60\text{cm}$, $l=120\text{cm}$ and $\epsilon_r=2.25$. The computed patterns in vertical plane fit well with the measurement data. The measurement result of VSWR of the double-discone antenna system shows that this construction still is broadband as the traditional single discone does.

With coaxial branch-pipe the integration of the antenna and the feedline can be made actualization and, on the basis, multi-discone system can be designed for the promotion of the antenna gain. It should be note that, both theoretical computing and measurement indicate the parasitic current on the outside surface of the rod between discone 1 and 2 must be restrained.

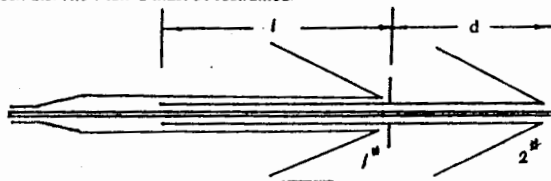


fig. the double-discone antenna system

Dielectric Resonator Antenna Elements with Enhanced Bandwidth

Gregory P. Junker¹, Ahmed A. Kishk^{*2}, and Allen W. Glisson²

¹501 W. Mariposa Ave., El Segundo, CA 90245

²Department of Electrical Engineering, The University of Mississippi
University, MS 38677

The use of a dielectric resonator (DR) as a radiating element has been a topic of considerable interest due to its small size, efficiency, and ability to perform multiple antenna tasks via simple mode coupling mechanisms. In a recent review of the dielectric resonator antenna (DRA) by Mongia and Bhartia, (R. K. Mongia and P. Bhartia, *Internat. J. Microwave and Millimeter-Wave Computer-Aided Engineering*, 2, No. 3, 230-247, 1994), approximate design equations for the prediction of source free DRA resonant frequencies and impedance bandwidth were given. Many of these simple relations were derived from experimental data, cavity models, and curve fitted data obtained from rigorous numerical methods. Simple relations such as these find utility as a starting point for design work. However, to design an actual radiating device, the feed mechanism must be taken into account since it can significantly influence the important antenna parameters such as impedance bandwidth and pattern integrity.

Rigorous numerical methods, together with hardware prototyping of ground plane backed, coaxial probe fed DRA elements operating in quasi-TE modes have been used in this investigation. Particular configurations of DRAs with impedance bandwidth consistently greater than 20% have been identified. One of the basic radiating elements under consideration in this investigation is the half-split cylindrical dielectric resonator operating in the HEM_{12} mode (G.P. Junker, A.A. Kishk, and A.W. Glisson, *Electron. Lett.* 29, No. 21, 1810-1811, 1993). Through proper selection of antenna parameters, this antenna mode has been identified as one which possesses very low radiation Q factor and large impedance bandwidth. Results of this numerical and experimental investigation shall be presented.

Through the use of numerical methods, broad-banding of other quasi-TE modes via the mechanism of concentric DRA elements has been investigated. The basic philosophy behind this design procedure is to concentrically load a half-split cylindrical DR of low permittivity with that of a relatively high permittivity DR. The parameters of the concentrically loaded DRA are selected so that the device exhibits multiple resonances of the same mode type over a frequency band which exceeds that of any of the constituent DR components. Results of this investigation shall be presented.

Analysis of Arbitrarily Shaped Dielectric Resonator Antenna Structures

A. J. Movahedi, A. W. Glisson*, and A. A. Kishk

Department of Electrical Engineering

University of Mississippi

University, MS 38677

The dielectric resonator antenna (DRA) radiating element has been the subject of considerable interest recently due to its small size, high efficiency, and ability to perform multiple antenna tasks via simple mode coupling mechanisms. The rigorous analysis of DRA elements, however, has been largely restricted to those with rotationally symmetry. The objective of this work is to present a numerical solution procedure for the rigorous modeling of arbitrarily shaped DRA elements in the presence of arbitrarily shaped conducting surfaces and/or wires. The equivalence principle is employed to obtain a set of coupled surface integral equations along with thin-wire integral equations when necessary. The PMCHW integral equation form is used for modeling dielectric interfaces, while the electric field integral equation is used for conducting surfaces and thin wires. The dielectric and conducting surfaces are modeled by planar triangular patches.

The analysis of electromagnetic radiation and scattering from a combination of arbitrarily shaped dielectric and conducting objects has been studied previously (S. M. Rao, T. K. Sarkar, P. Midya, and A. R. Djordjevic, *IEEE Trans. Antennas Propagat.*, AP-39, 1034-1037, 1991). In this work we add the capability to model thin wires, which may be located within or outside the dielectric region and which may be attached to a conducting surface. Of particular interest in this work is the modeling of DRA elements, where the dielectric region is of resonant size and acts as a radiating element. Thin wires in the vicinity of the dielectric or attached to conducting surfaces in the vicinity of the dielectric may be driven with delta-gap voltage sources to provide the excitation to the DRA. The program developed for modeling the DRA elements is validated for a variety of geometrical configurations for both radiation and scattering cases for which other analytical, measured or numerical data exists, including the specific cases of a probe-fed hemispherical DRA and a probe-fed cylindrical DRA.

Tropospheric and Ionospheric Propagation

D. A. Hill and M. E. Baginski

Electromagnetic Ground-wave Field of Vertical Antennas AP
R. W. P. King, Gordon McKay Laboratory, Harvard University, USA*

Analysis of Dual Polarisation Propagation Data for Tropospheric Channel Study AP
A. Rocha, J. Neves, Universidade de Aveiro, Portugal*

Wave Propagation in Curved Road Tunnels AP
M. Nilsson, Allgon System AB, Sweden, J. Slettenmark, Allgon Innovation AB, Sweden, C. Beckman, Allgon System AB, Sweden*

An Automated UTD Approach for Modeling Wave Propagation over Hilly Terrain Based on
Digital Maps AP
C. Yang, W. Chang, W. Hwu, National Taiwan University of Science and Technology, Taiwan,
ROC, H. Li, National Taiwan University, Taiwan, ROC*

Characterization of the Wave Propagation in the Ionospheric Channel by the
Scattering Function AP
M. Arshad, A. Bouirig, C. Gimenes, Equipe Radiopropagation, France*

Comparison of the Current Methods for Coverage Area Prediction for Communication in the HF
Band AP
S. G. Tanyer, C. B. Erol, Baskent University, Turkey*

Rainfall Induced Satellite Beacon Attenuation on Three 12 GHz Links in Equatorial and Tropical
Brazil AP
E. Couto de Miranda, M. S. Pontes, L. A. R. da Silva Mello, Pontifical Catholic University of
Rio de Janeiro, Brazil*

Mobile Propagation Measurements using CW and Sliding Correlator Techniques AP
G. Dyer, T. G. Gilbert, E. Sayadian, S. Henriksen, Stanford Telecommunications Inc., USA*

Reflection Coefficient by Inhomogeneous Ionized Media Having One Peak
Electron Density AP
K. Motojima, M. Ohki, Gunma University, Japan, H. Sakurai, Gunma College of Technology,
Japan, S. Kozaki, Gunma University, Japan*

An Investigation of Lightning-induced Sprites using a Non-linear, Inhomogeneous Atmospheric
Conductivity 268
M. E. Baginski, J. E. Mooney, L. S. Riggs, Auburn University, USA*

An Investigation of Lightning-Induced Sprites Using a Non-linear, Inhomogeneous Atmospheric Conductivity

Michael E. Baginski*, Jon E. Mooney, and Lloyd S. Riggs

Department of Electrical Engineering
200 Broun Hall • Auburn University, Alabama 36849

Sprites induced via lightning-related transient electric fields due to the re-configuration of charge following large positive cloud-to-ground strokes are investigated via a simulation of the Maxwell's equations. The research presents evidence that the "sprite" phenomenon is a direct result of energy coupled to the ionosphere by several complicated mechanisms. The primary region of interest is in the altitude range of $z = \sim 40 - 70$ km with the radial dimension spanning an area of 30 -60 km. Sprites developing in this region are commonly referred to as a Blue Jets. A measured nighttime conductivity profile is used in all simulations and a finite element code is employed in the solution. Maxwell's equations are solved accounting for the nonlinear atmospheric effects during the sprite event ($\sigma = \sigma(\rho, E, z, \text{etc})$). The fundamental equation used is shown below:

$$\nabla \times \nabla \times E = -\mu_0 \left(\sigma \frac{\partial E}{\partial t} + \frac{\partial J_s}{\partial t} \right) - \mu_0 \epsilon_0 \frac{\partial^2 E}{\partial t^2} \quad (1)$$

Several of the field signatures identified unusual traits. The temporal evolution of the current density clearly indicates an extremely long duration following the onset of the sprite event. This is primarily a result of the conductivity gradient forcing continuing current into the upper altitude regime.

Recent optical and electromagnetic measurements confirm much of the simulated schema. The research establishes, under "worse case" conditions, sufficient electrical energy or power is resident in the atmosphere to allow this optically measured event to occur. It is also strongly inferred that the primary mechanism for "triggering" a sprite event is a direct result of the gradient of the atmospheric conductivity complicating the electromagnetic response in the simulations.

Antennas for Mobile Communications

M. Geissler and M. Jensen

Extremely Low Cost Circularly Polarized Handset Antenna for L/S-Band Satellite Communication.....	270
<i>S. H. Huynh*, G. Cheng, M. Sanchez, Antcom Corporation, USA</i>	
A Dual Mode Handy Phone Antenna using Helical and Dipole Structures.....	271
<i>L. Desclos*, M. Madhian, A. Kuramoto, K. Tanabe, NEC Corporation, Japan</i>	
Patch and Dipole Type Configuration for Multi-mode System	272
<i>L. Desclos*, M. Madhian, A. Kuramoto, K. Tanabe, NEC Corporation, Japan</i>	
A Solution of the Read Zone of a Vertically-polarized Dipole RFID Tag Antenna Illuminated by a Pair of Switchable Circularly-polarized Base Station Antennas	273
<i>K. V. S. Rao*, D. W. Duan, H. K. Heinrich, IBM, Thomas J. Watson Research Center, USA</i>	
Sensitivity Analysis of a Planar Antenna with Respect to FDTD Modeling	274
<i>A. Christ*, K. Pokovic, M. Burkhardt, N. Kuster, Swiss Federal Institute of Technology (ETH), Switzerland</i>	

Extremely Low Cost Circularly Polarized Handset Antenna for L/S-Band Satellite Communication

Son H. Huynh*, Guan Cheng, Marco Sanchez

Alcom Corporation

21515 Hawthorne Blvd.

Torrance, CA 90503

Torrance, CA 90503
Lowest elevation angle
 10° 24°

Low-gain circularly polarized handset antenna designs that provide hemispherical patterns have always been a challenge for antenna engineers in general. This is especially true in the new L/S-band communication applications such as in Iridium, Globalstar, ICO, and Ellipso. It is even harder for the mechanical/packaging engineers and electrical engineers to work together in order to come up with a design that works electrically, and yet is visually appealing and cheap to mass-produce. It is essential nowadays for antenna engineers to have vast knowledge in mechanical engineering, material engineering, and packaging design to better assist them in the antenna design.

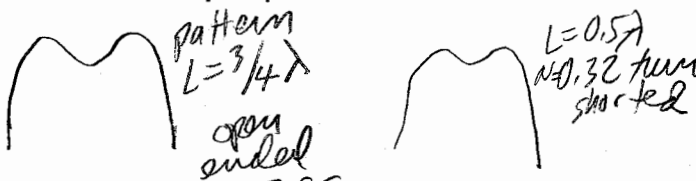
Handset antennas for the above applications require about 0 dBic gain at 10° elevation angle. They have to transmit and receive at the same time:

- either in one band as in Iridium:
Rec/Tx: 1.6160-1.6265 Ghz $\pm 5125 \text{ MHz}$
- or at two narrowly spaced frequencies as in ICO:
Rec: 1.995 Ghz, Tx: 2.185 Ghz $\pm 15 \text{ MHz}$
- or at two widely spaced frequencies as in Globalstar and Ellipso:
Rec: 2.4918 Ghz, Tx: 1.6183 Ghz $31/2 \pm 8.25 \text{ MHz}$

The gain of patch antenna is not enough to close the link between users and satellite down-link antennas. Conventional quadrifilar helix design approaches lead to a product that is too bulky and impractical to integrate into the handset unit and is too expensive to produce. ~~Cost \$130~~

Cost < \$30

This paper will discuss the innovative techniques that simplify the quadrifilar helix design. The new design approach will utilize hi-tech plastic engineering and fabrication technique for its electrical advantage. The overall package of the antenna will be small in size, extremely low in cost, and still maintain its optimal performance.



$N=0.85$
Print on Duriod ²⁷⁰ with feed network and then
wrap around cylinder. Laser etching
is too expensive.

A Dual Mode Handy Phone Antenna using Helical and Dipole Structures

Laurent Desclos*, Mohammad Madhian, A. Kuramoto* and K. Tanabe†
C&C Media Research Laboratories, NEC Corp.,

*Antenna system devlt. dept., Microwave Satellite Communications, NEC Corp.

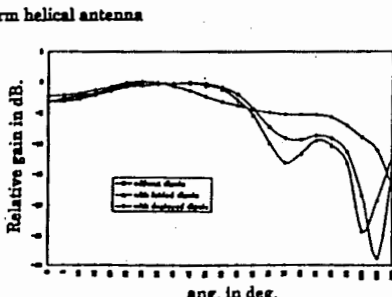
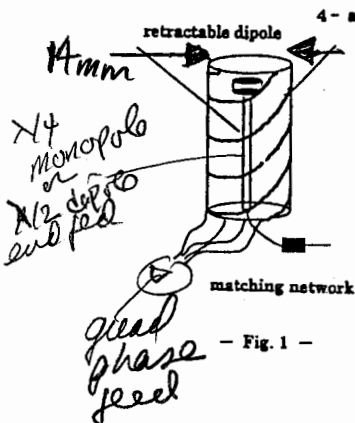
Abstract :

This paper describes a dual mode handy phone antenna by incorporating a dipole within a helical structure, developed for Satellite/Cellular dual mode communication.

Summary :

Recent advances in mobile communication technology have resulted in integration of different services such as combining Satellite and Terrestrial Cellular communication systems. Since operation frequencies, polarization and radiation patterns should be different, two antennas have to be used. Often the solution used is to separate them which requires space and is against the integration trend of actual handy communication system. In order to solve these problems, we propose a structure based on inclusion of a dipole type antenna within an helical type antenna. Helical antenna for generating circular polarization in the S frequency band with a beamwidth is designed to fulfill the requirements for a satellite communication system. It is based on a 4-arm helical optimized on its diameter, pitch, length. The dipole antenna which is to access a GSM alike system at 900 MHz is placed in the center of revolution of the helical antenna - Fig. 1-. Study of interaction of both antennas has been performed with a moment method. It is shown that the introduction of the dipole type antenna mainly affects the radiation pattern of the helical antenna but not the axial ratio which is staying within 2 dB at most. Measured performances show that it is possible not to perturb too much the radiation pattern of the helical antenna providing that the dipole is well positioned - Fig. 2 -.

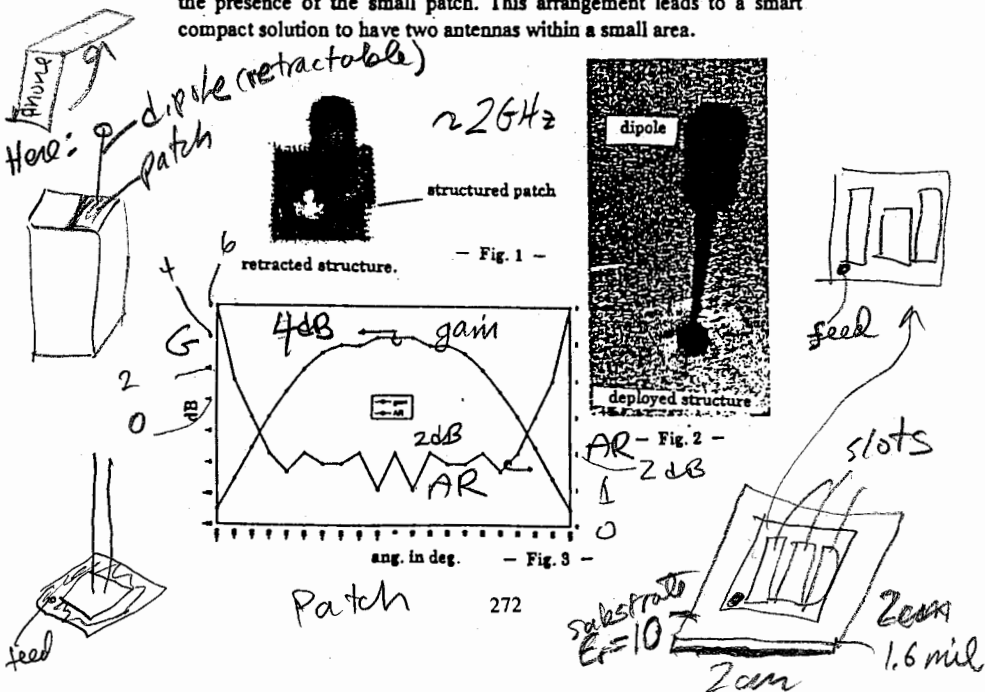
The developed structure provides a smart compact solution for dual mode handy phone systems.



It is retractable, but couldn't understand him

Results are for free space

Method:



Patch and Dipole type configuration for Multi—Mode system

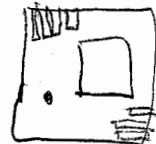
Laurent Desclos, Mohammad Madhian, A. Kuramoto* and K. Tanabe*

C&C Media Research Laboratories, NEC Corp.,

*Antenna system devt. dept., Microwave Satellite Communications, NEC Corp.

Summary : Integration of antennas for permitting both satellite and terrestrial communication access is emerging. For satellite communication the circular polarization is needed, however for the terrestrial communication the linear vertical polarization is often used. In this paper we describe an integrated patch dipole solution. The patch is fed through the substrate, to realize the circular polarization. A slot and a hole are made within the patch to mount the dipole type antenna to satisfy the terrestrial communication system requirements. The dipole can then be pull in or out of the patch configuration —Fig.1,2—. Since the introduction of a slot and hole creates a shift in the axial ratio and matching, we had to mechanize the behavior of the AR versus the matching and gain. It has been made through the introduction of slits on two edges of the patch. By adjusting the number of slits, their widths, lengths and separations, centering the AR is possible. All the simulations have been made using a moment method. A realization has been made having an overall size of 19 mm by 19 mm for the patch size in the S frequency band. The measured axial ratio, matching and axis gain are 2 dB, 30 dB and 4 dB respectively at the center frequency —Fig. 3—. The bandwidth is 0.75 %. The dipole radiation in this case is not affected by the presence of the small patch. This arrangement leads to a smart compact solution to have two antennas within a small area.

patch optimized for AR



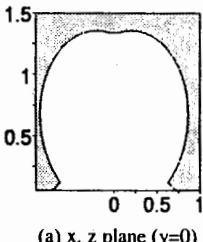
A Solution of the Read Zone of a Vertically-Polarized Dipole RFID Tag Antenna Illuminated By a Pair of Switchable Circularly-Polarized Base Station Antennas

K.V.S.Rao, D.-W. Duan and H. K. Heinrich

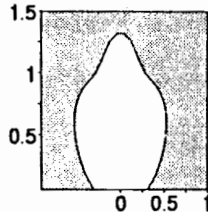
*IBM, Thomas J. Watson Research Center,
P.O.Box 218, Yorktown Heights, NY 10598*

Abstract : Radio frequency identification (RFID) system is a wireless communication system in which the radio link between the base station and the transponders are furnished by the modulated back-scattered waves. One of the most important characteristics of a RFID system is its "read zone", which is defined as the volume inside which the base station (with one or more base station antennas) can communicate with the transponders (or, tags). This paper presents a systematic approach to analyzing the read zone of an RFID system where the transponder antenna is a vertically-polarized half-wave dipole, and the base station antennas are a pair of circularly-polarized antennas.

In the analysis, whether a transponder can be read is determined by whether the voltage induced on the transponder exceeds a threshold voltage, which depends on the properties of the circuit attached to the transponder antenna. The induced voltage is computed based on the principle of receiving antennas, with the assistance of a series of coordinate transformations. The field of the base station antenna is computed using a formula for circularly-polarized microstrip antennas, and the effective height of the transponder antenna is computed using the expression for a half wave dipole. At a given point in space, an induced voltage is calculated for each base station antenna, and the maximum of these (two) voltages is used to compare with the threshold voltage in order to determine if the transponder is read. The dipole tag antenna is oriented vertically throughout the analysis. Contours of the constant induced voltages at the output terminals of the tag with 1 watt input power at the base station antenna are shown in Fig.1. Measurement of the read zone of RFID system has shown good agreement between theoretical analysis and experimental results.



(a) x, z plane (y=0)



(b) y, z plane(x=0)

Fig. 1 Typical Shape of Readzone for a Vertically Polarized Dipole Tag.
(Units are in meters)

Sensitivity Analysis of a Planar Antenna With Respect to FDTD Modeling

Andreas Christ*, Katja Poković, Michael Burkhardt and Niels Kuster

Swiss Federal Institute of Technology (ETH)

8092 Zurich, Switzerland

Phone: +41-1 632 2736, Fax: +41-1 632 1057, e-mail: christ@ifh.ee.ethz.ch

Introduction

The Finite-Difference Time-Domain (FDTD) method has been successfully used for the characterization of far- and near-field parameters for a variety of antenna configurations. Recently, it has gained increasing interest for use in the analysis and optimization of antennas for mobile communications devices (K.L.Virga and Y.Rahmat-Samii, IEEE-MTT, 10, 1879-1888, 1997), (S.-G.Pan et al., IEEE-AP, 10, 1475-1483, 1997). In our study, we have used the FDTD technique to characterize a planar antenna structure which is used for cellular phone base stations in the 900 MHz band. Of particular interest was the sensitivity of the assessed far- and near-field parameters with respect to FDTD specific modeling parameters. Knowledge of the influence of certain modeling parameters on the obtained results is essential for any further optimization process.

The antenna structure consists of a back-plate, a fed center-plate and a capacitively coupled directing plate which have been optimized to achieve the desired bandwidth (maximum dimensions $150 \times 170 \text{ mm}^2$). The entire antenna structure is covered by a radom housing. The thicknesses of the plates and the radom as well as the distances between the plates are much smaller than the plates' surface dimensions.

Objectives

The objective of this study was to characterize the described antenna in the far- and near-field, including far-field pattern, near-field and current distribution, bandwidth and feedpoint impedance. Furthermore, a reliable analysis of the sensitivity of the obtained results with respect to modeling parameters was of major interest.

Methods

The simulations were performed with a Yee-grid based FDTD algorithm. PML boundary conditions were used to truncate the computation domain. In order to properly represent the antenna structure, a computation domain of maximum 2.5 million voxels was used. The antenna model was excited using a voltage source with an internal resistance as described in (R.J.Luebers and H.S.Langdon, IEEE-AP, 7, 1000-1005, 1996), significantly reducing the calculation time. Measurements were performed for validation purposes. The far-field was measured in an anechoic chamber, and near-field scans were taken with the DASY3 measurement system (T.Schmid et al., IEEE-MTT, 1,105-113, 1996).

Results and Discussion

In both the horizontal and the vertical planes, the co- and crosspolar components of the far-field were calculated at a frequency of 915 MHz, which is the center of the specified bandwidth. Far-field patterns were in good agreement with the measurements and were found to be rather insensitive with respect to the modeling parameters. The accurate modeling of the thickness of the radom and its distance to the plates turned out to be crucial for the assessment of the precise feedpoint impedance and the antenna bandwidth. These findings were confirmed by the measurements. The calculated near-field distributions of the E- and H-fields at different distances above the front plate of the antenna were in excellent qualitative agreement with the measurements.

In summary, FDTD showed to be very robust and reliable for the assessment of the far-field patterns and the near-field distributions of the described antenna. The restrictions on gridding were identified and can be considered for further optimization processes of the described type of antenna.

Waveguiding Structures, Circuits, and Discontinuities

E. F. Kuester and D. P. Nyquist

Analysis of Planar Stratified Waveguides in the Presence of Perfect Matched Layers	276
<i>H. Derudder*, D. De Zutter, F. Olyslager, Dept. of Information Technology INTEC, Belgium</i>	
Transformation of Surface Waves in Homogeneous Absorbing Layers	277
<i>R. T. Ling*, J. D. Scholler, P. Y. Ufimtsev, Northrop Grumman Corp., USA</i>	
On the Electrical Properties of Interconnects in the Presence of Perforated Ground Planes	278
<i>A. W. Mathis*, A. F. Peterson, Georgia Institute of Technology, USA</i>	
Full-wave Perturbation Theory for Coupled Stripline Structures	279
<i>D. J. Infante*, D. P. Nyquist, Michigan State University, USA</i>	
Characteristic Impedance and Field Distribution in Coaxial Transmission Lines With Arbitrary Cross Section.....	280
<i>O. P. Perez*, L. C. da Silva, Catholic University of Rio de Janeiro, Brazil</i>	
Network Analysis and Measurement of an Inclined Microstrip-slotline Transition	281
<i>J. P. Kim*, W. S. Park, Pohang University of Science and Technology, Korea</i>	
Full-wave Analysis of Boxed Microstrip Discontinuities in Multilayered Anisotropic Substrates.....	282
<i>R. R. Boix*, E. Drake, M. Horno, University of Sevilla, Spain, T. K. Sarkar, Syracuse University, USA</i>	
Microstrip Bandstop Filters Based on Capacitive Crossover Coupling: Theory and Experiment	283
<i>J. Martel*, F. Medina, M. Horno, University of Sevilla, Spain.</i>	
Interdigital Capacitor in a Multilayered Medium	284
<i>J. F. Kiang*, National Chung-Hsing University, Taiwan, C. H. Chen, National Taiwan University, Taiwan</i>	
Closed Form Solutions for the Coupling Integrals of an Elliptic-to-rectangular Waveguide Junction	285
<i>K. L. Chan*, S. Judah, University of Hull, UK</i>	
A Krylov Subspace Based Solution to the Dielectric Waveguide Junction Problem	286
<i>K. Radhakrishnan*, W. C. Chew, University of Illinois at Urbana-Champaign, USA</i>	

ANALYSIS OF PLANAR STRATIFIED WAVEGUIDES IN THE PRESENCE OF PERFECT MATCHED LAYERS

Henk Derudder*, Daniel De Zutter and Frank Olyslager

Dept. of Information Technology INTEC, St. Pietersnieuwstraat 41, B-9000 Gent, Belgium. Tel: +32 9 264 33 54, Fax: +32 9 264 35 93. E-mail: henkd@intec.rug.ac.be

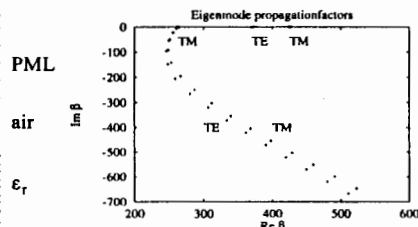
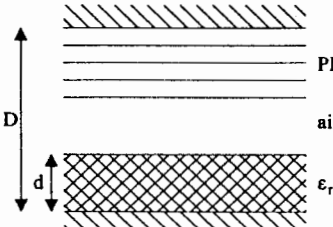
Abstract

This contribution focuses on the eigenmode analysis of planar stratified waveguides. This could be a simple slab waveguide as encountered in many optical problems, a parallel plate waveguide with a planar layered medium between the metallic plates or the dielectric on top of a ground plane type of structure found in MMIC's. As a matter of illustration we will further focus on this last type of structure, as shown in left hand side of the figure. In the lower half of the drawing this figure shows a substrate of thickness d with a relative dielectric constant ϵ_r on top of a ground plane. This open type of waveguide supports a series of discrete TE- and TM-modes and an infinite set of radiation modes. If one wants to use the complete set of eigenmodes to represent a field, these radiation modes often lead to numerical difficulties. Hence, while e.g. investigating the junction between two optical slab waveguides, this problem is sometimes circumvented by introducing an additional metal plane on top of the structure, creating a parallel plate waveguide. The distance D between both planes, is chosen to be very large. The large set of discrete eigenmodes of the parallel plate waveguide now serves as a (good) approximation for the original problem with the radiation modes.

Here we want to put forward a different way of tackling this problem. Rather than to modify the original waveguide problem by introducing an additional metal plane, we propose a planar stratified medium consisting of perfectly matched layers (PML). These PML's have been used with great success as absorbing boundary condition in the Finite Difference Time Domain method. The layers are terminated by a metal plane but when the field has propagated through the PML's its amplitude has decreased dramatically, such that the metal plane could as well be replaced by any other material.

The eigenmode analysis of the final structure consisting of the original waveguide and the PML's was performed by a propagator matrix formalism. A typical result for $d = 9$ mm, $\epsilon_r = 3.0$, and $\omega = 78.5398$ GHz, is given in the right hand side of the figure, showing one half of the complex β -plane for the propagation factors of the different eigenmodes. Without going into much detail, we see that 3 discrete eigenmodes are found on the real axis (one TE-mode and two TM-modes) together with a series of discrete eigenmodes with increasing imaginary part. It turns out that the position of the 3 real eigenvalues is not affected at all by the presence of the PML's. This result clearly illustrates that the PML's only absorb propagating plane waves and do not influence evanescent (non-homogeneous) plane waves. In our context this means that the propagating TE- and TM-modes of the original structure will not be influenced by the PML's. This will only be the case for the radiating ones.

In the oral presentation additional results will be presented as to the influence of the number of PML layers, of their specific constitutive parameters and of the distance between the original substrate and the PML region. We will further present results comparing the fields generated by a line source in the original problem (i.e. the two-dimensional Green's function of the problem) and the fields generated by the same source in the modified configuration.



Transformation of Surface Waves in Homogeneous Absorbing Layers

R.T. Ling, J.D. Scholler, P.Ya. Ufimtsev*

Northrop Grumman Corp.
8900 E. Washington Blvd.
Pico Rivera, CA 90660-3783

*Also with
Electrical Engineering Department
University of California at Los Angeles
Los Angeles, CA 90095-1594

Abstract

Surface waves in homogeneous absorbing layers are studied. The transformation of surface waves into other types of guided waves with frequency or thickness variations is analyzed. A guided wave diagram in the complex plane of the transverse wave number is used in this analysis. It is found that in such layers, the standing damped surface waves do not exist and the *continuous* transformation of surface waves into leaky waves is forbidden. Surface waves can only transform into non-physical waves with field strengths increasing exponentially in both the direction of propagation and in normal direction away from the layer into free space. The frequency at which surface waves transform into non-physical waves can be considered as an upper cutoff frequency of surface waves. At this frequency a surface wave becomes a regular plane wave incident on an absorbing layer under the Brewster angle. Numerical data for trajectories of transverse wave numbers are presented.

On the Electrical Properties of Interconnects in the Presence of Perforated Ground Planes

Andrew W. Mathis* and Andrew F. Peterson

Packaging Research Center
Georgia Institute of Technology
Atlanta, GA 30332-0250

The interconnects within an electronic package are frequently modeled as either a microstrip or stripline transmission line. Both of these transmission lines assume solid ground planes, but often, this is not the case. The manufacturing process may require that the ground planes be perforated, and these perforation may affect the electrical properties of the interconnect.

Previously, the authors have presented a numerical Green's function for analyzing a single microstrip transmission line above a perforated ground plane. The present analysis extends the above work to include multiconductor lines and both microstrip and stripline geometries. The ground planes are assumed to be periodically perforated with rectangular apertures.

The electric field integral equation (EFIE) is used to analyze the interconnects, and an appropriate numerical Green's function accounts for the apertures. The Green's function comprises the "standard" Green's function of a line source above a solid ground plane and a numerical correction factor. This correction factor is obtained by approximating the source as a series of plane waves, and for each plane wave solving the magnetic field integral equation (HFIE) for the equivalent magnetic current above the apertures. The scattered field from each plane wave is then summed to determine the total scattered field.

Data are presented that compare the above method with measured and numerical data obtained through other techniques. Data are also presented that show how the propagation constant and characteristic impedance of the transmission lines vary with proximity to the ground plane(s) and location with respect to the ground plane(s). From this data, design rules can be obtained.

Full-Wave Perturbation Theory for Coupled Stripline Structures

David J. Infante* and Dennis P. Nyquist

Department of Electrical Engineering

Michigan State University

East Lansing, MI 48824

Stripline waveguide structures are commonly used in microwave and millimeter-wave integrated circuit devices and as field applicators for the electromagnetic characterization of materials. Increasing clock speeds and the desire for broadband material measurements require knowledge of the behavior of such devices when driven at high frequency. In addition, the decreasing size of micro-electronic circuits has prompted a need for an understanding of coupling effects and leakage mechanisms which may lead to loss or distortion of signals present in circuits which employ stripline structures.

An integral equation formulation to determine the propagation-mode spectrum of coupled stripline structures has recently been presented by the authors. This method involves the development of a pair of electric field integral equations (EFIEs) which are based upon a Hertzian potential Green's function. These coupled EFIEs are converted to matrix form and solved numerically via a Galerkin's method using Chebychev basis functions.

Solution of the coupled strip EFIEs is a formidable task, both analytically and numerically. In order to reduce the complexity associated with this solution, a full-wave perturbation theory for coupled strips has been developed based on the full-wave EFIE formulation. For this method, a pair of modified integral equations are developed

$$\lim_{y \rightarrow h_1} \left\{ \int_{C_1} dx \tilde{k}_{1p}^{(0)} \cdot \left(k_0^2 + \tilde{\nabla} \tilde{\nabla} \cdot \right) \left[\int_{C_1} \tilde{g}_c(x, y | x', h_1) \cdot \tilde{k}_{1p}(x') dx' + \int_{C_2} \tilde{g}_c(x, y | x', h_2) \cdot \tilde{k}_{2p}(x') dx' \right] \right\} = 0$$

$$\lim_{y \rightarrow h_2} \left\{ \int_{C_1} dx \tilde{k}_{2p}^{(0)} \cdot \left(k_0^2 + \tilde{\nabla} \tilde{\nabla} \cdot \right) \left[\int_{C_1} \tilde{g}_c(x, y | x', h_1) \cdot \tilde{k}_{1p}(x') dx' + \int_{C_2} \tilde{g}_c(x, y | x', h_2) \cdot \tilde{k}_{2p}(x') dx' \right] \right\} = 0$$

Here $\tilde{\nabla}$ is the transform-domain differential operator, \tilde{g} is the transform-domain Green's function, and $\tilde{k}_{mp}^{(0)}$ is the current of the p th propagation mode along the isolated m th strip, having propagation constant $\pm \zeta_p^{(0)}$, and satisfying the isolated EFIE. In the case of loose, nearly degenerate coupling, the isolated eigenmodes of different strips are nearly equal, and it is assumed that the current distributions of the coupled system modes are approximately weighted replicas of the corresponding isolated currents.

In addition to reducing the time required for computation of current distributions, this method provides insight into the nature of coupling effects. Numerical results obtained using the perturbation method will be compared to those obtained using the method of moments solution of coupled EFIEs presented previously. Results will include current distributions associated with various modes, and propagation-mode dispersion characteristics indicating cutoff frequencies of higher order modes.

Characteristic Impedance and Field Distribution in Coaxial Transmission Lines With Arbitrary Cross Section

Oscar Polanco Perez and Luiz Costa da Silva
Catholic University of Rio de Janeiro
Rua Marques de Sao Vicente 225, Gavea, RJ, Brazil

A simple and accurate technique, based on dyadic Green's functions and the moment method, is proposed for the determination of the characteristic impedance and field distribution in coaxial cables with arbitrary cross section.

For the computation of the fields, the line is replaced by an equivalent structure, composed by the line and a rectangular waveguide circumscribing the line. In the equivalent structure, the contours of the inner and outer conductors are approximated by polygons.

The surface current densities, induced on both conductors, are determined by the moment method, using, as basis functions, pulses with domain coinciding with each side of the polygons:

$$\bar{J}_z = \sum_i \alpha_i p_i e^{-\mu_i} \bar{a}_i \dots \quad (1)$$

where z is the direction along the axis of the cable, k is the free space wave number, p_i are pulse functions and α_i are coefficients to be determined.

In the determination of α_i , the electric field generated by \vec{J}_i , as a function of α_i , are computed using the dyadic Green's function of the rectangular waveguide. The z component of the field results identically zero. Applying the boundary conditions to the polygonal contours, and testing functions equal to the basis functions, a homogeneous system of equations, with null determinant, is obtained, for the determination of α_i . Choosing $\alpha_i = 1$, the system is solved. Once α_i are known, the fields are computed, using, again, the dyadic Green's functions of the rectangular waveguide. The characteristic impedance is obtained from $Z_c = V/I$.

As examples of applications, it was considered, initially, a circular coaxial cable with known impedance of 50 Ohm. Using the present method, and approximating the contours of the conductors by polygons of 40 sides, a value of 49.68 Ohm was obtained for the impedance. The computed electric field showed an error less than 6% (if compared to exact analytical values), except at the boundary of the conductors. As a second example, the characteristic impedance of a rectangular coaxial line, with dimensions of 2.0x1.0 mm and 6.0x3.0 mm was calculated. A value of 50.46 Ohm was obtained. The value of this impedance, using an approximate, semi-analytical method (O. R. Cruzan and R. Garver, IRE Trans. on MTT, 488-495, 1965) was 50.54 Ohm.

Network Analysis and Measurement of an Inclined Microstrip-Slotline Transition

Jeong Phillip Kim* and Wee Sang Park

Department of Electronic and Electrical Engineering, Microwave Application Research Center, Pohang University of Science and Technology, San 31 Hyoja-dong, Nam-gu, Pohang, Kyungbuk 790-784, Korea

The transition between a microstrip line and a slotline has been used as a coupling structure in the design of multilayer microwave and millimeter-wave circuits. One example of the transition is found in the feed structure of a tapered slot antenna. Tapered slot antennas are usually fabricated on a thin substrate (h) having a low dielectric constant ϵ_r to reduce the cross-polarization in the radiation. For the slotline to be matched with the microstrip feed line whose width is W_m , the width of the slotline W_s should be very narrow, which is sometimes difficult to fabricate. One way to overcome the problem is to employ a quarter-wave transformer or a tapered line section. However, this attempt may result in a more complicated circuit and a narrow bandwidth.

This paper proposes an inclined microstrip-slotline transition to solve the matching problem. By using the modeling theory (J. P. Kim and W. S. Park, *Microwave Opt. Tech. Lett.*, vol. 15, no. 4, pp. 256-260, Jul. 1997.), a proper choice of the inclination angle θ_s between the slotline and microstrip line leads to a perfect impedance matching without any extra circuitry. One test circuit board containing a cascade of a microstrip-slotline transition and a slotline-microstrip transition was designed and fabricated. The structure parameters are $\epsilon_r = 2.2$, $h = 31 \text{ mil}$, $W_m = 2.4 \text{ mm}$, $W_s = 0.35 \text{ mm}$, $\theta_s = 60^\circ$, and the slotline length between the transitions is 50 mm. The stub lengths of microstrip line open and slotline short are 5.03 mm and 5.75 mm, respectively. The cascade was built for the convenience of measurement. The measured characteristics of the cascade are shown in Figure 1 along with the computed results from the network analysis. It is observed that the two results agree reasonably, indicating the validity of the modeling theory. Based on the network analysis and measurement, a linearly tapered slot antenna with antenna length 100 mm and flared angle 10° fed by an inclined microstrip-slotline transition was designed and fabricated, and the return loss was measured. Figure 2 shows the broadband characteristics of the antenna.

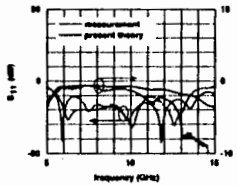


Figure 1

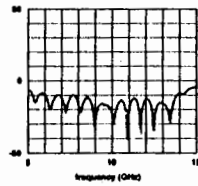


Figure 2

Full-wave analysis of boxed microstrip discontinuities in multilayered anisotropic substrates.

Rafael R. Boix⁽⁺⁾, Enrique Drake⁽⁺⁾, Manuel Horno⁽⁺⁾, Tapan K. Sarkar⁽⁺⁺⁾

(+) Facultad de Física, Avda. Reina Mercedes s/n, 41012, Sevilla, Spain.

E-mail: boix@cica.es. Telephone number: 34-54552891. Fax: 34-54239434.

(++) Dpt. Electrical & Computer Eng., 121 Link Hall, Syracuse NY 13244.

Many materials used as substrates for microwave integrated circuits or printed-circuit antennas exhibit dielectric anisotropy [N. G. Alexopoulos, IEEE-MTT, 10, 847-881, 1985]. Although many papers have been published dealing with the full-wave characterization of microstrip discontinuities on isotropic dielectric substrates, there are very few references in which the analysis of microstrip discontinuities on anisotropic dielectric substrates is addressed [S. S. Toncich et al., IEEE-MTT, 12, 2067-2073, 1993][Y. Chen et al., IEEE-MTT, 10, 1945-1950, 1994].

In this work the authors obtain the frequency-dependent scattering parameters of several boxed microstrip discontinuities in the case in which the metallizations are embedded in a multilayered substrate consisting of dielectric materials with biaxial anisotropy. As a first step towards the calculation of the scattering parameters, the microstrip lines involved in the discontinuities are excited by delta-gap generators, and the current densities on the metallizations are subsequently determined by solving an electric field integral equation via Galerkin's method in the spectral domain. Once the currents on the microstrip lines are known, matrix pencil method is used for de-embedding the scattering parameters as explained in [T. K. Sarkar et al., Int. Jour. MIMICAE, 3, 135-143, 1992]. The spectral dyadic Green's function for the boxed multilayered anisotropic substrate is computed by means of the recurrent algorithm described in [F. Medina et al., IEEE-MTT, 4, 504-511, 1989]. A novel technique has been developed for the efficient computation of the infinite sumations of infinite integrals appearing in the expressions of the elements of Galerkin's matrix. This technique is based on the numerical interpolation of the asymptotic behaviour of the spectral dyadic Green's function [R. R. Boix et al., JEWA, 10, 1047-1083, 1996].

The results obtained by the authors focus on studying microstrip discontinuities for which the effect of substrate anisotropy is specially relevant, such as coplanar microstrip gaps, microstrip gaps with overlay microstrip resonators [E. K. L. Yeung et al., 1, 143-149, 1995], and non-coplanar overlap microstrip gaps [M. J. Tsai et al., 3, 330-337, 1997]. All these microstrip discontinuities appear in bandpass microstrip filters, and these filters might operate out of the expected frequency band if substrate anisotropy were neglected when designing the filters.

Microstrip bandstop filters based on capacitive crossover coupling : theory and experiment

Jesús Martel*, Francisco Medina, Manuel Horno

Microwave Group, Dpt. of Electronics and Electromagnetism,

University of Sevilla, Avda. Reina Mercedes s/n, 41012, Sevilla, Spain.

E-mail: medina@cica.es. Telephone number: 34-54552891. Fax: 34-54239434.

Bandstop filters can be implemented in a simple way by using shunt stubs along a transmission line (G.L. Matthaei et al., *Microwave Filters...*, Artech House, 1980). However, this design presents some problems when microstrip technology is used, in particular if we are dealing with relatively narrow band filters (D.M. Pozar, *Microwave Engineering*, Addison Wesley, 1990). In these cases the required values of the characteristic impedances of the stub resonators often become too high to be realized in practice (because they lead to extremely small strip widths). In this communication, the authors propose a microstrip bandstop filter configuration which is essentially based on the same idea underlying the conventional stub resonator filter. However, the new configuration makes it possible to avoid the aforementioned limitation. In this filter, instead of shunt connected stubs, we use capacitively coupled resonant microstrip sections (C. Person et al., *European Mic. Conference*, pp. 1176-1180, 1992). Crossover coupling is provided by printing the main line and the resonators on both sides of the same substrate. This structure is placed on another dielectric layer with one of its faces metallized and grounded. The thickness of the substrate supporting the metallized pattern and its dielectric constant introduces additional flexibility in the design. This substrate can be chosen in such a way that the required characteristic impedances for the microstrip resonators are achievable with reasonable values of the microstrip widths.

A critical point in the design process of this type of filter is the determination of the electrical parameters of the equivalent circuit for the existing crossover discontinuities. The series and parallel capacitances of the π -equivalent circuit for this discontinuity are computed here by using a simple and accurate quasistatic analysis based on the excess charge technique (J. Martel et al., *IEEE-MTT*, 42, pp. 424-432, 1994). This analysis is good enough for the frequency range considered in this work and is much less computationally intensive than full-wave techniques (J.F. Carpentier et al., *IEE Proc., pt. H*, 142, pp. 275-281, 1995). The steps followed in the design process will be detailed in the presentation. This design can be carried out by using design charts or by computer optimization. We have built and measured two prototypes of third order Butterworth bandstop filters (central frequency $f_c = 6$ GHz; BW=15%). The agreement between the theoretical simulation of the filter and the measured response is quite good.

Interdigital Capacitor in a Multilayered Medium

*Jean-Fu Kiang and *Chun-Hsiung Chen

*Department of Electrical Engineering

National Chung-Hsing University

Taichung, Taiwan 402, ROC

*College of Electrical Engineering

National Taiwan University

Taipei, Taiwan 106, ROC

Interdigital capacitors are widely used in microwave integrated circuits and slow wave devices. Usually the dimension of an interdigital capacitor is much smaller than one wavelength, hence the quasi-static approach can be applied to calculate its lumped capacitance. For capacitors with simple conductor geometries, the conformal mapping technique or moment method in the spatial domain can be used to calculate the potential and the associated charge distributions. With complicated conductor geometries, segmentation technique can be used to treat the capacitor as several simple blocks interconnected. The total capacitance is the sum of the contribution from each block with corrections accounting for the fringing fields. The empirical rules are usually applied at this stage, and the accuracy can be doubtful if the geometrical parameters are too complicated.

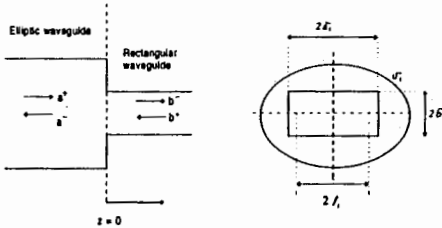
The main contribution of this work is to develop a rigorous solution to calculate the capacitance of an interdigital capacitor embedded in a multilayered medium. To derive the Green's function in the spectral domain, we first expressed the potential in each layer as a two-dimensional Fourier integral. Each spectral component consists of an upward decaying part and a downward decaying part. A coupling coefficient is defined to simplify the derivation. By imposing the continuity conditions between contiguous layers, a Green's function is obtained to express the potential distribution in each layer in terms of the charge distribution on the conductor surfaces.

Next, the method of moments is applied to solve for the charge distribution from which the capacitance is obtained. The self terms are extracted and calculated in the spatial domain to accelerate numerical convergence. The factors analyzed include the layered thickness, permittivity, finger number, finger width, slot width, and so on.

Closed form solutions for the coupling integrals of an elliptic-to-rectangular waveguide junction

K.L. Chan* and S.R. Judah
Dept. of Electronic Engineering, University of Hull, Hull, HU6 7RX

A concentric waveguide junction formed by a larger elliptic waveguide and a smaller rectangular waveguide is analysed using the mode matching method. By expressing the modal fields in the elliptic waveguide in terms of trigonometric functions, closed form expressions for evaluating the coupling integrals are derived.



Expressions for converting the Mathieu functions to trigonometric series are not available in the literature, however, by means of an integral relationship between Mathieu functions and trigonometric functions, we obtained expressions that evaluate the product of a radial and a circumferential Mathieu functions as a trigonometric series. For instance,

$$Je_{2p}(h, u)Se_{2p}(h, v) \cong \sqrt{\frac{\pi}{2}} \frac{(-1)^p}{N} \sum_{k=0}^{N-1} \cos(\beta \cos(kD)z) \cos(\beta \sin(kD)y) Se_{2p}(h, kD)$$

where $D = \frac{2\pi}{N}$, $S(\cdot)$ and $J(\cdot)$, are the circumferential and radial Mathieu functions, respectively, $\beta = hl$ where l is the semi-focal length of the elliptic waveguide.

Enforcing the boundary conditions at the junction plane, followed by the mode matching procedure, we get a modal coupling equation for the transverse electric fields as

$$\begin{bmatrix} a^{\text{TE}} \\ a^{\text{TM}} \end{bmatrix} = \begin{bmatrix} [\mathbf{H}] & [\mathbf{K}] \\ [\mathbf{G}] & [\mathbf{F}] \end{bmatrix} \begin{bmatrix} b^{\text{TE}} \\ b^{\text{TM}} \end{bmatrix}$$

where a, b are the modal coefficients of the elliptic and rectangular waveguides respectively. H_{mnpq} , K_{mnpq} , G_{mnpq} and F_{mnpq} are respectively the TE-TE-mode, TE-TM-mode, TM-TE-mode and TM-TM-mode coupling coefficients. K_{mnpq} is always equal to zero, which is well-known, and the other coupling coefficients can be evaluated by a general form

$$X_{mnpq} = N_{mn} N_{pq} \sum_{k=0}^{N-1} \Xi_{mn, k} \Omega_k$$

where Ω is a function of the waveguides dimensions and cutoff-wavenumbers, and it has different forms for different types of coupling coefficients, Ξ is the series coefficient that arises from the conversion of Mathieu functions to trigonometric functions and has the form

$$\Xi_{mn, k} = \sqrt{\frac{\pi}{2}} \frac{(j)^m}{N} S_m(h_{mn}, kD)$$

The closed form solutions obtained are helpful for the rapid computation of the coupling coefficients and this is invaluable in the design of dual mode waveguide filters etc., using elliptic apertures.

A Krylov Subspace Based Solution to the Dielectric Waveguide Junction Problem[†]

KALADHAR RADIHKRISHNAN* AND WENG CHO CHEW

CENTER FOR COMPUTATIONAL ELECTROMAGNETICS

DEPARTMENT OF ELECTRICAL AND COMPUTER ENGINEERING

UNIVERSITY OF ILLINOIS

URBANA, IL 61801

Prior to the advent of digital computers, analytic and variational techniques were used to analyze waveguide discontinuities. More recently, with the developments in the computational power of the computers, such discontinuities are routinely studied using numerical techniques.

In this paper, we use a Krylov subspace based algorithm to solve for the reflected and transmitted field from a dielectric waveguide junction. The finite difference formulation is used to obtain a governing equation based on the transverse component of the vector wave equation. The resulting equation can be expressed as

$$\bar{\mathcal{L}}_e \mathbf{E}_s + \frac{\partial^2}{\partial z^2} \mathbf{E}_s = \mathbf{s} \delta(z),$$

where $\bar{\mathcal{L}}_e$ is a linear operator. The generalized formal solution for such an equation in terms of operators is

$$\mathbf{E}_s = \frac{1}{2i} \bar{\mathcal{L}}_e^{-\frac{1}{2}} \cdot e^{i\bar{\mathcal{L}}_e^{\frac{1}{2}}|z|} \cdot \mathbf{s}.$$

In the presence of a junction, the field on either side of the junction can be written as

$$\mathbf{E}_{1s} = \frac{1}{2i} \bar{\mathcal{L}}_{1e}^{-\frac{1}{2}} \cdot \left[e^{i\bar{\mathcal{L}}_{1e}^{\frac{1}{2}}|z+d|} + e^{i\bar{\mathcal{L}}_{1e}^{\frac{1}{2}}z} \cdot \bar{\mathbf{R}}_{12} \cdot e^{i\bar{\mathcal{L}}_{1e}^{\frac{1}{2}}d} \right] \mathbf{s}_1,$$

$$\mathbf{E}_{2s} = \frac{1}{2i} \bar{\mathcal{L}}_{2e}^{-\frac{1}{2}} \cdot e^{i\bar{\mathcal{L}}_{2e}^{\frac{1}{2}}z} \cdot \bar{\mathbf{T}}_{12} \cdot e^{i\bar{\mathcal{L}}_{2e}^{\frac{1}{2}}d} \cdot \mathbf{s}_1.$$

The transverse electric field components can be used to derive an expression for the transverse magnetic field components. Then, by matching the tangential electric and magnetic field at the interface, we can obtain an expression for the reflected and transmitted field from the junction.

In the above expressions, $\bar{\mathcal{L}}_{1e}$ and $\bar{\mathcal{L}}_{2e}$ are represented by large, sparse asymmetric matrices. Carrying out matrix operations on large matrices is impractical in view of the high complexity involved. However, by using a Krylov subspace based algorithm, the sparsity of these matrices can be exploited to reduce them into a matrix of much smaller size. In view of the asymmetric nature of the matrices, the bi-Lanczos algorithm is used to reduce the large matrices ($N \times N$) to a tridiagonal matrix ($M \times M$). Typically M scales as \sqrt{N} . By using these tridiagonal matrices in place of the large matrices, the algorithm can be carried out at a complexity of just $O(N^{1.5})$.

[†]This work was supported by the MURI Program under grant F49620-96-1-0025, the NSF under grant ECS 93-02145, and the ONR under grant N00014-95-1-0872.

Biological Effects and Medical Applications

A. Taflove and O. P. Gandhi

Multigrid FDTD Code for Calculating Microwave Absorption Pattern in Human Head Radiated by Hand-held Antennas AP
R. Quintero-Illera, Z. Yun, M. J. White, M. F. Iskander, University of Utah, USA*

Application of FDTD and RGFIM to EM Interaction with Biological Tissue: A Comparison AP
M. A. Jensen, Brigham Young University, USA*

Visualization on SAR in a Monitoring System for Electromagnetic Influences on Humans in Cellular Telecommunications AP
L. Ololoska-Gagoska, S. Loskovska, M. Kacarska, L. Grcev, University Sts. Kiril and Metodij, Macedonia*

Automated SAR Measurements for Compliance Testing of Cellular Telephones AP
Q. Yu, M. Aronsson, D. Wu, O. P. Gandhi, University of Utah, USA*

Analysis of Coupling Phenomena in a TEM Concentric Array of Applicators Radiating into a Layered Biological Tissue Model AP
K. S. Nikita, G. D. Mitsis, National Technical University of Athens, Greece*

An FDTD Algorithm for Transient Propagation in Biological Tissue with a Cole-Cole Dispersion Relation AP
J. W. Schuster, R. J. Luebbers, Pennsylvania State University, USA*

Virtual Reality Based System for Monitoring Electromagnetic Influences on Humans in Cellular Telecommunications 288
L. Ololoska-Gagoska, S. Loskovska, M. Kacarska, L. Grcev, University Sts. Kiril and Metodij, Macedonia*

2-D FDTD Study of Fixed-focus Elliptical Reflector System for Breast Cancer Detection: Frequency Window for Optimum Operation AP
M. Popovic, S. C. Hagness, A. Taflove, Northwestern University, USA, J. E. Bridges, Interstitial, Inc., USA*

Variation of Emergency-room Electromagnetic-interference Potential AP
D. Davis, McGill University, Canada, B. Skulic, B. Segal, Jewish General Hospital, Canada, P. Vlach, T. Pavlasek, McGill University, Canada*

Virtual Reality Based System for Monitoring Electromagnetic Influences on Humans in Cellular Telecommunications

Ololoska-Gagoska L., *Loskovska S., Kacarska M., Grcev L.

University "Sts. Kiril and Metodij", Faculty of Electrical Engineering
Karpov II bb, 91000 Skopje, Macedonia
e-mail: suze@ereb.mf.ukim.edu.mk

With the enormous increment of supply and the growing use of electricity, in the recent time, there has been comprehension that the electric and magnetic fields (EMF) arising from the supply and use of electricity, may have adverse effects on human health. Furthermore, there has been an increasing public concern about the health risk of EMF waves emitting from cellular devices. Naturally, this awareness has spawned a growth in the wireless communications arena. Because portable handsets operate in close proximity to a human being, one particularly important consideration involves the interaction of the radiated EMF fields with the nearby biological tissue (S.P.A. Bren, IEEE Eng. in medi. and biology, 109-115, May/June 1995). To support the better understanding of EM influences, a system for monitoring EM influences on humans in living and working environments is underdevelopment. The system based on virtual reality (VR) offers to user to create and to investigate working and living environments, and to make judgments about the functional characteristics of devices placed in them. Additionally it considers the influences of EM processes to humans, synthesizing performances of 3D graphics interfaces with mathematical methods for determination of human's exposure parameters to EM fields.

The paper will present the visualization of EM influences on a human head while the cellular phone is used. A fundamental parameter when discussing the health risks of EM power absorption in the human body is the specific absorption rate (SAR). The SAR is the mass-normalized rate of EM energy absorbed by the body. At a specific location (x,y,z) SAR may be defined by: $SAR = \sigma |E|^2 / \rho$ [W/g], where σ is the tissue conductivity, ρ is the tissue mass density, E is the RMS value of the total field strength in the body.

In our near-field simulations, the scattering object is the human head, modeled by cubic cells with equal cell size with inhomogeneous dielectric constant and conductivity. The radiation source of the cellular device is modeled by an equivalent dipole antenna radiated a power of 0.6 W at frequency of 900 MHz. For numerical computations of the electric field and SAR distribution the finite difference approach is used.

Obtained results are similar like those report in the literature. The maximum SAR of 1.48 mW/g induced in the head is found for the distance of 2 cm, which is below the protection value of 1.6 mW/g for the ANSI/IEEE standards. The Figure 1 show SAR distribution obtained on the horizontal section of the human head model.



Figure 1

Wire and Active Antenna Elements

J. T. Williams and S. S. Gearhart

Multielement Top-loaded Vertical Antennas with Mutually Isolated Input Ports	290
<i>H. D. Foltz*, J. S. McLean, E. Guzman, G. E. Crook, University of Texas - Pan American, USA</i>	
Polarization-agile Wire Antenna Elements	291
<i>S. S. Gearhart*, University of Wisconsin, USA</i>	
Mode 0 Spiral Antenna Analysis & Design	292
<i>M. A. Acree*, V. P. Cable, Lockheed Martin Skunk Works, USA</i>	
Bandwidth Enhanced Normal Mode Helical Antennas	293
<i>S. D. Rogers*, J. C. Young, C. M. Butler, Clemson University, USA</i>	
Analysis and Design of High-temperature Superconducting Leaky-wave Antennas	294
<i>N. Li*, J. T. Williams, D. R. Jackson, University of Houston, USA</i>	
Using Voice-band Near Fields for Low-probability-of-intercept Communications	295
<i>E. K. Miller*, USA</i>	
Radiation of the Shielded Spheroidal Antenna	296
<i>E. D. Vinogradova*, P. Smith, University of Dundee, UK</i>	
Linear Analysis of Two Injection-locked Active Antennas	297
<i>C. Hsiao*, T. Chu, National Taiwan University, Taiwan, Republic of China</i>	
Mutual Coupling Effect on Injection-locked Active Antenna Array	298
<i>Y. Yang*, T. Chu, National Taiwan University, Taiwan, Republic of China</i>	
A 37 GHz Double Slot	299
<i>L. Desclos*, NEC Corporation, Japan</i>	

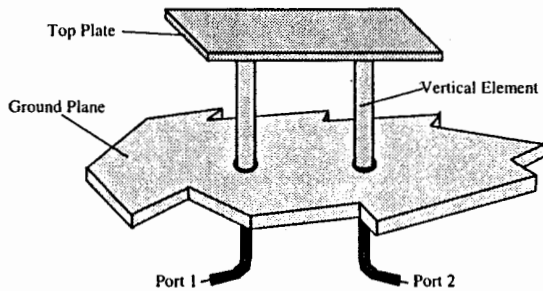
MUTIELEMENT TOP-LOADED VERTICAL ANTENNAS WITH MUTUALLY ISOLATED INPUT PORTS

H.D.Foltz, J.S.McLean, E.Guzman, G.E.Crook
Electrical Engineering, The University of Texas - Pan American
1201 West University Drive, Edinburg, TX 78539

In full-duplex communications systems, it is desirable to maintain high isolation between the transmit and receive channels. Most of this isolation is obtained through the use of filters and duplexers; however, the filter/duplexer requirements can be relaxed if separate, mutually isolated antennas are used. On the other hand, compact, colocated antenna structures are desirable for mobile, handheld, or portable operation.

One structure which can provide high isolation at a specified frequency consists of two or more vertical elements over a ground plane and under a single top-loading plate, as shown below. The geometry is similar to a folded antenna, but in this case each element is given a separate input port. It can be shown that in order for the ports to be isolated, both loop mode and monopole mode radiation must be present. The top plate serves the dual purpose of closing the loop and providing capacitive loading to allow alignment of the loop and monopole mode responses.

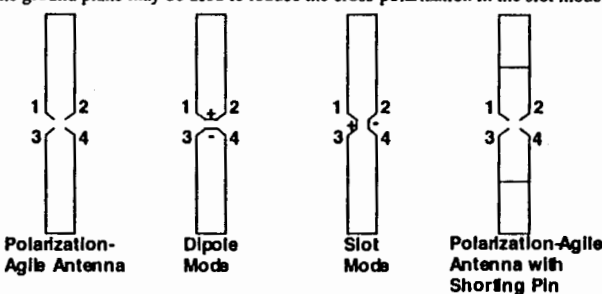
Design rules will be presented, along with measured data for input impedance, port-to-port isolation, efficiency, and radiation patterns. Experimental data on isolation degradation in the presence of nearby scatterers will also be presented.



POLARIZATION-AGILE WIRE ANTENNA ELEMENTS

Steven S. Gearhart
University of Wisconsin-Madison
Madison, WI 53706
gearhart@engr.wisc.edu

A new polarization-agile wire antenna element is presented. A polarization-agile antenna may be thought of as two orthogonally-polarized antennas that are isolated from each other. Using these two orthogonal antenna, a signal of any polarization may be transmitted through control of the relative magnitude and phase of the signal that is fed to each individual element. In this case, a single wire antenna with four feedpoints is used as the polarization agile antenna element. If feeds 1 and 2 are connected together and feeds 3 and 4 are connected together, the antenna radiates in the dipole mode. As expected, the radiation pattern of the dipole mode is polarized parallel to the antenna and the antenna the first resonance occurs at a frequency where the antenna approximately a half of a wavelength long. If feeds 1 and 3 are connected along with feeds 2 and 4, the antenna radiates in the slot mode. The slot-mode radiation pattern is polarized perpendicularly to the wires of the antenna and is resonant at a frequency where the antenna is $0.8\lambda_0$ long. A polarization-agile wire antenna with a length of 48 cm and a width of 8 cm has dipole-mode resonant frequencies of 2.37 and 7.33 GHz with respective impedances of 50 and 63 Ω according to NEC2. Note that only the low-impedance 1st and 3rd resonances of the dipole mode are considered. The first low-impedance (17 Ω) slot mode resonance occurs at 4.90 GHz. The resonant frequencies of the slot and dipole mode must converge for the antenna to be polarization agile at a given frequency. It has been found that the resonant frequencies and impedances of the two modes may be tuned using a shorting pin. Placing shorting pins 13.6 cm from the center of the antenna results in resonant frequency of 7.07 GHz for both the dipole (82 Ω) and the slot modes (60 Ω), making this antenna ideal for systems that require polarization agility. The theoretical cross-polarization levels of the polarization-agile antenna with shorting pins are -18dB for the slot mode and -34 dB for the dipole mode. The antenna may be fed using four coaxial cables connected to a ground plane one-quarter of a wavelength behind the antenna element. In addition to limiting the radiation to one half space, the ground plane may be used to reduce the cross-polarization in the slot mode.



Mode 0 Spiral Antenna Analysis & Design

M. A. Acree* & V. P. Cable
Lockheed Martin Skunk Works
Palmdale, CA 93599

Recent experimental work by Wang, et al. [AP-S Symp., ses. 95-6, Montreal, 1997] has shown that monopulse type null patterns are easily achieved from a 2-arm spiral by feeding both arms of the spiral with the same amplitude and phase referenced to the groundplane (mode-0). This straight forward approach seems ideally suited for creating a wideband monopulse antenna for circular polarization using mode-0 & mode-1. Potential DF applications which depend on a single small aperture with wide bandwidth and monopulse operation would benefit from the simplicity of such an antenna. However, experiments by Wang, et al., have indicated that the mode-0 spiral bandwidth was only a fraction of the mode-1 bandwidth normally attributed to a spiral.

This paper presents numerical & measured results for an improved monopulse spiral using mode-0 & mode-1 configurations. Bandwidth performance of mode-0 was adjusted using geometry and materials changes, and improved bandwidth tracking of mode-0 & mode-1 was achieved. The effects of these changes were investigated using MOM/FMM & FDTD numerical techniques, and confirming measurements were made on a simple 2-arm spiral breadboard. Data showing numerical as well as measured results will be presented. Data is also presented for a T-fed mode-0 spiral which exhibits improved impedance bandwidth characteristics over a center-fed circular patch antenna.

Bandwidth Enhanced Normal Mode Helical Antennas

Shawn D. Rogers*, John C. Young, and Chalmers M. Butler

Department of Electrical and Computer Engineering
105 Riggs Hall, Clemson University, Clemson, SC 29634-0915

Many modern wireless communication systems require low-profile antennas. To meet this requirement, we consider the helical antenna operating in the normal mode. A normal mode helix and a straight wire antenna having approximately the same wire length exhibit similar input impedance and far field patterns. One drawback to the helix operating in the normal mode is that its bandwidth is too limited for many applications. To increase the bandwidth, we have considered several potential remedies, one of which is discussed in this paper. It is well known that adding additional parasitic straight wires on either side of a driven dipole antenna may increase the bandwidth of the dipole (J.L. Wong and H.E. King, AP-21, no. 5, 725-727, Sept. 1973). One must be especially careful, however, to choose parasitic elements with the proper length and spacing. We use this basic idea to increase the bandwidth of the helical monopole. A structure similar to the sleeve dipole but applied to the helix has been used to design dual frequency antennas (P. Eratulii, et. al., Electronics Letters, v. 32, no. 12, 1051-1052, June 1996). The helix and its helical sleeve are both driven in the antenna of this reference. Several novel antenna structures are considered such as a driven helical antenna adjacent to parasitic helices and straight wires. Another candidate structure consists of a driven helix with helical parasites inside or outside of the driven element, which has the added benefit of conserving space. In any case, due to the large number of parameters in a helix, it is more difficult to design a broadband sleeve helical antenna than is the case for a sleeve dipole. It is not feasible to obtain optimum values of parameters by trial and error. Thus we employ a genetic algorithm routine (D.L. Carroll, A FORTRAN Genetic Algorithm Driver, <http://www.staff.uiuc.edu/~carroll/ga.html>) and efficient integral equation solution techniques to optimize the antenna system for bandwidth. Having an efficient numerical solution technique is necessary for this problem since the geometry of the antenna is redefined for each structure evaluated by the genetic algorithm. Since these antennas have a high degree of curvature, their solutions generally require a large number of unknowns for representing the geometry. An efficient solution technique which gets around this problem is used (S.D. Rogers and C.M. Butler, APS Symposium Digest, vol. I, 68-71, July 1997).

Analysis and Design of High-Temperature Superconducting Leaky-Wave Antennas

Na Li, Jeffery T. Williams, and David R. Jackson,

Applied Electromagnetics Laboratory
Department of Electrical Engineering
University of Houston
Houston, TX 77204-4793

We have developed a new class of leaky-wave antenna by taking advantage of the low loss and unique field penetration properties of high temperature (HTC) superconductors. These antennas are based upon the concept of creating a radial wave guiding structure that has a thin superconducting film through which the fields *leak*. The rate of leakage, and hence the radiation pattern, is controlled by appropriately tailoring the dimensions of the structure. These high-gain leaky-wave antennas are ideal for many millimeter-wave point-to-point communication applications. Their uniform monolithic geometry greatly simplifies the fabrication process, and these antennas do not require a complicated feed network, a simple waveguide feed is sufficient. This class of antenna is distinct in that the leakage effect upon which they are based is unique to superconducting materials. Therefore, the operation of these antennas is dependent upon the use of thin superconducting films. As is typical of many leaky-wave antenna designs, the radiation patterns of these structures can be scanned with frequency, but since the leakage is also dependent upon the intrinsic electrical properties of the superconducting film, the patterns can also be scanned with temperature.

In this presentation we will summarize the transverse equivalent network model that we developed to analyze the superconducting leaky-wave antennas, and we will present closed-form expressions that can be used for design. In particular, we will present results for the leaky-wave propagation constant, antenna efficiency, radiation patterns, bandwidth, and input return loss. Since these designs are most appropriate for the millimeter-wave frequency range, examples will be given for 94 GHz designs using YBaCuO superconducting films on LaAlO substrates. Particular attention will be given to the radiation and feed characteristics of these antennas and those issues most associated with applications.

USING VOICE-BAND NEAR FIELDS FOR LOW-PROBABILITY-OF-INTERCEPT COMMUNICATIONS

Edmund K. Miller

3225 Calle Celestial, Santa Fe, NM 87501-9613, emiller@popmail.esa.lanl.gov

Electromagnetic-field communication is normally based on propagating far fields. Whether antenna near fields might instead be used for limited-distance, low-probability-of-intercept (LPI) communication at voice-band frequencies is the subject of this paper. Straightforward analysis using closed-form expressions for the fields of electric dipoles (ED) and magnetic dipoles (MD) suggests that voiceband-frequency communication over distances of a few 10's of km may be feasible.

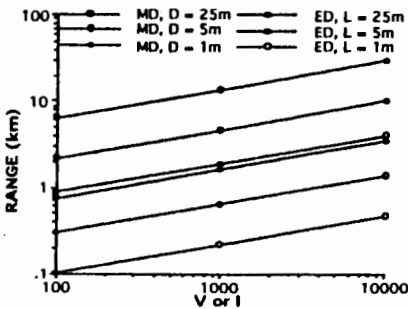
Producing useful electromagnetic fields at voiceband depends on the $1/R^2$ to $1/R^3$ near-field components. While the radiation field produced by 1-10 m size antennas at ULF frequencies will be insignificant because of the $(L/\lambda)^2$ fall off, the total field can remain substantial because of the reactive near field. For example, one cause of the buzzing heard on a car radio as the vehicle travels in the vicinity of a 60-Hz power line may be the near fields which rapidly attenuate in volume as the vehicle moves away from the line.

In considering the possibility of using ULF for LPI communications over a limited range, it is instructive to examine the field expressions for a short electric dipole and a small magnetic loop, as candidates for transmitting antennas. Using standard expressions for their fields and impedances, and assuming that an electric-field strength of $\sim 10 \mu\text{V/m}$ provides a usable signal, it can be shown that the potential range in meters varies with the antenna parameters as

$$r_{ED} = \left(\frac{5 \times 10^4 V_0 L^2}{[\log(L/a) - 1]} \right)^{1/3} = 22(V_0 L^2)^{1/3}$$

$$r_{MD} = \left(\frac{2.9 \times 10^{11} V_0 D^2}{[jD \{ \log(4D/a) - 1 \} / 2 + 10^3 R_{loss}]} \right)^{1/3} = 160.6(I_0 D^2)^{1/3}$$

and for an ED of length L and MD of diameter D , respectively, with a the wire radius, V_0 the excitation voltage and R_{loss} the resistive loss in the loop (assumed zero here) for which some results are shown below.



RADIATION OF THE SHIELDED SPHEROIDAL ANTENNA

E.D. Vinogradova* & P.D. Smith

Department of Mathematics, University of Dundee, Dundee, Scotland, UK

We analyse the radiation characteristics of a spheroidal antenna, modelled as a perfectly conducting spheroid excited by a voltage applied across a narrow circumferential slot, in the presence of a metallic spheroidal screen having two circular holes (see Fig.). The investigation uses a rigorous solution of the corresponding mixed boundary-value problem for Helmholtz equation. Solving the canonical problem makes it possible to study the influence of the screen on radiation features of this class of spheroidal antennas.

First the problem is reduced to the analysis of triple series equations with kernels employing prolate spheroidal angle functions, which depend on angle and wave parameters. Using features of these functions, the equations are reduced to ones involving kernels employing associated Legendre functions of the first kind involving only the angle parameter, and then to dual series equations containing Jakobi polynomials. Regularisation via Abel's integral equation technique finally reduces the problem to two independent Fredholm matrix equations of the second kind for the odd and even Fourier coefficients of the diffraction field. This transformation from a system of first kind to one of second kind provides the basis for an accurate and rapidly computable numerical solution obtained via truncation to a finite dimensional system.

Several features of this antenna can be varied, including the location of the feed, the shape (spherical to practically cylindrical depending on major to minor semi-axes ratio), and size and position of the outer screen. The frequency dependence of radiation resistance and far-field radiation pattern is investigated, and attention is focused on resonance properties over a wide band of frequencies.

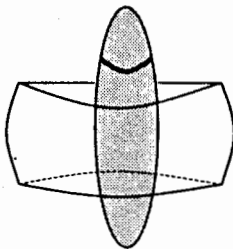


Fig. 1.
Spheroidal antenna with circumferential slot excitation and open spheroidal shell screen.

As well as the intrinsic interest of the radiation characteristics of this class of antenna, this rigorous solution of a new canonical scattering problem provides a valuable benchmark for validation of more general purpose numerical codes.

* Visiting Research Fellow from: Institute of Radiophysics & Electronics, Kharkov, Ukraine

Linear Analysis of Two Injection-Locked Active Antennas

Cheng-Cheng Hsiao and Tah-Hsiung Chu*

Department of Electrical Engineering,

National Taiwan University, Taipei, Taiwan, Republic of China

Tel: 886-02-23635251 ext. 541, Fax: 886-02-23638247

E-mail: thc@ew.ee.ntu.edu.tw

Injection-locked oscillator is an approach to stabilize an oscillator by impressing a small external signal. The formulation on analyzing its locking performance was firstly described in (*R. Adler, Proc. IEEE, vol.61, no.10, pp.1180-1185, 1973*). Recently, the injection locking technique is extended to synchronize an active antenna array for power combining or beam steering application. The design of an injection-locked active antenna array then requires to consider the effects of mutual coupling, each oscillator parameters and the injection signal strength to the locking performance of an injection-locked active antenna array.

In this study, we will present the formulation to linearly analyze the locking performance of two injection locked active antennas. Each active antenna consists of a FET oscillator. The injection signal can be applied to the gate port of FET as the transmission type injection or to the drain port of FET as the reflection type injection. Based on the connection-scattering method (*K.Gupta, R. Garg and R. Chadha, Computer Aided Design of Microwave Circuits, Artech House, ch.11, 1981*), a matrix equation to relate the input signals and output signals of each component in the two injection-locked active antennas is formulated. In this matrix equation, the antenna mutual coupling effect is represented by a mutual coupling coefficient. The FET is represented by its small signal S-parameter. After proper matrix manipulation, one can express the each active antenna output signal in terms of the injection signal, mutual coupling coefficient, FET S-parameter and the antenna input impedance. From which, one can derive an explicit formulation of locking bandwidth of the active antenna and effective Q of the oscillator.

By using the resulting equations, one can study the effects of each active antenna parameter, for example, antenna mutual coupling, FET S-parameter, feedback network or antenna input impedance to the locking performance. Numerical simulation will be presented. This linear analysis approach may be useful to find the explicit formulation for an injection-locked active antenna array.

Mutual Coupling Effect on Injection-Locked Active Antenna Array

Yuen-Ren Yang and Tah-Hsiung Chu*

Department of Electrical Engineering,

National Taiwan University, Taipei, Taiwan, Republic of China

Tel: 886-02-23635251 ext. 541, Fax: 886-02-23638247

E-mail: thc@ew.ee.ntu.edu.tw

An injection-locked active antenna array, with the application for spatial power combiner or phased-array antenna, is an array basically composed of modules of injection-locked oscillator and associated antenna. Since the antennas are closely distributed, the effect from the adjacent modules through antenna mutual coupling may change the state of oscillation and consequently vary the array locking capability. In (*K. Lee and T. Chu, 1996 AP-S/URSI Symp. pp.538-541, 1996*) a circuit model was proposed in which the antenna array is represented as an n-port admittance matrix and each port loaded with a nonlinear equivalent circuit of injection-locked oscillator. However, the calculation to solve these nonlinear circuit equations becomes complicated as the number of injection-locked module increases. In this paper, A load perturbation method is developed to study the mutual coupling effect on the array locking performance.

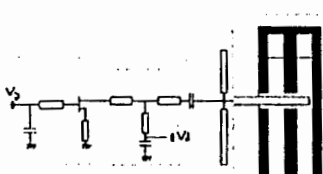
In this method all the equivalent external sources due to mutual coupling from the neighboring modules are considered as a perturbation of the load admittance of single injection-locked active antenna. In other words, one uses the formulation of single injection-locked active antenna by modifying its load admittance with a perturbation term contributed from mutual coupling. It then reduces the difficulty in the convergence problem encountered in a large nonlinear equation array. Both numerical simulation and experimental measurement are studied for a two element injection-locked active antenna array. They are shown that the locking performance is strongly dependent of the phase of perturbation admittance. Within a certain phase range, the required injection signal strength can be greatly reduced. While outside of this phase range, the array locking ability may be lost.

This load perturbation method is not only useful to quantitatively describe the effect of mutual coupling, but also gives the physical inside to interpret the array locking capability cased by mutual coupling.

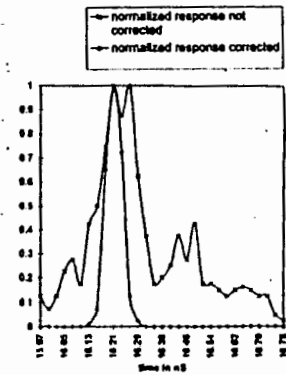
A 37 GHz Double-Slot GaAs Active Antenna

Laurent Desclos, Kenichi Maruhashi*, Mohammad Madhian
C&C Media Lab., * Kansai elec. Labs., NEC Corporation,

Summary : Development of compact identification and short range transmission systems requires integration of the active circuitry with the antenna. For millimeter wave range, GaAs is a candidate material for this purpose (C. Peixereiro, P. Dufrane, Y. Guillerme, A. Bouloard, E. Delhaye, B. Byzery, 26th EuMC, Prague, 9-12 Sept. 1996). In this paper we report the integration of a double-slot antenna with a 37 GHz range oscillator. The structure uses a grounded coplanar waveguide to avoid use of via holes and to optimize the transition between the antenna and the active circuit. A schematic circuit diagram for the CPWG oscillator and antenna is shown in Fig. 1. The active antenna size is 4mm x 2mm. The oscillator was designed using the method previously reported by the authors (K. Maruhashi, M. Madhian, L. Desclos, K. Onda, M. Kuzuhara, IEEE Trans. MTT, August 1996). Both separated circuit were designed to be matched to 50 Ohm enabling to be tested separately. The slot antenna has a double half wavelength slot configuration (Y. Qian, E. Yamashita, IEEE MTT S, Denver, 1996), with a separation of 0.7 mm. The length was chosen to compromise between gain and GaAs area. The slots are fed by a coplanar waveguide going through the center of each one. The end of the line is terminated in a short circuit via a capacitor. The active antenna IC was fabricated on a 3-inch undoped SI GaAs substrate. The HfJETs used in the IC have a gate length of 0.15 μ m and a total gate width of 200 μ m (25 μ m times 8 fingers). The calibration method was based on a time domain extraction of the antenna response - Fig. 2 - to isolate from the surrounding bounces and a reference to a waveguide measurement system. The antenna has a 2 dB gain in its normal direction. The output power of the oscillator varies between -4 to 2 dBm for a range of 37.6 to 38.2 GHz.



- Fig. 1 -



- Fig. 2 -

Formulations for Integral Equation Solutions

E. Michielssen and S. M. Rao

Scattering from Elliptical Cylinders of Infinite Extent using the Method of Ordered Multiple Interactions	302
<i>R. J. Adams*, G. S. Brown, Virginia Tech, USA</i>	
Extension of the Method of Ordered Multiple Interactions to Integral Equations of the First Kind	303
<i>R. J. Adams*, G. S. Brown, Virginia Tech, USA</i>	
Implicit Solution of Time Domain Integral Equation - Application to Three Dimensional Bodies	304
<i>S. M. Rao*, Auburn University, USA, T. K. Sarkar, Syracuse University, USA</i>	
Time Domain Integral Equation Finite Difference Modeling of Complex Antennas and Feed Networks	305
<i>K. Aygun*, S. E. Fisher, A. Ergin, B. Shanker, E. Michielssen, University of Illinois at Urbana-Champaign, USA</i>	
Green's Function-surface Integral Equation Solution of Plane Wave Scattering by Buried Infinite Conducting Cylinders of Arbitrary Cross-section at Oblique Incidence	306
<i>K. Michalski*, Texas A&M University, USA</i>	
Electromagnetic Coupling through Narrow Slot Apertures into a Half-space Containing a Conducting Element	307
<i>B. A. Lail*, S. P. Castillo, New Mexico State University, USA</i>	
Our Experiences with Object Oriented Design, Fortran 90, and Massively Parallel Computations	308
<i>W. A. Johnson*, R. E. Jorgenson, L. K. Warne, J. D. Kotulski, Sandia National Laboratories, USA, J. B. Grant, R. M. Sharpe, N. J. Champagne, Lawrence Livermore National Laboratories, USA, D. R. Wilton, D. R. Jackson, University of Houston, USA</i>	
Matrix Sparsification using Adaptive Localized Cosine Basis in the Method of Moments	309
<i>J. Spiegel*, Y. Levitan, Israel Institute of Technology, Israel</i>	
Low Frequency Characterization of a Loop Antenna	310
<i>I. Kouhia*, N. Didenko, E. Nive, NJIT, USA</i>	
Interaction of Electromagnetic Fields with a Material Sample in an Energized Microwave Cavity	311
<i>J. Zhang*, K. Chen, Michigan State University, USA</i>	

Scattering from Elliptical Cylinders of Infinite Extent Using the Method of Ordered Multiple Interactions

Robert J. Adams* and Gary S. Brown
ElectroMagnetic Interactions Laboratory
Bradley Department of Electrical Engineering
Virginia Tech, Blacksburg, VA 24061-0111

The Method of Ordered Multiple Interactions (MOMI) was originally developed to solve the problem of wave scattering from one-dimensional, extended rough surfaces having either Dirichlet or Neumann boundary conditions. As originally developed (Kapp and Brown, *IEEE A&P*, 44(5), 711-721, 1996), the method consists of decomposing the propagator matrix (P) of the magnetic field integral equation (MFIE) into its lower (L) and upper (U) triangular components ($P = L + U$). A few simple manipulations then lead to the MOMI integral equation which is itself a second kind integral equation having the new propagator matrix $P_M = (I - U)^{-1}(I - L)^{-1}LU$. The MOMI iterative series is obtained via straightforward Neumann iteration of the MOMI integral equation.

The MOMI series has been shown to be extremely robust for solving the reduced wave equation in the presence of an extended rough surface, with adequate convergence of the iterative series typically requiring one or two iterations. The MOMI series has never been observed to diverge for this problem. For these reasons, it has not been necessary to apply iterative minimization techniques such as the conjugate gradient algorithm to the MOMI integral equation.

In this talk we consider the conditions under which the MOMI series can provide a rapidly convergent solution to the problem of scattering from *closed* PEC objects in two dimensions. We begin with a straightforward application of the MOMI series to the MFIE for a closed body. It will be shown that, for a proper ordering of the unknowns in the MOMI integral equation, the Born term of the MOMI series often provides a very accurate approximation to the actual solution to the scattering problem, even at and near resonance. However, in most (but not all) cases the inclusion of higher order iterates eventually produces a divergent result.

To explain these results we develop a differential formulation of the MOMI integral equation. This development helps explain the convergence problems exhibited by the MOMI series when applied to the MFIE for closed bodies. Given this understanding, a combined field formulation is proposed to ameliorate these difficulties and a method for determining which combined field formulation is optimal is presented. The difficulties encountered in using MOMI as initially proposed with a combined field formulation are also briefly discussed. Finally, results are presented for the TE case displaying the rapid convergence rates of the MOMI series for the combined field formulation for scattering from elliptical cylinders of various sizes having axial ratios in the range of 1-10.

Extension of the Method of Ordered Multiple Interactions to Integral Equations of the First Kind

Robert J. Adams* and Gary S. Brown
ElectroMagnetic Interactions Laboratory
Bradley Department of Electrical Engineering
Virginia Tech, Blacksburg, VA 24061-0111

The Method of Ordered Multiple Interactions (MOMI) was originally developed (Kapp and Brown, *IEEE A&P*, 44(5), 711-721, 1996) to solve the problem of wave scattering from one-dimensional, extended rough surfaces having either Dirichlet or Neumann boundary conditions. The method as originally developed consists of a simple recasting of the magnetic field integral equation (a Fredholm equation of the second kind) into a new second kind integral equation with a modified propagator. The robustness of the MOMI series resulting from Neumann iteration of this new integral equation has been attributed to the manner in which the series re-sums important multiple scattering terms present in the Neumann series for the original form of the magnetic field integral equation (MFIE).

An essential aspect of the MOMI series as originally developed is the assumption that the propagator's coupling of forward and backward directions on the surface is weak and can be accommodated via decoupled forward and backward iterations. The validity of this assumption is borne out by the robustness of the MOMI series as applied to the magnetic field integral equation. In terms of the kernel function of the MFIE, this coupling is weak because, once the limit is taken in which the observation point approaches the surface, the remaining kernel function is nonsingular. This is physically attributable to the fact that the magnetic field near a constant-current sheet is finite (i.e., the singular contributions cancel).

In this talk we consider the modifications of the MOMI series necessary to achieve a similar decoupling for first kind integral equations. Unlike the kernel function for the MFIE, the kernel functions of the electric field integral equations (EFIEs) in two dimensions contain nonremovable singularities. We demonstrate that direct application of MOMI to these integral equations leads to iterative series which are much less robust than the MOMI series for the MFIE. Among others, the convergence properties of the resultant series depend on the size of the discretization interval.

These results suggest that a method for achieving a more robust series is to decompose the propagator matrix as $P = L + B + U$ where B is a banded matrix (having a bandwidth on the order of one wavelength) instead of the decomposition $P = L + U$ suggested by *Kapp and Brown*. This new decomposition of the propagator matrix then leads to a modified form of the MOMI series. We note that this modified series is different from the straightforward inclusion of a nonzero diagonal term in the propagator matrix. Finally, the convergence properties of the resultant MOMI series are illustrated for a variety of rough surfaces.

Implicit Solution of Time Domain Integral Equation - Application to Three Dimensional Bodies

S. M. Rao*, Department of EE, Auburn University, Auburn, AL 36849.

T. K. Sarkar, Department of ECE, Syracuse University, Syracuse, NY 13244.

In this work, we develop an implicit solution to calculate the transient scattering from three dimensional conducting bodies of arbitrary shape illuminated by a transient electromagnetic plane wave. Starting from Maxwell's equations and using equivalence principle, a time domain integral equation for a conducting scatterer may be developed, given by

$$AJ(r', t - \frac{|r - r'|}{c}) = F(r, t) \quad (1)$$

where A represents the integro-differential operator, J represents the induced current on the conductor and $F(r, t)$ represents the known excitation field. Also in (1), r , r' , and c represent the location of the observation point, location of the source point, and wave speed of the electromagnetic wave. For a numerical solution, we divide the structure into a suitable grid, the time axis into equal intervals Δt , and denote $t_j = j\Delta t$, $j = 0, 1, 2, \dots, \infty$. Then, at $r = r_m$ and $t = t_n$, (1) may be written as,

$$AJ(r', t_n - \frac{|r_m - r'|}{c}) = F(r_m, t_n) \quad (2)$$

which can be rewritten in the following form, given by

$$A_1 J(r', t_n - \frac{|r_m - r'|}{c}) + A_2 J(r', t_n - \frac{|r_m - r'|}{c}) = F(r_m, t_n) \quad (3)$$

where

$$A = \begin{cases} A_1 & \text{if } \frac{|r_m - r'|}{c} < \Delta t \\ A_2 & \text{if } \frac{|r_m - r'|}{c} \geq \Delta t \end{cases} \quad (4)$$

Note that in (4), the currents for the operator A_2 are retarded in time, by at least Δt , and hence are known. Here we assume that the currents are known until $t = t_{n-1}$ while solving for the currents at $t = t_n$.

Now, for the explicit scheme, we choose $\Delta t \leq \frac{R_{min}}{c}$ where R_{min} represents the minimum of all the distances between any two distinct observation points in the grid scheme. In contrast, for the implicit scheme, we choose $\Delta t > \frac{R_{max}}{c}$ which results in a sparse matrix for the operator A_1 and the sparsity of the matrix depends on the choice of Δt . Although the implicit method requires a storage and inversion of a sparse matrix, the method is superior to the explicit scheme since the results are unconditionally stable. Further, the implicit method is more efficient since, in general, a relatively larger time step is utilized. Numerical results will be presented for several geometrical shapes and compared with other data.

TIME DOMAIN INTEGRAL EQUATION-FINITE DIFFERENCE MODELING OF COMPLEX ANTENNAS AND FEED NETWORKS

Kemal Aygün*, Stephen E. Fisher, Arif Ergin, Balasubramaniam Shanker,
and Eric Michielssen

Center for Computational Electromagnetics
Department of Electrical and Computer Engineering
University of Illinois at Urbana-Champaign
1406 W. Green St., Urbana, IL 61801
e-mail: kaygun@decwa.ece.uiuc.edu

Time domain integral equation (TDIE) based methods have been used previously in the analysis of transient electromagnetic scattering and radiation phenomena. They are often preferred over finite difference time domain (FDTD) techniques because (i) they only require a discretization of the scatterer surface, (ii) they implicitly impose the radiation condition, and (iii) they are devoid of grid dispersion errors.

In this paper, a novel algorithm is presented for analyzing transient radiation from complex antennas that consist of multi element broadband wire radiators mounted on arbitrarily shaped three-dimensional conducting bodies. The algorithm simultaneously characterizes the antenna's transient radiation properties and feed network performance using a hybrid integral equation- finite difference scheme.

The transient currents on the wire and surface radiator are computed using a Marching-On-in-Time (MOT) algorithm. Boundary conditions on the electric field are enforced on open surfaces and wires, while boundary conditions on the magnetic field are imposed on closed surfaces. The resulting electric and magnetic field integral equations are discretized by a sophisticated and stable MOT algorithm that handles interactions between different types of basis functions for modeling currents on the surfaces, wires, and surface-wire junctions.

The wire array is fed using a complex transmission line feed network that is modeled using a one dimensional FDTD scheme. Coupling between the feed network and the exterior antenna is accounted for in a self consistent manner. The resulting hybrid MOT-FDTD scheme simultaneously solves for both the antenna and feed network currents at each time step.

The above algorithm has been applied to the analysis of broadband radiation from log-periodic monopole arrays mounted on complex wedge-like platforms that are fed using impedance modulated feeders. The transient antenna currents and radiation fields have been computed and validated against Fourier transformed frequency domain data. Results illustrating the accuracy and the efficacy of this technique will be presented. More specifically, it will be shown that the proposed algorithm is computationally more efficient than frequency domain techniques when applied to the analysis of electrically large broadband radiators.

GREEN'S FUNCTION-SURFACE INTEGRAL EQUATION SOLUTION
OF PLANE WAVE SCATTERING BY BURIED
INFINITE CONDUCTING CYLINDERS OF
ARBITRARY CROSS-SECTION AT
OBLIQUE INCIDENCE

Krzysztof A. Michalski
Department of Electrical Engineering
Texas A&M University
College Station, TX 77843-3128

ABSTRACT

The mixed-potential integral equation (MPIE) approach (K. A. Michalski, Arch. Elek. Übertragung, 39, 317-322, 1985) is applied to an infinite conducting cylinder of arbitrary cross-section, buried in a multilayered planar medium and excited by an obliquely incident plane wave. Two implementations of the MPIE are compared: the original one (K. A. Michalski and D. Zheng, IEEE Trans. Antennas Propagat., 38, 335-344, 1990), in which the so-called correction factor, which arises in the case of non-planar conductors, is incorporated in the vector potential kernel, and the modified one (K. A. Michalski and J. R. Mosig, IEEE Trans. Antennas Propagat., 45, 508-519, 1997), in which this factor is merged with the scalar potential term. The advantage of the latter approach is that the spectral integral associated with the correction factor converges faster than that arising in the original formulation.

The spectral integrals that arise in the MPIE kernels are evaluated using the partition-extrapolation technique (Squire, Int. J. Computer Math., B-5, 81-91, 1975), in which an infinite integral is computed as a sum of a series of partial integrals over finite subdomains, accelerated by an extrapolation method.

As in the corresponding propagation problem (K. A. Michalski and D. Zheng, IEEE Trans. Microwave Theory Tech., 37, 2005-2010, 1989), in the case of oblique incidence the field structure is a hybrid combination of fields transverse-magnetic (TM) and transverse-electric (TE) to the cylinder axis. Consequently, both the longitudinal and transverse surface currents are excited. Only for normal incidence the TM and TE parts of the problem become uncoupled.

The MPIE is solved for the induced longitudinal and transverse surface currents by a method of moments procedure using first- and second-order subsectional basis functions. From the induced surface currents, the far-field radiation patterns are computed.

Electromagnetic Coupling Through Narrow Slot Apertures Into a Half-Space Containing a Conducting Element

Brian A. Lail and Steven P. Castillo

The Klipsch School of Electrical and Computer Engineering

New Mexico State University

Dept. 3-O, Box 30001

Las Cruces, NM 88003

Coupling to wires via narrow slot apertures is of interest in general electromagnetic interference and compatibility problems. In this paper, we consider electromagnetic penetration of narrow slot apertures with depth and width when a finite-length thin wire is present in the coupled region. Slot depth and width is accounted for with an equivalent antenna radius (L.K.Warne and K.C. Chen, IEEE Trans. AP 37, 824-834, 1989). This approach has been verified experimentally (A. Taranto, M.S. thesis, NMSU, 1990). Additionally, coupling into complex cavities through narrow slot apertures has also been studied (R.P. Jedlicka, Ph.D. Dissertation, NMSU, 1995). In this work an incident plane wave couples into a half space containing a finite-length thin wire.

The physical problem consists of an infinite ground plane containing a narrow slot aperture having depth and width located at the origin, a finite-length thin wire displaced distance δ from the ground plane, and an incident plane wave. An equivalent problem is derived using equivalence and image theory. In the equivalent problem the ground plane and aperture are replaced with an equivalent magnetic dipole. Induced electric currents and their image arise from the wire. Boundary conditions are applied at the ground plane and the wire to arrive at two governing integro-differential equations. These equations are coupled with the unknowns being equivalent magnetic currents along the aperture and induced electric currents on the wire. The Galerkin technique yields a matrix equation form that is solved for the currents. Finally, the coupled fields are determined from the currents.

Of interest in this work is the peak coupling to the wire as a function of frequency. We will present results that illustrate the effects of slot width, length and depth, along with wire length, on the peak coupling as the frequency is varied.

OUR EXPERIENCES WITH OBJECT ORIENTED DESIGN, FORTRAN 90, AND MASSIVELY PARALLEL COMPUTATIONS

W. A. Johnson*, R. E. Jorgenson, , L. K. Warne, Dept., 9735, Sandia National, Laboratories
J. D. Kotulski, Dept. 9352, Sandia National Laboratories
J. B. Grant, R. M. Sharpe, N. J. Champagne, Electronics Engineering Department, Lawrence Livermore National Laboratories
D. R. Wilton, D. R. Jackson, Dept. of Electrical and Computer Engineering, University of Houston

EIGER (Electromagnetic Interactions GeneRalized) is a general purpose frequency domain electromagnetics code aimed at integrating a variety of frequency domain analysis methods into a single package. The code suite consists of a pre-processor, computational engine, and post- processor. FORTRAN 90 and object oriented design have yielded a computational engine, with great generality, flexibility, and extensibility. The capabilities to treat, surfaces, wires, wire-surface junctions, multi-layer media, periodic structures, discrete body of revolution symmetries, surface curvature, and dielectric media are present as well as the flexibility to choose different integral equation operators.

The topics of interest include: how the abstract object oriented design and it's FORTRAN 90 implementation have allowed for great generality and flexibility in the computational engine; how this approach has simplified the addition of new features; and our experience in porting and running this code on both serial, and massively parallel computers.

An example of the code's generality is the introduction of two sided elements to enhance the dynamic range of coupling problems. Extension of capabilities is illustrated by addition of discrete body of revolution symmetry and sub-cell models for thin slots. A static code has also been developed within this framework to model micro-electro-mechanical systems. This code includes static integral equations, finite elements, and hybrid finite element-integral equation treatments.

Sample problems will include antenna systems, frequency selective surfaces, layered media, and coupling.

Sandia is a multiprogram laboratory operated by Sandia Corporation, a Lockheed Martin Company, for the United States Department of Energy under contract DE-AC04-94AL85000. This work was performed in part under the auspices of the U. S. Department of Energy by Lawrence Livermore National Laboratory under contract number W-7405-ENG-48.

Matrix Sparsification Using Adaptive Localized Cosine Basis in the Method of Moments

J. Spiegel and Y. Levitan

Department of Electrical Engineering

Technion - Israel Institute of Technology

Haifa 32000, Israel.

e-mail: levitan@ee.technion.ac.il

A new approach of matrix sparsification is used in conjunction with the method of moments. Here, a library of bases in a tree format, consisting of smooth localized cosine functions, is used. The adapted best-basis search procedure is applied with a threshold measure as the cost function. This means that the set of basis functions that gives the smallest number of terms above a given threshold level is chosen. This adaptive transform can be seen as an extension of the fixed transform used in the impedance matrix localization method (IML) (F. X. Canning, IEEE Trans. AP-41, May 1993). In this search procedure, we start with basis functions that are extended over the entire structure and possess high resolution in the spatial-frequency domain, and proceed with basis functions that gradually become more localized in the space domain but have less resolution in the spatial-frequency domain. At each step, we increase the resolution in the space domain by two. The result is that we have basis functions associated with a dyadic decomposition of the structure. The best-basis, at the end of the procedure, is the one that renders the most sparse impedance matrix according to the criterion defined by the cost function. The best-basis search ends when no better decomposition is obtained, or at a pre-determined level.

The new method has been applied to the cases of 2-D scattering by a metallic strip and a strip with a crack. In both cases, high sparseness levels have been attained. An interesting point, besides the achievement of high sparseness level, is that the best-basis tree reflects the geometry of the structure under consideration.

LOW FREQUENCY CHARACTERIZATION OF A LOOP ANTENNA

Irene Koukhta, Nikolai Didenko and Edip Niver*

Electrical and Computer Engineering Department
New Jersey Institute of Technology
Newark, NJ 07102

The conventional solution of an integral solution for the loop antenna in free space can be expressed analytically using Fourier series. However, solutions based on a delta gap feed model yield divergent results for the susceptance in the input admittance. To overcome such diverging results, alternative solutions using equivalent magnetic frill current feed models were implemented. Although low frequency models for delta gap feed were reported, no generalized low frequency expansions for the input admittance have been reported previously. In this work, such generalized low frequency expansions are developed for both delta-gap and magnetic frill feed models of loop antennas. Validity of such expansions around $ka = 0$ and $ka \neq 0$, where a is the radius of the loop and k is the wavenumber, have been investigated and were compared with the published results. One other advantage of having such expansions limited to only few terms is to associate each term with the equivalent circuit parameters such as an input inductance, resistance, capacitance, radiation conductance and susceptance of the antenna.

Interaction of Electromagnetic Fields with a Material Sample in an Energized Microwave Cavity

Jianping Zhang and Kun-Mu Chen
Department of Electrical Engineering
Michigan State University
East Lansing, MI 48824
Tel: (517)355-6502, Fax:(517)353-1980
E-mail: zhangjia@egr.msu.edu

In the study of the interaction of microwave radiation with non-ionic materials, a material sample is placed in a cylindrical or a rectangular EM cavity which is excited with a fundamental cavity mode. We aim to quantify the electric field inside the material sample induced by the cavity mode, based on an Electric Field Integral Equation (EFIE) through Galerkin's method.

To analyze this problem, we need an appropriate dyadic Green's function for the cavity. The cavity field induces electric charge on the surface of a material sample of finite size. Thus, the divergence of electric field does not vanish at all points inside the cavity. Therefore, the total electric field inside the cavity can not be expanded into simple cavity eigenmodes which are pure solenoidal. Instead, an eigenmode with an irrotational electric field is needed in addition. We have derived an electric dyadic Green's function in terms of three vector wave functions, \hat{L}_{nml} , \hat{M}_{nml} and \hat{N}_{nml} functions where \hat{L}_{nml} function gives an irrotational electric field. The same electric dyadic Green's function can be obtained if the derivation is based on the magnetic field and a magnetic dyadic Green's function. After the appropriate dyadic Green's function is obtained, an electric field integral equation (EFIE) for the induced electric field inside the material sample is derived. This EFIE is then numerically solved by discretizing the sample into a large number of volume elements.

In the numerical calculation of the EFIE, we have encountered difficulty in the convergence of the numerical results. This is due to poor convergence of the dyadic Green's function we have employed. To overcome this difficulty, a triple summation over cavity eigenmodes is reduced to a double summation using a relation (Collin, Field Theory of Guided Waves, p.814, 1991) to save computation time. Also the volume elements of the material sample is divided into two groups, interior volume elements and boundary layer volume elements, and the EFIE's in different formulations are applied to these two groups of volume elements. This scheme accelerates the convergence of numerical results and saves computation time.

Complex Media

D. L. Jaggard and Y. M. M. Antar

Wire Media as Complex Media with Electrically Large Inclusions	314
<i>C. A. Moses*, N. Engheta, University of Pennsylvania, U.S.A</i>	
Scattering and Knotted Media.....	315
<i>O. Manuar*, D. L. Jaggard, University of Pennsylvania, USA</i>	
Resonant Modes of Single and Stacked Circular Microstrip Patches in Multilayered Substrates Containing Chiral Media.....	316
<i>R. R. Boix*, V. Losada, M. Horro, University of Sevilla, Spain</i>	
A Comprehensive Study of Discontinuities in Chirowaveguides	317
<i>T. X. Wu*, D. L. Jaggard, University of Pennsylvania, USA</i>	
Electromagnetic Wave Propagation and Radiation from a Waveguide Filled with a Gyromagnetic Uniaxial Chiral Medium	318
<i>D. Cheng*, Y. M. M. Antar, Royal Military College of Canada, Canada</i>	

Wire Media as Complex Media with Electrically Large Inclusions

Charles A. Moses* and Nader Engheta
Moore School of Electrical Engineering

University of Pennsylvania

Philadelphia, Pennsylvania 19104, U.S.A

Tel: (215) 898-9777, Fax: (215) 573-2068

E-mail: engheta@pender.ee.upenn.edu

We recently introduced an idea for *Wire Media* as a new type of artificial complex media. These media can be considered as special cases of electromagnetic FeedForward/FeedBackward (FF/FB) media, which were suggested by us previously [C. A. Moses and N. Engheta, "An Idea for Electromagnetic FeedForward/FeedBackward Media: I. Plane Wave Propagation in Axial Direction," presented in the *1997 URSI North American Radio Science Meeting*, Montreal, Canada, July 13--18, 1997; and C. A. Moses and N. Engheta, "FeedForward/FeedBackward and Wire Media as Electromagnetic Complex Media," a talk in the *1998 URSI International Symposium on EM Theory*, Thessaloniki, Greece, May 25--28, 1998]. A wire medium may be conceptually constructed by embedding many parallel, finite-length, identical wire inclusions within some host medium; the wires may be placed on a periodic grid or dispersed randomly. Unlike some conventional artificial materials for which the inclusions are taken to be small compared to the wavelength, in wire media the wire inclusions, all being identical in size, are allowed to be of any arbitrary length, from a fraction of a wavelength to multiple wavelengths. However, the spatial periodicities (in the case of a periodic distribution) are still small compared to the wavelength. Because the wire inclusions are permitted to be electrically large, the effective tensorial material parameters of wire media may show interesting dependencies on direction of wave propagation (as well as on other parameters; e.g. frequency, wire length, element spacings). In our work we show that even though the inclusions may be electrically large, the resulting structure can often-times still be regarded as a complex *medium* under certain conditions.

In our theoretical analysis of electromagnetic wave propagation through wire media, we have studied various characteristics and interesting features of wave interaction with these media. We have theoretically investigated wave propagation in both unbounded and semi-infinite wire media, and have obtained wavenumber surfaces for these cases. Our results reveal some of the salient features of wire media and, based on these results, we believe wire media may find some potential applications in future microwave devices, e.g., as substrates in printed antennas, as radome for beamforming, and as waveguide material for mode control.

In this talk, we present our theoretical results for wavenumber surfaces in unbounded and semi-infinite wire media. We also mention how the knowledge of wave interaction with wire media can assist in understanding oblique plane wave propagation in FF/FB media.

Scattering and Knotted Media

Omar Manuar[†] and Dwight L. Jaggard

Complex Media Laboratory
School of Engineering and Applied Science
University of Pennsylvania
Philadelphia, PA 19104-6391

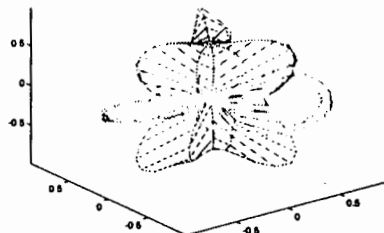
†Also Biochemistry and Biophysics
School of Medicine
University of Pennsylvania
Philadelphia, PA 19104-6059

Background

We previously studied the backscattering of polarized electromagnetic waves from individual wire structures in the shape of trefoil knots and related unknots [O. Manuar and D. L. Jaggard, *Elec. Lett.* 33(4), 278-280 (February 1997)]. The determination of topology of a structure is relevant to biological macromolecules, for example. We asked whether we could see the difference in the topologies of a knot and its related unknot in the radiation scattered from each. We found for the backscattering cross-section at a fixed direction of incidence it is the symmetry presented to the incident wave rather than the topology that is of primary importance in determining the polarization of the scattered wave.

Knotted Media

Here we are interested in groups of knots which together form *knotted media*. We use a range of incidence directions for each given structure and study the backscattering at each direction. Averaging over these angles can be interpreted as the interaction of waves with a medium composed of identical, non-interacting knots at different orientations. In addition to backscattering, we also consider scattering at a fixed angle with respect to the incidence direction over the same range of incidence angles. The figure to the right shows an example of such a backscattering pattern from a trefoil: the backscatter is represented by the central cushion; it is superimposed on the trefoil which appears as several loops protruding from the scattering cushion.



We summarize the angular scattering information using the Mueller matrix formalism. It provides a concise description of the effect of a scattering system on a wave in terms of the intensity, degree of polarization, and polarization. From first studies, it appears that Mueller matrices may also be used to distinguish some trefoils from their untrefoil counterparts.

Resonant modes of single and stacked circular microstrip patches in multilayered substrates containing chiral media.

Rafael R. Boix*, Vicente Losada, Manuel Horno

Grupo de Microondas, Departamento de Electrónica y Electromagnetismo.

Facultad de Física, Avda. Reina Mercedes s/n, 41012, Sevilla, Spain.

E-mail: boix@cica.es. Telephone number: 34-54552891. Fax: 34-54239434.

In the microwave frequency band microstrip patch resonators are used as antennas and as components of integrated circuits oscillators and filters. In antenna applications, microstrip patches are commonly arranged in a stacked configuration in order to achieve either dual-frequency operation [S. A. Long, D. Walton, IEEE-AP, 3, 270-273, 1979] or wider bandwidth [A. N. Tulintseff, S. M. Ali, J. A. Kong, IEEE-AP, 3, 381-390, 1991]. Although dielectric materials have been traditionally used as substrates of microstrip patches, in the last few years some interest has arisen on studying the resonance and radiation properties of microstrip patches printed on complex materials such as magnetized ferrites [D. M. Pozar, IEEE-AP, 9, 1084-1092, 1992] and chiral materials [D. M. Pozar, IEEE-AP, 10, 1260-1263, 1992], [A. Toscano, L. Vigni, JEW, 5, 567-592, 1997]. Concerning microstrip patch antennas printed on chiral substrates, it has been reported that these antennas have disadvantages because they radiate more surface wave power and show higher cross-polarization levels than antennas of the same size printed on dielectric materials [D. M. Pozar, IEEE-AP, 10, 1260-1263, 1992]. However, it has been recently shown that microstrip antennas on chiral substrates also have advantages because they present wider bandwidth and bigger directivity than similar antennas printed on dielectric substrates [A. Toscano, L. Vigni, JEW, 5, 567-592, 1997].

In this work the authors focus on the numerical computation of the resonant frequencies, quality factors and radiation patterns of single and stacked circular microstrip patches embedded in a multilayered substrate which may consist of both dielectric materials and/or biisotropic chiral materials. In spite of substrate chirality, the structures analyzed show azimuthal symmetry around the revolution axis of the circular patches from an electromagnetic point of view. Owing to this, spectral techniques in the Hankel transform domain can be applied to their analysis. In particular, Galerkin's method in the Hankel transform domain [K. Araki, T. Itoh, IEEE-AP, 1, 81-89, 1981] is used for obtaining the resonant frequencies and quality factors of the first resonant modes of the circular patches. Once Galerkin's method has been applied and the current densities on the patches are known, the radiation patterns are obtained in terms of the Hankel transforms of the tangential electric field at the limiting plane of the multilayered substrate by means of the stationary phase method [K. Araki, T. Itoh, IEEE-AP, 1, 81-89, 1981].

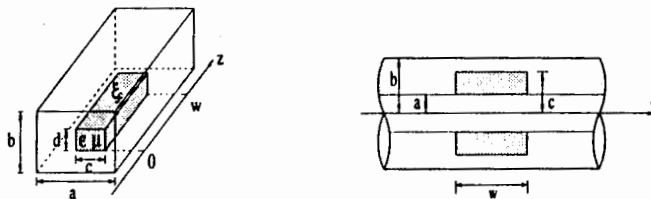
A Comprehensive Study of Discontinuities in Chirowaveguides

Thomas Xinzhang Wu* and Dwight L. Jaggard
Complex Media Laboratory
Moore School of Electrical Engineering
University of Pennsylvania
Philadelphia, PA 19104-6390

We provide a comprehensive study of two- and three-dimensional discontinuities in chirowaveguides. We focus on the effects of discontinuities for metallic waveguide partially filled with chiral media. Our procedure is to treat the discontinuity problem by a multi-mode coupled-mode method. We use the eigenfunctions of hollow metallic waveguide as basis functions to expand the fields in the chiral media partially filled region and then insert those expressions together with the chiral constitutive relations into Maxwell's equations. Using the orthogonality relations of the metallic waveguide, we obtain a set of multi-mode coupled-mode equations. In our analysis, we take the multimode equations and consider the influence of higher-order modes rather than using only two modes as in traditional coupled-mode theory. We diagonalize the coupling matrix whose eigenvalues and eigenfunctions are associated with the eigenvalues and eigenfunctions of the partially filled chirowaveguide. After matrix manipulations, we obtain a multi-mode scattering matrix for the entire structure. From these results we find the scattering properties of the discontinuities.

To check the validity of our method, we have first analyzed coaxial waveguide partially filled with lossy chiral media. Our results are compared with those obtained by the mode-matching method and excellent agreement is found. We have also checked our results for achiral dielectric material partially filled rectangular waveguide and excellent agreement between our calculation and experimental data as well as data from the mode-matching method is again found.

Based on our analysis, we have numerically calculated the scattering parameters for chiral media partially filled rectangular waveguide and coaxial waveguide as examples. We find: (1) the sensitivity of the scattering parameters to chirality admittance increases as the chirality admittance increases; (2) the dielectric constant has a great influence on the scattering parameters; and (3) for the rectangular waveguide case, the influence of the height is always large but the influence of the width decreases as the width increases. Our results are explained by underlying physical principles.



Electromagnetic wave propagation and radiation from a waveguide filled with a gyromagnetic uniaxial chiral medium

Dajun Cheng* and Yahia M. M. Antar

Department of Electrical and Computer Engineering

Royal Military College of Canada

Kingston, Ont. K7K 5L0, Canada

Increasing attention has recently been paid to the area of interaction of electromagnetic waves with composite materials. In the present study, a concept of gyromagnetic uniaxial chiral medium is proposed to generalize the well-studied gyromagnetic medium and the uniaxial material with chirality. The constitutive relations of this medium can be written as $\mathbf{D} = [\epsilon] \cdot \mathbf{E} - [\zeta] \cdot \mathbf{H}$ and $\mathbf{B} = [\mu] \cdot \mathbf{H} + [\xi] \cdot \mathbf{E}$. Here, the permittivity, permeability and cross-coupling tensor are $[\epsilon] = \epsilon_c [I] + \epsilon_z \mathbf{e}_z \mathbf{e}_z$, $[\mu] = \mu_c [I] + \mu_z \mathbf{e}_z \mathbf{e}_z - i g \mathbf{e}_z \times [I]_c$, and $[\zeta] = i (\mu_0 \epsilon_0)^{1/2} (\alpha [I]_c + \gamma \mathbf{e}_z \mathbf{e}_z)$. In practice, a general form of gyromagnetic uniaxial chiral medium can be created by mixing three sets of small metal helices in a host gyromagnetic medium (e.g., magnetically biased ferrite), with the axes of two sets perpendicular and parallel to the external magnetic field, respectively, and the other set distributed in random orientations and locations. In the present study and based on the concept of characteristic waves and the method of angular spectral expansion, electromagnetic waves in this medium are represented in terms of the cylindrical vector wave functions. A dispersion equation is obtained to determine the propagation constants of electromagnetic waves in a circular waveguide filled with this medium. By ignoring the diffraction effects of the edge, radiation from an open-end guide is formulated.

General relations for the propagation constant of the n -th mode are obtained. For the lowest order $n=1$ mode, numerical results of the propagation constant and radiation pattern are presented, respectively. It is revealed that the axial chirality parameter γ and off-diagonal parameter g have little influence on the normalized propagation constant k_z/k_0 , respectively. However, k_z/k_0 will decrease as the transverse chirality parameter α increases. Keeping the constitutive parameters as constants, increasing $k_0 a$ would result in greater k_z/k_0 . It is also found that the uniaxial chirality parameters α , γ would sharpen the halfpower beamwidth, respectively, while the off-diagonal parameter g has little influence.

Combining Method of Moments with High Frequency Techniques

E. Arvas and G. Theile

Hybrid Scattering by Large Objects with Cavity-like Features using the Free-space Green's Function.....	320
<i>S. W. Altizer, J. S. Avestas*, J. M. Stamm, Naval Air Warfare Center, USA</i>	
Hybrid Methods Combining the Moment Method and High Frequency Techniques for 2-D and 3-D Bodies.....	321
<i>A. Sullivan*, Air Force Research Laboratory, USA, L. Carin, Duke University, USA</i>	
Scattering from a Dielectric-coated Large Conducting Cylinder: A Hybrid MoM/Go Method	322
<i>D. Worasawate*, E. Arvas, Syracuse University, USA</i>	
Hybrid Analysis of Scattering for a Large Body with Cracks	323
<i>X. C. Nie, Y. B. Yan, S. Y. Shi, D. B. Ge*, H. Huang, Xidian University, P.R.China</i>	
The Coupling Between Antennas on Conductive Construction.....	324
<i>Y. Shaohua*, C. Xinke, Guangzhou Communication Research Institute, China, Y. Enyao, Gulin Institute of Electronic Technology, China</i>	

HYBRID SCATTERING BY LARGE OBJECTS WITH CAVITY-LIKE FEATURES USING THE FREE-SPACE GREEN'S FUNCTION

Stuart W. Altizer, John S. Asvestas*, and James M. Stamm

RF Sensors Branch, Naval Air Warfare Center, Aircraft Division, Patuxent River, MD, USA.

ABSTRACT

We will present a new hybrid method for computing electromagnetic scattering from an electrically large scatterer. The scatterer is perfectly conducting and its surface (which is very many square wavelengths large) has cavity-like features (recesses, grooves, etc.). The cavities may be filled with material other than that of the surrounding medium. The geometry of the scatterer as well as of the cavities is arbitrary. The incident electromagnetic wave is a plane wave that varies harmonically in time.

Our approach is similar to that in (Jin, J.-M., Ni, S.S., and S.-W. Lee, IEEE Trans. Antennas Propagat., 43, 1130-1139, 1995). There, the authors use the high-frequency method of shooting and bouncing rays (SBR) on the large part of the scatterer and the resulting field as an input to a finite-element method (FEM) for determining the fields in the cavity. This is an elegant method and appears to yield very good results. As the authors admit, however, it has the drawback that it uses a dyadic Green's function that is geometry dependent; specifically, its tangential component must be equal to zero on the original scatterer when the entrance to each cavity is covered with a perfectly conducting surface. This dyadic is not explicitly known and not easy to compute (even approximately) when there are strong interactions among the various components of the scatterer.

In our approach we also use SBR to compute contributions from parts of the scatterer that do not have cavities. For the cavity contributions, however, we use a system of boundary-integral equations. These equations are derived from integral representations of the fields both in the cavities and exterior to them. Moreover, they are defined on the walls of the cavities and on the imaginary surfaces that cover the entrances to these cavities. The system of integral equations can be solved numerically using boundary elements. Besides the incident fields, part of the input to this system is the contribution over the openings of the cavities of the SBR electric currents.

The essence of our contribution lies in the fact that we do not use a specialized Green's function in the integral equations but the free-space Green's function in its dyadic form. In contrast to the Green's function in the above reference, the free-space Green's function is explicitly known and easy to compute.

In the meeting we will present the analysis that leads to the system of integral equations as well as expressions for the fields everywhere in space.

Hybrid Methods Combining the Moment Method and High Frequency Techniques for 2-D and 3-D Bodies

Anders Sullivan*

Air Force Research Laboratory
 Eglin Air Force Base, Florida 32542

Lawrence Carin

Department of Electrical Engineering, Duke University
 Durham, North Carolina 27708

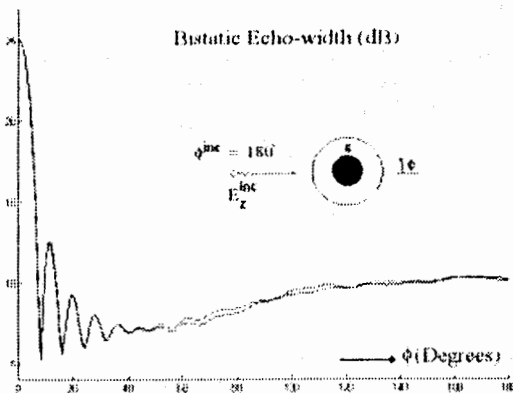
Hybrid methods combining the method of moments (MoM) and high frequency techniques such as physical optics (PO) and the geometrical theory of diffraction (GTD) are examined for electrically large, perfectly conducting, two and three-dimensional bodies. Hybrid methods have found great utility for cases where strictly MoM solutions become prohibitive due to the rapidly increasing CPU and memory requirements, and for cases where high frequency techniques alone fail to capture nonspecular second order effects such as tip diffraction, surface curvature discontinuity, and creeping waves. In certain cases, high frequency methods are also subject to nonphysical singularities at caustics and shadow boundaries. In the hybrid formulation, typical MoM subsectional basis elements are employed over corners, edges, and rapidly varying sections of the body, while high frequency basis functions are employed over interior regions of the body. The only practical limitation of these hybrid methods is that the region of the scatterer where the high frequency approximation is applied must be large (with respect to wavelength) and relatively smooth. Such schemes have been used by others to calculate the scattered fields from electrically large bodies. The new feature in this study is that asymptotic techniques are used to evaluate many of the highly oscillatory integrals that result from the hybrid formulation.

Methods such as stationary phase and uniform asymptotics (L. B. Felsen and N. Marcuvitz, *Radiation and Scattering of Waves*, Prentice Hall, 1973) yield analytic approximations for many of these integrals (which represent elements in the hybrid MoM impedance matrix), thereby significantly reducing computation time. The induced surface currents and scattered fields from the asymptotic-hybrid formulation are compared with standard MoM solutions and are shown to produce remarkably accurate results. Moreover, the present formulation is shown to reduce computation time by an order of magnitude or more, in some cases, when compared to traditional MoM solutions. Results are presented for a two-dimensional cylinder with a triangular cross section and a long slender body of revolution. Plane wave incidence is assumed.

SCATTERING FROM A DIELECTRIC-COATED LARGE CONDUCTING CYLINDER: A HYBRID MOM/GO METHOD

Denchal Worasawate* and Ercument Arvas
Dept. of EECS, Syracuse University, Syracuse, N.Y. 13244

A simple Geometrical Optics and MOM hybrid method is used to compute the electromagnetic scattering from a large perfectly conducting cylinder of arbitrary cross section which is coated by a dielectric layer. The system is assumed to be excited by a TM plane wave. The surface equivalence principle is used to replace the system by equivalent electric and magnetic surface currents residing on the outer surface of the coating, and the induced electric current on the surface of the conductor. The surfaces are approximated by linear segments, and MOM is used to come up with a matrix equation for the unknown expansion coefficients. The size of this equation is reduced considerably by approximating the values for the currents on the lit side of the structure. These approximate values are found analytically by replacing a linear segment of the structure with an infinite conducting plane coated with the same dielectric material. The figure below shows the bistatic echo width of a conducting cylinder of radius 3.4λ which is coated by a dielectric layer of thickness 0.1λ and dielectric constant of 2.5. The size of MOM matrix was 1080X1080 and that of the GO/MOM matrix is 690X690. The results agree very well. The memory and the CPU needed with the hybrid method are much smaller than the direct MOM method. One limitation of the method is that, the lit side should be smooth.



Hybrid Analysis of Scattering for a Large Body with Cracks

X.C.Nie, Y.B.Yan, S.Y.Shi, D.B.Ge and H.Huang
Department of Physics, Xidian University

710071, Xi'an, P.R.China
email: dbge@xidian.edu.cn

With increasing of sophistication of RCS reduction techniques, studies of contribution of small features such as wires, cracks have been drawn great interests in recent years. A hybrid method on the basis of high frequency technique combined with a numerical method (for example, J.M.Jin, S.S.Ni, and S.W.Lee, IEEE Trans. AP-43,1130-1138, 1995) has to be resorted because the object under investigation and the cracks on it are of different electric dimensions, respectively. Here we consider a two-dimensional object with cracks and apply the hybridization of Iterative Physical Optics (IPO) and MoM or FDTD to treat this problem.

Considering the equivalence principle, the computation of scattering of an object with cracks is first divided into two regions: the external and the internal regions with respect to the crack, while the appropriate equivalent electric and magnetic currents are put on the opening aperture of the crack. The opening can be furthermore filled with PEC and the external problem is then split into a scattering problem of PEC object without crack and a radiation problem of magnetic currents spreading on the PEC object. We treat the former problem by using the IPO method that may include multi-reflections if the object is concave. Concerning the radiation of magnetic currents, the MoM is applied to calculate the external field. On the other hand, the mode-matching method is used to compute the internal field at the opening provided the crack being rectangular. Finally, we apply the generalized network formulation (R.F.Harrington and J.R.Mautz, IEEE Trans. AP-24,870-873, 1976) to determine the magnetic currents on the opening aperture by matching the boundary conditions. Moreover, as a key step, the magnetic currents on the opening can also be calculated by the FDTD instead of mode-matching method. This approach may extend the application of proposed scheme to the scattering of an object with cracks of more complex shape. We compute the monostatic and bistatic RCS for some simple objects with cracks by proposed hybrid method, and compare them with the one obtained directly from FDTD. The two results are in good agreement showing the feasibility of proposed method.

The Coupling between Antennas on conductive Construction

Yang Shaohua, Chen xinke

Guangzhou Communication Research Institute, China

Yang Enyao

Guilin Institute of Electronic Technology, China

In communication and electronic system it is necessary to mount two antennas, or even more, on the conductive construction. For example, to mount two antennas on top of a vehicle, or one antenna on the top while another one on the ground nearby. It is important to compute the level of coupling between the antennas, since they are located closely with the result that one is in the vicinity of the other. This hybrid method combining MM and GTD is adopted to compute the coupling level of two typical situations. For fig.1(a), it is necessary to add four edge diffractive lines beside directive line and reflective line of the top; fig.1(b) shows the typical diffractive line structure in the case of the conductive stair construction. The current distribution and coupling level between antennas will change when they are in the space where scatterers exit. This fluctuation can be shown in the variation of impedance matrix, that is, the effect of diffractive lines can be summed up in additional matrix [ΔZ]. Fig 2 shows the computing results corresponding to fig 1. The dimensions of the flat model structure are: $L \cdot W \cdot H = 2m \cdot 1.3m \cdot 1.8m$ and the two antennas are of the same height, $h=0.2m$. The height(H) of conductive stair varies from 1λ to 8λ in computation.

It should be noted that it is problematic, for computation in the case of conductive stair, to use MM only and it is simple and practical to use the hybrid method which combines MM and GTD.

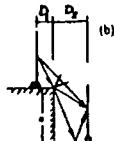
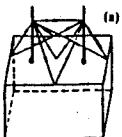


fig.1

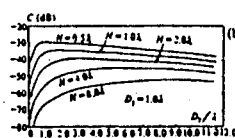
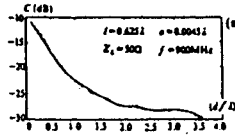


fig.2

Inverse Scattering for Target Recognition

L. Carin and K. J. Langenberg

Scattering Mechanism Characterization using Adaptive Decomposition with a Vectorized Dictionary.....	326
<i>N. S. Subotic*, J. W. Burns, ERIM International, Inc., USA</i>	
Extraction of Target Parameters using the Frequency Correlation Function: A Feasibility Study.....	327
<i>S. R. Legault*, K. Sarabandi, University of Michigan, USA</i>	
Wave-based Target Identification with Short-pulse Scattering Data	328
<i>P. K. Bharadwaj*, L. Carin, Duke University, USA</i>	
Investigation of Bandwidth Effects in Natural Resonance Based Target Recognition.....	329
<i>G. Turhan-Sayan*, Middle East Technical University, Turkey</i>	
Inverse Scattering of Electrically Large Regions with a Gaussian-beam Forward Model.....	330
<i>B. Rao*, L. Carin, Duke University, USA</i>	
Identification of Metallic Objects using Low Frequency Magnetic Fields	331
<i>L. S. Riggs*, J. E. Mooney, D. Lawrence, L. Lowe, T. Barnett, Auburn University, USA</i>	

SCATTERING MECHANISM CHARACTERIZATION USING ADAPTIVE DECOMPOSITION WITH A VECTORIZED DICTIONARY

Nikola S. Subotic* and Joseph W. Burns

ERIM International, Inc.

P.O. Box 134008 Ann Arbor, MI 48113-4008

subotic@erim-int.com, burns@erim-int.com

In this paper we present an extension of adaptive decomposition techniques to vector data and dictionaries for scattering mechanism characterization. The ability to classify and characterize scattering mechanisms in radar data is useful for target radar cross section diagnosis and automatic target recognition applications. Recently, several researchers (N.S. Subotic, J.W. Burns and D. Pandelis, *1997 IEEE URSI Radio Sci. Mtg. Digest*, p.258; M.R. McClure and L. Carin, *Matching Pursuits with a Wave-Based Dictionary, IEEE Trans. Sig. Proc.*, Vol. 45, No. 12, pp. 2912-2927) have applied scalar adaptive signal decomposition techniques to scattering mechanism identification using the Matching Pursuits algorithm (S. Mallat and Z. Zhang, *IEEE Trans. Sig. Proc.*, Vol. 41, pp 3397-3415). This presentation will describe two extensions to the previous work designed to improve scatterer discrimination and classification performance. First, the reweighted minimum norm algorithm described by Gorodnitsky and Rao (Gorodnitsky, I.F., and B.D. Rao, *IEEE Trans. Signal Proc.*, Vol. 45, No. 3, pp. 600-616) is used as the decomposition algorithm in place of Matching Pursuits, and second, the algorithm is formulated such that the data and dictionary take a vector form.

Adaptive techniques decompose radar signals using a very general "dictionary" of functions which can represent disparate scattering mechanisms and are chosen to closely model anticipated characteristics of the signal. Scattering mechanisms can be classified by adaptively mapping measured data onto appropriate dictionaries of functions that describe specific scattering behavior. In the previous work, scattering mechanisms were classified by identifying their frequency dependence. The approach is motivated by the observation that asymptotic solutions for the high frequency scattering from targets, such as the Geometric Theory of Diffraction (GTD), describe the scattering from canonical local geometries by simple models with distinct frequency dependencies. In the previous work, the Matching Pursuit decomposition algorithm was used with a GTD-based dictionary. Accurate mechanism classification was obtained when the algorithm was applied to scalar data with sufficient frequency bandwidth that individual scattering centers were separated by several Fourier resolution cells.

In our recent work, the reweighted minimum norm algorithm was used in place of Matching Pursuits as the adaptive decomposition algorithm to improve classification performance when scattering centers were not well resolved. The reweighted algorithm refines an initial low resolution initial estimate of the dictionary coefficient to a final localized energy solution. The iterations are based on weighted norm minimization of the dependent variable with the weights being a function of the preceding iterative solutions. Since all the dictionary elements are evaluated at each iteration, it was anticipated that it would avoid the tendency of Matching Pursuits in low resolution situations to spend most of its time correcting for any mistakes made in the classifying the first few terms. Even with scalar data, the reweighted minimum norm technique was able to correctly type scatterers at much smaller scatterer separations.

To further enhance scatterer discrimination, the algorithm was generalized to consider vector data, such as that obtainable from a polarimetric radar. This simply involved defining a dictionary of frequency-weighted, complex exponentials with appropriate polarization states. As before, the weights correspond to frequency dependencies suggested by GTD. The richer diversity of the data and dictionary allows more scatterer types to be distinguished than those provided using only frequency-weighted exponentials with scalar data or polarization states alone with vector data.

In the presentation, we will describe the formulation and implementation of the algorithm. We will show the mechanism classification performance obtained when the algorithm was applied to numerically-simulated and experimentally-measured data, and algorithm performance determined from Monte Carlo simulations will be compared to Carmer-Rao bounds.

Extraction of Target Parameters using the Frequency Correlation Function: A Feasibility Study

Stéphane R. Legault* and Kamal Sarabandi

Radiation Laboratory

Department of Electrical Engineering and Computer Science

University of Michigan, Ann Arbor, MI 48109-2122

The remote sensing community has made significant progress in recent years and this vast research effort is supported by an increased world wide interest in the management of our dwindling natural resources. Even with the perfection of synthetic aperture radars, the extraction of parameters of interest such as biomass and vertical extent for vegetation canopies remains at best a complicated process. This is true despite the advent of multi-frequency and multi-polarization systems which greatly increase the number of independent observables. In contrast to examining the correlation of signals with respect to observation angle or polarization, we propose the use of frequency correlation across the bandwidth of the signal in an effort to provide a new distinct measurable for target identification and classification.

Over frequency bandwidths of interest the scattering properties of the individual elements making up a complex distributed target change only slightly with frequency. This implies that the frequency dependent part of the scattering process is predominantly due to variations in the electrical path lengths of the multiple interactions. Examination of the correlation function over the bandwidth of the returned radar signal therefore yields an interference pattern associated with the distribution and the structure of the scatterers making up the medium. This suggests the possibility of extracting those parameters of a distributed target which relate, such as vertical extent, to its structure.

The feasibility of this technique is investigated experimentally and theoretically. A sizeable number of radar measurements of various crops form the major part of the experimental data collected. These experiments were conducted at various angles of incidence at L, C and X band. This data is used in conjunction with a theoretical model in order to identify the role played by the various parameters of a target and its frequency correlation function. To this end a heuristic model for a layer of random scatterers above a lossy medium is presented. A discussion of both the experimental and the theoretical results will be provided.

Wave-Based Target Identification with Short-Pulse Scattering Data

Priya K. Bharadwaj* and Lawrence Carin

Department of Electrical and Computer Engineering

Duke University

Durham, NC 27708-0291

Matching pursuits is an algorithm by which a given waveform is projected onto a dictionary of elements, with which the data is parsed. By representing the data in as compact a decomposition as possible, its principal features are extracted, setting the stage for target detection and identification. Consequently, we have developed what we have termed a wave-based dictionary, appropriate for short-pulse scattering, with dictionary elements representative of wavefronts, resonances, and chirps. As discussed below, this data parsing scheme plays an integral role in the target identification framework.

The identification algorithm is based on the reasonable assumption that a decision will be made using a few measured waveforms from a given target (a few "looks"), representative of several aspects (sensor-target orientations). Since the target is unknown, we do not know the actual target-sensor aspect for a given waveform (*i.e.*, it is hidden). The different waveforms (in general from different target-sensor orientations) can therefore be viewed as transitions from one hidden state (orientation) to another. In the training phase, the target is segmented into multiple states, representative of characteristic target-sensor orientations. Each state is characterized by a zone of target-sensor angles, within which the wave phenomenology is relatively similar. The multiple measured waveforms to be processed are representative of different target-sensor orientations, and therefore constitute state transitions (from one measured waveform, at a particular sensor-target orientation, to another waveform, at a second sensor-target orientation). Within each state, the data is parsed or segmented using the aforementioned wave-based dictionary, with this decomposition parameterized statistically, reflecting the statistical variation of such within a given state. These statistics characterize the variability of the segmentation within a particular state and are determined during the wave-based training phase.

The state transitions are represented via a hidden Markov model (HMM), much as in word-recognition schemes for speech processing. The states of the HMM are defined as ranges of target-sensor angles over which the underlying wave phenomenology is relatively constant (or similar). Within each such range of angles (*i.e.*, within each such state), the wave-based matching-pursuits scheme provides the data parsing. In this talk, we present the basic processing paradigm, and discuss example results for *identification* of several canonical targets.

Investigation of Bandwidth Effects in Natural Resonance Based Target Recognition

Gönül Turhan-Sayan

Electrical and Electronics Engineering Department
Middle East Technical University, 06531 Ankara, Turkey

Classification of radar targets from the measured backscattered data is an important problem in inverse scattering. The aspect and polarization dependent nature of electromagnetic scattering makes this problem quite difficult to solve. Accordingly, one of the recent trends in target recognition is to use special signal shaping techniques to describe targets in an aspect and polarization independent manner. The target recognition techniques known as K-pulse and E-pulse techniques are based on the annihilation of a target's natural resonances as the set of complex natural resonance (CNR) frequencies of a scatterer identifies that object being independent from the aspect and polarization. In such a technique, every target of concern is classified by means of a time-limited characteristic signal whose Laplace domain zeroes correspond to the CNR frequencies of the target over a given frequency band. These characteristic time signals synthesized for each of the targets to be recognized can be stored in a computer to represent a set of digital filters. At the time of recognition, the received unknown signal is passed through each of these filters and the filter producing a time-limited response (due to proper pole-zero cancellation) identifies the unknown target. Among many factors affecting the success of recognition, the bandwidth of the scattered signal used for the synthesis of a characteristic signal has the utmost importance. The widest possible bandwidth in the resonance region starting from the lowest possible frequency produces the best characterization as the related synthesis data must contain all the critical information about the natural resonance behaviour of the target, especially that information about the dominant resonances. In practice, however, the available database for the recognition problem may not comply with these requirements leading to some deterioration in the recognition performance.

The objective of this paper is to investigate the effects of the signal bandwidth in the performance of the natural resonance based target recognition techniques. It is believed that the results of this investigation will help to clarify the uncertainties about choosing the signal bandwidths not only in the signal shaping phase but also in the phase of active target recognition. The importance of the match between the bandwidths of the signals used in the synthesis procedure and that of the test (unknown) signal will also be demonstrated in this paper through simulation problems for varying bandwidth conditions and for a realistic set of targets.

Inverse Scattering of Electrically Large Regions with a Gaussian-Beam Forward Model

Bimba Rao* and Lawrence Carin
Department of Electrical and Computer Engineering
Duke University
Durham, NC 27708-0291

Inverse scattering algorithms require an accurate and efficient forward model. There has recently been a focus on the use of forward solvers that satisfy Maxwell's equations rigorously, resulting in inverse-scattering algorithms that are quite accurate. However, the limitations of current computers and the overhead on rigorous forward solvers often restrict the electrical size of the problems that can be considered. In the research presented here, we utilize a beam-tracing algorithm as a forward solver, thereby yielding accurate field solutions over electrically large regions. We demonstrate results of inverse scattering over regions that constitute thousands of square wavelengths.

An issue with regard to beam-tracing algorithms involves the mapping of initial (antenna) fields onto the Gaussian beams, the latter subsequently propagated through the domain under test. Previous work with Gaussian beams was characterized by an almost *ad hoc* mapping of started fields to beams. Here this mapping is performed rigorously through use of several signal-processing algorithms. In particular, here we demonstrate results computed via Gabor and wavelet transforms, as well as through use of the method of matching pursuits.

In the work presented here, we demonstrate how the beam tracing algorithm can be placed into the context of an inverse-scattering algorithm. In this regard we address appropriate simplifications and assumptions that must be made, and their impact on the result accuracy. Moreover, we present results for several inhomogeneous distributions, which we approximate via inversion. We address the range of parameters over which the inversion results are accurate, the issue of local minima, and regularization techniques that improve inversion accuracy.

Identification of Metallic Objects Using Low Frequency Magnetic Fields

Lloyd S. Riggs*, Jon E. Mooney, Dan Lawrence, Larry Lowe, and Tom Barnett

Department of Electrical Engineering
200 Broun Hall • Auburn University, Alabama 36849

At the present time, the AN/PSS-12 is the U.S. Army's only fielded mine detector. Although this detector is quite sensitive and can detect low metal content mines, its overall value to the foot soldier is severely limited due to many false alarms generated by buried metallic clutter. In fact, in highly cluttered environments, the detector is rendered, for all intents and purposes, useless. In short, a metal detector is not a mine detector!

Baum has shown (Interaction Note 499, Nov. 1993) that the quasi-magnetostatic scattering from conducting scatterers is characterized by natural frequencies (SEM) which are negative and real. Equivalently, the time domain response is characterized by a sum of weighted exponentials. This model affords an opportunity for metallic object identification in that each metallic object is characterized by a small number of distinct exponential decay rates.

We have recently demonstrated in a laboratory setting the ability to discriminate among a set of metallic objects with simple shapes. In general, we view the problem of identification as one of inference from incomplete information calling for a full application of probability theory. Following this philosophy, we have employed a generalized likelihood ratio test (GLRT) as the basis for our identification algorithm. The apparatus and techniques used to measure the objects transfer function will be discussed. We will review several methods for extracting exponential decay rates from measured data including a differential corrections method and a genetic algorithm.

Extracting non-oscillatory exponential decays from measured data can present a challenge. A response containing multiple decay rates can be approximated reasonably well under certain conditions by a model with fewer poles. Furthermore, if the error between the true and approximate model is on the order of the measurement noise, then the lower order (approximate) model is sufficient to characterize the underlying true model. We will demonstrate, through numerical experimentation, that when the maximum error (between the true model and a lower order approximate model) is less than the standard deviation of the noise, most pole extraction methods (Prony's method, Pencil-of-Functions method, Genetic Algorithm, Differential Corrections Method, etc.) cannot identify the parameters (poles and residues) of the true model but instead converge to the parameters of the lower order approximate model. Furthermore, we show that the differential corrections method in white Gaussian noise provides an efficient estimate of model parameters in that the estimate of model parameters have variances near that of the Cramer-Rao lower bound.

Author Index

Name	Page	Name	Page		
A					
Abdin, A.	35	Buckles, S.	33		
Acree, M. A.	292	Bulkin, V.	71		
Adams, R. J.	108,302,303	Burkhardt, M.	72,73,274		
Agi, K.	119	Burkholder, R. J.	109		
Alaydrus, M.	190	Burns, J. W.	326		
Altizer, S. W.	320	Butler, C. M.	169,214,259,293		
Anantha, V.	50	Buxton, C. G.	2		
Ando, M.	122	Byahun, U. M.	193		
Andrenko, A. S.	122	Byers, A.	150		
Antar, Y. M. M.	218,318	C			
Archambeault, B. R.	98	Cable, V. P.	292		
Armogida, A.	53	Cangellaris, A.	44		
Arnautovski, V.	112	Cangellaris, A. C.	200		
Arvas, E.	151,322	Caputa, K.	194,197		
Asvestas, J. S.	61,320	Carin, L.	167,168,184,217,321,328,330		
Awadallah, R. S.	183,185	Castillo, S.	33		
Aygun, K.	305	Castillo, S. P.	307		
Ayyildiz, K.	151	Caswell, E. D.	111		
B		Cendes, Z.	41		
Baginski, M. E.	268	Champagne, N. J.	308		
Baharav, Z.	244	Chan, C. H.	32,186		
Bardati, F.	69	Chan, K. L.	285		
Bardi, I.	41	Chan, T. K.	178		
Barnett, T.	331	Chang, C. C.	189		
Baroni, M.	54	Chang, F. C.	164		
Basilio, L. I.	9	Chatterjee, D.	11,12		
Baum, C. E.	103	Chavannes, N.	73		
Beaumont, E.	232	Chen, C.	138,139		
Beck, F. B.	96	Chen, C. H.	284		
Bharadwaj, P. K.	328	Chen, G.	189		
Bhobe, A.	5	Chen, K.	311		
Biswas, R.	117	Chen, K. M.	66,189		
Bit-Babik, G.	215	Chen, V. C.	23		
Boix, R. R.	282,316	Chen, Y.	8,83,99		
Boots, B.	150	Cheng, D.	218,318		
Borgioli, A.	155	Cheng, G.	270		
Botros, Y. Y.	203	Cheng, G. G.	257,260		
Brandfab, M.	15	Chew, W. C.	18,37,132,182,286		
Brandfass, M.	18	Chiang, H. S.	144		
Breakall, J. K.	61	Chive, M.	240		
Brown, E. R.	114	Chou, H.	49,51		
Brown, G. S.	108,183,185,302,303	Christ, A.	274		
		Chu, T.	297,298		
		Chung, J. K.	144		

Author Index

Name	Page	Name	Page
Chung, Y.	225	Engheta, N.	134,163,314
Cocchi, A.	97	Enyao, Y.	263,324
Cockrell, C. R.	96	Ergin, A.	305
Coetzee, J. C.	57	Erricolo, D.	48
Conde, M. E.	235	Espinoza, C.	142
Courtney, C.	228	Estrada, J.	232
Cown, B.	232	F	
Crook, G.	142	Faiz, M. M.	4
Crook, G. E.	290	Fan, G.	31,92
Crosta, G.	14	Fedosova, N. H.	193
Crouch, D.	117	Feinerman, A. D.	252
Cuhaci, M.	261	Felsen, L. B.	170
Cwik, T.	104,155	Feng, M.	154
D		Fiddy, M. A.	19
Dauvignac, J. Y.	100	Fikioris, G.	160
Davis, A. M. J.	219	Fisher, S. E.	305
Davis, B. A.	108	Foltz, H.	142
Davis, W. A.	111,234	Foltz, H. D.	262,290
Dawson, T. W.	188,194	Fontana, T. P.	62
Dean, I.	242	Forest, F. W.	102
Dean, J.	106	Freire, M. J.	158
DeBoer, D. R.	256	G	
Denison, D.	258	Gai, W.	235
Derudder, H.	276	Gallivan, K.	110
Desclos, L.	271,272,299	Garreau, P.	232
Deshpande, M. D.	96	Ge, D. B.	174,220,323
Diaz, L.	60	Gearhart, S. S.	291
Didenko, N.	310	Gedney, S. D.	43
Ding, Z.	172	Geng, N.	167,168,217
Dixon, J.	75	Gershon, E.	107
Dogaru, T.	184,217	Gheorma, I. -	207
Drake, E.	282	Glisson, A. W.	264,265
Drayton, R. F.	250	Goggans, P. M.	67,68
Duan, D. W.	273	Gong, J.	91
Dubois, L.	240	Gordon, R. K.	202
E		Goto, K.	52
Economou, D.	215	Gozani, J.	176,177
Ederra, I.	209	Graglia, R. D.	207
Egger, O.	196	Grant, J. B.	308
Eibert, T. F.	190	Grcev, L.	112,191,288
El-Shenawee, M.	182	Grechka, A. V.	26
Ellis, T.	120,123	Greenwood, A. D.	94
Elsherbeni, A. Z.	35	Grzesik, J. A.	222

Author Index

Name	Page	Name	Page
Guo, Y. X.	3	Jensen, M. A.	153
Guzman, E.	262,290	Jiang, Y.	93
H		Jin, J.	37,92,94
Haas, M.	17	Johnson, J. M.	59
Hagness, S. C.	149	Johnson, W. A.	308
Hajj, G.	136	Jorgenson, R. E.	308
Hall, W. F.	36	Joubert, J.	57
Hamada, L.	242	Judah, S. R.	285
Hansen, V. W.	190	Junker, G. P.	264
Hanson, G.	161	K	
Hanson, G. W.	103	Kacarska, M.	191,288
Harrison, L. A.	202	Kan, Y.	66
Haupt, R. L.	225	Kang, Y. W.	252
Havrilla, M. J.	229	Kapadia, R.	7
Heinrich, H. K.	273	Kashyap, S.	24
Heyman, E.	81,82,170	Kastner, R.	81,82,107
Hill, D. A.	233	Katehi, L. P.	148
Ho, K.	117	Katehi, L. P. B.	120,123,249
Holtzman, R.	82	Katsenelenbaum, B.	209
Hon, B. P. d.	170	Katz, D. S.	104
Horno, M.	158,282,283,316	Kelley, D. F.	30
Houshmand, B.	25	Kelly, P. K.	5,60
Hsiao, C.	297	Kempel, L. C.	90
Huang, H.	323	Kesler, M. P.	116
Huang, K. S.	144	Khan, S. M.	47
Huang, Y.	141	Kiang, J. F.	144,152,195,284
Huber, C.	17	Kim, J. P.	281
Humbert, W. R.	230	Kim, K. T.	162
Hussar, P.	46	King, R. W. P.	192
Hutchcraft, W. E.	202	Kishk, A. A.	264,265
Huynh, S. H.	257,260,270	Kobayashi, K.	216
I		Konecny, R. S.	235
Infante, D. J.	279	Koshikawa, S.	216
Ishihara, T.	52	Kotulski, J. D.	308
Ishimaru, A.	178	Kouhata, I.	310
Iskander, M. F.	146	Kuga, Y.	178
Ito, K.	242	Kuramoto, A.	271,272
J		Kuster, N.	72,73,196,274
Jackson, D. R.	6,9,294,308	Kuzuoglu, M.	79,205
Jaggard, A. D.	127,128	Kwon, D. -	109
Jaggard, D. L.	166,315,317	L	
Jandhyala, V.	154,182	Lail, B. A.	307
		Lam, T.	7

Author Index

Name	Page	Name	Page
Lane, R.	140	Manara, G.	53
Langenberg, K. J.	15	Mancini, D. C.	252
Lawrence, D.	331	Manuar, O.	315
Lee, J.	202	Maponi, P.	16
Lee, M.	140	Marco, F. D.	69
Lee, R.	42	Margetis, D.	160
Lee, R. Q.	10	Marrocco, G.	69
Lee, S.	70	Martel, J.	283
Legault, S. R.	327	Martin, A. Q.	93
Lehner, G.	17	Mathis, A. W.	278
Leung, W.	117	Mayer, K.	15
Leung, Y. F.	32	McGahan, R. V.	19
Leviatan, Y.	244,309	McLaughlin, D. J.	143
Li, H.	138,139,140	McLean, J. S.	142,262,290
Li, N.	294	McMahon, O. B.	114
Li, Q.	186	Medina, A.	142
Li, Q. L.	220	Medina, F.	283
Liepin, U. R.	63	Mehrotra, A.	6
Lin, H.	138,139	Mesa, F.	158
Ling, H.	23,145	Michalski, K.	306
Ling, R. T.	201,277	Michielissen, E.	110,132,154,182,305
Liu, G.	95	Miller, E. K.	295
Liu, J. J.	178	Miller, J.	28,29,85,133
Liu, Q. H.	31,84	Miller, R.	133,245
Liu, S. P.	152	Mioc, F.	54
Liu, T.	138,139	Mirzabekov, A.	253
Lo, W. T.	152	Misici, L.	16
Lodder, D. R. A.	213	Mitra, R.	8,40,71,79,83,99,205,251
Long, S. A.	6,9	Mix, J.	75
Losada, V.	316	Mohammadian, A. H.	36
Loskovska, S.	191,288	Mojahedi, M.	119
LoVetri, J.	24	Mokole, E.	171
Lowe, L.	331	Monorchio, A.	53,97
Lucas, E. W.	62	Mooney, J. E.	172,268,331
Luebbers, R. J.	30,239	Moore, R.	179
Luevano, M.	142	Morales-Porras, A.	19
Luk, K. M.	3	Morris, J. B.	19
M			
Mack, M.	231	Moses, C. A.	314
Madhian, M.	271,272	Motil, W.	228
Mak, C. L.	3	Motoi, N.	216
Malik, S.	81	Movahedi, A. J.	265
Malloy, K. J.	119	Mrozowski, M.	159
Maloney, J. G.	116	Mudaliar, S.	181
		Murav'ev, V. V.	193

Author Index

Name	Page	Name	Page		
N					
Nagraj, S.	226	Popovski, B.	112		
Najafabadi, R. M.	223	Pouliguen, P.	212		
Navsariwala, U.	43	Power, J. G.	235		
Nealy, J. R.	2	Preissig, R. S.	206		
Nepa, P.	53	Prescott, G.	12		
Nevels, R.	28,29,85,133,245	Pribetich, J.	240		
Nie, X. C.	323	Primak, S.	24		
Nima, F.	56	Prussner, L.	204		
Nive, E.	310	Pursel, J. D.	67,68		
Niver, E.	7	R			
Niyompong, M.	150	Radhakrishnan, K.	286		
Nurnberger, M. W.	105	Rahmat-Samii, Y.	59,130		
Nyquist, D. P.	229,279	Ramahi, O. M.	78,86,87,98		
Nystrom, J. F.	34	Rao, B.	330		
O		Rao, K. V. S.	273		
Okoniewski, M.	197	Rao, S. M.	304		
Oliker, E.	204	Rebeiz, G. M.	120,123,249		
Oliker, V.	46,204	Reddy, C. J.	96		
Ololoska, L.	191	Rehnmark, S.	151		
Ololoska-Gagoska, L.	288	Rengarajan, S. R.	56,58		
Olyslager, F.	276	Riblet, G. P.	208		
Oz, J.	129	Richie, J. E.	102		
Ozzaim, C.	259	Rieger, W.	17		
P		Riggs, L. S.	172,268,331		
Pantic-Tanner, Z.	231	Rockway, J. D.	178		
Park, D.	83	Rogers, S. D.	293		
Park, S.	226	Romanovsky, J.	204		
Park, W. S.	281	Ros, A. E.	74		
Parker, C. D.	114	Rothwell, E. J.	189		
Pathak, P. H.	49,51,109	Rousseau, P.	49		
Pelosi, G.	97,100	Rowell, C.	36		
Perez, O. P.	280	Rucker, W. M.	17		
Peterson, A. F.	206,278	Ruehli, A.	44		
Pichot, C.	100	Rumsey, I.	5		
Piket-May, M.	5,75,150	S			
Pisano, A. P.	248	Sadayappan, P.	42		
Pisano, III, F. A.	169	Saito, K.	242		
Pitsch, A.	15	Sanchez, M.	260,270		
Plumb, R. G.	11,12	Santos, H. J. D. L.	121		
Pokovic, K.	196,274	Sarabandi, K.	327		
Popovic, Z.	75	Sarkar, T. K.	226,282,304		
		Sayama, S.	52		
		Schamiloglu, E.	119		

Author Index

Name	Page	Name	Page
Scharstein, R. W.	219,238	Suk, J.	189
Schmid, T.	196	Sullivan, A.	321
Schmier, R. G.	62	Sun, K.	8
Schoessow, P.	235	Suzuki, T.	118
Scholler, J. D.	277	Symons, W. C.	213
Schuster, J.	239	T	
Scott, Jr., W. R.	70,230	Taflove, A.	50,149
Selfridge, R. H.	153	Takagi, K.	216
Selleri, S.	100	Tamelo, A. A.	193
Sengupta, D.	154	Tanabe, K.	271,272
Shaker, J.	261	Tavzashvili, K.	215
Shankar, V.	36	Temkin, R.	258
Shanker, B.	154,305	Terril, N. D.	234
Shaohua, Y.	263,324	Thomas, J. B.	136
Shapiro, M.	258	Thomy, V.	240
Sharpe, R. M.	308	Thumm, M.	209
Shi, S. Y.	220,323	Tian, X.	145
Shifman, Y.	244	Tiberio, R.	54
Shifrin, Y. S.	63	Tirone, L.	69
Shumpert, J. D.	120,123	Toccafondi, A.	54
Shumpert, T.	106	Toland, B.	222
Sigalas, M. M.	117	Tong, M.	8
Silva, L. C. d.	280	Toporkov, J. V.	185
Smaddar, S. N.	171	Tricoles, G.	22
Smelyanskiy, M.	105	Trosko, J. E.	189
Smith, C. E.	35	Trott, K. D.	90
Smith, G.	116	Tsang, L.	186
Smith, P. D.	296	Turhan-Sayan, G.	329
Song, J. M.	132	Tuttle, G.	117
Sorolla, M.	209	U	
Sowa, M. J.	143	Ufimtsev, P. Y.	201,277
Spasenovski, B.	112	Upham, B. L.	189
Spiegel, J.	309	Uslenghi, P. L. E.	48
Spitsyn, V. G.	241	Uzunoglu, N.	215
Spitsyna, N. V.	241	V	
Stamm, J. M.	61,320	Vanoverschelde, C.	240
Steffes, P. G.	256	Veliev, E. I.	216
Steinberg, B. Z.	107,129	Veremey, V.	40,251
Stevens, W. G.	143	Vescovo, R.	64,224
Stillman, G.	154	Vinogradova, E. D.	296
Stuchly, M. A.	188,194,197	Vogel, W. J.	145
Stutzman, W. L.	2	Volakis, J. L.	105,203
Subotic, N. S.	326		
Sudanthy, S.	142		

Author Index

Name	Page	Name	Page
Vorgul, I. Y.	173	Zaridze, R.	215
W		Zhang, B.	24
Wahid, P. F.	4	Zhang, J.	189,311
Waller, M.	106	Zhao, J. -	18
Wang, J.	250	Ziolkowski, R. W.	80,81,82,131
Wang, J. J. H.	223	Zirilli, F.	16
Wang, Y.	23	Zou, P.	235
Warne, L. K.	308	Zuffada, C.	136
Wedge, S.	91	Zunoubi, M.	37
Weijers, B.	143	Zutter, D. D.	276
Weile, D. S.	110		
Werner, D. H.	126		
White, M. J.	146		
Whites, K. W.	180		
Wilczewski, F.	190		
Williams, J. T.	6,9,294		
Wilson, D.	155		
Wilson, M.	231		
Wilton, D. R.	308		
Wittwer, D. C.	80		
Wolfe, C. T.	43		
Wong, T.	235		
Worasawate, D.	322		
Wu, F.	180		
Wu, T. X.	166,317		
X			
Xinke, C.	263,324		
Xu, X.	95		
Y			
Yan, Y. B.	174,323		
Yang, H. Y. D.	115		
Yang, M.	99		
Yang, Y.	298		
Yasan, E.	148		
Young, J. C.	293		
Young, J. L.	34		
Young, L.	136		
Yu, D. S.	195		
Yu, P. K. L.	118		
Yun, Z.	146		
Z			
Zaman, A.	10		



1999 IEEE AP-S INTERNATIONAL SYMPOSIUM AND USNC/URSI NATIONAL RADIO SCIENCE MEETING

Orlando, Florida July 11-16, 1999

<http://www-ece.engr.ucf.edu/apursi99>

The 1999 AP-S International Symposium sponsored by the IEEE Antenna and Propagation Society and URSI (International Union of Radio Science) meeting sponsored by USNC Commissions A, B, D, E, F, and K, will be held jointly at the Renaissance Orlando Resort in Orlando, Florida, July 11-16. The technical sessions, workshops and short courses will be coordinated between the two symposia to provide a comprehensive and well-balanced program.

Paper submission

This year we will continue the use of both electronic and hard copy paper submission. The Conference Digest will be available both in CD-ROM format and in hard copy format.

Authors are invited to submit papers on all topics of interest to the AP-S and URSI membership. In addition there will be an AP-S Student Paper Competition and an URSI Student Paper Competition. Suggested topics and general information can be found in <http://www-ece.engr.ucf.edu/apursi99>

General Chair: Christos Christodoulou
ECE Department, University of Central Florida
Orlando, FL 32816
(407) 823-5831 (W)
cgc@ece.engr.ucf.edu

General Vice-Chair: Michael Thursby
EE Department, Florida Institute of Technology
Melbourne, FL 32901
(407) 768-8000 ext 6160
mht@as1.fit.edu

All technical inquiries should be addressed to:

Chair: William Croswell
Harris Corporation
1037 Homewood Ave
Melbourne, FL 32940
(407) 729-3110 (H) (407) 242-3152 (W)

Co-Chair: Parveen Wahid
ECE Department, University of Central Florida
Orlando, FL 32816
(407) 823-2610 (W)
pfw@ece.engr.ucf.edu

